Changes in the cytoskeleton and signalling pathways in differentiated human neuroblastoma cells following MPP$^+$ exposure

Katy Elizabeth Beck

A thesis submitted in partial fulfilment of the requirements of The Nottingham Trent University for the degree of Doctor of Philosophy

December 2004

DECLARATION

This work has not been accepted for any other degree and is not concurrently being submitted for any other degree.

We certify that the work submitted was carried out by the author. Due acknowledgement has been made of any assistance received.

Signed..(candidate)

Signed..(Director of studies)

ACKNOWLEDGEMENTS

ABSTRACT

Changes in the cytoskeleton and signalling pathways in differentiated human neuroblastoma cells following MPP$^+$ exposure

1-methyl-4-phenyl-1,2,3,6 tetrahydropyridine (MPTP), via its active metabolite, 1-methyl-4-phenylpyridinium (MPP$^+$), provides a Parkinsonian model for investigating (a) the mechanisms of cell death and (b) neuroprotective strategies. The majority of research uses either animal models or mitotic cell lines, exposed to MPTP/MPP$^+$ over relatively short exposure times. In the work presented, the human neuroblastoma (SH-SY5Y) cell line was differentiated biochemically and morphologically to provide a viable, mature phenotype for extended time periods. Following a 7-day pre-differentiation regime, cells were exposed to cytotoxic and sub-cytotoxic concentrations of MPP$^+$ over 72 h, and to sub-cytotoxic concentrations for up to 14 days. In the latter case cell viability is not significantly reduced but subtle biochemical changes occur that may replicate the neurodegenerative process *in-vivo*.

The effects of MPP$^+$ and proteasomal inhibition on the cytoskeleton were investigated, in particular the neurofilament (NF) and microtubule (MT) systems. Results suggest that changes in post-translational modification/distribution of NFs represent down-stream markers of MPP$^+$ toxicity in this system. Following 24 h exposure to cytotoxic, and 14 days exposure to sub-cytotoxic MPP$^+$ concentrations, phosphorylated NF-H and NF-M levels increased, associated with an increase in the ratio of phosphorylated NF-M to NF-H. Immunocytochemical analyses of cells exposed to cytotoxic MPP$^+$ levels revealed phosphorylated NF-H/NF-M as a discrete accumulation adjacent to and impinging on the nucleus. Similarly, in cells exposed to sub-cytotoxic MPP$^+$ concentrations, NF-H/NF-M was located as a perinuclear halo. MPP$^+$ exposure significantly increased levels of ubiquitinated proteins, suggestive of impaired proteasomal activity. Evidence was provided for proteasomal degradation of NFs and tubulin since they accumulated following proteasomal inhibition using a specific inhibitor. This project established a novel role for the transamidating/GTPase enzyme, tissue transglutaminase (tTG) in MPP$^+$ toxicity. MPP$^+$ increased tTG activity, despite reducing tTG protein levels, whilst inhibition of tTG activity exacerbated MPP$^+$ toxicity.

The effects of specific MAPK pathway inhibitors on MPP$^+$ toxicity revealed a dynamic balance between pathways. Protection conferred by MEK and p38 inhibitors was dependent on the level of MPP$^+$ toxicity whilst inhibition of the JNK pathway attenuated MPP$^+$ toxicity. The role of CDK-5 in this system was also investigated since it is predominantly expressed in post-mitotic neurones, is implicated in Alzheimer's disease and has recently been identified in brainstem and cortical Lewy bodies. Butyrolactone 1, a selective CDK-5 inhibitor significantly protected cells treated for up to 14 days with MPP$^+$. This study is the first to show protection against MPP$^+$ toxicity using a selective CDK-5 inhibitor (Butyrolactone I) in a human neuronal cell system.

AAV; Adeno-associated virus
AIF; Apoptosis inducing factor
ANT; Adenine nucleotide translocator
AOEs; Anti-oxidant enzymes
AP; Alkaline phosphatase
APP; β-amyloid precursor protein
BCIP; 5-bromo-4-chloro-3-indolyl-phosphate (di-sodium salt)
BL-1; Butyrolactone 1
BSA; Bovine serum albumin
CDK-5; Cyclin-dependent kinase 5
CIP; CDK-5 inhibitor protein
DA; Dopamine
DMEM; Dulbecco's Modified Eagles Medium
DMSO; dimethyl sulfoxide
EDTA; Ethylenediamine
ELISA; Enzyme Linked Immunosorbant Assay
ERK; Extracellular signal related kinase
FBS; Foetal bovine serum
FITC; Fluorescein Isothiocyanate
GRD; Glutathione reductase
GSH Px; Glutathione peroxidase
GSH: Glutathione
GSSH; Oxidised glutathione
GTP; Guanosine 5′triphosphate
HRP; Horseradish peroxidase
JIP; JNK interacting protein
JNK: c-jun N-terminal kinase
LPA; Lysophosphatidic acid
MAO; monoamine oxidase
MAPK; Mitogen activated protein kinase
MAPs; Microtubule associated proteins
MEK; ERK kinase
MEKK; ERK kinase kinase
MF; Microfilaments
MKK; MAPK kinase
MKKK; MAPK kinase kinase
MPDP$^+$; 1-methyl-4-phenyl-2,3 dihydropyridinium
MPP$^+$; 1-methyl-4-phenylpyridinium ion
MPTP; 1-methyl-4-phenyl-1,2,3,6 tetrahydropyridine
MT; Microtubules
MTOC; Microtubule organising centre
MTP; Mitochondrial transition pore
MTT; 3-[4-5-Dimethylthiazol-2-y1]-2,5-diphenyl tetrazolium bromide
NBT; Nitro Blue Tetrazolium
NF; Neurofilaments
NMDA; N-methyl-D aspartate
NO; Nitric oxide
NOS; Nitric oxide synthase
PBS; Phosphate buffered saline
PD; Parkinson's disease
PI-3K; Phosphatidylinositol 3-kinase
PLC; Phospholipase C
PMSF; Phenylmethylsulphonyl fluoride
PT; Permeability transition
RA; Retinoic acid

RNS: Reactive nitrogen species
ROS; Reactive oxygen species
SDS PAGE; Sodium dodecylsulphate polyacrylamide gel electrophoresis
SEM; Standard error of the mean
SOD; Superoxide dismutase
STS; Staurosporine
TBS; Tris buffered saline
TG; Transglutaminase
TGF-β; Transforming growth factor-β
tTG; Tissue transglutaminase
UPP: Ubiquitin-proteasome pathway

LIST OF CONTENTS

LIST OF FIGURES

LIST OF TABLES

CHAPTER I

GENERAL INTRODUCTION

CHAPTER 1. GENERAL INTRODUCTION

1.1 Parkinson's Disease

Parkinson's disease (PD) is a progressive, extrapyramidal, neurodegenerative disorder, commonly related to old age. It is reported to affect more than 2 % of the population over 65 years and exhibits an increased incidence with age. More rarely, early onset cases are reported at less than 40 years of age (reviewed by Blum *et al.*, 2001). The majority of PD cases are late onset and idiopathic but recently more novel theories have been hypothesised including involvement of environmental exogenous or endogenous neurotoxins in genetically predisposed individuals (Jenner, 2001; Barzilai and Melamed, 2003). Genetic factors account for approximately 0.5 % of PD cases. Rare, autosomal dominant and recessive transmission patterns of the disease have been implicated in hereditary PD. For a comprehensive review of the genetic contributions to PD, see Huang *et al,* (2004).

1.1.1 Disease pathology

It is widely accepted that the underlying cause of PD pathology is due to a progressive loss of dopamine (DA), resulting from death of neuromelanin containing DA fibres in a midbrain structure, the substantia nigra pars compacta. Degeneration of neurones follows a specific pattern, the ventral area being most susceptible, causing striatal DA loss. Since the brain contains an excess of dopaminergic fibres, patients can remain asymptomatic until approximately 80 % are lost. Non-nigral lesions also contribute to disease pathology resulting in cognitive and psychological impairments i.e. dementia (Blum *et al.,* 2001 and references therein). The principle events that initiate idiopathic PD are not fully elucidated but several contributable molecular mechanisms are proposed (reviewed by Schapira, 2004) (see Fig 1.1). The primary insult is considered to be ATP depletion due to a systemic mitochondrial complex I defect (Schapira *et al.,* 1989; Cassarino and Bennett Jr, 1999; Orth and Schapira, 2002) thus contributing to oxidative stress (see Jenner and Olanow, 1996; Hunot *et al.,* 1997). However, an integral role for impaired proteasomal function is also currently gaining favour (Chung *et al.,* 2001; McNaught *et al.,* 2003). Although disease pathology cannot be treated at this time, therapy aims to alleviate symptoms

via restoration of the acetylcholine/DA imbalance. Current treatment options are not entirely ideal; over-stimulation of DA can result in hyperkinesias (uncontrolled writhing movements), raised noradrenaline levels can induce hypermania and patients can experience periodic insensitivities to drugs. Alternative treatment options are then required, including drugs that mimic DA action or enhance DA release, monoamine oxidase B (MAO B) inhibitors, drugs that release DA and acetylcholine antagonists (Rang, Dale & Ritter, 1995). Therefore research aimed at designing more effective treatment is necessary. For this to proceed, continued and detailed understanding of the aetiology and pathogenicity of PD is required.

Whether familial or sporadic in manifestation, remaining neurones of the PD brain commonly contain characteristic, cytoplasmic inclusions termed Lewy bodies. An exception is autosomal recessive juvenile onset Parkinsonism (Kitada *et al.,* 1998). PD can be placed within a spectrum of neurodegenerative disorders whose pathology exhibits similar inclusions, including, dementia with Lewy bodies/diffuse Lewy body disease and Alzheimer's disease (Schmidt *et al.,* 1991; Rampello *et al.,* 2004). Of significance is that Lewy bodies have been found in elderly patients not diagnosed with PD, suggesting that their formation may precede clinical symptoms (Del Tredici *et al.,* 2002). The formation, structure and role of the Lewy body are discussed in detail in section 1.8.
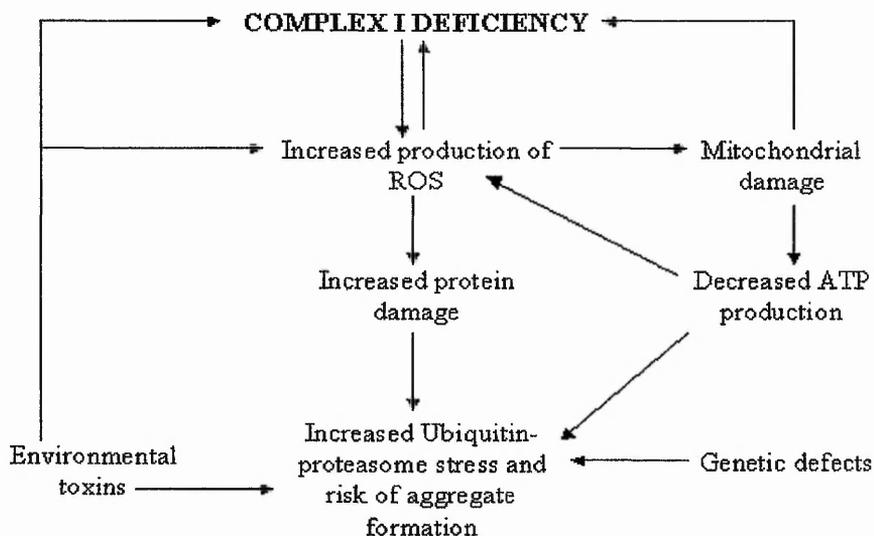
Figure 1.1 Overview of the currently considered pathogenic mechanisms in PD. (Taken from Schapira, 2004 with modifications).

1.2 MPTP - a model for Parkinson's disease

1.2.1 Identification of MPTP as a Parkinsonian neurotoxin

Several experimental neurotoxins are used in PD models, including 6-hydroxydopamine, DA and MPTP (1-methyl-4-phenyl-1,2,3,6 tetrahydropyridine) (reviewed by Blum *et al.*, 2001). MPTP is the most established model for PD but recently a model using the pesticide, rotenone, has emerged (Betarbet *et al.*, 2000; Cassarino *et al.*, 1999) and significantly, both MPTP and rotenone are inhibitors of complex I of the mitochondrial electron transport chain (discussed in section 1.3.1). MPTP is a potent, lipid soluble, six member cyclic tertiary allyamine and thermal degradation product of a meperidine-type narcotic analgesic 1-methyl-4-phenyl-4-propionoxypiperidine (Ziering *et al.*, 1947). MPTP was first described to induce a human Parkinsonian state in 1979, after it was injected as a narcotic analgesic (Davis *et al.*, 1979). It was later reported in a group of drug addicts in California who were intravenously injecting a "synthetic heroin" in which MPTP was identified as a synthetic by-product (Langston *et al.*, 1983). The pathological, biochemical and symptomatic state induced by MPTP bears some striking similarities to idiopathic Parkinsonism but with acute onset (Davis *et al.*, 1979; Langston *et al.*, 1983; Burns *et al.*, 1983). Patients responded to first line treatment for the alleviation of PD, hence indicating a similar pharmacological response (Langston *et al.*, 1983). The compound was reported to selectively destroy dopaminergic neurones of the pars compacta of the substantia nigra in man (Langston *et al.*, 1983), non-human primates (Burns *et al.*, 1983) and mice (Heikkila *et al.*, 1984).

1.2.2 Bio-activation of MPTP

It was subsequently determined that MPTP requires bio-activation to an active metabolite 1-methyl-4-phenylpyridinium ion (MPP$^+$), via a four-electron oxidation process (Chiba *et al.*, 1984; Markey *et al.*, 1984; Langston *et al.*, 1984). *In-vivo* this process is localised to glial cells which take up MPTP in a non-specific manner and accommodate its oxidative metabolism predominantly via monoamine oxidase B (MAO B), but to some extent by MAO A, to an intermediate compound 1-methyl-4-phenyl-2,3 dihydropyridinium (MPDP$^+$) via a two-electron oxidation process

(Heikkila *et al.,* 1985; Chiba *et al.,* 1985; Castagnoli *et al.,* 1985). MPDP$^+$ auto-oxidises to MPP$^+$ (D'Amato *et al.,* 1986), which on escape from glial cells, (either through diffusion or by damaging the glial cells), undergoes active, selective uptake into pre-synaptic striatal dopaminergic neurones via the DA uptake system and noradrenergic nerve terminals (Javitch *et al.,* 1985; Tipton and Singer, 1993). The bio-activation of MPTP is detailed in Figure 1.2. Interestingly MPTP and MPDP$^+$ are mechanism-based inhibitors as well as substrates for MAO A and MAO B, hence termed "suicide substrates". The extent of MPTP oxidation is therefore dependent on the level of MAO B present (reviewed by Tipton and Singer, 1993), whilst MPTP, MPDP$^+$ and MPP$^+$ are competitive inhibitors of the enzymes (reviewed by Ramsey and Singer, 1986). MPP$^+$ undergoes energy dependent concentration within the mitochondria in dopaminergic neurones, driven by the mitochondrial membrane potential (Ramsay & Singer, 1986) and binds with high affinity to neuromelanin. Neuromelanin is present in high concentrations in the substantia nigra of primates, functioning to further concentrate MPP$^+$ in dopaminergic neurones in this region, accounting for the selective neurotoxic action of MPP$^+$ (D'Amato *et al.,* 1986; D'Amato *et al.,* 1987).
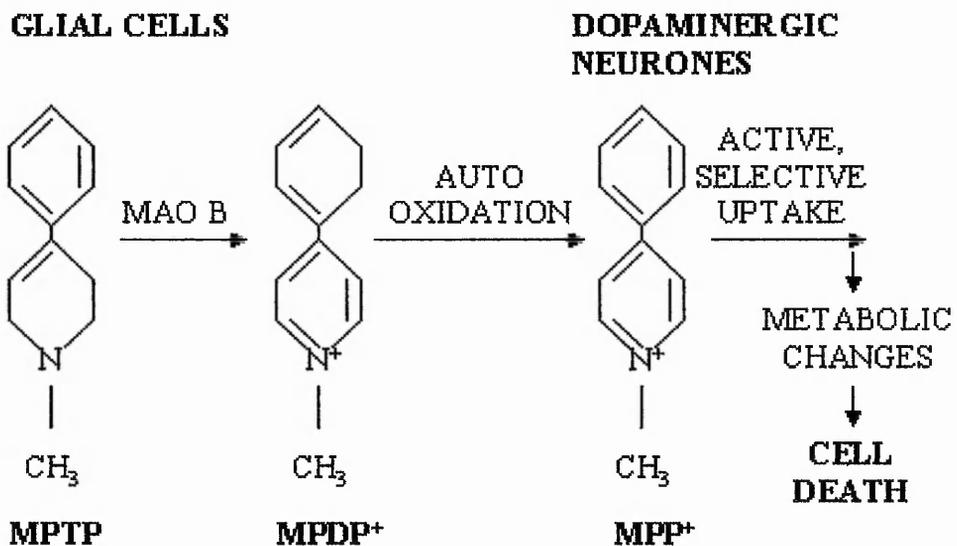
Figure 1.2 Mechanism of MPTP bio-activation to MPP$^+$ (Javitch *et al.,* (1985) with modifications).

1.2.3   Models of MPTP toxicity

The MPTP Parkinsonian model has instigated a wealth of research that has significantly enhanced the current understanding of the pathology and pathogenesis of PD. Many models exist for investigation of MPTP including whole animal study and primary/continuous cell culture systems. The non-human primate MPTP model using squirrel monkeys (Forno *et al.,* 1988, 1993) is considered the gold standard for investigation of the motor deficit in PD and shares many similarities with the disease including selective dopaminergic destruction and complex I deficiency (Meredith *et al.,* 2002, 2004 and references therein). This model provided important early information regarding symptomatic and biochemical deficits associated with MPTP toxicity and as such, has been extensively used to evaluate neuroprotective/ neurorestorative agents and surgical techniques (Jenner, 2003). The recent development of a chronic mouse MPTP model in which granular and filamentous inclusions showing a likeness to Lewy bodies were observed 6 months after MPTP treatment, offers an exciting possibility that disease pathology may be further replicated *in-vivo* (Petroske *et al.,* 2001; Meredith *et al.,* 2002).

1.2.4   Differences in species sensitivity to MPTP toxicity

Regardless of whether an *in-vivo* or cell culture system is employed, species origin is a significant consideration. A difference in species sensitivity to MPTP and MPP$^+$ has been observed and also the observation that aged animals exhibit greater sensitivity to the toxin (reviewed by Tipton and Singer 1993; Gupta *et al.,* 1986). It has been noted that rodents are less sensitive to MPTP. However certain strains of mice i.e. C57BL/6 are sensitive to the toxin (Petroske *et al.,* 2001). For example, rhesus monkeys retained MPP$^+$ within the brain for over 20 days whilst in mice, MPTP and MPP$^+$ were only present at low concentrations and for no longer than 2 h after administration (Markey *et al.,* 1984). Pifl *et al,* (1993) propose several reasons for species differences in sensitivity to the toxin including; MAO predominance and binding affinity, differences in MAO B binding sites and MAO B activity, differences in binding of MPP$^+$ to neuromelanin within dopaminergic neurones and differences in the cellular uptake mechanism of the neurotoxin between species. Sensitivity to the effects of MPP$^+$ can be proposed to be dependent on the level of

expression of the DA transporter (which can differ in density within DA neurones in different brain regions), the ability of cells to produce ATP anaerobically if oxidative phosphorylation were inhibited, and indeed the sensitivity of cells to oxidative stress (Pifl *et al.*, 1993).

1.3 Mechanisms of MPP$^+$ induced toxicity

1.3.1 Inhibition of complex I of the mitochondrial electron transport chain

The exact mechanisms by which MPP$^+$ induces death of dopaminergic neurones of the substantia nigra and cell culture models remain unresolved. However it is accepted that MPP$^+$ inhibits mitochondrial complex I of the electron transport chain, thus inhibiting oxidation of NAD$^+$ linked substrates (Nicklas *et al.*, 1985; Ramsay *et al.*, 1986), and subsequently reduces cellular ATP levels (Chan *et al.*, 1991). MPP$^+$ is also reported to cause loss of mitochondrial membrane potential, altered calcium homeostasis (see section 1.3.3) and free radical formation (see section 1.3.2) (reviewed by Blum *et al.*, 2001). Using mouse fibroblast cells cloned with the human or rat DA transporter, Pifl *et al.*, (1993) hypothesised that a subsequent increase in anaerobic glycolysis is observed as the cell attempts to compensate for MPP$^+$ induced inhibition of complex I, since the pH of the culture medium became acidic suggesting the presence of lactate. Hence cell survival following MPTP exposure may in part be dependant on ability to produce ATP via glycolysis, and the contribution of mitochondrial oxidation and glycolysis to the energy requirements of the cell. The chain of events by which MPP$^+$ causes inhibition of mitochondrial respiration is reviewed by Tipton & Singer, (1993). MPP$^+$ accumulates inside the mitochondrial matrix via the electrochemical potential of the membrane. MPP$^+$ then enters a hydrophobic binding region, inhibiting chain progression that would lead to oxidative phosphorylation and ATP production, namely cessation of electron transport from NADH dehydrogenase. Indeed, Ramsey *et al*, (1987) identified that in interacting with NADH dehydrogenase, MPP$^+$ prevents electron transfer from the Fe-S cluster of highest potential in complex I to coenzyme Q.

1.3.2   Oxidative stress

1.3.2.1   Anti-oxidant defence systems in the brain

Reactive oxygen species (ROS) are generated during oxidation-reduction (redox) reactions, resulting in oxidative stress. In the brain, ROS are formed extracellularly and intracellularly in response to internal and external toxins and as a consequence of normal cell metabolism including; normal O_2 intake and aerobic respiration, DA metabolism, oxidative metabolism of some substrates, infection, Ca^{2+} mediated activation of glutamate receptors and degeneration of fatty acids (reviewed by Prasad *et al.,* 1999). Cells therefore require an anti-oxidant defence system, which is achieved both through dietary obtained anti-oxidants and endogenous anti-oxidant enzymes (AOEs). Figure 1.3 details the generation of principal ROS, and their associated AOEs, which include superoxide dismutase (SOD), catalase, glutathione reductase (GRD) and glutathione peroxidases (GSH Px). When the production of ROS exceeds the available anti-oxidant defence systems, or there is a reduction in anti-oxidant defence systems, cellular damage can occur (Prasad *et al.,* 1999). The level of AOEs is comparatively low in the brain and is found to reduce with aging. In turn oxidative stress is implicated in a number of neurodegenerative diseases including PD, where the substantia nigra is considered particularly prone to attack due to DA deamination/auto-oxidation processes, a high concentration of unsaturated fatty acids, mitochondrial dysfunction, increased levels of free iron and reduced anti-oxidant defence (reviewed by a Cassarino *et al.,* 1999; Presad *et al.,* 1999; Eberhardt and Schulz, 2003).
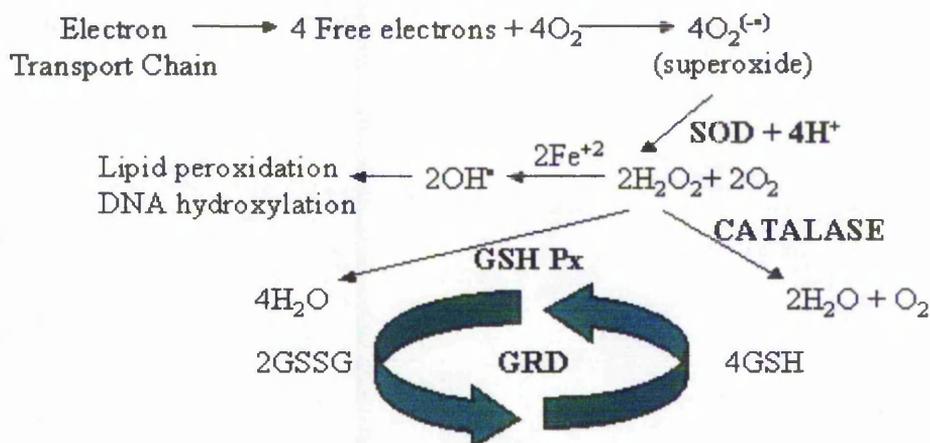
Fig 1.3 Reactive oxygen species produced by the mitochondria and associated anti-oxidant defence systems (taken from Cassarino and Bennett Jr, 1999; Prasad *et al.*, 1999).
Normal aerobic respiration produces ROS, a percentage of which is due to leakage of partially reduced O_2 within the electron transport chain. Leakage of electrons onto molecular O_2 produces the superoxide anion ($O_2^{-\bullet}$). SOD can react with $O_2^{-\bullet}$ to form H_2O_2 and O_2. H_2O_2 is in turn detoxified by catalase to produce H_2O and O_2. Iron can react with H_2O_2 to give the highly reactive hydroxyl radical ($OH^\bullet$). GSH Px detoxifies H_2O_2 produced from $O_2^{-\bullet}$ by oxidising glutathione (GSH) which also acts as an AOE, whilst GRD reduces oxidised GSH, (GSSH) back to GSH. Disruption to the mitochondrial electron transport chain therefore impairs ATP production but also increases ROS.

1.3.2.2   The oxidative stress hypothesis for MPTP toxicity

Oxidative stress was initially proposed to contribute to MPP^+ neurotoxicity by Johannesson *et al.*, (1985), who implicated MPP^+ involvement in redox reactions via formation of partially reduced free radical species. Subsequently Lai *et al.*, (1993) concluded that reactive oxygen species generation may play a role in MPTP and MPP^+ toxicity, damaging critical bio-molecules (lipid peroxidation, protein peroxidation and DNA damage) via one or both of the following mechanisms:

(a) $MPDP^+$ auto-oxidation may produce $O_2^{-\bullet}$ radicals from molecular O_2 culminating in the production of the $OH^\bullet$ radical (Zang and Mistra, 1992). (b) Leakage of

reducing equivalents onto molecular oxygen due to mitochondrial disruption may cause $O_2^{\bullet -}$ generation.

Importantly, MPP^+ and $MPDP^+$ can also increase DA release resulting in increased $OH^{\bullet}$ generation from elevated DA oxidation processes (Vidaluc, 1996). Involvement of oxidative stress in MPTP neurotoxicity is supported by the protection afforded by anti-oxidative agents (Lai *et al.,* 1993; Gonzalez-Polo *et al.,* 2004), whilst depletion of glutathione, a naturally occurring anti-oxidant, was found to potentiate MPTP and MPP^+ toxicity in dopaminergic neurones *in-vivo* (Wullner *et al.,* 1996). Additionally, Cassarino *et al,* (1997) demonstrate *in-vivo* and in cell culture systems using SH-SY5Y cells that MPP^+ induced elevation of ROS and elevated activity of AOEs, in particular SOD and catalase. The same group demonstrated that ROS and AOE activity was similarly elevated in PD cybrids (SH-SY5Y cells containing mitochondrial DNA from the platelets of PD patients), but this elevation was not altered by further addition of MPP^+. The authors note that since the only difference between control and PD cybrids was the mitochondria and mitochondrial DNA, results suggest that elevated ROS and AOE activity were due to the PD mitochondrial complex I defect. Thus the general consensus is that oxidative stress plays a role in MPP^+ toxicity. That said, it has been suggested that MPP^+ does not induce oxidative stress directly but rather it increases the vulnerability of cells to oxidative stress (Lee *et al.,* 2000). Additionally, Nakamura *et al,* (2000), determined that MPP^+, employed at a concentration that was selectively toxic to primary dopaminergic neurones did not selectively increase SOD activity in dopaminergic neurones and had no effect on glutathione levels. However, contrary to these findings, MPP^+ has been shown in my laboratory to reduce glutathione levels in mitotic SH-SY5Y cells (Begoña Caneda-Ferron, unpublished observations).

A key consideration is that ROS can activate intracellular signalling cascades; they can mediate protein phosphorylation and increase intracellular Ca^{2+}, thus inducing signal transduction (Suzuki *et al.,* 1997; Kamata and Hirata, 1999). Such signalling pathways include the mitogen activated protein kinase (MAPK) cascades, sub-families of which include the c-Jun N-terminal kinase/stress activated protein kinase

(JNK/SAPK) cascade and the p38 MAPK cascade, and also the NF - κB cascade (see section 1.5).

1.3.2.3   The role of Nitric oxide in MPTP toxicity

In addition to ROS, reactive nitrogen species (RNS) can mediate cellular damage. Nitric oxide ($NO^{\bullet}$) is synthesised from L-arginine and O_2 by sub-types (neuronal, inducible and endothelial), of nitric oxide synthase (NOS) enzymes. $NO^{\bullet}$ is an important intracellular messenger, controlling for example, neurotransmitter release from synaptic vesicles, smooth muscle relaxation, blood flow, inflammation and immune responses (reviewed by Suzuki *et al.,* 1997; Leist and Nicotera, 1998; Eberhardt and Schulz, 2003). $NO^{\bullet}$ evokes these effects in part through its ability to mediate partially reversible covalent modifications of proteins i.e. S-nitrosylation (Leist and Nicotera, 1998). At elevated levels $NO^{\bullet}$ can become toxic. On reaction with the superoxide anion ($O_2^{-\bullet}$), $NO^{\bullet}$ can generate peroxynitrite ($ONOO^-$), a powerful oxidant, which induces DNA/mitochondrial damage and irreversible protein modification via nitration/hydroxylation of protein tyrosine residues and oxidation of thiols. The $ONOO^-$ radical is unstable and rapidly decomposes to $OH^{\bullet}$ and $NO_2^{\bullet}$ (Prasad *et al.,* 1999). NOS activation and subsequent $ONOO^-$ formation has been implicated in MPTP mediated toxicity (Przedborski *et al.,* 1996; Halasz *et al.,* 2004). The role for $NO^{\bullet}$ is potentiated by studies that show NOS inhibition to attenuate MPTP toxicity. Indeed, Kurosaki *et al,* (2002) and Wanatabe *et al,* (2004), reported that neuronal NOS inhibitor, 7-nitroindazole, conferred protection against MPTP induced loss of striatal DA and DA metabolite, 3,4-dihydroxyphenyl acetic acid (DOPAC). However studies have suggested that 7-nitroindazole does not specifically inhibit NOS and may also inhibit MAO B (Lee *et al.,* 2000 and references therein). In both *in-vivo* and cell culture studies by Kurosaki *et al,* (2002) and Lee *et al,* (2000), the non specific NOS inhibitor, L-NAME, had no beneficial effect on MPTP/MPP^+ toxicity. However, a role for inducible NOS has also been implicated in MPTP toxicity.

1.3.3 Calcium homeostasis

MPTP/MPP$^+$ can have additional effects on calcium homeostasis since inhibition of complex I of the electron transport chain and subsequent ATP depletion can impair the plasma membrane Ca^{2+}-ATPase, which actively extrudes Ca^{2+} from the cell, resulting in increased free cytosolic Ca^{2+} concentrations (Kass *et al.,* 1988; Urani *et al.,* 1994; Chen *et al.,* 1995). In isolated hepatocytes MPP$^+$ has been shown to increase free cytosolic calcium and cause ATP depletion without affecting the plasma membrane Ca^{2+}-ATPase by initiating the release of mitochondrial Ca^{2+} (Kass *et al.,* 1988), possibly via the mitochondrial transition pore (MTP). The mitochondrial transition pore (MTP) is a non-selective, high conductance pore, spanning the inner and outer mitochondrial membranes. The MTP allows the passage of solutes between the mitochondrial matrix and the cytoplasm and can induce a permeability transition (PT, Cassarino and Bennett, 1999). In conjunction with inhibition of complex I, Cassarino *et al.,* (1999) report the ability of MPP$^+$, via an oxidative mechanism, to open brain MTPs inducing a PT and subsequent release of Ca^{2+} and also cytochrome c (oxidation of which is coupled to the reduction of O$_2$ to H$_2$O at complex IV of the electron transport chain), a signal that can induce an apoptotic cell death programme through activation of caspases (Orrenius *et al.,* 2003). Therefore the result of impaired calcium homeostasis can include disturbance of the cytoskeleton and initiation of Ca^{2+} induced cytotoxic processes including activation of kinases, proteases, endonucleases and NOS, that contribute to cell death (Leist and Nicotera, 1998; Blum *et al.,* 2001). Indeed, Mandelkow *et al,* (1991) demonstrate that Ca^{2+} induces microtubules to disassemble *in-vitro* (see section 1.4.2). Of significance is that Ca^{2+} is required for tissue transglutaminase (tTG) activity, an enzyme which catalyses the post-translational modification of proteins (refer to section 1.6). Additionally, increased intracellular Ca^{2+} can activate calpains (cysteine proteases). Calpains, whose activity is regulated by an endogenous inhibitor, calpastatin, do not exhibit cleavage specificity. As such calpain activity can promote cell survival or cell death (reviewed by Orrenius *et al.,* 2003). Ray *et al,* (2000) report up-regulation of calpains at the mRNA and protein levels following MPTP induced spinal cord degeneration in mice whilst Crocker *et al,* (2003) showed that calpain inhibition attenuated neuronal and behavioural deficits in MPTP treated mice.

1.3.4 Excitotoxicity

By depletion of ATP via inhibition of mitochondrial respiration, MPP^+ renders neurones more susceptible to excitotoxic attack, although the exact role of MPP^+ remains unresolved (reviewed by Eberhardt and Schulz, 2003). Excitotoxicity refers to hyper-stimulation of glutamate receptor sub-types i.e. the N-methyl-D aspartate (NMDA) receptor by excitatory amino acids such as glutamate. These receptors act as ligand-gated Ca^{2+} channels. Following activation they promote a sustained increase in intracellular Ca^{2+} levels and the synthesis of NOS, which can induce cell death as detailed in section 1.3.3 (Leist & Nicotera, 1998).

The major proposed mechanisms for MPTP toxicity are summarised in Figure 1.4
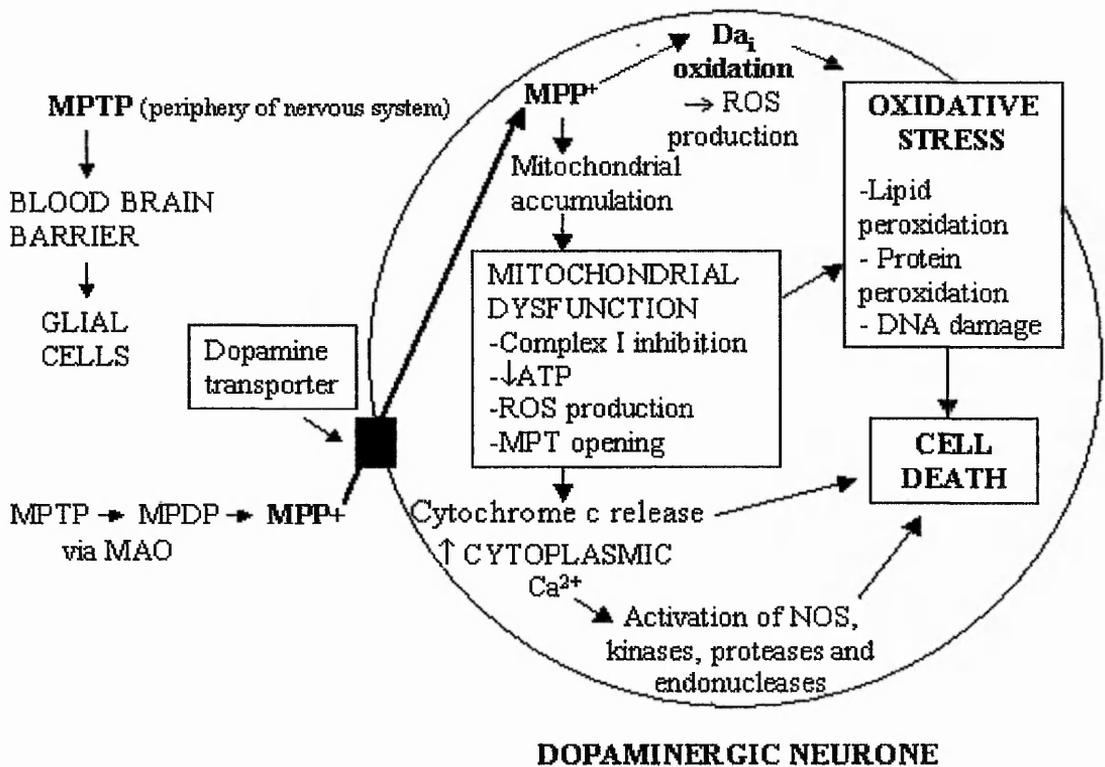
Figure 1.4 Overview of proposed mechanisms of MPTP toxicity *in-vivo* (Taken from Blum et al., (2001) with modifications).

In-vivo MPTP undergoes bio-activation within glial cells to its active metabolite, MPP^+ via MAO oxidation processes. MPP^+ undergoes selective uptake into dopaminergic neurones on the DA transporter and is concentrated within the mitochondria. MPP^+ inhibits complex I of the electron transport chain causing reduced ATP production, and ROS formation, which can result in opening of the MTP with subsequent release of Ca^{2+} and cytochrome c, to activate death processes. Disrupted ATP synthesis inhibits the ATP-requiring plasma membrane Ca^{2+}-ATPase thus disrupting Ca^{2+} extrusion from the cell and may induce hyper-stimulation of glutamate receptors, which can act as Ca^{2+} channels. Disturbed Ca^{2+} homeostasis can activate NOS with resultant $NO^{\bullet}$ and RNS production, and can also disrupt the cytoskeleton. MPP^+ also produces ROS/oxidative stress through both DA oxidation and inhibition of the electron transport chain.

14

1.4 The neuronal cytoskeleton

The neuronal cytoskeleton is a dynamic structure that extends throughout the cytoplasm, incorporating three cytoskeletal complexes; microtubules (MTs), intermediate filaments and microfilaments (MFs), formed from tubulin, neurofilament (NF) and actin proteins respectively. Collectively, these complexes are responsible for spatial organisation, communication, transport systems, cell shape and mechanical stability of the cell. Whilst these components differ in properties and spatial arrangement, it is their complex interaction that promotes cytoskeletal functions (Alberts *et al.*, 1994; Siegel, 1999). Post-translational modifications of neuronal cytoskeletal elements are normal cellular processes independently regulated by the cell that can act to increase the functional repertoire and specialism of that particular element within the cell (Laurent & Fleury, 1993). Disruption to the cytoskeleton, particularly, the NF and MT systems is extensively documented in neurotoxicity and neurodegenerative diseases including PD, Alzheimer's disease, Huntington's disease and Amyotrophic lateral sclerosis. As such considerable current research aims to understand the nature of interactions between cytoskeletal systems and indeed how they are damaged during disease processes, which often culminates in aberrant protein aggregation.

1.4.1 Microfilaments

The globular, monomeric subunits of MFs are actin proteins (G-actin). Polymerisation of G-actin follows ATP binding to monomers. In turn, two actin polymers form a two-stranded helical MF (F-actin) with a diameter of 5-9 nm (Carlier, 1991). MFs are dynamic, polar structures – assembly and disassembly occurs preferentially at the plus end of the filament. Whilst polymerisation requires ATP binding, it does not require ATP hydrolysis. However, ATP is hydrolysed soon after polymerisation, the resultant ADP is trapped within the filament. Nucleotide hydrolysis acts to destabilise interactions between actin subunits and therefore promotes de-polymerisation events (Carlier, 1991; Alberts *et al.*, 1994).

MFs are abundantly found within growing nerve processes; the major role of MFs in neuronal cells is to maintain cell shape (Shepherd, 1994). MFs are flexible and can

form linear bundles, two-dimensional networks and three-dimensional gels (Alberts *et al.,* 1994). MFs, in conjunction with myosin, play a major role in muscle contraction. However, in non-muscle cells, actin does provide a loose contractile network. MFs are predominantly located beneath the plasma membrane, forming the 'cell cortex'. Additionally MFs contribute to, and can independently maintain, cell polarity, and co-ordinate cell movement through dynamic cell surface extensions such as pseudopodia, lamellipodia and in the growth cone of developing axon, filopodia (Alberts *et al.,* 1994). The MF network is supported structurally and functionally by actin binding proteins and other accessory proteins, and is responsive to cell surface signals through interaction with heterotrimeric G proteins and GTPases (Alberts *et al.,* 1994, Mathews and Van Holde, 1996).

1.4.2 *Microtubules*

MTs are an integral part of the cytoskeleton of all cells and as such coordinate diverse cellular functions such as organelle motility/vesicle transport, chromosome segregation during mitosis, cell movement and cell stability (reviewed by Alberts *et al.,* 1994; Downing and Nogales, 1998). In neuronal cells, MTs, in conjunction with microtubule associated proteins (MAPs), play a major role in neurite outgrowth and axon stabilisation (Shea and Beermann, 1994; Nixon, 1998) and intracellular transport (Shea and Flanagan, 2001) (discussed in detail in section 1.4.4).

1.4.2.1 *Structure and assembly*

MTs are formed from α and β-tubulin proteins, of which a number of isotypes exist (reviewed by Downing and Nogales, 1998). α and β-tubulin sub-units form dimers (termed the tubulin molecule). The tubulin molecule binds GTP, which permits polymerisation in a process termed nucleation. The tubulin polymer is termed a 'protofilament' and comprises alternate α and β-tubulin sub-units. Protofilaments (usually 13) align and assemble into a helical, cylindrical polymer, the MT (see Figure 1.5). MTs exhibit polarity and undergo continual polymerisation/depolymerisation events as detailed in section 1.4.2.2. Elongation of a MT occurs predominantly at the plus ('fast growing') end. Rate of polymerisation

is proportional to the concentration of free tubulin; therefore elongation continues until growth and dissociation events reach equilibrium (steady state) (reviewed in Alberts *et al.,* 1996). MT (but not MT sub-units) can be post-translationally modified, i.e via glutamylation, detyrosination or acetylation and phosphorylation. The role of these modifications with respect to stabilisation of the MT remains controversial. Palazzo *et al,* (2003) review that whilst detyrosinated tubulin accumulates in stable MTs, it does not cause stabilisation. This study also questions previous literature, which suggests that decreasing tubulin acetylation reduces MT stability. Instead Palazzo *et al,* (2003) propose that MTs are stabilised and then accumulate acetylated tubulin. This is particularly important for neuronal cells where MTs provide a major transport system for trafficking proteins and organelles (see section 1.4.4). The stability and interaction of MTs with other cell components is highly dependent upon microtubule-associated proteins (MAPs) of which two major classes exist; high molecular weight proteins, and tau proteins, which in neuronal cells exhibit a particular regional distribution. NB2a/d1 cells induced to differentiate with dbcAMP were shown to require tau for initial neurite outgrowth whilst MAP1B were required at the later stages of neurite outgrowth and stabilisation (Shea and Beermann, 1994 and references therein).

Microtubule structure
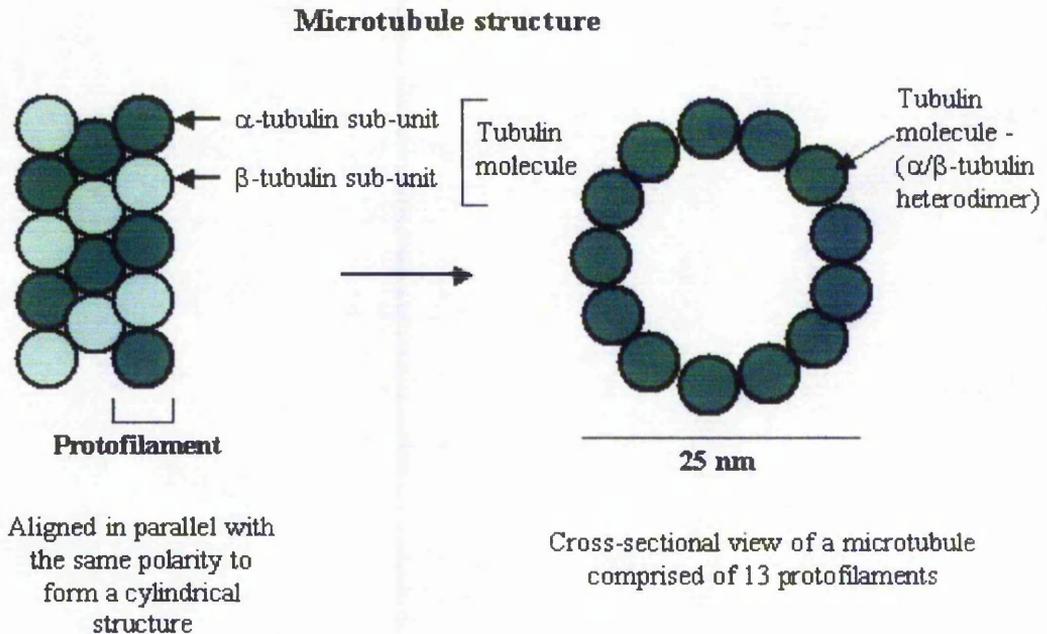
Figure 1.5 Microtubule structure
α/β tubulin heterodimers bind GTP and polymerise to form protofilaments. Protofilaments (generally 13) then assemble into a helical, cylindrical comformation to form the MT. Current literature suggests that the plus end of the MT is crowned by β-tubulin subunits (see Downing and Nogales, 1998).

1.4.2.2 Dynamic instability of microtubules

The MT plus end polymerises and de-polymerises continually, and as such appears to grow and shrink both *in-vitro* and *in-vivo* (Tanaka *et al.*, 1991). This process, termed 'dynamic instability', was initially described by Mitchison and Kirschner, (1984) and is important so that MTs can correctly position themselves and spatially organise the cytoplasm. In brief, the process requires a shift in energy that is provided by hydrolysis of tubulin-bound GTP nucleotides. Similarly to MF polymerisation, GTP binding to tubulin molecules, but not hydrolysis, is required for polymerisation. Delayed hydrolysis of β-tubulin-bound GTP yields GDP, which is maintained within the polymer and acts to weaken the interactions between sub-units. Whilst polymerisation rate is high, tubulin molecules are added to the polymer quicker than bound GTP can be hydrolysed. The bound GTP 'caps' the end of the protofilament, acting to stabilise the MT in linear conformation (Mandelkow *et al.*, 1991). When the tubulin polymerisation rate is decreased, the GTP cap is hydrolysed and the

protofilaments begin to disassemble. Additionally, a third structural state was hypothesised by Tran *et al,* (1997), on the basis of findings that severed plus and particularly minus ends of MTs did not always disassociate, but could indeed be stable or resume elongation.

1.4.3   Neurofilaments

1.4.3.1   Neurofilament structure

Intermediate filaments are non-polarised, fibrous, highly elongated molecules approximately 10 nm in diameter. They share an amino-terminal head domain and a carboxyl-terminal tail domain, and are classified into five types. They display a highly conserved central α-helical domain of 310 amino acids, containing heptad repeats which permit parallel α-helices to form coiled-coil dimers (Xu *et al.,* 1996) (See Fig 1.6). NFs are unique, neurone specific intermediate filaments. As obligate heteropolymers, each NF triplet comprises three type IV proteins, NF-heavy (NF-H), NF-medium (NF-M) and NF-light (NF-L) with approximate molecular masses of 115 kDa, 95 kDa and 68 kDa respectively. However due to hyperphosphorylation of the NF-H and NF-M carboxyl terminal tail domains, which are also rich in glutamic acid residues and repetitive sequences regions, NF-H, NF-M and NF-L are detected at molecular masses of approximately 200 kDa, 140-160 kDa and 70 kDa respectively, when separated by sodium-dodecylsulphate polyacrylamide gel electrophoresis. The length of the carboxyl-terminal domain differs between NF sub-units and is accountable for the difference in mass (Lee *et al.,* 1988).

1.4.3.2   Neurofilament expression in axon development and stability

Axons are enriched with NFs. NFs contribute to morphology and provide strength and stability to the axonal cytoskeletal network by promoting radial growth (Nixon, 1998). The relative proportion of NF sub-units undergoes changes during neuronal development. During embryonic neurogenesis NF-L and NF-M are co-expressed, whilst NF-H expression occurs later in development (Nixon and Sihag, 1991; Nakagawa *et al.,* 1995; Julien, 1999). Considerable research has focussed on the role of individual NF sub-units in axonal development and stability.   In order to

19

determine the contribution of each sub-unit to radial axonal growth, Xu *et al,* (1996) used transgenic mice with altered sub-unit complement. Results showed that over-expression of any one sub-unit inhibited radial growth. To promote further radial axon growth, NF-L was critically required in combination with NF-H or NF-M. Additionally, studies have shown that NF-M and NF-H sub-units were unable to assemble into filaments in NF-L knock-out mice. Importantly, NF-M knock-outs were more detrimental to radial axonal growth than NF-H knock outs (reviewed by Julien, 1999).

Whilst NF-L is considered integral to NF assembly, NF-H and NF-M are highly interactive components (Julien, 1999). The carboxyl tail domains of NF-H and NF-M extend as side arms and mediate a 50-55 nm spaced cross-linkage between NF triplets and other cytoplasmic components including MTs and membrane bound organelles (Miyasaka *et al.,* 1993; Leterrier *et al.,* 1996), thus promoting NFs to 'bundle' in parallel arrays. Indeed Nakagawa *et al,* (1995) report that the carboxyl tail domain of NF-M is structurally involved in both cross-bridge formation and promoting elongation of NFs. NFs may also bind to actin filaments, an important consideration since this would collectively associate MFs, NFs and MTs with the cell membrane (Leterrier *et al.,* 1996). Using the delivery of specific anti-cytoskeletal protein antibodies into permeablised NB2a/d1 cells during dbcAMP mediated neurite outgrowth, Shea and Beermann, (1994) demonstrated that the later stages of neurite outgrowth and axon stability were sensitive to anti- NF antiserum, due to disruption of interactions between NFs and MTs that ensued.

Post-translation modification of NFs via phosphorylation of the carboxyl tail domain is associated with axonal development and maturation (reviewed by Shea *et al.,* 2003). Indeed phosphorylation events (detailed in chapter III, section 3.1.3) slow the rate of NF transport within the axon, likely increasing axonal calibre (Marzalek *et al.,* 1996; Ackerley *et al.,* 2003). Indeed Shea *et al,* (2003) demonstrate an inverse relationship between NF phosphorylation and transport. Axonal transport of cytoskeletal proteins is detailed in section 1.4.4.

Extensive research has investigated the structural form of NF proteins as they translocate into, and travel along the axon (as sub-units or in polymeric form), and

also their phosphorylation status. However, findings are not straightforward and remain to be fully resolved. It is important to note that even though NFs are essentially considered to be associated with axon stabilisation, they remain dynamic in nature – evidence suggests that phosphorylation and filament polymerisation, are reversible (reviewed by Nixon, 1998; Shea *et al.,* 1997b). Early studies suggested that NF sub-units were polymerised within the cell body and transported along the axon in polymer form (Lasek *et al.,* 1984). This theory has recently been hotly disputed in favour of a sub-unit, transport model (reviewed by Terada, 2003). However, collective evidence suggests that NF sub-unit, individual NF, or non-filamentous oligomer transport systems may exist simultaneously (Shea *et al.,* 1997b; 1998, Yabe *et al.,* 1999). It is generally accepted that different populations of NFs exist within the axon; NFs exhibiting limited carboxyl terminal domain phosphorylation and NF-NF interactions, and highly phosphorylated NFs, exhibiting extensive NF-NF interaction and subsequent slow transport, were simultaneously reported in axonal neurites of NB2a/d1 cells (Yabe *et al.,* 2001). Likewise the NFs at the front of the transporting wave are rich in hypo-phosphoylated (fast moving) NFs, whilst the tail end is highly phosphorylated and subsequently slow moving (Shea and Flanagan, 2001).

The phosphorylation state of NF proteins depend upon a dynamic balance between protein kinase and phosphatase activities. Phosphatase activity is thought to be particularly important during labile stages of axon outgrowth (Grant *et al.,* 2001). Protein phosphatase 2A (PP2A) is proposed to play an important role in regulation of NF head domain phosphorylation and has also been shown to dephosphorylate tail domain KSP motifs that are phosphorylated by CDK-5 (Grant *et al.,* 2001). In dorsal root ganglion, okadaic acid treatment was shown to reduce the electrophoretic mobility of NFs, which suggested increased phosphorylation (Grant *et al.,* 2001 and references therein).
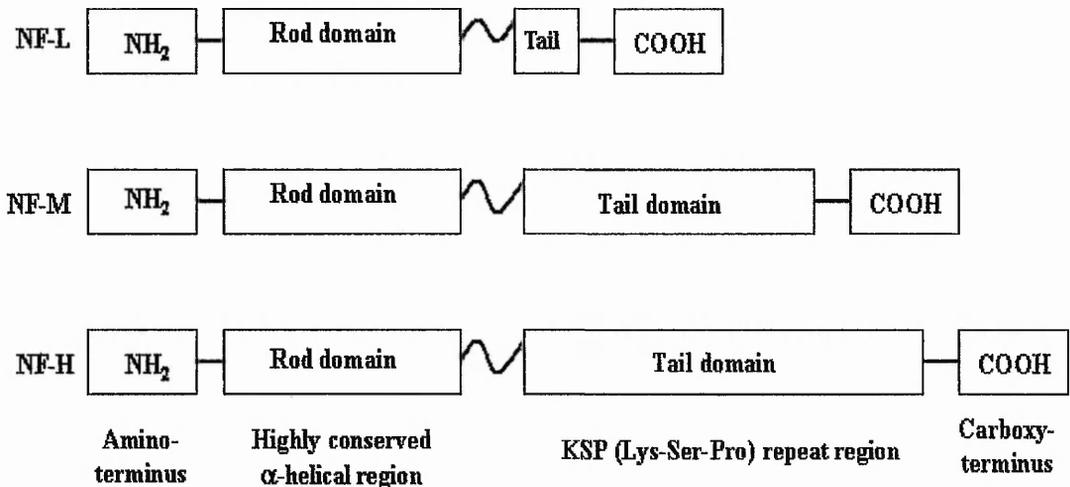
Figure 1.6 NF structure (Taken from Schmidt *et al,* (1991) with modifications).
NF-H, NF-M and NF-L exhibit an amino-terminal domain, a conserved α-helical rod domain and a carboxyl-tail domain. The length of the carboxyl-tail domain varies between the NF sub-units and permits post-translational modification of the molecule by phosphorylation, within specific KSP repeat regions.

1.4.4 Transport of cytoskeletal proteins

Protein synthesis occurs within the neuronal cell body and as such, transport systems are required to correctly distribute organelles and proteins, including cytoskeletal components within the axon. Transport is categorised as being anterograde (away from the cell body) or reterograde (towards the cell body). Historically, transport systems have been classified as slow (sub-classified as slow component a, SCa [transport rate; 0.1 – 1.0 mm/day] and SCb [transport rate; 1.0 – 3.0 mm/day]), transporting axonal cytoskeletal polymers, or fast (transport rate; 0.5 – 1.0 µm/s), transporting membranous organelles (reviewed by Nixon, 1998; Prahlad *et al.,* 2000). Transport of cellular components at either rate involves associated motor proteins that move through the axon in association with the MT network. Whilst motor proteins associated with fast transport have been identified, the slow transport motors remain more elusive (Terada, 2003). Whilst the historical concepts of fast and slow transport in terms of overall transport rate remain, growing evidence suggests that slow and fast transport may be a continuum of a single system in which proteins simply spend different lengths of time associated with their motors (reviewed by

Shea and Flanagan, 2001). In support of this theory, Roy *et al,* (2000) established that NFs move intermittently within axons, spending 20 % of their time moving and the other 80 % pausing. Other evidence suggests that NF proteins can undergo transport attached to MT-associated motor proteins such as kinesin and dyenin, which mediate fast axonal transport in anterograde and retrograde fashion, respectively (Yabe *et al.,* 1999; Prahlad *et al.,* 2000). Additionally, it has been found that tubulin heterodimers or polymers (but not MTs) are transported along the axon also in association with MT-dependent kinesin (Miller and Joshi, 1996; Funakoshi *et al.,* 1996; Terada *et al.,* 1996).

1.4.4.1 Disruption of axonal transport systems might contribute to neurodegenerative disease

Given that axonal transport is so critical for normal cellular function, disruption of the system would likely be detrimental to the cell. Many neurodegenerative diseases are characterised by aberrant inclusions that form within the cell body. Basic consideration would suggest that in order for proteins and other materials to abnormally accumulate, they must either be prevented from translocating into the axon, transported in retrograde fashion from the axon back to the cell body, or indeed prevented from undergoing normal degradation, for example through the ubiquitin-proteasome pathway (refer to section 1.7). Indeed Katsuse *et al,* (2003), graded the formation of cortical Lewy bodies on the basis of immunohistochemical analysis of α-synuclein and also investigated accumulation of axonally transported substances. Results showed that Lewy bodies contained axonal substrates, β-amyloid precursor protein (APP), chromogranin-A, synphilin-1 and synaptophysin and that accumulation of these substances increased as the Lewy body matured, suggesting that axonal transport was blocked. As previously stated, NF phosphorylation events are coupled to the slowing of NF axonal transport. Of significance is the finding that phosphorylation of NFs promotes their dissociation from kinesin motors (Yabe and Shea, 2000). Indeed, Shea *et al,* (2004a) report that Cyclin-dependent kinase-5 (CDK-5) (see section 1.5.2) induces NF phosphorylation and mediates normal NF distribution in cortical neurones, but that over-expression of the kinase induces phosphorylated NFs to accumulate within the perikarya. The authors propose that

CDK-5, via hyper-phosphorylation of NFs, might increase dissociation of NF from its motor proteins, both slowing transport and perhaps potentiating NF-NF bundling.

1.5   Intracellular kinases

1.5.1   Mitogen activated protein kinases (MAPKs)

The mitogen activated protein kinases (MAPKs) function to propagate intracellular signals in response to extracellular stimuli, from the cell membrane to downstream cytoplasmic and nuclear targets. The MAPKs encompass 3 major pathways; extracellular signal related kinase (ERK), c-jun N-terminal kinase (JNK) and p38. ERK, JNK and p38 pathways are evolutionarily conserved and exist in all eukaroyotic cells (Hagemann and Blank, 2001). They respond to a large number of stimuli controlling cell growth, differentiation, environmental adaptation and apoptosis (Grewal et al., 1999; Mielke and Herdegen, 2000; Waetzig and Herdegen, 2004). All pathways transfer signals downstream of the cell membrane in parallel hierarchical cascades through sequential phosphorylation events as detailed in Figure 1.7. Extracellular stimuli channel activating signals through transmembrane receptors that first induce activation of serine threonine kinases termed MAPK kinase kinases (MKKK). MKKK phosphorylates and activates dual specificity MAPK kinase (MKK), which phosphorylates and activates MAPK (ERK/JNK/p38), also serine threonine kinases (Hancock, 1997; Garrington and Johnson, 1999). Activated MAPKs phosphorylate diverse targets that can be cytoplasmic or nuclear and include transcription factors, protein kinases, phospholipases, membrane receptors and cytoskeletal proteins including NFs and tau (Meilke and Herdegen, 2000; Garrington and Johnson, 1999; Grewel et al., 1999; Clarke et al., 2003; Chang et al., 2003; Bogoyevitch and Court, 2004). A summary of MAPK substrates as reviewed by the fore-mentioned authors is provided in Table 1.1. For maximal MAPK activation, dual specificity MKK phosphorylates threonine and tryrosine residues in a TyrXxxThr conformation. The identity of Xxx is dependent on the MAPK pathway; glutamic acid for the ERK pathway, proline for the JNK pathway and glycine for the p38 pathway (Hagemann and Blank, 2001).

By virtue of phosphorylation of downstream kinases, the MAPK pathways amplify the signal whilst cross-talk between pathways is evident at all levels (Schaeffer and Weber, 1999) (see Figure 1.7). Numerous MKKKs, MKKs and MAPK have been identified allowing for differential activation of pathways (as reviewed by Garrington and Johnson, 1999; Hagemann and Blank, 2001). A phenomenal amount of research has investigated potential stimuli for the MAPK pathways to reveal that different pathways are activated in response to specific stimuli. It has been historically considered that the ERK pathway is "pro-survival" and activated in response to mitogenic stimuli that promote growth and differentiation whilst JNK and p38 pathways are activated in response to stressful or pro-inflammatory stimuli (Xia *et al.*, 1995; Wang *et al.*, 1998). However, this is by no means conclusive as discussed in chapter V, section 5.1. With so many signals diverging on the MAPK pathways the cell must evoke a degree of specificity. Organised sub-cellular localisation of pathway intermediates and direct substrate-enzyme interactions promote specificity. Scaffolding proteins, for example JNK interacting protein (JIP), MEK partner 1 (MP1) and MEKK1 and specific regulatory binding proteins promote binding between specific proteins and specific MAPK modules (Garrington and Johnson, 1999; Schaeffer and Weber, 1999; Hagemann and Blank, 2001). Additionally, MAPK phosphatases regulate the magnitude and duration of MAPK signals within the MAPK pathways. These phosphatases are classified by their ability to act in a tyrosine-specific, threonine-specific or dual (tyrosine/threonine)-specific manner and achieve substrate specificity via specific protein-protein interactions that are mediated by the amino-terminal domain of the phosphatase (Keyse *et al.*, 2000).
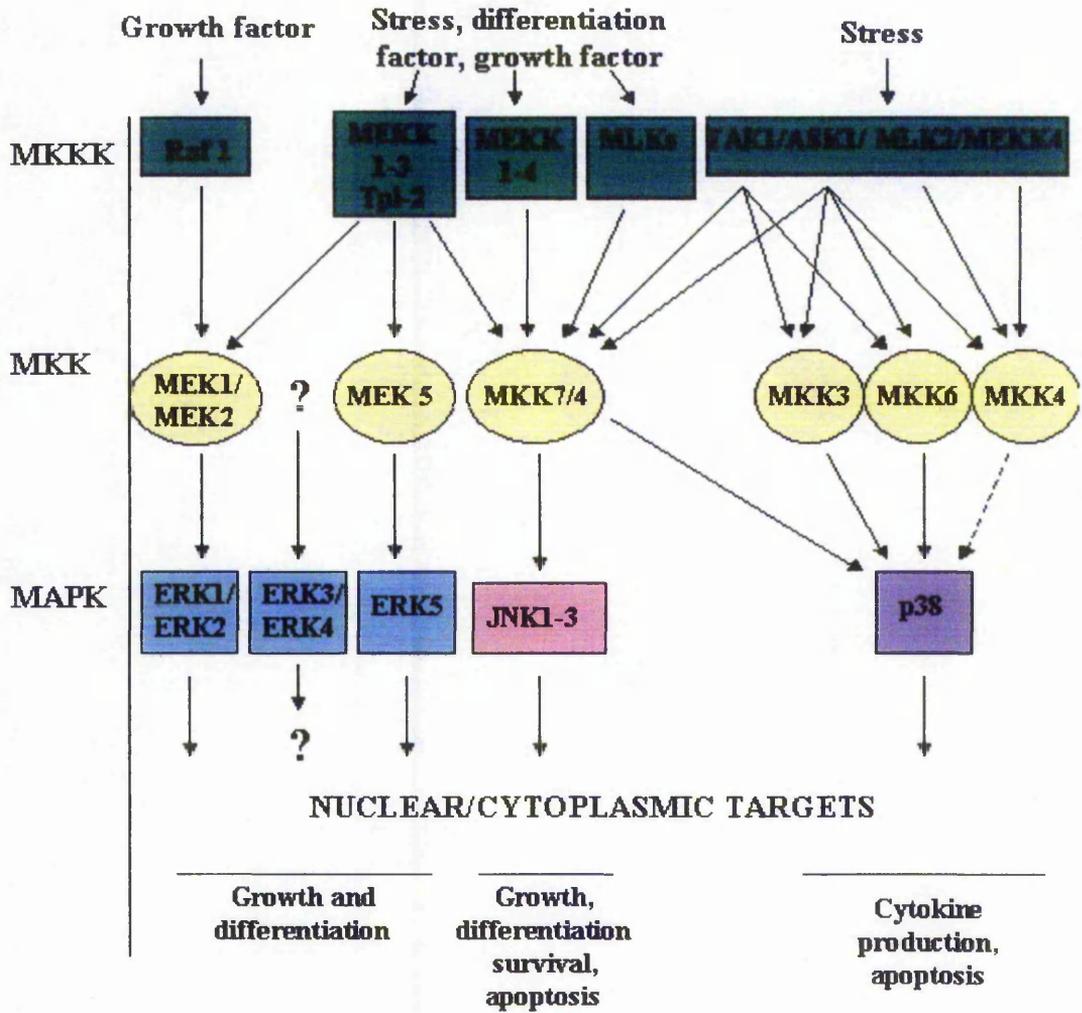
Figure 1.7 Overview of the MAPK pathways
The ERK, JNK and p38 pathways comprising of MKKK, MKK and MAPK modules. Examples at each level of the pathway are given to demonstrate the hierarchical nature of the MAPK pathways but this list is not complete. For reviews see Hagemann and Blank, (2001), Garrington and Johnson, (1999) and Bogoyevitch and Court, (2004). Note that the historically proposed pathway outcomes are shown but are not exclusive. The role of the MAPK pathways in cell survival/death is discussed is chapter V, section 5.1.   ------► represents a tentative modification.

1.5.1.1   The ERK pathway

To date 8 ERK proteins have been identified; however ERK1 and 2 (p42/p44) remain the most highly characterised (Bogoyevitch and Court, 2004). Attention is now turning to ERKs 3-8 whose cellular functions are less identified. Indeed whilst ERK 1 and 2 share 90 % homology, this homology is not extended to ERKs 3-8 which may be reflected in their differing targets. For example ERK 3 is not activated by traditional MEKs owing to a different phosphorylation motif (serine – glutamic acid – glycine rather than threonine – glutamic acid – tyrosine). Big MAPK (BMK), as ERK5 is often known, is a 98 kDa protein with an extended c-terminal domain (Bogoyevitch and Court, 2004). ERK 5 is not activated through the archetypal Ras-Raf cascade described below. Instead it is activated via MEKK 2 and MEKK 3 (MKKKs) and can play an important role in cell differentiation, in proliferation and indeed survival via phosphorylation/activation of the pro-survival transcription factor MEF2C (Sun *et al.,* 2001; Zhao *et al.,* 1999 and references therein). A detailed review of the discovery, molecular characteristics and identified cellular functions of ERKs 3-8 is given by Bogoyevitch and Court, (2004). ERK 1 and 2 can be activated via MEKKs 1-3 and are also activated by Raf via the ERK cascade. In brief, extracellular signals i.e. growth factors activate and autophosphorylate receptor tyrosine kinases at the cell membrane. Activated tyrosine kinase receptors dock an adaptor protein, Grb2, in a complex with the GTP-exchange factor, Sos (Son of sevenless), which activates a small G protein i.e. Ras or Rap. In turn Ras recruits Raf to the cell membrane, which signals to ERK via MEK (reviewed by Hagemann and Blank, 2001).

1.5.1.2   The JNK and p38 pathways

JNKs are widely expressed in mammalian cells including the brain. The JNK family is encoded by 3 genes to yield 3 isoforms; JNK1, JNK2 and JNK3 from which 10 splice variants are formed (Gupta *et al.,* 1996). Gene products range from approximately 46-57 kDa owing to the presence of an extended C –terminus on JNK 3 (Mielke and Herdegen, 2000). JNKs share 90 % homology in mammals; whilst JNK1 and JNK2 are ubiquitously expressed, JNK3 is selective to the brain, heart and testes (Mielke and Herdegen, 2000). Within the brain the expression of JNK

isoforms follows specific patterns (Mielke and Herdegen, 2000). Indeed the human neuroblastoma SH-SY5Y cell line expresses all three JNK isoforms, which reportedly respond differentially to stressful stimuli (Mielke *et al.*, 2000). This finding is mirrored by Coffey *et al,* (2002) using cerebellar neurones who show that JNK2 and 3 were selectively activated by neuronal stress induced by trophic factor withdrawal. In addition such studies highlight that JNK activation depends on the stimulus and indeed the cell system employed.

Five isoforms of p38 have been identified; p38α, p38β, p38γ, p38δ and p38-2. However only p38α and p38β are expressed in the brain (reviewed by Harper and LoGrasso, 2001).

MKKKs that regulate JNKs include mixed lineage kinases (MLK): MLK1-4, dual-leucine-zipper-bearing kinase (DLK), zipper sterile-α-motif kinase (ZAK), apoptosis-inducing kinases (ASK1, ASK2), transforming growth factor-β-activated kinase 1 (TAK1) and triplolethal 2 (TPL2) (Davis, 2000) all activate JNK (Gallo and Johnson, 2002). As shown in Figure 1.7, considerable cross-talk occurs between p38 and JNK pathways and many MKKKs including MEKKs, MLKs, TAK1 and ASK1 that regulate JNK also regulate p38. MLKs can be characterised by structural features including Src Homology (SH) domains, leucine zippers (which permit homodimerisation and subsequent autophosphorylation) (Gallo and Johnson, 2002) and small GTPase binding domains as described below (Tibbles and Woodgett, 1999). The processes by which activation of the MKKKs occurs to induce downstream activation of JNK and p38 MAPKs are less established than the Ras-Raf-MEK pathway, which activates ERK1/2. However, data suggests that MEKK1 can mediate Ras-dependant JNK activation via growth factor receptors (Pomérance *et al.,* 1998). Additionally other monomeric G proteins i.e. Rho family members, cdc42 and Rac are implicated in regulation of JNK and p38 pathways via activation of MEKK1 and 4 and also certain MLKs (reviewed by Tibbles and Woodgett, 1999; Davis, 2000; Hergmann and Blank, 2001). Under certain conditions JNK can also be activated via G-protein coupled receptors and by Fas receptor ligation. Binding of certain stimuli including inflammatory cytokines to tumour necrosis factor (TNF1) receptors are proposed to activate JNK and p38 pathways via ASK 1 and GCK

(germinal centre kinase; JNK only) proteins in a GTP-independent manner (Tibbles and Woodgett, 1999) whilst interleukin 1 (IL-1) stimulates JNK and p38 pathways by binding to IL-1 receptors; stimulation occurs via IL-1 receptor-interacting kinases (Tibbles and Woodgett 1999).

TARGET LOCATION	ERK	JNK	p38
CYTOSOLIC	Neurofilament	Neurofilament	Tau
	Myelin basic protein	Tau, MAP1B MAP2	Light chain myosin II (*in-vitro*)
	MAPs; tau, MAP2C, MAP4	Bcl-2	Mnk1/2
	Membrane associated proteins; i.e. Epidermal growth factor receptor, Phospholipase A2, synapsin I	Glucocorticoid receptor	MAPKAP2/3/5
	Cytoplasmic kinases; i.e. Rsk2, RskB, MAPKAP 2/3, MNK1/2, Msk 1	p53	
NUCLEAR	ETS family transcription factors	c-Jun	AFT2
	c-Jun	AFT2	CREB
	c-Myc	ELK1	ELK1
	c-Myb	NFAT4	MEF2C
	Stat 3/5		CHOP
	Estrogen receptor		
	lamins		

Table 1.1. Overview of neuronal targets of the MAPK pathways
A large number of MAPK targets have been identified, an overview of which are given. The distinct sub-cellular localisation of target substrates confers a degree of specificity to the MAPK modules. A major role of the MAPKs is to mediate activation or inactivation of nuclear transcription factors via phosphorylation following translocation to the nucleus, thereby directly effecting the expression of specific genes.

1.5.2   Cyclin-Dependant Kinase-5

Cyclin-dependent kinase 5 (CDK-5) is a member of the cyclin dependent kinase (CDK) family of small serine/threonine kinases, which regulate the progression of cells through the cell cycle. CDK-5 shares 58 % sequence homology with CDK-1 and 61 % homology with CDK-2 and cell division cycle kinase 2 (cdc-2) (for review see Shelton and Johnson, 2004). However CDK-5 is unique, whilst it is expressed in almost all tissues, it does not play an active role in the cell cycle. Rather CDK-5 activity is mostly confined to the CNS in post-mitotic neurones. CDK-5 is not dependent on cyclins for kinase activity but is dependant on binding of a regulatory sub-unit of which p35 and p39 are the most widely characterised. p35 and p39 confer 57 % homology and are expressed predominantly in the CNS. Therefore the activity of CDK-5 is confined to the CNS due to the specific location of its activating partners (Dhavan and Tsai, 2001). In addition to cyclin binding, CDKs require activation by phosphorylation at distinct threonine residues. Phosphorylation may play a role in mediating maximal CDK-5 activity (Sharma *et al.,* 1999a) but remains controversial at present (Shelton and Johnson, 2004).

CDK-5 activity is regulated in part through controlled degradation of p35, which has been demonstrated *in-vivo* and *in-vitro* to occur through the ubiquitin-proteasome pathway (UPP; see section 1.7.1) (Patrick *et al.,* 1998; Saito *et al.,* 1998). Indeed proteasomal inhibition stabilised p35 *in-vivo* (Patrick *et al.,* 1998). p35 is targeted for UPP-mediated degradation following phosphorylation by CDK-5. Therefore, by stimulating p35 degradation, active CDK-5 provides a negative feedback mechanism to regulate its own activity (Patrick *et al.,* 1999). Alternative kinases may also be involved in p35 phosphorylation (Kerokoski *et al.,* 2002). Under certain pathological conditions, p35 can be cleaved at the amino terminal to p25 by calpains (Patrick *et al.,* 1999; Lee *et al.,* 2000) (discussed in detail in chapter V, section 5.1.2). The p25 sub-unit can also activate CDK-5 and exhibits greater stability. If the cleaved p10 terminal is important for ubiquitination and UPP targeting, it may be attributable to the stability of p25 (Patrick *et al.,* 1998). Phosphorylation of p35 by CDK-5 has been shown to occur at distinct sites; as already discussed, phosphorylation can mediate degradation of p35 or alternatively, it can suppress the cleavage of p35 to p25 by

calpains, hypothesised to protect against p25 production in the developing brain (Saito *et al.*, 2003).

Identification of the substrate-binding site shows that CDK-5 binds substrates in a highly specific, proline directed manner (Sharma *et al.*, 1999b; Dhavan and Tsai, 2001). CDK-5 binds a plethora of substrates and exhibits many roles in brain development and disease, as reviewed by Dhavan and Tsai, (2001); Cruz and Tsai, (2004); Shelton and Johnson, (2004) and summarised in table 1.2. The role of CDK-5 in neurodegenerative disease is discussed in detail in chapter V. With respect to the role of CDK-5 in brain development, Ohshima *et al*, (1996) demonstrated that CDK-5 knockout mice suffered perinatal mortality associated with significant brain developmental defects. Knockout mice were lacking cortical laminar structure and cerebellar foliation whilst brain stem/spinal cord neurones exhibited accumulations of NFs which immunostained for phosphorylated and non-phosphorylated NF epitopes, which was suggested by the authors as implicating disrupted axonal transport. Thus CDK-5 is critical in brain development. p35 knock mice also show abnormal corticogenesis but are viable and fertile, probably due to compensatory effects of p39. p39 knockout mice do not show defects, however double p35/p39 knockout mice suffer the same developmental defects as CDK-5 knockout mice (reviewed by Dhaan and Tsai, 2001). CDK-5 is associated with neuronal differentiation and survival pathways (Li *et al.*, 2003). Indeed Fu *et al*, (2002), report increased CDK-5 and p35/p39 expression and increased CDK-5 activation during retinoic acid induced differentiation of NT2 cells whilst Pigino *et al*, (1997), demonstrate a role for CDK-5 in axon formation and guidance in developing cerebellar macroneurones. Additionally CDK-5 mediates phosphorylation of NF, influencing NF transport (Grant *et al.*, 2001; Shea *et al.*, 2004a) and can influence MT motor systems by phoshorylating the dynein-interacting protein, Nudel (Smith and Tsai, 2004 and references therein).

CDK-5 FUNCTIONS	ASSOCIATED REFERENCES
Synaptic transmission and plasticity associated with memory and learning	Li *et al.*, 2001; Fischer *et al.*, 2002; Dhavan *et al.*, 2002
Synaptic vesicle endocytosis/exocytosis and synapse formation at the neuromuscular junction	Samuels and Tsai, 2003; Fletcher *et al.*, 1999; Fu *et al.*, 2001
Corticogenesis	Ohshima *et al.*, 1996
Cell motility, axon dynamics and axon pathfinding	Humbert *et al.*, 2000; Pigino *et al.*, 1997
Interactions with MTs / MAPs / MT motor, dynein	Pigino *et al.*, 1997; Niethammer *et al.*, 2000; Hashiguchi *et al.*, 2002
NF phosphorylation	Grant *et al.*, 2001; Shea *et al.*, 2004a
Activation of cell survival pathways	Li *et al.*, 2003
Cell adhesion	Li *et al.*, 2000
Control of dopaminergic/glutaminergic signalling pathways	Bibb *et al.*, 2001a; Chergui *et al.*, 2004
Adaptive changes in the brain associated with chronic cocaine exposure	Bibb *et al.*, 2001b
Cross-talk with MAPK pathways	Sharma *et al.*, 2002; Li *et al.*, 2002

Table 1.2   Summary of the major roles of CDK-5 in brain development and function and associated references.

1.6   Tissue Transglutaminase

Tissue transglutaminase (tTG) is a type II protein product of eight evolutionary related genes encoding active transglutaminase (TG) sub-types in humans. The sub-types are known as blood coagulation factor FXIIIa and TG1-7 (Wu and Zern, 1994). A ninth, catalytically inactive homologue, erythrocyte band 4.2, has also been characterised (see Lorand and Graham, 2003). tTG is reportedly located in both mammalian central and peripheral nervous systems including the brain (Miller and Anderton, 1986). Given the ubiquitous nature of the enzyme and its internal (cytosolic and nuclear) and external (cell surface and extracellular matrix) location,

its cellular functions are diverse (Lesort *et al.,* 1998; Fesus and Piacentini, 2004). They include involvement in the following; cell survival (Oliverio *et al.,* 1999), apoptotic pathways (Piacentini *et al.,* 2002), differentiation (Tucholski *et al.,* 2001), cell adhesion processes (Verderio *et al.,* 1998; 1999), wound healing *in-vivo* (Haroon *et al.,* 1999), cell signalling (Antonyak *et al.,* 2002; Lopez-Carballo *et al.,* 2002; Tucholski and Johnson, 2003) and cell growth (reviewed by Lesort *et al.,* 2000a; Griffin *et al.,* 2002). The role of tTG in cell differentiation is addressed in detail in chapter III, section 3.1.4. Indeed the mouse tTG gene promotor has been shown to contain a retinoid response element (Nagy *et al.,* 1996). The role of tTG in cell survival/death and indeed neurodegeneration, is discussed in chapter VI with respect to MPP$^+$ toxicity.

The structural and functional domains of the human tTG gene are detailed in Figure 1.8 showing the catalytic site of cysteine, histidine and aspartic acid residues which remains conserved across enzymatically active TG sub-types (see Griffin *et al.,* 2002). Multifunctional in nature, tTG acts to post-translationally modify proteins by transamidation of specific polypeptide bound glutamate residues, resulting in protein cross linking or incorporation of polyamines into substrates (Greenberg *et al.,* 1991) (see Figure 1.9). If H$_2$O replaces an amine substrate in the active site, glutamine deamination or Ca^{2+} -dependent isopeptide hydrolysis can occur *in-vitro* (Parameswaran *et al.,* 1997). The transamidation reaction is Ca^{2+} dependant since Ca^{2+} modifies the enzyme to expose the active site, thus allowing the enzyme to become catalytically active (Greenberg *et al.,* 1991). tTG also binds and hydrolyses Guanosine 5′ triphosphate (GTP) and ATP. ATP/GTP hydrolysis occurs within the same domain of the tTG molecule but at distinct sites (Lesort *et al.,* 2000a). Whereas Ca^{2+} binding increases tTG activity, GTP binding brings about a conformational change to the enzyme that both inhibits tTG activity and reduces Ca^{2+} binding, shown both *in-vitro* and *in-situ* using SH-SY5Y cells (see Lesort *et al.,* 2000a; Zhang *et al.,* 1998a). tTG is a substrate for calpains (Zhang *et al.,* 1998b) and GTP binding has also been shown to protect SH-SY5Y cells from proteolytic cleavage (Zhang *et al.,* 1998a). Therefore Lesort *et al.,* (2000a) propose that nucleotide and Ca^{2+} binding may act to modulate tTG turnover in cells.

HUMAN TISSUE TRANSGLUTAMINASE

FUNCTIONAL DOMAINS
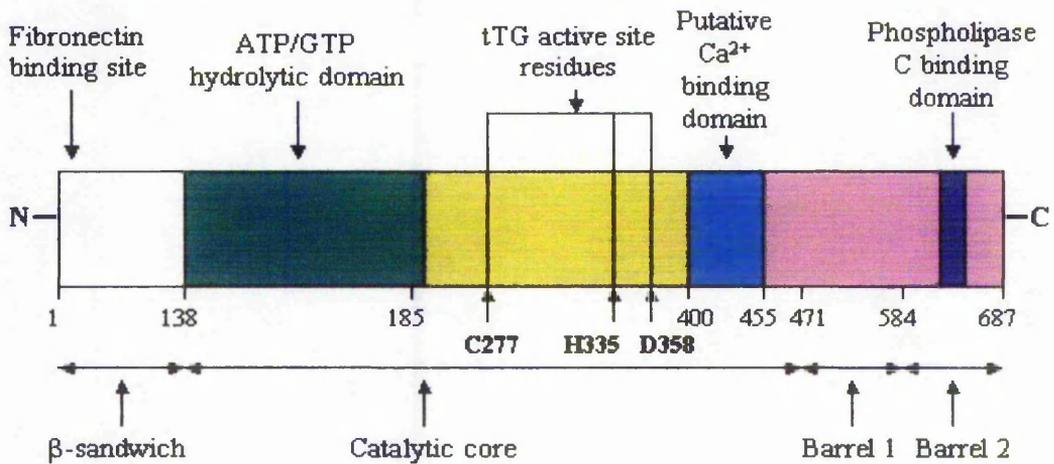
STRUCTURAL DOMAINS

Figure 1.8 Diagram showing structural and functional domains of the human tTG gene (taken from Lesort *et al.*, (2000a) with modifications).
The human tTG gene sequenced against the sequence alignment of Factor XIII-A subunit (Yee *et al.,* 1994). The gene is located on chromosome 20q12 and is 32.5 kb comprising 13 exons and 12 introns. The full length protein is 687 amino acids with an approximate mass of 77 kDa. Human tTG confers 80-90 % sequence homology with bovine, mouse and guinea pig tTG. (for review see Lesort *et al.*, 2000a).

Independent to its transamidating activity, a unique function of tTG is its ability to also function as a signal transducing G protein; Nakaoka *et al,* (1994) discovered that rat liver G alpha (h), (a GTP binding protein) was in fact tTG. As a GTP binding protein, rat liver tTG was shown to mediate alpha(1)-adrenoreceptor stimulation of PLC-delta 1 (Nakaoka *et al.,* 1994; Feng *et al.,* 1996). Thus tTG-GTP is able to partake in intracellular signalling pathways although not in a method identical to classical G proteins. In SH-SY5Y cells this was demonstrated by Zhang *et al.,* (1999) whereby the contribution of tTG in phosphoinositide hydrolysis was much lower than the classical G protein G(q/11) and was also bimodal depending on tTG expression levels.

Isopeptide bond

$$H_2N\text{-}(CH_2)_4\text{<} \quad \xrightarrow{\text{tTG + Ca}^{++}} \quad NH_4^+$$

Lys(K)
(polypeptide
bound lysine)

+

$$\text{-}(CH_2)_2\text{-C-NH}_2 \text{ (Gln, Q)}$$
(polypeptide bound
glutamine)

$$\text{<}(CH_2)_2\text{-C-NH-}(CH_2)_4\text{-<}$$

A. CROSSLINKING

(γ-gluatamyl)polyamine bond

$$\text{-}(CH_2)_2\text{-C-NH-}(CH_2)_4\text{-NH}_3^+$$

+

$$^+H_3N\text{-}(CH_2)_4\text{-NH}_3^+ \quad \xrightarrow{\text{tTG + Ca}^{++}} \quad NH_4^+$$

Putrescine
(polyamine)

**B. POLYAMINE
INCORPORATION**
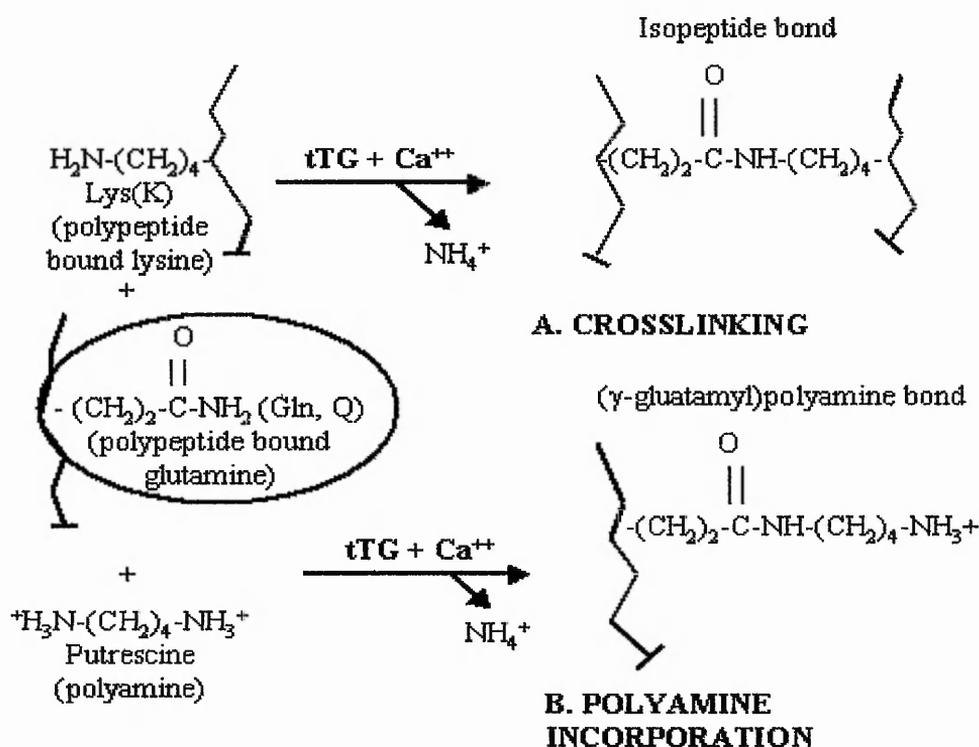
Figure 1.9 Protein cross-linking and incorporation reactions mediated by tTG (taken from Lesort *et al.,* 2000a with modifications).
A. Formation of an ε-(γ-glutamyl)lysine isopeptide bond. tTG catalyses an acyl transfer reaction between the γ-carboxamide group of a polypeptide bound glutamine and the ε-amino group of a polypeptide bound lysine group. B. Formation of a (γ-glutamyl)polyamine bond. tTG can catalyse the incorporation of a polyamine into a polypeptide bound glutamine.

1.7   Protein degradation pathways

Critical to normal cellular function is the degradation of mutated/mis-folded and redundant proteins, to prevent their accumulation into aggregates that can be harmful to the cell. As such "cellular quality control systems" exist to ensure that correct protein transcription/translation and folding is achieved and that mis-folded proteins are appropriately degraded (Kopito, 2000). The endoplasmic reticulum (ER) is the location for biosynthesis of proteins, steroids and certain lipids. Assisted by chaperone proteins, the ER controls the folding, assembly and post-translational modification of newly synthesised proteins (Alberts *et al.,* 1994). Under normal cellular conditions mis-folded proteins are translocated from the lumen of the ER to the cytosol for degradation (Kopito, 2000). Under certain detrimental conditions

including impaired Ca^{2+} homeostasis, hypoxia, growth factor depletion and proteasomal impairment, protein folding can be impaired, which can result in accumulated proteins in the ER lumen and the cytosol termed "ER stress" (Rao and Bredesen, 2004). The cell responds to ER stress via specific sensor proteins that transiently halt protein synthesis, enlist chaperones to prevent protein aggregation and promote translocation and degradation of ER proteins, known as the "unfolded protein response" (reviewed by Rao and Bredesen, 2004). The principle system for cellular protein degradation is the ubiquitin-proteasome pathway (UPP) (detailed in section 1.7.1). However, the cell also relies on lysosomal proteolysis pathways. Lysosomes are acidic organelles, which contain hydrolytic enzymes (Alberts *et al.*, 1994). Between 5 and 7 lysosomal degradation pathways are proposed to exist including macroautophagy, microautophagy and chaperone- mediated autophagy (Majeski and Dice, 2004). Cross-talk between the UPP and lysosome degradation pathways is proposed to occur and perturbation of both pathways is linked to normal aging (Keller *et al.*, 2004).

1.7.1   *The ubiquitin-proteasome pathway*

The UPP is responsible for targeted degradation of abnormal and short-lived proteins from the cell, including regulatory proteins that control the cell cycle and signal transduction, with subsequent recycling of amino acids (McNaught and Jenner, 2001; Shoesmith Berke and Paulson, 2003). The 26S proteasome is a 2000 kDa multi sub-unit protease, located in the cytosol and nucleus of eukaryotic cells. It comprises a catalytic core (20S subunit) and two regulatory subunits (19S). The catalytic core is formed from 4 rings of α or β sub-units (encoded by over 15 genes) with 7 sub-units per ring. Two rings of β sub-units form the central domain of the 20S flanked either side by a ring of α sub-units. The structure therefore forms a cylindrical conformation within which ATP dependent proteolysis occurs on the β sub-units, whilst α-sub-units confer stability to 20S proteasome (Ding and Keller, 2001). Substrates are fed into the catalytic 20S through narrow pores at either end (Ding and Keller, 2001). The 26S proteasome has several active sites and can be described as having chymotrypsin, trypsin and post-acidic – like activities as it mediates the hydrolysis of proteins at the C-terminus of hydrophobic, basic and acidic residues,

respectively (reviewed by McNaught and Jenner, 2001). The 20S proteasome is capped on either or both ends with the 19S regulatory sub-unit, an interaction that causes the narrow pore through the 20S to open. The 19S regulator comprises a lid (formed from 8 non-ATPase sub-units), which functions to recognise substrates and cleave ubiquitin chains (which can be recycled). The lid covers a base sub-unit (formed from 6 ATPase subunits), which function to unfold the protein so that it may be channelled into the 20S proteasome (Hartmann-Peterson *et al.*, 2003 and references therein).

The process by which the 26S proteasome degrades proteins is detailed in Figure 1.10. The 26S proteasome requires that most proteins are ubiquitinated for recognition and entry into the proteasome (Hartmann-Peterson *et al.*, 2003). However, it has been proposed by Shringarpure *et al*, (2003) that under certain circumstances 20S proteasomal degradation can be both ubiquitin and ATP independent. Using cultured cells with inactivated E1 ubiquitin-conjugation activity, oxidised intracellular proteins were still degraded through the proteasome. This activity was proposed to be consequential of oxidised proteins being partially unfolded, which presents hydrophobic sites to the proteasome (required for recognition) and reduces the requirement for ATP in the unfolding process (Shringarpure *et al.*, 2003). Additionally the fore-mentioned study proposes that the 26S proteasome is damaged by oxidative stress whereas the 20S is not, concluding that the 20S, rather than the 26S is involved in degrading oxidised proteins.
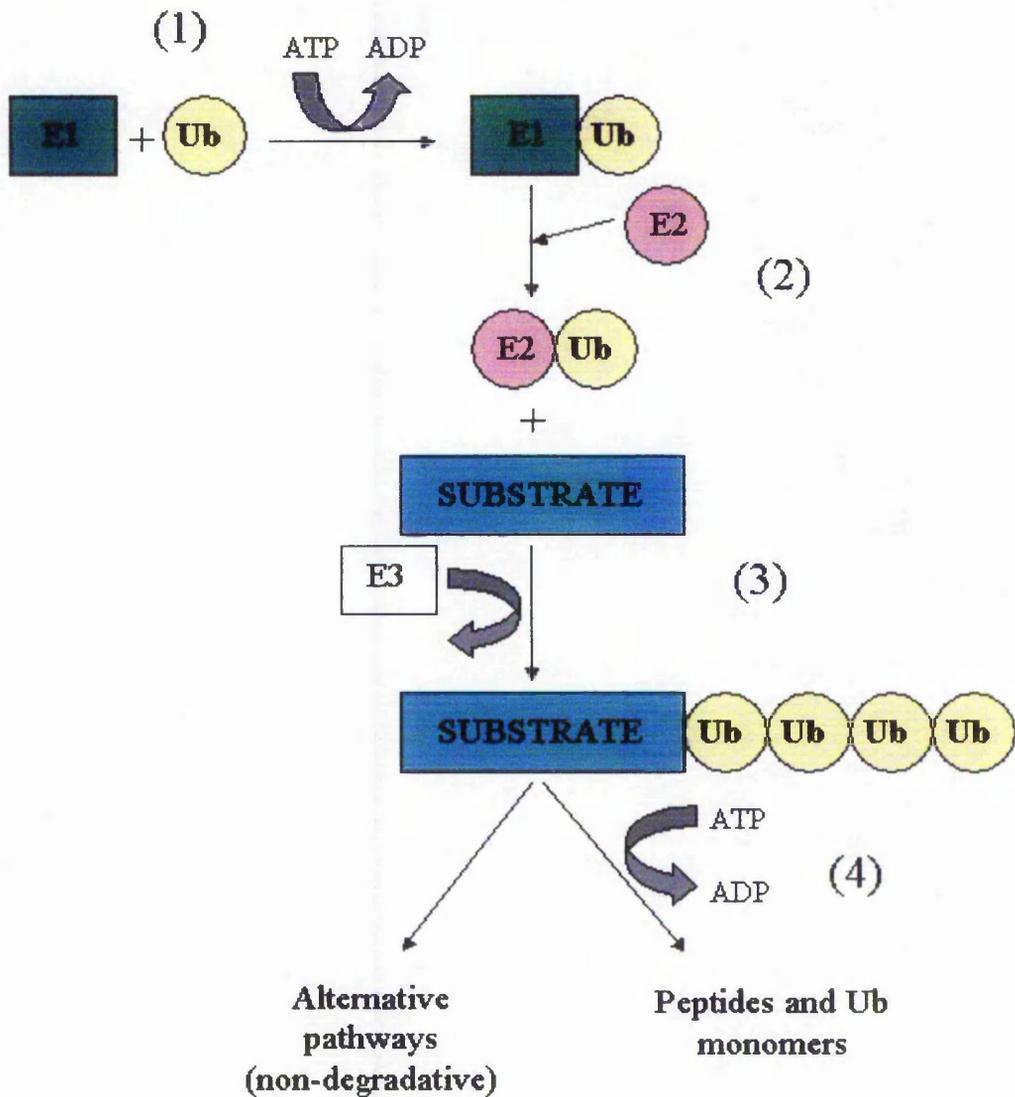
Figure 1.10   Degradation of proteins via the 26S proteasome (Chung *et al.*, 2001).

Most substrates require ubiquitination before transfer to the 26S proteasome. Ubiquitin (a 76 amino acid protein) is first activated by ubiquitin-activating enzyme (E1) in the presence of ATP (1) then transferred to a ubiquitin-conjugating enzyme (E2) (2). E2 in conjunction with a ubiquitin protein ligase (E3) mediates attachment of ubiquitin to a lysine residue on the target substrate (3). When a chain of at least 4 ubiquitin molecules is attached, the substrate can be recognised by the proteasome and degraded into short peptides in an ATP dependant manor within the 20S catalytic core (4). Ubiquitination is highly controlled and can be positively and negatively regulated. For example ubiquitin chain elongation factors (E4s i.e. C terminus of Hsc70-interacting protein [CHIP]) catalyse proteins bound to the E2-E3 complex promoting polyubiquitination. Negative regulation occurs via deubiquitinating enzymes i.e ubiquitin C-terminal hydrolases. The degradation process is also regulated by chaperone proteins (reviewed by Shoesmith Burke and Paulson, 2003). Many E3 enzymes exist to confer substrate recognition and selectivity (Layfield *et al.*, 2003).

1.7.1.1 MPP$^+$ and proteasome inhibition

It has been recently demonstrated that MPP$^+$ can inhibit the proteasome, although research is very limited at this time. It has been shown in my laboratory in a mitotic SH-SH5Y system that 2 mM MPP$^+$ could significantly inhibit the proteasome within 24 h. Significantly glutathione levels were reduced preceding proteasomal inhibition by MPP$^+$ thus augmenting oxidative stress (Begoñã Caneda-Ferron, unpublished observations). Jha et al, (2002), demonstrated that reduced glutathione levels in PC12 cells correlated with reduced ubiquitin-protein conjugates due to inhibition of E1 (ubiquitin-activating) activity. In a study by Höglinger et al, (2003) using primary mesencephalic cultures, MPP$^+$ was shown to reduce proteasomal activity via ATP depletion and also increase ROS levels. Proteasome inhibition did not increase ROS but did increase levels of oxidised proteins due to reduced proteolysis. However under critical conditions of ATP depletion and ROS elevation, proteasomal impairment by MG132 was shown to exacerbate MPP$^+$ toxicity by increasing the sensitivity of cells to levels of ROS that would normally remain sub-cytotoxic. Contrary to Höglinger et al, (2003), a study by Shamoto-Nagai et al, (2003) using rotenone, (also a complex I inhibitor), in mitotic SH-SY5Y cells, reported that rotenone increased oxidised protein levels, which were prone to aggregation and also that rotenone oxidatively modified the 20S proteasome, as demonstrated by a reduction in proteasomal activity in the absence of ATP depletion or reduction in proteasome levels. This is in agreement with findings in my laboratory using mitotic SH-SY5Y cells whereby MPP$^+$-mediated impaired proteasomal activity is dependent on reduced glutathione levels but is not dependent on ATP depletion (Begoñã Caneda-Ferron, unpublished observations).

The link between MPP$^+$ toxicity and proteasome impairment further strengthens the potential role of the proteasome in the pathogenesis of PD. Indeed levels of oxidised proteins are elevated in all areas of the PD brain (Halliwell and Jenner, 1998) and 20S/26S proteasome sub-units have been identified with Lewy bodies, the pathological hall-mark of PD (detailed in section 1.8.1) (McNaught and Jenner, 2001 and references therein). Significantly familial PD has been linked to a number of identified genetic mutations that have in common involvement in protein folding and degradation via the ubiquitin-proteosome pathway thus augmenting conditions for

protein aggregation. Mutations include point mutations (A53T and A30P) in the gene encoding for α-synuclein (Polymeropoulos *et al.,* 1996; 1997; Krüger *et al.,* 1998) and mutations of the parkin (an E3 ligase) (Kitada *et al.,* 1998) and Ubiquitin C terminal hydrolase L1 genes (Leroy *et al.,* 1998). A study by Bennett et al, (1999) using SH-SY5Y cells transiently expressing wild-type and mutant (A53T) α-synuclein, a major component of Lewy bodies, demonstrated firstly that the mutant protein had a longer half life than wild-type α-synuclein and secondly that both wild-type and mutant proteins were degraded through the proteasome. McNaught and Jenner, (2001) provide direct, albeit very limited, evidence of reduced chymotrypsin-like, trypsin-like and post-acidic-like activities in the substantia nigra of PD brains. Importantly this research suggests that idiopathic PD brains exhibit accumulation of normal and mutated proteins because the proteasome itself is impaired, whereas in cases of familial PD, proteins accumulate because genetic mutations prevent their ubiquitination and subsequent recognition by the proteasome (McNaught and Jenner, 2001).

1.8 The Lewy body and associated intracellular inclusions in MPTP-induced Parkinsonism

1.8.1 The Lewy body

Lewy bodies are cytoplasmic inclusions containing filamentous, insoluble proteins, but are also rich in lipids (Gai *et al.,* 2000). In cases of idiopathic PD, Lewy bodies are detected within brain stem nuclei (substantia nigra, locus coeruleus and dorsal motor vagal nucleus) and less frequently, the cerebral cortex (Gai *et al.,* 2000). Brain stem Lewy bodies are eosinophillic whereas cortical Lewy bodies poorly stain for eosin or do not stain at all (Schmidt *et al.,* 1991). The morphology and structural composition of Lewy bodies is highly heterogeneous and shows regional variation. Approximately 40-55 % of mature, PD Lewy bodies represent classically defined, concentric inclusions comprising a dense core containing filamentous material and lipids and a peripheral region of radiating filaments. However, Lewy bodies exhibiting a more homogeneous distribution of composite proteins co-exist (Forno *et al.,* 1986; Gai *et al.,* 2000). The fact that a spectrum of Lewy body morphologies

exists may represent different developmental stages (Gai *et al.,* 2000). Lewy bodies comprise largely of α-synuclein (and synphilin 1 [α-synuclein interacting protein]), ubiquitin and NFs (Forno *et al.,* 1986; Schmidt *et al.,* 1991; Spillantini *et al.,* 1997, 1998; Gai *et al.,* 2000), proteasomeal sub-units (McNaught and Jenner, 2001) and MAPs (Galloway *et al.,* 1992).

1.8.2   Structural components of Lewy bodies

1.8.2.1   α-synuclein and ubiquitin

α-synuclein is a member of four cytosolic proteins (α, β, and γ-synuclein and synoretin) of 127-140 residues which exhibit a high degree of homology. α and β synuclein proteins are abundant at the pre-synaptic nerve terminal. (Schlüter *et al.,* 2003). Ubiquitin is small protein (76 amino acids) required for the degradation of many cytosolic, nuclear and ER proteins through the 26S proteasome (Alves-Rodrigues *et al.,* 1998) as detailed in section 1.7.1. A host of evidence demonstrates that insoluble α-synuclein and ubiquitin-protein conjugates are both prominent components of the Lewy body (Gai *et al.,* 2000; Meredith *et al.,* 2002; Spillantini *et al.,* 1998) whilst mutations in the α-synuclein and ubiquitin C terminal hydrolase L1 genes are linked with familial PD (see section 1.7.1.1). In traditional concentric Lewy bodies, α-synuclein is distributed in the peripheral and outer domains. In contrast ubiquitin is generally found in the central domain (Gai *et al.,* 2000; Chung *et al.,* 2001). In normal cells the concentration of α-synuclein is highly controlled but under conditions of oxidative stress, or where the α-synuclein is mutated, α-synuclein levels increase. This promotes oligomerisation of protein monomers, forming structured toxic protofibrils and fibrils which are consequently found in Lewy bodies (reviewed by Bazilai and Melamed, 2003).

1.8.2.2   Cytoskeletal elements

Numerous studies using post mortem brains provide evidence that NF proteins are key components in Lewy bodies associated with PD (Forno *et al.,* 1986; Schmidt *et al.,* 1991; Galloway *et al.,* 1992; Pollanen *et al.,* 1993). Of the three NF proteins, NF-

H and NF-M are reported to be most commonly associated with Lewy bodies (Pollanen *et al.,* 1993). Significantly, Lewy bodies contain many phosphorylated NF epitopes (Forno *et al.,* 1986). In a comparative study of brainstem, PNS and cortical Lewy bodies, Schmidt *et al,* (1991), determined that phosphorylated NF-M epitopes were homogenously detected throughout almost all cortical Lewy bodies whereas other NF antibodies did not stain more than 10 % of these inclusions. Similarly, a peripheral ring of NF and phosphorylated NF immunoreactivity was detected in brain stem Lewy bodies (Forno *et al.,* 1986). There is strong evidence to suggest that phosphorylation of these epitopes is at least in part mediated by CDK-5 since brain stem and cortical Lewy bodies were found to be immunoreactive for this kinase, following a similar staining pattern to NF-H and NF-M (Brion and Couck, 1995). CDK-5 imunoreactivity was in turn found to co-localise with regulatory sub-unit p35 in PD Lewy bodies, suggesting that CDK-5 be in an active state (Nakamura *et al.,* 1997). Conversely anti-ERK 1 and anti cdc2-p34 did not label Lewy bodies (Brion and Couck, 1995). Tubulin sub-units and MAP2 have also been identified in Lewy bodies (Galloway *et al.,* 1988, 1992).

1.8.3   *Formation of a Lewy body and inclusion formation in in-vivo models of PD*

The ability of a cell to instigate the degradation of accumulated, mutated or mis-folded proteins is generally achieved through the ubiquitin-proteasome system or the lysosomal system following sequestration of damaged proteins from the cytosol by chaperone proteins (Meredith *et al.,* 2004). The mechanism by which Lewy body formation occurs in PD, and associated inclusions form in toxin-induced PD models, remains unresolved. The employment of neurotoxins may more accurately reproduce disease pathology than using models in which Lewy body associated proteins are over-expressed. This point is reviewed by Meredith *et al,* (2004) who state that over-expression of proteins e.g. α-synuclein may never reproduce true Lewy bodies because they lack the oxidative stress that can sustain cellular damage and impair normal protein degradation systems that is achieved using neurotoxic agents.

Eosinophilic inclusion bodies ultrastructurally similar to Lewy bodies were found at predilection sites for Lewy bodies in aged MPTP treated squirrel monkeys (Forno *et al.,* 1988, 1993). However evidence suggests that MPTP induced Parkinsonism in

monkeys may be reversible (Eidelberg *et al.,* 1986) and that Lewy body structure is not accurately replicated owing to the lack of a central core and filamentous halo (reviewed by Meredith *et al.,* 2004). In a more recent study, Petroske *et al.,* (2001) developed a mouse MPTP model whereby mice were co-administered with MPTP and probenecid. Probenecid is a lipid soluble derivative of benzoic acid that competitively inhibits renal tubular secretion of other drugs (Rang, Dale and Ritter, 1995). Thus it reduces the clearance of MPTP and its metabolites from the kidney and the brain and therefore exacerbates neurotoxicity. Sustained nigrostriatal degeneration and motor deficits were observed for 6 months post treatment (Petroske *et al.,* 2001) In a further study employing the chronic MPTP/probenecid model, Meredith *et al,* (2002) have demonstrated both granular and filamentous inclusions in the substantia nigra and cortex that were immunoreactive for α-synuclein. Significantly the MPTP/probenecid treatment induced formation of secondary lysosomes containing lipofuscin granules that were α-synuclein positive. Lipofuscin granules are protein-lipid aggregates that form under conditions of oxidative stress and low pH, causing lysosomal dysfunction (Meredith *et al.,* 2004; Keller *et al.,* 2004). Of interest is that the dopaminergic neurones of α-synuclein knock-out mice show resistance to MPTP (Dauer *et al.,* 2002).

Meredith *et al,* (2004) recently proposed a mechanism for PD and MPTP induced Parkinsonism based on α-synuclein accumulation (shown in Figure 1.11); the ubiquitin-proteasome system is the most commonly used system for protein degradation but generally requires ATP. Since damaged neurones have reduced ATP levels (and impaired UPP), it is hypothesised that accumulating proteins are moved to the lysosomes for degradation, aided by chaperones such as heat shock proteins, the presence of which has been reported in Lewy bodies (McLean *et al.,* 2002). Within the lysosome, lipofuscin granules, lipids and neuromelanin accumulate until the lysosome breaks down releasing its contents into the cytoplasm. It is proposed that lipofuscin granules may provide nucleation centres for Lewy body formation.
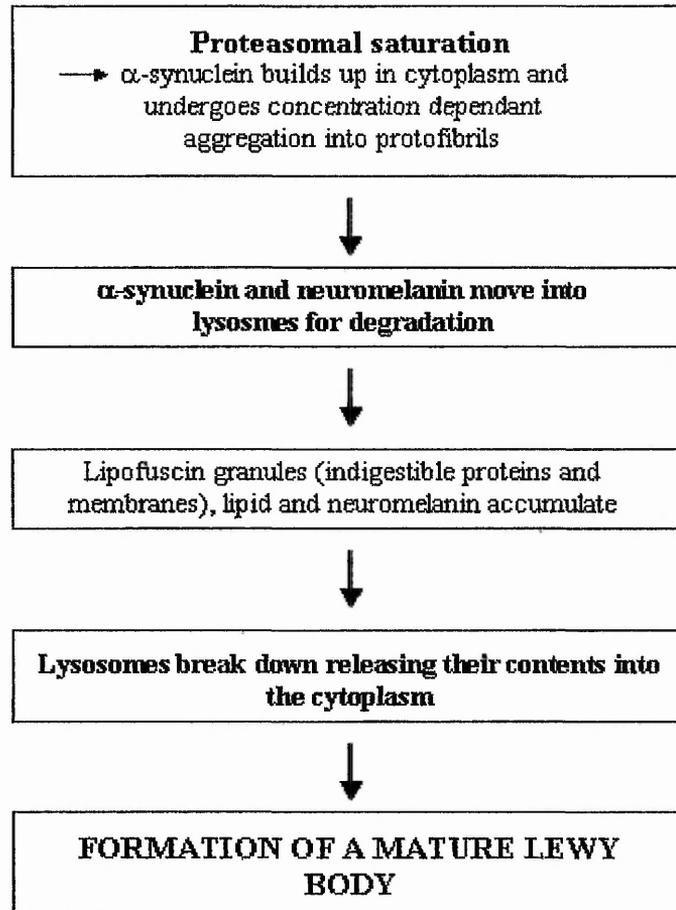
Figure 1.11 Proposed mechanism of Lewy body formation (taken from Meredith *et al*, (2004), with modifications). See text for details.

1.8.4   Aggresomes

Recent research has proven that *in-vitro*, where proteins become accumulated due to over expression, mutation, or inhibition of the proteasome system, cells will accumulate these proteins into a structure that has been termed an aggresome (Johnston *et al.,* 1998). In turn an aggresome was defined by the authors as "a general cellular response to the presence of aggregated, un-degraded protein formed when the capacity of the proteasome is exceeded by the production of aggregation prone, mis-folded proteins". The concept of aggregated proteins forming inclusion bodies has long been accepted and linked to various neurodegenerative disorders. However it has been reported that aggresomes form by the ordered retrograde transport of proteins on dynein MT associated motors. Thus the ability of a cell to specifically mediate aggresome formation may shed important light on the formation of Lewy bodies. Indeed, links between aggresomes and Lewy bodies have been made on the basis of structural resemblance and similarities in the conditions under which they can form (McNaught *et al.,* 2002). Reduced proteasomal activity is characteristic of PD whilst mutated proteins in the presence of oxidative stress increase the risk of protein aggregation (Shamoto-Nagai *et al.,* 2003). This link is heightened by studies that show proteasomal inhibition in cells over-expressing the E3 ligase, Parkin to cause aggresome like structures in neuronal cells (Ardley *et al.,* 2003). In addition endogenous Parkin was present in aggresomes induced not only by proteasome inhibition but also oxidative stress and pro-apoptotic inducers in human neuroblastoma SH-SY5Y cells. In this system, over-expression of wild-type Parkin was found to reduce aggresome formation but the subsequent effect that this had on cell survival was dependant on the type of stress to which cells were exposed (Muqit *et al.,* 2003). Indeed, similarly to Lewy bodies, the role of an aggresome within a cell, albeit toxic and damaging, or a protective mechanism to sequester and contain damaged, accumulating proteins in the face of reduced proteasomal activity, remains to be fully elucidated.

1.8.4.1   The role of axonal transport systems and aggresome formation

An interesting perspective on inclusion formation considers axonal transport systems, which are required to carry proteins within the cell. As previously described the MT network provides a transport system via association with motor proteins (Downing and Nogales, 1998). Shea *et al*, (2004b) report that oxidative stress affects the dynamics of NF transport. The authors proposed that NF inclusions might sequester motor proteins, so that the cellular mechanisms that could potentially alleviate inclusion formation are in turn compromised. Additionally, Muchowski *et al*, (2002) propose that inclusion body formation may trap bio-molecules required for normal cellular functions i.e. chaperones and transcription factors. The MT system has been reportedly required for the formation of aggresomes (Johnston *et al.*, 1998; Zhao *et al.*, 2003) and also for *in-vitro* inclusions that mimic Huntington's disease pathology (Muchowski *et al.*, 2002). Aggresomes form at the microtubule organising centre (MTOC) and require an intact MT network presumably to traffic proteins in retrograde fashion (Johnston *et al.*, 1998; Ardley *et al.*, 2003; Muquit *et al.*, 2004) because treatment with MT disrupting agents prevented aggresome formation. However the MT network is not required for stability of the aggresome, since MT disruption did not affect existing aggresomes (Johnston *et al.*, 1998).

1.8.4.2   Intracellular inclusions; protective sequestration of harmful proteins or promoters of cell death?

The role of intracellular inclusions, whether protective or pro-death, in neurodegenerative disease *per se* or cell culture models that mimic the disease state, remains highly controversial. As reviewed by Orr, (2004), it is crucial that this be determined since disruption of such inclusions is the focus of many studies. A recent study by Arrasate *et al*, (2004) used a unique approach to determine that formation of intracellular inclusion bodies in live striatal neurones transfected with mutant huntingtin, correlated with increased cell survival. The authors used automated microscopy to analyse a particular neurone at any one time following transfection with the mutant protein allowing the relationship between inclusion body formation and survival to be exacted. The study hypothesised that the pro-survival effect of inclusion body formation was attributable to a corresponding reduction in diffuse

intracellular huntingtin. Thus supporting the aggresome theory that inclusions may act to sequester harmful proteins within the cell (Johnston *et al.,* 1998). Furthermore, Hasegawa *et al,* (2004) noted that microtubule depolymerisation prevented formation of α-synuclein aggregates in iron treated SH-SY5Y cells but did increase apoptosis. In another study, deregulated CDK-5 activity in mice expressing a mutant superoxide dismutase to model ALS, caused hyperphosphorylation of NFs and tau (Nguyen *et al.,* 2001). The study proposed that consequent perikaryal NF inclusions were, to an extent, protective, by acting as a "phosphorylation sink" for CDK-5 activity. However, the study also suggested that the protective effects of CDK-5 activity reached a threshold level since they were not apparent when CDK-5 activity was very high (Nguyen *et al.,* 2001), thus implying that the role of inclusion bodies may in fact be variable.

1.9   Aims of project

The MPTP model continues to reveal valuable insight into PD pathology. Ultimately *in-vivo* models provide important experimental systems, particularly for neuroprotective studies. However, cell culture systems have gained favour owing to their comparable simplicity and pliability, and provide a most useful basis on which to investigate underlying disease pathology at the sub-cellular level. Due to an observed difference in species sensitivity to MPTP, the most applicable cell culture system would be of human origin. For this project the SH-SY5Y human neuroblastoma cell line was employed. The initial aim of the project was to establish a differentiated phenotype in these cells using all-trans retinoic acid, to provide a system with greater analogy to cells *in-vivo*. Of significance to the project was that cells could also be maintained in a viable differentiated state for extended time periods to permit the study of low (sub-cytotoxic) concentrations of the active metabolite, MPP^+. Whilst previous studies have investigated the effects of $MPTP/MPP^+$ in SH-SY5Y cells, mitotic cells are often used, or if cells are differentiated the time course of MPP^+ exposure is relatively short. Additionally, high concentrations of the toxin are commonly used. The use of low concentrations of MPP^+ over extended time periods in a pre-differentiated system is novel and important since it more closely mimics the chronic neurodegenerative PD process.

Using a pre-differentiated SH-SY5Y system, the aim was to determine potential markers of MPP$^+$ toxicity, with emphasis on the post-translational modification and distribution of specific cytoskeletal elements. Particular focus was given to the NF and MT networks, given their presence in proteinacious inclusions and the pathological hallmark of PD, the Lewy body. Additionally the aim was to explore evidence for, and consequences of, impaired proteasomal activity in this system, since a role for impaired proteasome function has recently gained interest in PD. An investigation into the role of tTG in the MPP$^+$ Parkinsonian model is also warranted given that the cross-link catalysed by the enzyme has been found to colocalise with α-synuclein in Lewy bodies, and its cross-linking activity has been implicated in other neurodegenerative diseases. Therefore this project aimed to investigate the effects of MPP$^+$ on tTG protein levels and activity and to assess the effects of tTG inhibitors on MPP$^+$ toxicity in the SH-SY5Y system.

Of critical importance to PD research is the discovery of neuroprotective strategies. This project aimed to assess the relative merits of specific chemical inhibitors to MAPK pathways with respect to maintaining cell viability and cell morphology following both short term and extended exposures to MPP$^+$. Given the recent interest in the CDK-5 pathway in neurodegeneration, and the lack of investigation of the enzyme in cell culture systems, this project sought to investigate the role of CDK-5 in MPP$^+$ toxicity using a specific inhibitor.

CHAPTER II

MATERIALS AND METHODS

2.1 MATERIALS

Materials are listed with their corresponding product code and the company from which they were purchased.

2.1.1 Cell culture

2.1.1.1 Reagents

Dulbecco's Modified Eagles Medium (DMEM) (12-614F), foetal bovine serum (14-801-F), Penicillin/streptomycin (17-603E), L-Glutamine (17-603E), Trypsin/EDTA solution (02-007E), all purchased from BioWhittaker UK Ltd. Berkshire, UK.

DMEM/Ham's F12 medium (D6421), Roswell Park Memorial Institute (RPMI) - 1640 medium (R0883), horse serum (H1270), MEM non-essential amino acids solution (M7145), trypan blue solution (0.4 %) (T8154), all purchased from Sigma-Aldrich Chemical Company, Poole, UK.

2.2.1.2 Plastic ware

All sterile plastic ware was tissue culture treated and supplied by Sarstedt, Leicester, UK.
Cryotube vials (Nunc brand products), Merck Ltd. Leicester, UK.
Nunc Lab-Tek CC chamber slides (permanox) (177445), Scientific Laboratory Supplies Ltd, Nottingham UK.

2.1.2 General laboratory reagents

All laboratory reagents were of the highest grade and purchased from Sigma-Aldrich Chemical Company, Poole, UK, unless otherwise specified in the text.

2.1.3 Specialised laboratory reagents

3-(4,5-dimethylthiazol-2-yl)-2,5-diphenyltetrazolium bromide (MTT) (M2128), Sigma-Aldrich Chemical Company, Poole, UK.
3MM chromatography paper (CJF240090), Fisher Scientific, Leicestershire, UK.
5-bromo-4-chloro-3-indolyl-phosphate (di-sodium salt) (BCIP) (MB1018), Melford Laboratories Ltd, Ipswich, UK.
Acrylogel 3 solution Electran (containing 2.5 % NN'-methylenebisacrylamide, final ratio 29:1:0.9) (443735T), VWR International Ltd, Poole, UK.
all-trans Retinoic acid (R2625), Sigma-Aldrich Chemical Company, Poole, UK.
Bio-Rad protein assay dye reagent concentrate (500-0006), Bio-Rad Laboratories Ltd, Hemel Hempstead, UK.
Dimethylsulfoxide (DMSO) (D/4120/PB08), Fisher Scientific UK Ltd, Loughborough, UK
ECL Western blotting detection reagents (RPN2109), Amersham Pharmacia Biotech UK Ltd, Bucks, UK.
EZ-Link 5-(biotinamido)pentylamine (21345), Perbio Science UK Ltd, Cheshire, UK.

Folin and Ciocalteu's phenol reagent (J/4100/08), Fisher Scientific UK, Leicestershire, UK.

GBX developer/replenisher (P7042), Sigma-Aldrich Chemical Company, Poole, UK.

GBX fixer/replenisher (P7167), Sigma-Aldrich Chemical Company, Poole, UK.

Igepal CA-630 (I3021), Sigma-Aldrich Chemical Company, Poole, UK.

Ionomycin calcium salt (I0634), Sigma-Aldrich Chemical Company, Poole, UK.

MG132 (47490), Calbiochem, Nottingham, UK.

MPP+ Iodide (D048), Sigma-Aldrich Chemical Company, Poole, UK.

Nitro Blue Tetrazolium (NBT) (MB1019), Melford Laboratories Ltd, Ipswich, UK.

Nitrocellulose 0.22 µM pore size (WP2HY00010), Genetic Research Instrumentation, Essex, UK.

Phenylmethylsulfonyl fluoride (PMSF) (P7626), Sigma-Aldrich Chemical Company, Poole, UK.

Pre-stained SDS molecular weight standard markers (SDS-7B), Sigma-Aldrich Chemical Company, Poole, UK.

Protease inhibitor cocktail (P8340), Sigma-Aldrich Chemical Company, Poole, UK.

Putrescine (tetramethylenediamine) Dihydrochloride (P7505), Sigma-Aldrich Chemical Company, Poole, UK.

R283 (tTG inhibitor), a kind gift from Professor M. Griffin, The Nottingham Trent University, UK

Sodium-orthovanadate (S6508), Sigma-Aldrich Chemical Company, Poole, UK.

Vectashield mounting medium (H-1000), Vector Laboratories Ltd, Peterborough, UK.

Vectashield mounting medium with propidium iodide (H-1300), Vector Laboratories Ltd, Peterborough, UK.

Vialight HS kit, (LT07-111), LumiTech Ltd, Nottingham UK.

XAR-5 Kodak film (F5388), Sigma-Aldrich Chemical Company, Poole, UK.

Dithiothreitol (DTT) (MB1015), Melford Laboratories Ltd, Ipswich, UK.

2.1.4 Kinase inhibitors

Butyrolactone I (CC-210), Biomol Research Laboratories Inc, distributed by Affiniti Research products Ltd, Exeter, UK.

CEP-11004 mixed lineage kinase inhibitor, Cephalon Inc.

PD98059 MEK inhibitor (513000), Calbiochem, Nottingham UK.

SB202190 p38 MAP kinase inhibitor (559388), Calbiochem, Nottingham UK.

Staurosporine (S4400), Sigma-Aldrich Chemical Company, Poole, UK.

Stock solutions of inhibitors were prepared in DMSO to give a final concentration of 10 mM.

2.1.5 Antibodies

2.1.5.1 Primary antibodies

Anti- ERK 1 (K-23) antibody (sc-94), Santa Cruz Biotech, Santa Cruz, California.

Anti-p35 (C-19) antibody (sc-820), Santa Cruz Biotech, Santa Cruz, California.

Anti-phospho ERK 1/2 (E-4) antibody (sc-7383), Santa Cruz Biotech, Santa Cruz, California.

Anti-phospho-JNK (G-7) MAP kinase antibody (sc-6254), Santa Cruz Biotech, Santa Cruz, California.

Monoclonal anti-α-tubulin (clone B-5-1-2) (T5168), Sigma-Aldrich Chemical Company, Poole, UK.

Monoclonal anti-β-tubulin (clone TUB 2.1) (T4026), Sigma-Aldrich Chemical Company, Poole, UK.

Monoclonal anti-Growth associated protein-43 (GAP-43) (clone GAP-7B10) (G9264), Sigma-Aldrich Chemical Company, Poole, UK.

Monoclonal Bcl-2 (clone Bcl-2-100) (B3170), Sigma-Aldrich Chemical Company, Poole, UK.

Neurofilament 200 kDa monoclonal (clone RT97), (NCL-NF200), Vector Laboratories Ltd, Peterborough, UK.

Neurofilament 200 monoclonal antibody (clone N52) (N0142), Sigma-Aldrich Chemical Company, Poole, UK.

NeutrAvidin horseradish peroxidase conjugated (31001), Perbio Science UK Ltd, Cheshire, UK.

Rabbit polyclonal antibody to ubiquitin-protein conjugates, (clone UG9510) Affinity research products Ltd, Exeter, UK.

SMI31 anti-phospho-neurofilaments, Sternberger Monoclonals Inc, Maryland, USA.

Transglutaminase II Ab-1 (clone CUB 7402) (MS-224-P), Stratech Scientific Ltd, Cambridgeshire, UK.

2.1.5.2 Secondary antibodies

Goat anti-mouse immunoglobulins alkaline phosphatase conjugated (D0486)
Goat anti-mouse immunoglogulin horseradish peroxidase conjugated (P0447)
Goat anti-rabbit immunoglobulins alkaline phosphatase conjugated (D0487)
Goat anti-rabbit immunoglogulins horseradish peroxidase conjugated (P0447)
Rabbit anti-mouse immunoglobulins FITC conjugated (F0261)
All purchased from DAKO Ltd, Cambridgeshire, UK.

2.1.6   Specialised equipment

ATTO HorizBlot, ATTO corporation, Japan.

Bio-Rad mode 680 microplate reader, Bio-Rad Laboratories Ltd, Hemel Hempstead, UK.

Bio-Rad Power Pac 300, Bio-Rad Laboratories Ltd, Hemel Hempstead, UK.

Bio-Rad Trans-Blot electrophoretic transfer system, Bio-Rad Laboratories Ltd, Hemel Hempstead, UK.

GeneTools/GeneSnap gel analysis/quantification system, Syngene, Cambridge, UK.

Leica CLSM confocal laser microscope, Leica, Germany.

Lucy I microplate luminometer, Anthos, UK.

MIKRO 22R microfuge, Hettich, Germany.

Mini-PROTEAN II system, Bio-Rad Laboratories Ltd, Hemel Hempstead, UK

Nikon Digital Net camera DN100, Nikon, Japan.

Nikon Eclipse TS 100 inverted microscope, Nikon, Japan.

Pharmacia electrophoresis power supply EPS 500/400, Pharmacia, UK.

Sanyo Harrier 18/80 refridgerated centrifuge, Sanyo Gallenkamp PLC, Leicestershire, UK.

Soniprep 150, MSE scientific instruments, UK.

Tecan SPECTRA Fluor plate reader, Tecan UK Ltd, Reading, UK.

Walker class II microbiological safety cabinet, Walker safety cabinets Ltd, Derbyshire, UK.

2. 2 METHODS

2.2.1 Cell culture

Three clones of the human SH-SY5Y neuroblastoma cell line were used. The first (to be referred to as the 'Leicester clone') was a kind gift from Professor S.R. Nahorski, Pharmaceutical Sciences, Leicester University. The second was obtained from European Collection of Animal and Cell Cultures ('ECACC clone'). The third was a kind gift from Professor M. Griffin, School of Science, formerly of The Nottingham Trent University and originated from Dr G.V.W. Johnson, Department of Psychiatry and Behavioural Neurobiology, University of Alabama ('Johnson clone').

2.2.1.1 Maintenance of SH-SY5Y clones

Cell culture was carried out in a class II safety cabinet using aseptic technique. Cells were cultured in 25 cm^2 (T25), 75 cm^2 (T75) and 175 cm^2 (T175) flasks in 'growth medium' containing at final concentration:

- Leicester clone – 90 % (v/v) Dulbecco's Modified Eagles Medium (DMEM), 10 % (v/v) foetal bovine serum (FBS), 2 mM L-Glutamine, 100 units/ml penicillin/10 µg/ml streptomycin.

- ECACC clone – 90 % (v/v) Dulbecco's Modified Eagles Medium (DMEM)/Ham's F12 (1:1), 10 % (v/v) heat inactivated FBS (serum heated at 60 °C for 30 min), 2 mM L-Glutamine, 1 % (v/v) non essential amino acids, 200 units/ml penicillin / 0.2 mg/ml streptomycin.

- Johnson clone – 85 % (v/v) RPMI-1640, 10 % (v/v) heat inactivated horse serum, 5 % (v/v) heat inactivated FBS, 2 mM L-Glutamine, 200 units/ml penicillin / 0.2 mg/ml streptomycin.

Components of growth medium for clones were used as recommended by their source. Cells were incubated at 37 °C in a humidified atmosphere of 95 % (v/v) air/5 % (v/v) carbon dioxide until 70-90 % confluent.

2.2.1.2 Sub-culture

Cells were assessed via light microscopy for viability. Growth medium was removed using a Pasteur pipette and the cell monolayer rinsed twice with DMEM to remove serum. Cells were detached from the substratum using trypsin (100 μg/ml)/ Ethylenediamine (EDTA) (40 μg/ml) in DMEM at 37 °C. Growth medium, ten times the volume of trypsin solution, was added to quench the action of trypsin. The suspension was transferred to a sterile centrifuge tube and centrifuged at 150 x g for five minutes. Supernatant was removed and the pellet re-suspended in 1 ml fresh growth medium. A volume of cell suspension, typically 20-50 μl was transferred to an appropriate sterile flask containing fresh growth medium. Cells were then incubated as described in section 2.2.1.1.

2.2.1.3 Viable cell counting and seeding

To seed cells at a given density, a 1:10 dilution of cell suspension prepared during sub-culture was made in Trypan Blue solution (0.4 % [v/v]), typically 180 μl Trypan blue and 20 μl cell suspension (see section 2.2.3.2). A viable cell count was performed in four fields (each 1.0 mm^2) on a haemocytometer (0.1 mm depth chamber) using light microscopy at x 10 magnification. Cell density/ml was calculated as follows:

cell density = mean cell number (from four fields) x 10^4 x dilution factor

This value was used to determine the volume of cell suspension required to achieve the desired cell density in a known volume of fresh growth medium. Once seeded, cells were incubated in a humidified atmosphere of 95 % (v/v) air/5 % (v/v) CO_2 at 37 °C.

2.2.1.4 Cryo-preservation of cells

Cells underwent long-term storage in the gaseous phase of liquid nitrogen in freezing medium containing, at final concentration, 95 % (v/v) FBS and 5 % (v/v) sterile dimethyl sulfoxide (DMSO). Cells were grown as described in section 2.2.1.1, harvested using trypsin (as described in section 2.2.1.2) transferred to a sterile centrifuge tube, a sample diluted 1:2 with Trypan blue and counted as described in

section 2.2.1.3. The cells were then sedimented by centrifugation at 150 x g for 5 min. Supernatant was removed and the centrifuge tube gently tapped to dislodge the cell pellet. The pellet was re-suspended in ice-cold freezing medium to give a density of 2 x 10^6 cells/ml. The suspension was immediately transferred to cryovials on ice in 1 ml aliquots and rapidly transferred to a - 70 °C freezer overnight before transferring to liquid nitrogen for long term storage.

2.2.1.5 Resuscitation of cryo-preserved cells

Having removed a vial of cells from liquid nitrogen storage, cells were thawed rapidly by suspending the vial in a 37 °C water bath. Cells were immediately transferred to a sterile centrifuge tube containing 10 ml fresh growth medium. The cell suspension was centrifuged at 150 x g for 5 min. Supernatant was removed and cells re-suspended in 1 ml fresh growth medium using a Pasteur pipette before transfer into a sterile T25 flask containing 10 ml growth medium. Cells were incubated in a humidified atmosphere of 95 % (v/v) air/5 % (v/v) carbon dioxide at 37 °C until 70-90 % confluent then sub-cultured as detailed in section 2.2.1.2.

2.2.1.6 Differentiation of SH-SY5Y human neuroblastoma cells

Cells were seeded in growth medium as detailed in section 2.2.1.3 (typically 5000 cells/well of a 96 well plate or 400,000 cells in a T25 flask) and allowed to recover. Approximately 24 h after seeding, medium was carefully removed and replaced with differentiating medium (see below), then incubated in a humidified atmosphere of 95 % (v/v) air/5 % (v/v) carbon dioxide at 37 °C in the dark. SH-SY5Y cells were induced to differentiate in medium containing at final concentration:
- Leicester clone - DMEM containing 2 % (v/v) FBS, 2 mM L-Glutamine, 100 units/µl penicillin / 10 µg/ml streptomycin and 10 µM all-trans retinoic acid
- ECACC clone - DMEM/Ham's F12 containing 1 % (v/v) heat inactivated FBS, 2 mM L-Glutamine, 200 units/µl penicillin / 0.2 mg/ml streptomycin, 1 % (v/v) non essential amino acids and 10 µM all-trans retinoic acid or 1 nM staurosporine (STS).

- Johnson clone – RPMI-1640 containing 4 % (v/v) heat inactivated horse serum, 1 % (v/v) heat inactivated FBS, 2 mM L-Glutamine, 200 units/µl penicillin / 0.2 mg/ml streptomycin and 10 µM all-trans retinoic acid.

Components of differentiating medium for clones were used as recommended by their source. Cells were maintained, with differentiating media exchanged on days 3 or 4, for 7 days after which toxicity assays were commenced. Cells were induced to differentiate using 10 µM all-trans retinoic acid unless otherwise stated. In accordance with ECACC guidelines, ECACC clone cells were not differentiated beyond passage 20.

2.2.1.7 Coomassie blue staining

Medium was aspirated from cells using a Pasteur pipette. Cells were fixed for 20 min at - 20 °C in 90 % (v/v) methanol/Tris Buffered Saline (TBS: [50 mM Trizma base, 200 mM NaCl, pH 7.4]). Fixing solution was removed by inversion of the plate and cells were stained for 1-2 min in Coomassie brilliant blue G protein staining solution (de-stain solution [25 % (v/v) ethanol, 10 % (v/v) glacial acetic acid] containing 0.25 % (w/v) Coomassie brilliant blue G). Cells were rinsed twice in distilled water to remove excess stain and left to air-dry.

2.2.2 Quantification of axon outgrowth

In order to quantify outgrowth of axon-like processes, live cells cultured in T25 flasks were observed using phase contrast microscopy at x 100 magnification. Counts were made of total cell number and number of axon-like processes greater than two cell bodies in length in four random fields per flask. Axon outgrowth was expressed as a percentage of total cell number (axons/100 cells).

2.2.3 Assessment of cell viability

2.2.3.1 MTT tetrazolium salt assay for anchorage dependant cells

3-[4-5-Dimethylthiazol-2-y1]-2,5-diphenyl tetrazolium bromide (MTT) is a substrate that is taken up by cells and reduced by mitochondrial and endoplasmic reticulum dehydrogenase enzymes, to yield a purple formazan product that accumulates within cells depending on cell integrity and viability (Cookson *et al.,* 1995). Typically viability was assayed in cells cultured in 96 well plates where 10 μl 5 mg/ml MTT/Phosphate Buffered Saline (PBS: [137 mM NaCl, 2.68 mM KCl, 8.1 mM Na$_2$HPO$_4$, 1.47 mM KH$_2$PO$_4$, pH 7.4]) were added to the culture medium and incubated at 37 °C in a humidified atmosphere of 95 % (v/v) air/5 % (v/v) carbon dioxide for 1 h. After this time, all medium was removed from the cells and replaced with 100 μl DMSO. The plate was then agitated on an orbital shaker to dissolve the formazan product. Absorbance was read spectrophotometrically using a multi-plate reader at 570 nm. Absorbance results were expressed as mean percentage cell viability compared to controls ± standard error of the mean (SEM).

2.2.3.2 Trypan blue exclusion assay

Trypan blue is taken up by dead cells where it stains the cytoplasm, causing cells to shine bright blue when observed by light microscopy. Cells were induced to differentiate in 96 well plates as detailed in section 2.2.1.6. Medium was removed and each well rinsed twice with 100 μl DMEM to remove serum. To detach cells, 20 μl trypsin (100 μg/ml)/EDTA (40 μg/ml) in DMEM were added and cells incubated in a humidified atmosphere of 95 % (v/v) air/5 % (v/v) carbon dioxide at 37 °C for 5 min. Growth medium (30 μl) was added to quench the action of trypsin. The cell suspension was diluted 1:2 with 50 μl trypan blue (0.4 % [v/v]) and counted in a haemocytometer chamber as described in section 2.2.1.3. In each case total and dead cells were counted. The mean number of dead cells could then be expressed as a percentage of the total cell count ± SEM.

2.2.3.3 ATP assay

The ViaLight HS kit was used according to manufacturer's guidelines. This kit is based upon the bioluminescent measurement of ATP, utilising luciferase enzyme which catalyses the formation of light from ATP and luciferin. Cells were cultured in 96 well plates as described in section 2.2.1.1 and differentiated as described in section 2.2.1.6. To assay ATP, 100 µl nucleotide releasing agent were added to each well (containing 100 µl medium). After 5 min, extracts were transferred to a white luminometer microtitre plate. Using a luminometer 20 µl ATP monitoring reagent were added per well. Emitted light intensity was proportional to ATP concentration. Results were expressed as mean percentage cell viability compared to controls ± SEM.

2.2.4 MPP⁺/MPTP toxicity studies in mitotic and differentiated SH-SY5Y cells

Cells were seeded in growth medium at 10,000 or 5,000 cells/96 well for mitotic and differentiated studies, respectively and allowed to recover overnight. For cells to remain mitotic, medium was removed and replaced with fresh growth medium supplemented with MPP⁺. For cells to be differentiated over 7 days as detailed in section 2.2.1.6, medium was removed and replaced with differentiating medium. On day 7 medium was carefully removed and replaced with fresh differentiating medium supplemented with MPP⁺. Cells were incubated at 37 °C in a humidified atmosphere in 95 % (v/v) air/5 % (v/v) carbon dioxide in the dark. Cells were incubated with MPP⁺ for periods of up to 14 days; media treatments were changed twice weekly. Cell viability was assessed at given time points using the MTT assay, as detailed in section 2.2.2.1. Results of toxin treated cells are presented as mean percentage reduction of non-toxin treated controls ± SEM.

2.2.5   Protein extraction systems

2.2.5.1   *Total protein extraction from cells for detection of cytoskeletal proteins and tissue transglutaminase during differentiation and in response to MPP$^+$ treatment*

To extract total protein from cells the medium was carefully decanted from the flask and the monolayer washed twice with 1 ml PBS to remove serum. 500 µl ice cold extraction buffer (50 mM Trizma base pH 6.8, 150 mM NaCl, 5 mM EDTA, 1 % (w/v) sodium dodecylsulphate (SDS), 2 mM PMSF, 0.2 % (v/v) protease inhibitor cocktail) was pipetted directly onto the monolayer to lyse cells. The flask was agitated to ensure cell detachment and the extract immediately transferred to an Eppendorf tube on ice. For experiments where a significant number of cells were floating, they were included in the extraction; medium and PBS washes were collected and centrifuged at 150 x g for 5 min. The resultant pellet was added to the adherent cell extract. Total extracts were sonicated (six pulses) on ice, boiled for 1 min then vortex mixed to ensure homogeneity. Aliquots of samples were stored at - 20 °C prior to protein estimation by the Lowry method (see methods section 2.2.6.1).

2.2.5.2   *Differential cell extraction for detection of MAPK signalling pathway proteins*

For detection of proteins associated with MAPK signalling pathways, cells were seeded into 6 well plates at 80,000 cells/well and differentiated as detailed in methods section 2.2.1.6. On day 7, medium was carefully removed and replaced with fresh differentiating media (control wells), 10 µM MPP$^+$ or 5 mM MPP$^+$, chosen according to preliminary experiments to represent sub-cytotoxic and cytotoxic concentrations of toxins following short-term exposures. Cells were incubated with toxins and corresponding controls over a 24 h time-course. At given incubation times, media were carefully removed and replaced with 300 µl ice cold extraction buffer (50 mM Tris pH 6.8, 5 mM EDTA pH 6.8, 1 % (v/v) Igepal, 0.1 % (w/v) SDS, 150 mM NaCl, 1 mM sodium orthovanadate, 2 mM PMSF, 0.2 % (v/v) protease inhibitor cocktail). Cells were detached by gentle agitatation then transferred to an Eppendorf tube on ice. Samples were vortex mixed for 30 s then microfuged at

19000 x g for 10 min at 4 °C to pellet the insoluble fraction. Supernantant was aliquoted on ice and stored along with the insoluble pellet at - 20 °C prior to protein estimation by the Lowry method (see methods section 2.2.6.1). Note that following employment of the Lowry method all standards and samples were microfuged at 19000 x g for 1 min to spin down a precipitate that forms in the presence of this extraction buffer.

2.2.6 Estimation of protein in cell extracts

2.2.6.1 Micro-Lowry method

The protein content of samples was estimated using the Lowry method (Lowry *et al.*, 1951 (with modifications)). A calibration graph was constructed using bovine serum albumin (BSA) to represent 0-100 µg protein. Protein standards and test samples, both in extraction buffer, were diluted appropriately to a final volume of 100 µl in extraction buffer.

The working Lowry reagent was prepared as 2 % (w/v) $NaCO_3$, 1 % (w/v) $CuSO_4$, 2.7 % (w/v) NaK tartrate in 0.1 M NaOH immediately before use. 1 ml of reagent was added to each standard and sample, which were then vortex mixed and incubated at room temperature for 15 min. The reaction was developed over 30 min at room temperature, via addition of 100 µl Folin Ciocalteu's phenol reagent diluted 1:1 with distilled water. The solutions were vortex mixed and absorbances measured spectrophotometrically on a multiplate reader at 750 nm. A typical standard calibration curve of mean absorbance for standards (blanked for zero protein) versus protein concentration (µg/assay) is shown in Figure 2.1 from which the protein content of the samples could be estimated.
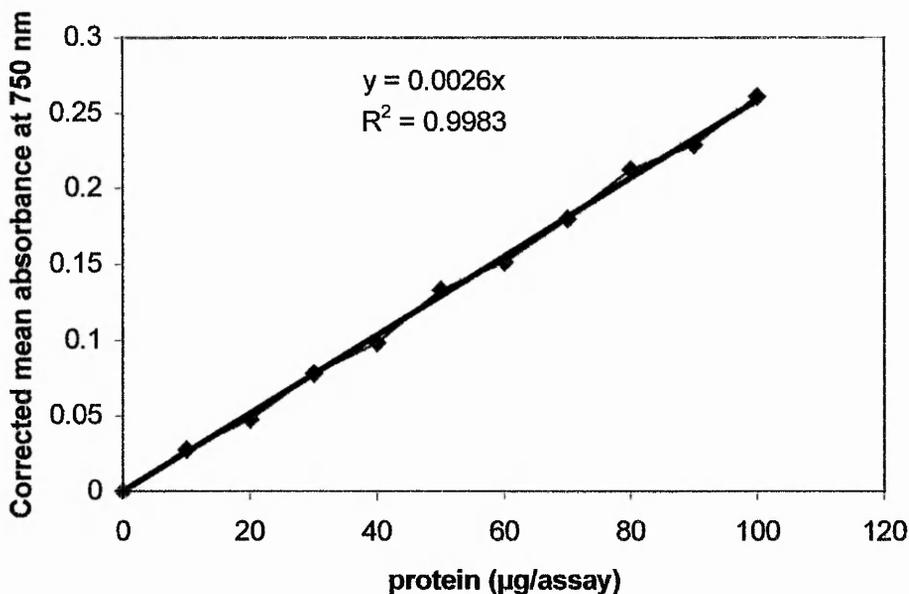
Figure 2.1 Standard calibration graph for BSA using the micro-lowry method

2.2.6.2 Bio-Rad protein assay

The Bio-Rad protein assay was used in accordance with the manufacturer's guidelines. A calibration graph ranging from of 0-100 μg protein was prepared from BSA as detailed in section 2.2.6.1. Samples were prepared as described in section 2.2.6.1. Bio-Rad dye reagent (neat reagent diluted 5 times with distilled water to a final volume of 5 ml) was added to each standard and sample, which were then vortex mixed. After a period of between 5 min and 1 h, absorbances were read at 620 nm.

2.2.7 Denaturing sodium dodecylsulphate polyacrylamide gel electrophoresis (SDS-PAGE)

2.2.7.1 Preparation of acrylamide resolving gels

SDS-PAGE separates proteins in a sample according to their size and molecular mass. Hence small proteins of lower molecular mass diffuse more rapidly than larger proteins and therefore travel further through the gel. SDS-PAGE was carried out as follows: -

1. The Bio-Rad mini Protean II apparatus was assembled according to the manufacturer's guidelines. In brief two glass plates were held, typically 1.5 mm apart, by vertical spacers.

2. For each gel, 10 ml gel mix was prepared as detailed in Table 2.1 and degassed under vacuum for 10 min. It should be noted that the 40 % acrylamide stock includes NN'- methylenebisacrylamide to give a final ratio of 29:1. For each 10 ml gel mix 100 μl 10 % (w/v) ammonium per sulphate (APS) and 10 μl TEMED were used as polymerisation agents, added immediately before the gel was poured.

3. Gels were poured approximately 2.5 cm from the top of the glass plates and covered with a layer of water-saturated butan-2-ol to exclude air. The gel mix was allowed to polymerise at room temperature for 30-45 min.

2.2.7.2 Preparation of stacking gel

Once the resolving gel had polymerised, the butan-2-ol was rinsed away with SDS-PAGE buffer (0.0256 M Tris base; 0.192 M Glycine; 0.1 % SDS). Typically 3 ml 4 % (v/v) acrylamide stacking gel were used per gel (see Table 2.2) and degassed under vacuum over 10 min. The volumes of reagents required to prepare 100 ml stock stacking gel mix are shown in Table 2.2. To polymerise 3 ml of the stacking gel stock, 12 μl TEMED and 30 μl APS were added immediately before pouring. Stacking gel mix was poured above the resolving gel to the top of the glass plates. Combs were positioned (10 wells) within the gel

to form individual wells. The gel was allowed to polymerise for 30 min at room temperature before removal of the combs and transfer of the gel to an electrophoresis running chamber to be submerged in SDS-PAGE buffer.

Reagent	7.5% Acrylamide	10% Acrylamide	12% Acrylamide	15% Acrylamide
40 % Acrylamide stock	1.88 ml	2.50 ml	3.00 ml	3.75 ml
1.5 M Tris buffer (pH 8.8)	2.50 ml	2.50 ml	2.50 ml	2.50 ml
10 % SDS	100 µl	100 µl	100 µl	100 µl
Millipore (distilled) water	5.50 ml	4.90 ml	4.40 ml	3.65 ml

Table 2.1 Preparation of Acrylamide resolving gels

Table 2.1 details the methods for preparation of acrylamide resolving gels. Separation of proteins within a sample can be varied according to the percentage of acrylamide within the resolving gel. For greater separation of high molecular weight proteins, a lower percentage acrylamide gel would be used and vice versa.

Reagent	Volume (ml) (to make 100 ml)
40 % Acrylamide stock	10
0.5 M Tris buffer pH 6.8	25
10 % SDS	1
Millipore (distilled) water	64

Table 2.2 Preparation of 100 ml stock 4 % acrylamide stacking gel.

2.2.7.3   Preparation of samples for SDS-PAGE

Samples (typically 20-50 µg protein), were diluted 1:1 in 2 x concentrated reducing electrophoresis sample buffer (4 % (w/v) SDS; 30 % (v/v) glycerol; 0.1 M Tris HCL pH 6.8; 100 mM DTT; 0.01 % (w/v) Bromophenol blue). Samples and pre-stained molecular weight markers (10 µl/gel) were heated to 100 °C for 5 min then microfuged at high speed for 10 s to recover all the sample prior to loading and separation at a constant current (40 mA/gel). Current was stopped as the dye front ran off the bottom of the gel.

2.2.7.4   Acetone precipitation

Where the calculated volume of sample was too large to be loaded into the well of a gel, acetone precipitation was used. The required sample volume, in an Eppendorf tube, was vortex mixed with 5 times its volume of ice-cold acetone prior to incubation at - 20 °C for a minimum of 2 h. The mixture was then microfuged at 19000 x g for 10 min. Supernatant was carefully removed and discarded and the pellet re-suspended in an appropriate volume of reducing electrophoresis sample buffer for loading.

2.2.8   Western blotting and immunoprobing of proteins

2.2.8.1   Western blotting

Proteins separated by SDS-PAGE were transferred electrophoretically to a nitrocellulose membrane by Western blotting using one of two methods:

Wet blotting (Bio-Rad Trans-Blot electrophoretic transfer system): - Four pieces of filter paper and one piece of nitrocellulose were cut to the same size as the gel and pre-saturated with electroblotting buffer (48 mM Trizma base, 39 mM glycine, 20 % (v/v) methanol, 0.0375 % (w/v) SDS). The gel was laid on top of the sheet of nitrocellulose. This was sandwiched on each side with two pieces of filter paper and two fibre pads. Care was taken during this procedure to ensure that air pockets were not trapped. The sandwich was held in a plastic case submerged in electroblotting

buffer in a tank. For overnight blotting, 30 V were applied over 16 h at room temperature. The process could also be carried out in 1 h 30 min at 100 V according to manufacturer's instructions.

Semi-dry blotting (ATTO HorizBlot): - The internal blotter surfaces were flooded with distilled water. The gel was laid on top of a piece of nitrocellulose of equal size. Again care was taken to ensure that any air pockets were removed. This was sandwiched on either side by six pieces of filter paper of equal size, all pre-saturated with electroblotting buffer. Excess buffer was removed from the blotter surface and a current of 2 mA/cm gel was applied over 1 h 30 min.

2.2.8.2 *Immunoprobing*

2.2.8.2.1 *Preparation of nitrocellulose for immunoprobing*

Protein transferred to nitrocellulose during the blotting process was stained with copper pthalocyanine 3,4´4,"4,'" tetrasulphonic acid tetrasodium salt (0.05 % (w/v) in 12 mM HCl), to ensure adequate transfer and to allow for photography (GeneTools gel analysis system). The nitrocellulose was then cut as required for immunoprobing and de-stained in 12 mM NaOH.

2.2.8.2.2 *Blocking of non-specific antibody binding and immunoprobing with primary and secondary antibodies*

Non-specific antibody binding was prevented by blocking of nitrocellulose for 1 h in 3 % (w/v) marvel milk/TBS or 3 % (w/v) BSA/TBS with gentle shaking. Nitrocellulose sections were incubated with primary antibody diluted in blocking agent overnight at 4 °C with gentle shaking. Information regarding the epitope specificity and required dilutions of primary monoclonal antibodies used are detailed in Table 2.3. Unbound primary antibody was removed by washing with TBS/0.1 % (v/v) Tween 20 for 6 x 10 min washes with vigorous shaking. Nitrocellulose sections were incubated with an alkaline phosphatase - or horseradish peroxidase (HRP) - conjugated secondary antibody diluted 1:1000 in blocking agent for development via colourmetric or enhanced chemiluminescence methods respectively (see sections

2.2.8.2.3 and 2.2.8.2.4), for 2 h at room temperature with gentle shaking. Unbound antibody was washed again as above.

2.2.8.2.3 Alkaline phosphatase development system

Blots were washed for 5 min in distilled water then equilibrated for a further 5 min in substrate buffer (0.75 M Tris, pH 9.5). Immunoprobing was developed in the dark by addition of alkaline phosphatase substrate solution [20ml substrate buffer; 44 µl NBT (75 mg/ml in 70 % (v/v) DMF); 33 µl BCIP (50 mg/ml)], prepared immediately prior to use. The reaction was allowed to proceed until bands had appeared. To stop the reaction the substrate was poured off and the nitrocellulose rinsed with distilled water. Nitrocellulose was dried between sheets of filter paper.

2.2.8.2.4 Enhanced Chemiluminescence (ECL) development system

ECL was performed using a kit from Amersham Pharmacia Biotech UK Ltd, according to manufacturers instructions. In brief, solution A and solution B were mixed in equal volumes to a final volume of 1 ml / 9 x 6 cm^2 nitrocellulose then immediately incubated with the nitrocellulose for 1 min. Excess ECL substrate was drained and the nitrocellulose was placed protein-side facing downwards onto SaranWrap. The SaranWrap was folded so as to envelop the nitrocellulose. Care was taken to avoid trapping air pockets. The nitrocellulose was placed protein-side facing upwards into a film cassette and held in place with masking tape. Photographic film was exposed to nitrocellulose in the dark for the required time, dependent on the primary antibody used. Film was removed from the cassette and placed immediately into developing solution (diluted 1:5 in water) for 1 min, rinsed in water then transferred to fixing solution (diluted 1:5 in water) for a further minute. The film was washed again and then allowed to dry at room temperature.

2.2.8.2.5 Stripping and re-probing membranes

Primary and secondary antibodies could be completely removed from membranes and membranes re-probed several times. Membrane was submerged in stripping buffer (100 mM 2-mercaptoethanol, 2 % (w/v) SDS, 62.5 mM Tris-HCl pH 6.7) and

incubated at 50 °C for 30 min with occasional agitation. The membrane was washed 2 x 10 min in TBS/0.1 % (v/v) Tween-20, then blocked and re-probed as detailed in section 2.2.8.2.2.

2.2.8.2.6   Quantification of Western blots

To allow for quantitative comparison of protein band intensity following Western blotting and immunoprobing, a process of manual band quantification was performed using the GeneTools quantification system (Syngene), according to manufacturer's guidelines. In brief, equal sized boxes were drawn around bands to be quantified. For each band an equal sized box was also drawn to represent background. In drawing boxes, raw volume figures were generated which represent the number of pixels in each box multiplied by the grey shade value of each pixel. The background value for each band was subtracted from the band value to give a corrected pixel volume.

Antibody	Epitope specificity	Working Dilution (Western blotting)	Working Dilution (immuno-cytochemistry)
N52 (monoclonal)	Anti-NF-H/NF-M (phosphorylation independent)	1:500 – 1:1000	1:200
SMI31 (monoclonal)	Anti-NF-H /NF-M (phosphorylation dependent)	1:1000	1:500
RT97 (monoclonal)	Anti-NF-H (phosphorylation dependent)	1:500	N/A
CUB-7402 (monoclonal)	Anti-transglutaminase II, cellular/tissue Ab-1	1:1000	1:20
TUB 1/2 (monoclonal)	Anti-β-tubulin	1:500	1:200
B512 (monoclonal)	Anti-α-tubulin	1:500	1:200
Bcl-2 (monoclonal)	Anti-human Bcl-2	1:1000	N/A
Phospo-ERK 1/2 (monoclonal)	Anti-phosphorylated ERK1/2	1:500	N/A
Phospho-JNK 1/2 (monoclonal)	Anti-phosphorylated JNK1/2	1:100	N/A
GAP-7B10 (monoclonal)	Anti-GAP-43	N/A	1:20
Total ERK 1/2 (polyclonal)	Anti-total ERK 1/2	1:500 – 1:1000	N/A
UG9510 (polyclonal)	Anti-ubiquitin-protein conjugates	1:1000	N/A
p35 (polyclonal)	Anti- p35	N/A	1:20

Table 2.3 Epitope specificity and working dilutions required for primary antibodies for Western blotting and immunocytochemistry techniques.

2.2.9   Immunocytochemical analysis of proteins

2.2.9.1   Seeding and differentiation of cells

SH-SY5Y cells were seeded in 300 µl growth media into an eight well permanox chamber slide at a density of 10,000 cells/chamber and induced to differentiate as detailed in section 2.2.1.6.

2.2.9.2   Fixing of cells

With care, differentiation medium was removed and cells washed twice in PBS to remove serum. Cells were fixed using two protocols: -

1. Cells were fixed in 200 µl ice-cold 90 % (v/v) methanol / TBS at - 20 °C for 10 min. Methanol was removed and cells were again washed twice with PBS. Cells were further permeabilised in 200 µl 0.5 % (v/v) Triton X-100/PBS for 10 min at room temperature, washed in PBS as before and then allowed to air-dry.

2. Cells were permeabilised prior to fixing (to remove soluble proteins) in 200 µl 0.01 % Igepal in 5 mM $MgCl_2$/PBS for 5 min at room temperature. This was removed and the cells washed twice in PBS. Cells were then fixed in ice-cold 90 % (v/v) methanol / TBS at - 20 °C for 10 min and washed a further two times in PBS. Slides were stored at 4 °C until immunoprobing was performed.

2.2.9.3   Immunoprobing of cells

Cells were re-hydrated in PBS for 20 min at room temperature. Non-specific antibody binding was prevented by blocking with 3 % (w/v) bovine serum albumin BSA/PBS for 1 h at room temperature with gentle shaking. Cells were incubated with primary antibody diluted in the above blocking agent overnight at 4 °C. Cells were washed in PBS for 3 x 5 min in their chambers then incubated with Fluorescein Isothiocyanate (FITC) conjugated secondary antibody diluted 1:50 in blocking agent for 2 h at room temperature, in the dark. Excess secondary antibody was removed by

3 x 5 min washes in PBS in the dark. Slides were carefully air-dried. Vectashield preservative solution ± propidium iodide was applied to the slide before a cover slip was placed over the cells and glued into place. The slide was then stored at - 20 °C in the dark to prevent bleaching of fluorescence signal prior to viewing by confocal laser microscopy.

2.2.10 Assessment of TG activity in MPP$^+$ treated cells.

The ability of TG enzymes to incorporate polyamines into proteins can be exploited to determine the level of TG activity within cells. A method by Zhang *et al.,* (1998a) (with modifications) was used to visual proteins into which a pseudo-substrate for TG became incorporated. Cells were seeded into T25 flasks and differentiated as detailed in section 2.2.1.6. On day seven medium was removed and replaced with fresh differentiating medium or fresh medium supplemented with MPP$^+$. 1 h prior to the end of MPP$^+$ incubation, EZ-link 5-(biotinamido) pentylamine (50 mM) was added to each flask at a final concentration of 2 mM. Following 1 h incubation, cells were extracted as detailed in section 2.2.5.1. Ionomycin (1 mM in DMEM) was used as a positive control; cells were differentiated as above, however 2 mM EZ-link 5-(biotinamido) pentylamine was added for 1 hr prior to 15 min incubation with 10 μM ionomycin. Protein in extracts was estimated using the Lowry method as detailed in section 2.2.6.1 and separated by SDS-PAGE. Following Western blotting, nitrocellulose was blocked in 3 % (w/v) marvel milk/TBS and incubated overnight at 4 °C with Neutravidin HRP conjugated secondary antibody (2 μg/ml) (which binds to incorporated amines), diluted in blocking solution. Unbound antibody was washed 6 x 10 minutes in TBS/0.1 % (v/v) Tween-20. Incorporation of EZ-link 5-(biotinamido) pentylamine was revealed by ECL as detailed in section 2.2.8.2.4.

2.2.11 Statistical analysis

Data was presented as mean ± the standard error of the mean (SEM). Statistical analysis was performed using two-tailed, homoscedastic, Student's t-Tests. Statistical significance was accepted at $p < 0.05$ or $p < 0.01$.

CHAPTER III

ESTABLISHMENT OF A DIFFERENTIATED PHENOTYPE IN AN SH-SY5Y HUMAN NEUROBLASTOMA CELL LINE

3.1 INTRODUCTION

3.1.1 SH-SY5Y human neuroblastoma cell line – a potential model for MPP$^+$ studies

Whilst animal models provided early important information with regards to symptomatic, pathological and behavioural defects that result following exposure to MPTP, their application is limited and hindered by ethical considerations. *In-vitro* studies of homogenous cell populations allow the investigation of sub-cellular biochemical processes with much tighter control of the environmental conditions of a particular cell type. Employment of a neuroblastoma human cell line should allow development of a model with greater analogy to neurones *in-vivo*. Thus a study of the effects of neurotoxins on *in-vitro* cultures of human neuroblastoma cells is warranted.

The SH-SY5Y cell line is the third cloned sub-line from a parent neuroblastoma cell line SK-N-SH (SK-N-SH→ SH-SY→ SH-SY5→ SH-SY5Y). SK-N-SH was established in 1970 from the metastatic bone tumour of a young female (Biedler *et al.*, 1973). Early characterisation of the SK-N-SH cell line by Ross *et al,* (1983) and Ciccarone *et al,* (1989) suggested that it comprised of three morphologically distinct cell types. One type, the parent of the SH-SY5Y cell line, SH-SY, was neuroblast like with a small cell body giving rise to short neuritic processes (N type). This cell type was poorly adherent but capable of forming focal aggregates (Biedler *et al.*, 1978). The second cell type was epithelial/fibroblast like, morphologically larger, flatter and highly substrate adherent (S type). The third was an intermediate cell type expressing properties of both other cell types (I type). The cell types were not only morphological different but biochemically distinct also. Further research indicated that cells could undergo spontaneous bi-directional phenotypic and biochemical inter-conversion between neuroblast like and fibroblast like types, a process termed transdifferentiation (Ross *et al.*, 1983).

The SK-N-SH cell line was regarded as predominantly adrenergic but multipotential with regard to neuronal enzyme expression (Biedler *et al.*, 1978). As a serially isolated neuroblast clone, SH-SY5Y expresses tyrosine hydroxylase activity (and

therefore can convert tyrosine to DA) and also dopamine β hydroxylase activity (for conversion of DA to norepinephrine) (Ciccarone *et al.,* 1989). The cells can also convert glutamate to GABA (Biedler *et al.,* 1978). The SH-SY5Y clone has been widely exploited in neurochemical investigations including those involving MPTP and MPP$^+$ (Song *et al.,* 1997; Song and Ehrich, 1997a, 1997b, 1998). Apart from its human origin, the clone has the advantage over the murine N2a clone, previously used and characterised in our laboratory, of being able to transport DA due to expression of the DA receptor, hence facilitating MPP$^+$ uptake (reviewed by Song and Ehrich, 1998). In contrast to MPP$^+$, MPTP is taken up into cells via a non-catecholaminergic mechanism (Song and Ehrich, 1998).

3.1.2 Differentiation of the SH-SY5Y cell line

A major advantage of this cell line is its reported ability to produce terminally differentiated cells with a mature neuronal phenotype using chemical agents (Hartley *et al.,* 1996; Lo Presti *et al.,* 1992; Tieu *et al.,* 1999). Neuronal differentiation is a complex process involving intracellular and extracellular signalling molecules including hormones, cytokines, morphogens and trophic support along with interactions between cells and their substratum (reviewed by Lopez-Carballo *et al.,* 2002). This process requires cells to withdraw from the cell cycle into the Go phase and exhibit neurite outgrowth in response to cellular signals (Pahlman *et al.,* 1984). Considerable research has been carried out to assess the potential of various differentiating agents in the SH-SY5Y cell line. Such agents have included all-trans retinoic acid, staurosporine, 12-0-tetradecanoylphorbol-13-acetate (TPA), nerve growth factor (NGF), herbimycin and insulin (reviewed by Tieu *et al.,* 1999). Tieu *et al,* (1999) review the major biochemical, morphological and functional changes exhibited by SH-SY5Y upon differentiation induced by chemical agents, to include the following: inhibition of proliferation; increased neurite process length; increased noradrenaline, neuron specific enolase activity and growth associated protein – 43 (GAP-43).

3.1.2.1 Neuronal differentiation induced by all-trans retinoic acid

All-trans retinoic acid has been successfully employed most commonly as a chemical differentiating agent in SH-SY5Y cells (Hartley *et al.,* 1996, 1997; Sharma *et al.,* 1999; Tieu *et al.,* 1999). The mode of action of retinoic acid in differentiating cells continues to be elucidated. Retinoic acid is the biologically active derivative of Vitamin A and plays a key role in embryonic development *in-vivo* (reviewed by Chambaut-Gurein *et al.,* 2000). Following entry into the nucleus, retinoic acid binds two isoforms of ligand activated nuclear transcription factors, (which belong to the super family of nuclear hormone receptors), retinoic acid receptors (RARs) and retinoid X receptors (RXRs). These in turn bind retinoic acid responsive elements (RAREs), controlling the activity of specific genes (Lopez-Carballo *et al.,* 2002; Ruiz-Leon and Pascual, 2003). In this way retinoic acid instigates the control of target genes, the down stream consequence of which support the differentiation and survival of cells. Lopez-Carballo *et al,* (2002) have found that mRNA levels and protein expression of differentiation-inhibiting basic helix-loop-helix (bHLH) transcription factors ID1, ID2 and ID3 are down regulated during early retinoic acid induced regulation in SH-SY5Y cells, with a concomitant increase in expression of differentiation promoting genes, NEUROD6 and NEUROD1. These changes in gene expression were surmised to require increased PI3-K and a concomitant Akt phosphorylation, a signalling pathway that is also important in cell survival (Brunet *et al.,* 2001; Brazil *et al.,* 2004). Antonyak *et al.,* (2002) report that whilst both PI3-K and ERK were activated by retinoic acid in NIH3T3 mouse fibroblast cells, only PI3-K was necessary for retinoic acid induced tissue transglutaminase expression and subsequent mediation of tissue transglutaminase GTP binding activity, prerequisites for differentiation (see section 3.1.4 for further details). In one study, retinoic acid is proposed to induce Myocyte enhancing factor 2 (MEF-2), a transcription factor believed, via p38α activation, to prevent apoptosis during neuronal development (Okamoto *et al.,* 2000) The authors propose MEF-2 to work in concert with bHLH transcription factors. Retinoic acid also stimulates expression of tropomyosin receptor kinase B (TrkB) receptors in SH-SY5Y cells, which bind the neurotrophin brain derived neurotrophic factor (BDNF), a union which promotes neurite generation (Encinas *et al.,* 1999; Ruiz-Leon and Pascual, 2003).

3.1.2.2 *Markers of retinoic acid induced differentiation*

If a cell culture model is to boast that it is "pre-differentiated" it should be supported by morphological and biochemical studies. Ideally a marker protein can be identified and its presence monitored in cell extracts during a differentiation time course. Tieu *et al*, (1999) report that retinoic acid induced differentiation results in up regulation of the anti-apoptotic gene Bcl-2. Expression of GAP-43, which is highly abundant within the neuronal growth cone, is regulated during neuronal differentiation but its exact role remains unresolved; indeed literature suggests that its expression may be transient (Encinas *et al.,* 1999; Lopez-Carballo *et al*, 2002; Chambaut-Guerin *et al*, 2000). Up-regulated tTG expression and activity is also characteristic of retinoic acid induced differentiation in SH-SY5Y cells (Tucholski et al., 2001) (discussed in detail in section 3.1.4). The period of time over which SH-SY5Y can survive in the presence of retinoic acid can be extensive. For example, Hartley *et al*, (1996) differentiated SH-SY5Y cells in 10 μM retinoic acid in the presence of reduced foetal bovine serum (1 %) over 28 days with weekly media changes. Numbers of mitotically active cells were significantly reduced by 8 days of retinoic acid treatment. It has to be noted that the presence of biochemical markers associated with neuronal differentiation can be transient (as was noted for GAP-43 above) and their presence therefore dependent on time post retinoic acid treatment.

3.1.3 The neuronal cytoskeleton and associated post-translational modifications

Due to the unique morphology and functional requirements of neurones, their cytoskeletal organisation is specially designed. They comprise of a cell body (within which most cytoskeletal proteins are synthesised), from which short dendritic processes and a long axon extend during the differentiation process. Along the axon electrical impulses (action potentials) travel in anterograde fashion (away from the cell body). This is an ion-dependent, cyclic process of depolarisation/repolarisation of the membrane brought about by transient increases in membrane permeability to Na^{2+} and K^+, acting to propagate the signal down the axon.

Of significance in neuronal cells are phosphorylation and dephosphorylation events of NFs. The general consensus appears to be that phosphorylation of NFs can occur as they travel along the axon, thus promoting incorporation into the cytoskeleton, but also in the cell perikaryon (Shea *et al.,* 1988, 1990). Recent research has suggested that a soluble pool of phosphorylated NF-H remains in the cell perikarya of mature neurones (Shea *et al.,* 1997b). An overall increase in phosphorylation reduces the mobility of NFs and promotes their incorporation into stationary complexes, thus contributing to neurite outgrowth and stabilisation (Nixon, 1998; Shea *et al.,* 2003). Such phosphorylation events occur some time after NF expression and are considered to signify neuronal maturation. Phosphorylation occurs via KSP (Lys-Ser-Pro) repeats located in the tail domains of NF sub-units (Giasson & Mushynski, 1996), catalysed by a number of independently regulated enzymes i.e. glycogen synthase kinase-3, ERK, CDK-5, and SAPK/JNK (Guidato *et al.,* 1996; Giasson & Mushynski, 1996; Veeranna *et al.,* 1998 and Sun *et al.,* 1996). Being of human origin, SH-SY5Y cells contain KSP repeats of which 34 of the 43-44 present are KSPXP repeats, major phosphorylation targets of CDK-5. As such CDK-5 activity is proposed to be of particular significance in NF phosphorylation in this cell line (Sharma *et al.,* 1999c). Integrins in turn, have been shown to influence CDK-5 activity (Li *et al.,* 2000). Integrins are trans-membrane, heterodimeric receptors which play important roles in cell adhesion, nerve regeneration and migration through interactions with extracellular matrix components such as laminin (reviewed by Li *et al.,* 2000). Retinoic acid has been shown to upregulate α_1 and β_1 integrin expression in SH-SY5Y cells during differentiation and, via binding of integrins with laminin, this has been shown to upregulate the CDK-5 activator p35 leading to CDK-5 activation and subsequent NF-H phosphorylation and neurite outgrowth (Li *et al.,* 2000).

Hartley *et al,* (1996), noted that markers of neuronal maturity i.e. NF heavy chain (NF-H) phosphorylation increased over the differentiation period in SH-SY5Y cells in conjunction with reduced vimentin (intermediate filament protein) and increased synapsin levels. Sharma *et al,* (1999c) demonstrated increased NF-H and NF-M chain phosphorylation correlating with long neurite formation, following 6 days differentiation with 10 μM retinoic acid/10 % heat inactivated FBS with media changed every 24 h. In comparison, non-differentiated cells contained predominantly

de-phosphorylated NFs. In the same differentiated cells, NF light chain phosphorylation state remained unchanged in this study.

Prior to differentiation neuronal cells exhibit short neurites. As noted earlier, upon differentiation an axon forms, requiring specialised cytoskeletal function and organisation. Within this process, one neurite outgrows all others. *In-vivo*, axon generation is a highly specialised process involving environmental signals to determine which neurite will become the axon and the direction of this neuronal outgrowth. A proportion of remaining neurites may form dendritic processes (Siegel, 1999) exhibiting mixed polarity MTs and high MAP-2 expression. Macleod *et al,* (2001), reported that when SH-SY5Y cells were differentiated with 10 μM retinoic acid for 6 days with media replaced at 48 h intervals, cells developed immunopositivity for the neuronal marker MAP-2 and the G_0 associated cell cycle protein p21^{waf}. During axon outgrowth, tau expression and phosphorylation are critical for the initial elongation process (Siegel, 1999). Sharma *et al,* (1999) demonstrated that tubulin levels were unaffected by retinoic induced differentiation whilst tau expression increased, a finding supported by Hartley *et al,* (1996).

3.1.4 Tissue Transglutaminase (tTG)

In-vitro studies with SH-SY5Y indicate that elevated tTG expression and activity occurs concomitantly with neurite outgrowth and reduction in cell proliferation in response to retinoic acid treatment (Tucholski *et al.,* 2001). Through wild type and mutant tTG transfection studies Tucholski *et al* (2001) highlight the necessity for transamidation activity rather than simply protein expression for morphological differentiation. Miller and Anderton, (1986) propose that tTG plays a role in cell function/survival via NF modification. Of significance is that Singh *et al,* (2003) propose an additional role for tTG following retinoic acid induced activation. They propose that tTG activation causes transamidation of the small G-protein RhoA, causing RhoA to become constitutively active. Active RhoA binds and activates RhoA-associated kinase-2 (ROCK-2) leading to formation of stress fibres and focal adhesion complexes and, significantly, promoting the activation of ERK 1/2 and p38γ, which may control gene expression for differentiation. Moreover tTG has been shown to increase adenylyl cyclase activation. This causes enhanced cAMP

production and consequently greater cAMP-response element-binding protein (CREB) activation, said to play an important role in neuronal differentiation (Tucholski and Johnson, 2003).

3.1.5   Anti-apoptotic protooncogene Bcl-2

The Bcl-2 gene belongs to the Bcl-2 family that collectively includes a number of similar genes that can be described as either pro or anti-apoptotic in function. They represent key regulators in apoptosis, functioning at different levels of the apoptotic pathway to activate downstream signalling pathways and can themselves be regulated both post-transcriptionally and post-translationally, thus altering their function accordingly. The major target of this family is the mitochondrion and hence it can regulate apoptosis via control of cytochrome c release (reviewed by Blum *et al.*, 2001). Bcl-2 is itself anti-apoptotic and *in-vivo* studies suggest that Bcl-2 expression can protect neurones from cell death during development (Farlie *et al.*, 1995). Of interest is that in cell culture systems, Bcl-2 expression has been reported to increase in response to retinoic acid induced differentiation. Indeed Tieu *et al,* (1999) reported that in SH-SY5Y cells induced to differentiate by retinoic acid, Bcl-2 expression was shown to increase with a concomitant decrease in p53 expression over a 6 day differentiation time course. This was hypothesised to involve indirect activation of PKC by retinoic acid, in turn influencing p53 expression that acts to negatively regulate Bcl-2. Hence although not directly involved in the morphological transformation of cells undergoing differentiation, Bcl-2 may represent a biochemical marker associated with the differentiation process, suggesting that apoptotic pathways and those associated with morphological and biochemical differentiation may at some point converge.

3.1.6   Aims of chapter

The aim of this chapter was to establish and characterise the differentiation process afforded by all-trans retinoic acid in three clones of the SH-SY5Y cell line. The first clone to be used was a kind gift from Professor S.R. Nahorski, Pharmaceutical Sciences, Leicester University. Studies using a second clone from ECACC commenced several months into the project. The third clone was a kind gift from

Professor M. Griffin, formally of the School of Biomedical and Natural Sciences, The Nottingham Trent University and originated from Dr G.V.W. Johnson, Department of Psychiatry and Behavioural Neurobiology, University of Alabama. This clone was not made available until a late stage of the project. The morphological characteristics of the differentiation process were analysed and biochemical markers of differentiation established, to achieve terminally differentiated, viable cells, with a view to employing a pre-differentiated system in subsequent MPP^+ studies.

3.2 RESULTS

3.2.1 Preliminary characterisation of the SH-SY5Y cell line using the Leicester clone

Initial studies with SH-SY5Y cells were performed using a clone kindly received from Professor S.R. Nahorski, Pharmaceutical Sciences, Leicester University and recommended for the study of NFs by Professor B Anderton, Institute of Psychiatry, Kings College, London.

The SH-SY5Y cell line was previously uncharacterised in my laboratory at the Nottingham Trent University. Many preliminary studies on differentiation were performed using this clone including successful establishment of a differentiation protocol afforded by all-trans retinoic acid; retinoic acid and foetal bovine serum (FBS) concentrations were defined to support morphologically differentiated, viable cells. It was envisaged that a protocol be determined whereby cells were cultured in reduced serum conditions over an extended time period so as to maximise the window of opportunity for toxicological studies. Mitotic cells exhibited short extensions; however treatment of cells with retinoic acid increased their number. When stained with coomassie blue, differentiation was characterised by the presence of long, sweeping, spiny axon-like processes extending from rounded cell bodies and a reduction in cell proliferation. Figure 3.1 shows morphological differentiation of the Leicester clone following a protocol in which cells were seeded in growth medium at varying densities (1000, 2500, 5000 cells/well) into 96 well plates and allowed to recover for 24 h. The aim was to establish the lowest serum concentration that allowed cells to survive/differentiate in retinoic acid. Medium was replaced with medium containing 1 %, 2 %, 5 % or 10 % FBS $\pm$ 10 or 20 μM retinoic acid. Medium was replaced at 48 h intervals over a 6 day time course, after which, cells were fixed and stained with coomassie blue. At day 6 it was clear that 20 μM retinoic acid was toxic to cells irrespective of FBS concentration (see Fig 3.1B for 2 % FBS), At the lower densities (1000/2500 cells/well) 10 μM retinoic acid maintained differentiation most effectively in the presence of 2 % serum as determined by morphological observations (see Fig 1D) and MTT assay (results not shown). At this

FBS concentration control cells remained healthy, exhibiting many neuritic processes. At lower FBS concentrations, 10 μM retinoic acid resulted in cell death (Fig 3.1F). Thus results suggested the most effective retinoic acid concentration to be 10 μM in accordance with previous studies (Hartley *et al.,* 1996; 1997; Sharma *et al.,* 1999) with 2 % FBS.

Having established a suitable differentiation protocol for the SH-SY5Y Leicester clone in terms of morphological assessment, it was necessary to biochemically assess this differentiation state to determine whether cells had become terminally differentiated. As discussed, NF phosphorylation status is indicative of neuronal maturation and can be used as a marker of differentiation in neuroblastoma cells. NF status can be assessed using various immunobiochemical techniques, therefore an essential aspect of this work was to determine the antibody repertoire suitable for detection of "total" NFs (NF protein, irrespective of phosphorylation status) and phosphorylated NFs in SH-SY5Y cells. However, it became apparent that this clone did not exhibit the characteristics described by other authors for SH-SY5Y cells: -

- Cells could not be maintained in a healthy differentiated state beyond six days, in contrast to published studies showing sustained viability for up to twenty-eight days (Hartley *et al.,* 1996).

- Total and phosphorylated NF proteins were scarcely detectable in cell extracts using a variety of extraction methods in conjunction with several NF-specific antibodies.

The Leicester clone was subsequently abandoned since it was deemed to be unsuitable for the proposed work. However important progress had been made in terms of method development. An alternative SH-SY5Y clone was purchased from ECACC to continue the investigation.
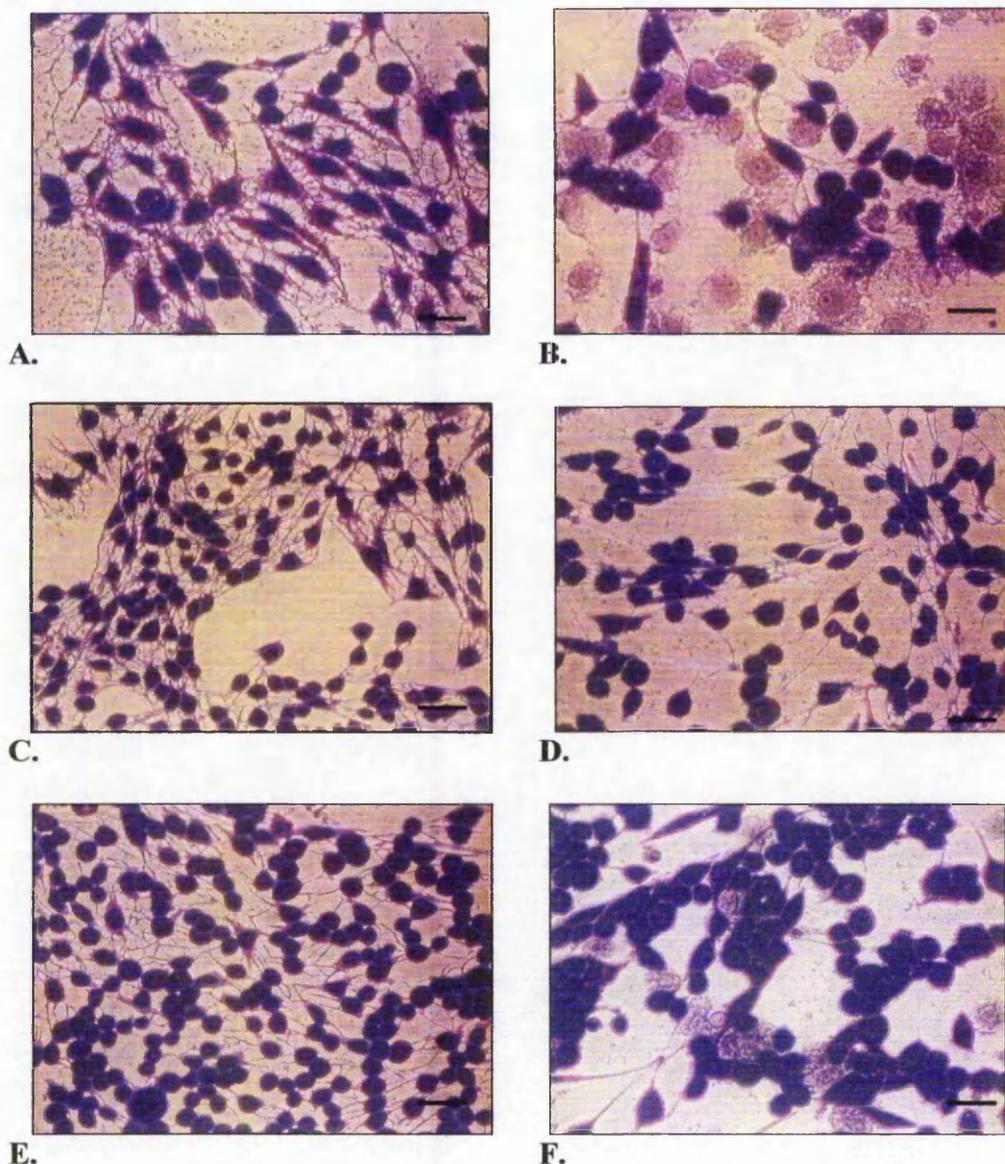
Figure 3.1 Morphological assessment of retinoic acid induced differentiation in the Leicester clone.
Figure 3.1 shows as follows: - (A) Mitotic cells cultured in growth medium containing 10 % FBS, (B) cell death caused by 6 days culture with 2 % FBS and 20 µM retinoic acid, (C) control cells cultured with 2 % FBS, (D) cells cultured with 2 % FBS and 10 µM retinoic acid, (E) control cells cultured with 1 % FBS, (F) cells cultured with 1 % FBS and 10 µM retinoic acid. Initial seeding density in all examples was 1000 cells/well. B-D are following a 6-day differentiation protocol. Cells were fixed in methanol/TBS and stained with Coomassie brilliant blue as detailed in methods section 2.2.1.7. Cells were visualised using light microscopy. Scale bar represents 40 µm.

3.2.2 Differentiation studies using the ECACC SH-SY5Y clone

3.2.2.1 Initial characterisation of retinoic acid treatment

The SH-SY5Y cell line was purchased from ECACC at the lowest passage number available, which was passage 11. This was considered important since according to ECACC guidelines, SH-SY5Y cells should not be used beyond passage 20, since the loss of neuronal characteristics has been ascribed to high passage number. As for the Leicester clone, initial experiments sought to establish suitable seeding density and serum conditions in the presence of retinoic acid to give differentiated, viable cells. Unpredictably and despite numerous attempts, cells would not routinely differentiate until they had reached passage 18. In some instances, cells would not differentiate at all and therefore would not be used in experiments. In accordance with ECACC guidelines cells were not used beyond passage 20. In subsequent experiments the ECACC clone was evaluated for suitability as a pre-differentiated human cell system in neurotoxicity studies.

3.2.2.2 Morphological assessment following differentiation with all-trans retinoic acid.

In initial experiments employing the ECACC SH-SY5Y clone a differentiation protocol was tested whereby cells were induced to differentiate 24 h post seeding in growth medium containing FBS at a range of concentrations from 1 % to 10 % of the total volume, supplemented with 10 µM retinoic acid. Medium was changed once over a 7-day time course (routinely day 3 or day 4). Figure 3.2 shows the morphological transition of ECACC clone cells from mitotic cells to neurone-like, differentiated cells over 7 days of treatment with 1 % FBS in the presence of 10 µM retinoic acid. Mitotic cells appear small and irregular in shape but exhibit many short processes. Within 24 h of retinoic acid treatment, longer axon-like processes had begun to grow. Cells appeared healthy and differentiated beyond this time point with no indication of apoptosis, providing cells were not over confluent. Refer to chapter V, Figure 5.19 to observe the morphology of differentiated cells 14 days beyond the differentiation time course.
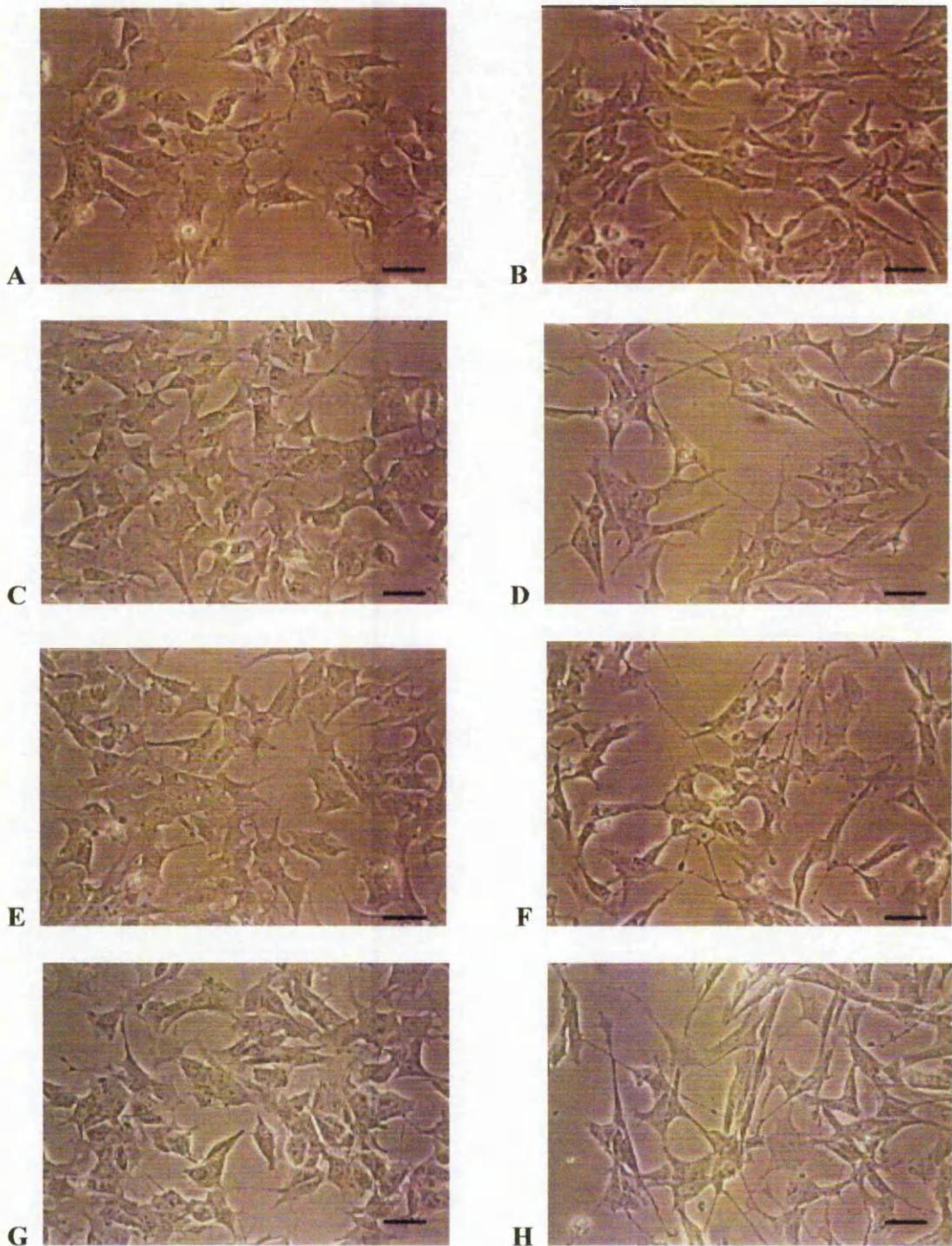
Figure 3.2 Morphological assessment of retinoic acid induced differentiation of the ECACC SH-SY5Y clone.
A, C, E and G represent mitotic cells at day 1, 3, 5 and 7 respectively. B, D, F and H represent differentiating cells at corresponding time points. Cells were seeded in growth media at a density of 80,000 cells/ml approximately 24 h prior to replacement of medium for differentiating medium (1 % FBS, 10 µM retinoic acid) then incubated in 95 % (v/v) air/5 % (v/v) CO_2 at 37 $^{\circ}$C in the dark. Media was changed on day 3. Cells were visualised using phase contrast microscopy at x 200 magnification. Scale bar represents 20 µm.

3.2.2.3   The effect of retinoic acid induced differentiation on cell proliferation.

Reduction in cell proliferation is a marker of terminal differentiation as cells leave the cell cycle and enter G_0 phase. The proliferation rate of retinoic acid treated cells compared with mitotic cells was observed to be lower. Figure 3.3 quantifies this effect from cell counts performed on mitotic cells and cells induced to differentiate over 5 days. Results indicate that for mitotic and differentiating cells alike, growth rate proceeded at a similar rate until day 3 in culture (2 days after addition of retinoic acid) when cell number for mitotic cells began to exceed that of corresponding retinoic acid treated cells. The plateau in cell number for mitotic cells at days 5 and 6 in culture were due to cells reaching confluency. Thus results suggested that, within the chosen protocol, retinoic acid had indeed reduced cell proliferation as expected.
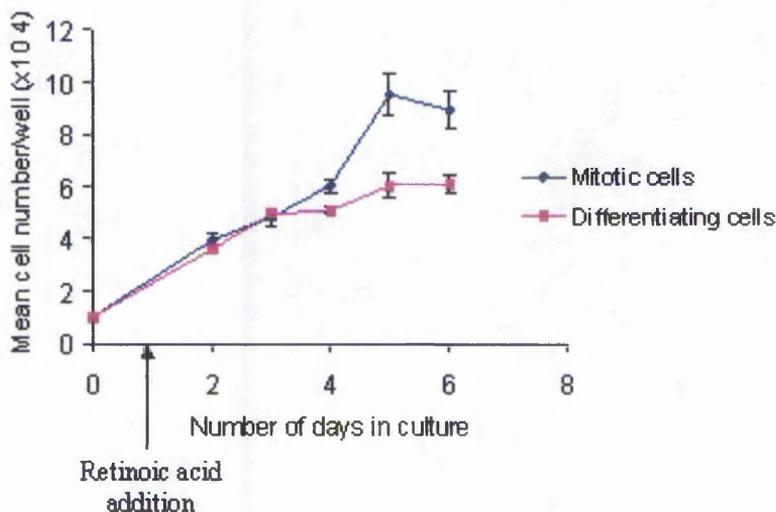
Figure 3.3. Graph to show the relationship between number of days in culture and mean cell number /100μl (x10^4) in mitotic and differentiating ECACC clone SH-SY5Y cells.
Two 96 well plates were seeded, one to remain mitotic, the other to be differentiated. Cells were seeded at 10,000 cells/96well. At 24 h intervals post seeding cells were detached using trypsin and total cell counts performed (as detailed in methods section 2.2.1.3) Mean cell number from four replicate wells of mitotic and differentiated cells was determined and expressed as mean cell number/well ± SEM.

3.2.2.4   Assessment of cell viability following 7 days exposure to retinoic acid

Given the intended use of pre-differentiated cells in toxicological studies, the viability of cells following retinoic acid treatment was established to ensure that differentiation was not detrimental to cells. In Figure 3.4, viability of cells treated for 7 days with 10 µM retinoic acid was assessed using two methods. Figure 3.4A shows results of the trypan blue exclusion assays. Results suggested there was no difference in viability following retinoic acid treatment compared to mitotic cells.

In a second method the MTT reduction assay was performed. The MTT tetrazolium salt can be taken up by the cell and reduced via endoplasmic reticulum and mitochondrial dehydrogenase enzymes to yield a product that can be measured spectrophotometrically. This assay is dependant on cell integrity and viability and is, more specifically, a measure of metabolic activity. Following retinoic acid treatment under reduced serum conditions, MTT reduction/cell was increased compared to mitotic controls and cells cultured in reduced serum alone (Fig 3.4B).
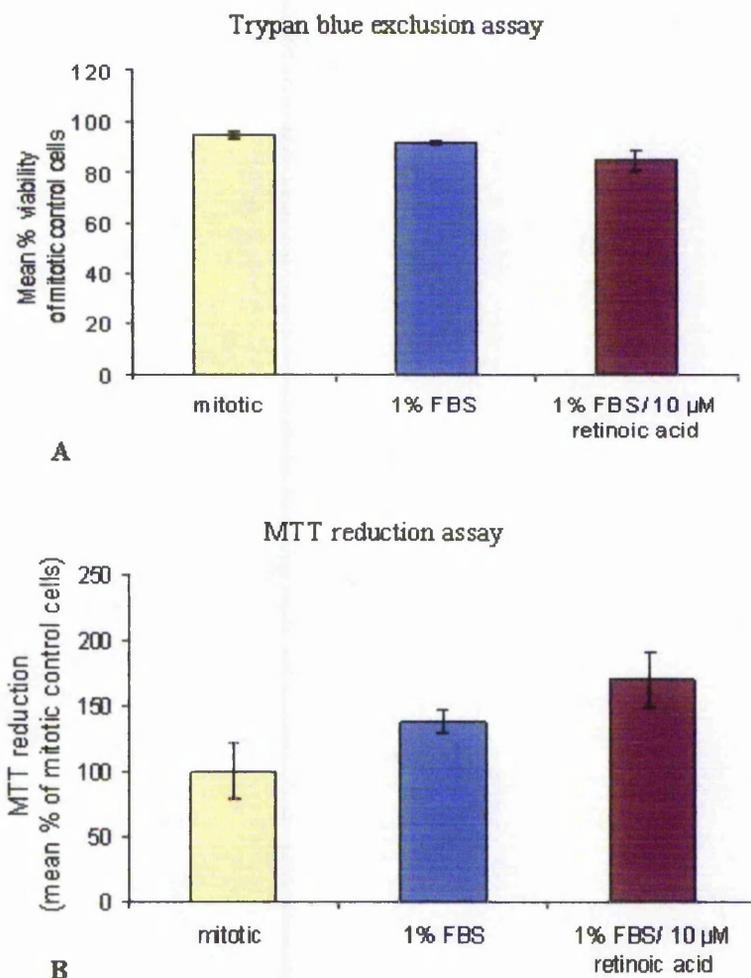
Figure 3.4 Assessment of cell viability in ECACC SH-SY5Y cells under conditions of reduced serum in the presence/absence of retinoic acid.
A, shows cell viability (mean % of mitotic control ± SEM) determined by Trypan Blue exclusion assays (triplicate wells) whilst B shows MTT reduction/cell (mean % of mitotic control ± SEM) (7 replicate wells). Cells were seeded at 5000 cells/96 well. After 24 h medium was exchanged for fresh growth medium, medium containing 1 % FBS or differentiating medium (1 % FBS/ 10 μM retinoic acid) and incubated in 95 % (v/v) air/5 % (v/v) CO_2 at 37 °C in the dark for 7 days with treatments changed on day 3. MTT reduction and Trypan blue exclusion assays were performed as detailed in methods sections 2.2.3.1 and 2.2.3.2 respectively.

3.2.2.5   Establishment of biochemical markers of retinoic acid induced differentiation.

3.2.2.5.1   Effects of retinoic acid on NF-H levels and specific phosphorylation status

Total NF status was investigated using the commercial Neurofilament 200 monoclonal antibody (clone N52). This antibody was raised against the carboxy terminal tail domain of enzymatically de-phosphorylated pig NF-H but exhibits species cross-reactivity. It is said to be phosphorylation independent given that it does not discriminate between phosphorylated and de-phosphorylated epitopes. The N52 antibody gives rise to a doublet in which the two bands do not always separate clearly following SDS-PAGE as shown in Figure 3.5 (compare to Figure 3.15). In this system a gel mobility shift associated with NF phosphorylation was not detectable.

NF-H protein levels ("total NF-H") were assessed over the retinoic acid induced differentiation time course using N52. The N52 doublet was corrected against corresponding bands probed with a reference protein, total ERK 1/2, to account for any differences in protein loading as detailed in methods section 2.2.8.2.6. Figure 3.5 shows examples of total NF-H after 1 day and 7 days exposure to retinoic acid. Results show that following 24 h retinoic acid treatment, NF-H protein level was slightly reduced compared to mitotic controls but that this level of NF-H was then maintained over the differentiation time course.
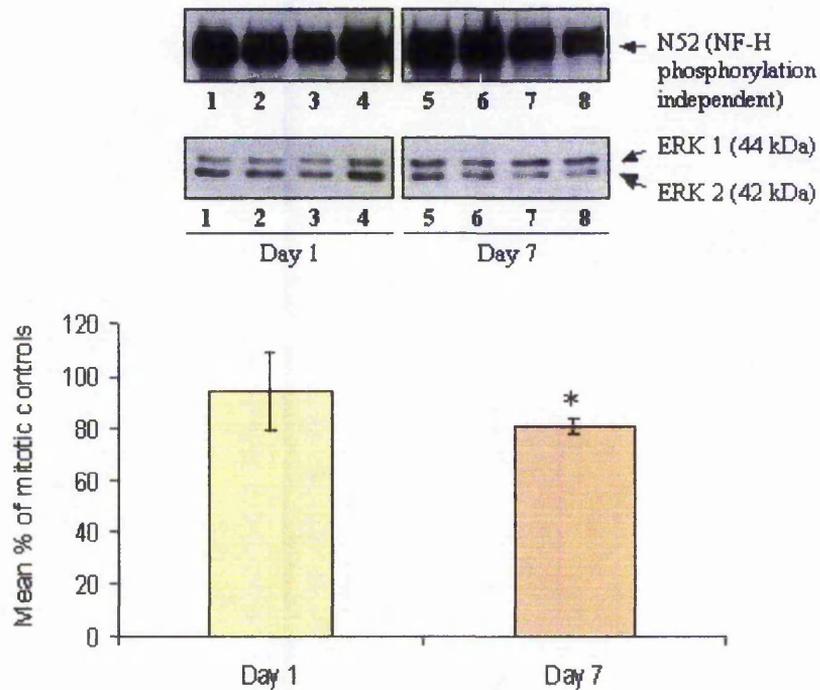
Figure 3.5 Assessment of NF-H levels during retinoic acid induced differentiation in the ECACC clone using N52.
Cells were induced to differentiate as detailed in methods section 2.2.1.6 or allowed to remain mitotic (controls). On day 1 and 7 of the time course cells were extracted as detailed in methods section 2.2.5.1. 30 μg protein was loaded/lane and separated on acrylamide gels by SDS-PAGE. Protein was transferred to nitrocellulose membrane by Western blotting and probed with N52 (NF-H phosphorylation independent) (1:500) or anti-total ERK 1/2 (1:1000) Primary antibody binding was detected by ECL as detailed in methods sections 2.2.8.2.4. A representative blot is shown. Band intensity was quantified. Lanes 1-8 represent the following; lanes 1,2 and 5,6 – mitotic controls: lanes 3,4 and 7,8 – 10 μM retinoic acid/1 % FBS treated. Results were corrected for loading differences against corresponding total ERK bands and expressed as mean % of mitotic control ± SEM. Statistical analysis of mitotic versus RA treated cells based on combined data from 3 independent experiments (2 replicate flasks per experiment) (n = 3) was carried out using two-tailed t-Tests. Statistical significance was accepted at $p < 0.05$ (*).

Specific neurofilament phosphorylation was assessed using two antibodies: 1. SMI31, which detects phosphorylated NF-H and also cross-reacts with NF-M (Sternberger Monoclonals Inc). 2. RT97, which detects phosphorylated NF-H alone. In all experiments, phosphorylated NF-H/NF-M bands were corrected against corresponding total ERK 1/2 bands. Results were then expressed as a percentage of corresponding controls. Additionally, using SMI31, the ratio of phosphorylated NF-M:NF-H was ascertained.

Using RT97 as shown in Figure 3.6 a reduction in NF-H phosphorylation was detected over 7 days. Figure 3.7 shows specific NF-H and NF-M phosphorylation at day 3, 5 and 7 of retinoic acid induced differentiation following immunoprobing with SMI31. It appears that retinoic acid induces differential effects on phosphorylation of the NF-H/NF-M sub-types (Fig 3.7A, B, C). NF-H is markedly reduced compared to mitotic controls by day 7 of the time course. NF-M phosphorylation was better maintained over the differentiation time course. As shown in Figure 3.7D, the ratio of NF-M phosphorylation to NF-H phosphorylation in retinoic acid versus mitotic treated cells was increased 1.9 fold by day 7 of the differentiation time course.
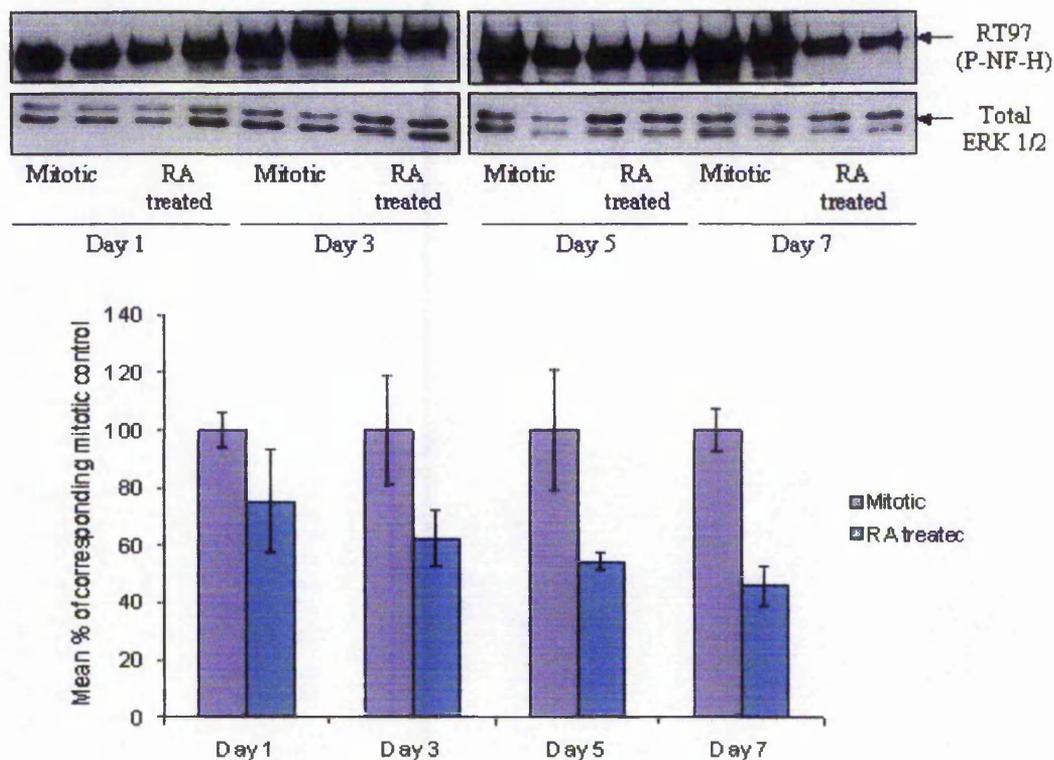
Figure 3.6 Assessment of specific phosphorylation status of NF-H during retinoic acid induced differentiation in the ECACC clone using RT97.
Cells were induced to differentiate as detailed in methods section 2.2.1.6 or allowed to remain mitotic (controls). On day 1, 3, 5 and 7 cells were extracted in duplicate as detailed in methods section 2.2.5.1. 30 μg protein was loaded/lane and separated on acrylamide gels by SDS-PAGE. Protein was transferred to nitrocellulose membrane by Western blotting and probed with anti-phosphorylated NF-H antibody, RT97 (1:500). Primary antibody binding was detected by enhanced chemiluminescence as detailed in methods sections 2.2.8.2.4. Band intensity was quantified and corrected against corresponding total ERK bands to account for differences in protein loading. Results were expressed as mean % of mitotic control (two replicate flasks). The range of the data is shown.

A. SMI31

→ NF-H-P
→ NF-M-P

B. Total ERK

← ERK 1
← ERK 2

Mitotic RA	Mitotic RA	Mitotic RA	Mitotic RA
Day 1	Day 3	Day 5	Day 7

C. Quantitative analysis of NF-H and NF-M phosphorylation
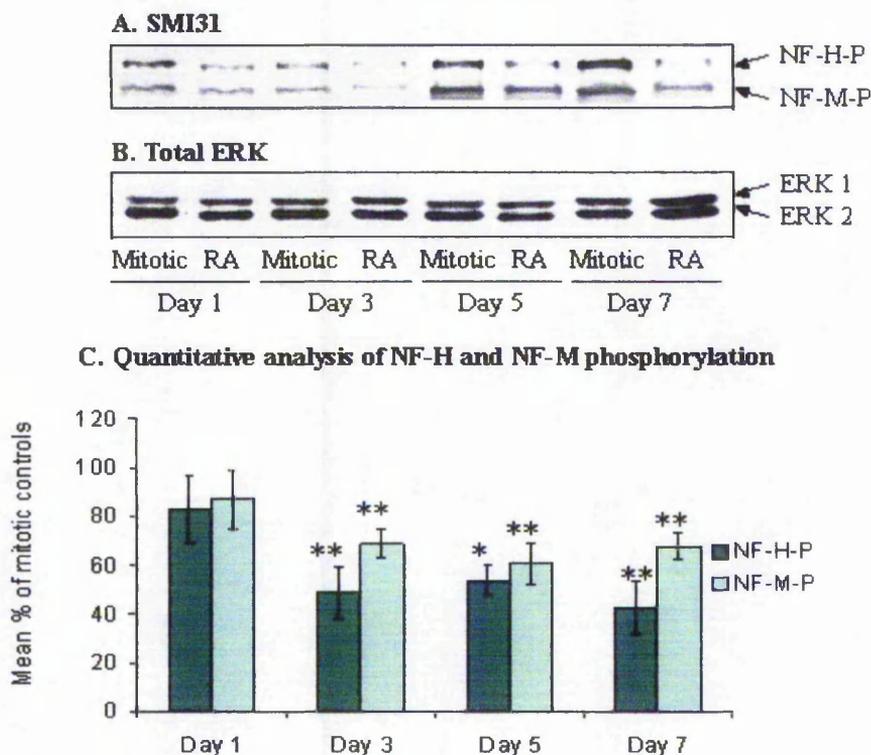
D. NF-M-P:NF-H-P ratio

NF-M:NF-H phosphorylation	Mitotic (SEM)	Retinoic acid (SEM)
Day 1	1.079 ± 0.06	1.359 ± 0.31
Day 3	1.114 ± 0.03	1.277 ± 0.13
Day 5	1.277 ± 0.27	1.512 ± 0.41
Day 7	0.876 ± 0.05	1.656 ± 0.56

Figure 3.7 Assessment of the specific phosphorylation status of NF-H and NF-M during retinoic acid induced differentiation in the ECACC clone using SMI31.
Cells were induced to differentiate as detailed in methods section 2.2.1.6 or allowed to remain mitotic (controls). On day 1, 3, 5 and 7 cells were extracted as detailed in methods section 2.2.5.1. 30 µg protein separated on acrylamide gels by SDS-PAGE. Protein was transferred to nitrocellulose membrane by Western blotting and probed with anti- phosphorylated NF-H/NF-M antibody, SMI31 (1:1000) panel A) and total ERK 1/2 (1:500) (panel B). Primary antibody binding was detected by alkaline phosphatase as detailed in methods sections 2.2.8.2.3. Phosphorylated NF-H and NF-M band intensities were quantified and corrected against corresponding total ERK 1/2 bands as detailed in methods section 2.2.8.2.6. Combined values for differentiated cells from three independent experiments (2 replicate flasks per experiment) (n = 3) were expressed as mean % of mitotic controls ± SEM (panel C). Statistical significance was assessed using two-tailed t-Tests where statistical significance was accepted at $p < 0.05$ (*) and $p < 0.01$ (**). The NF-M:NF-H phosphorylation ratio was calculated (panel D).

3.2.2.5.2 Determination of kinases responsible for NF phosphorylation in the ECACC SH-SY5Y clone

In order to further characterise NF phosphorylation in the ECACC SH-SY5Y system, preliminary assessment of role of kinases proposed to be instrumental in NF phosphorylation in this cell line was performed. Differentiation medium (1 % FBS, 10 μM retinoic acid) was supplemented with chemical inhibitors to MEK (PD98059 [5 μM]), JNK (mixed lineage kinase inhibitor, CEP-11004 [10 nM]) and CDK-5 (butyrolactone 1 [BL-1; 1 μM]) and incubated with cells over 7 days (for further information regarding MAPK and CDK-5 inhibitors, refer to Chapter V, sections 5.2.1.1 and 5.2.2). Inhibitors were used at a concentration that did not reduce viability beyond 50 %. The effects of such treatments on cell morphology and neuritogenesis are shown in Figure 3.8. In this experiment PD98059 treated cells exhibited reduced axon-like outgrowth in response to retinoic acid treatment. Conversely, CEP-11004 induced an increase in axon-like outgrowth compared to control cells. BL-1 had no effect on neuritogenesis.

Total NF levels were analysed in cell extracts by Western blotting, in conjunction with specific NF-phosphorylation to determine the effect of kinase inhibition. All MAPK/CDK-5 inhibitors appeared to cause some increase in total NF-H levels (Fig 3.9B) in two independent experiments. The MEK inhibitor (PD98059) and the CDK-5 inhibitor (BL-1) both caused some reduction in NF phosphorylation (Figure 3.9C). The effect of kinase inhibition on ERK phosphorylation was also assessed (see Fig 3.10). Both PD98059 and BL-1 reduced ERK phosphorylation by approximately 25 % whilst CEP-11004 increased ERK phosphorylation. Further trials would be required to confirm these initial findings.

A. Morphology

a. 10 µM retinoic acid (RA)

b. RA + 5 µM PD 98059

c. RA + 10 nM CEP-11004

d.　RA + 1 µM BL-1
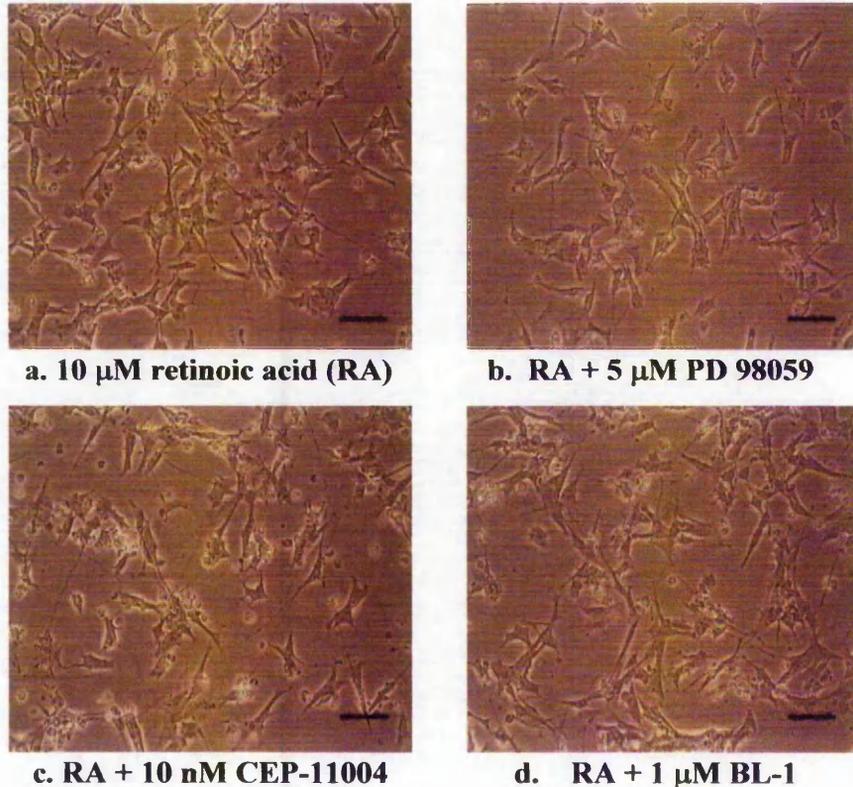
B. Axon counts
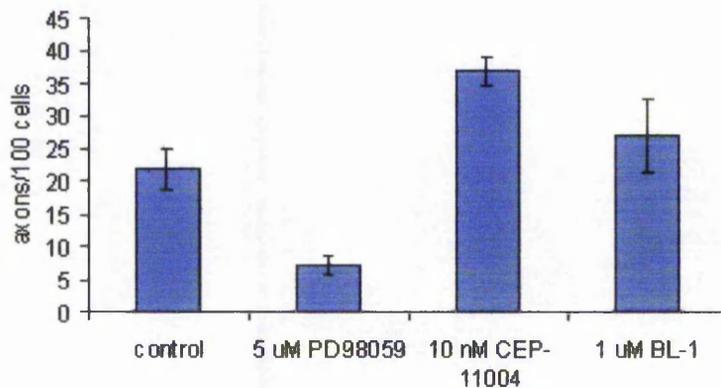
Figure 3.8 Effects of MAPK and CDK-5 inhibitors on neuritogenesis.
400,000 cells were seeded into T25 flasks and allowed to recover over 24 h. Medium was removed and replaced with differentiation medium (1 % FBS, 10 µM retinoic acid) ± MAPK and CDK-5 inhibitors (MEK inhibitor, PD98059; mixed lineage kinase inhibitor, CEP-11004; CDK-5 inhibitor, butyrolactone 1 [BL-1]) as indicated in a-d above and incubated in 95 % (v/v) air/5 % (v/v) CO_2 at 37 $^{\circ}$C in the dark. Medium was changed on day 4. Cells were visualised use phase contrast microscopy on day 7. Scale bar represents 40 µm. Total cell number and number of axons were counted in 4 random fields from triplicate flasks on the same day. Results are expressed as mean axon number/100 cells ± SEM.

A. Western blots

Controls   10 nM CEP-11004

Controls   5 μM PD98059   1 μM BL-1
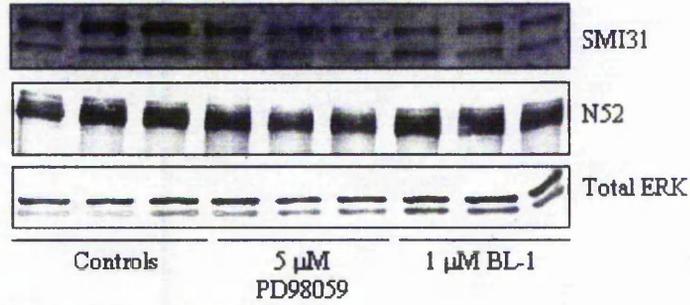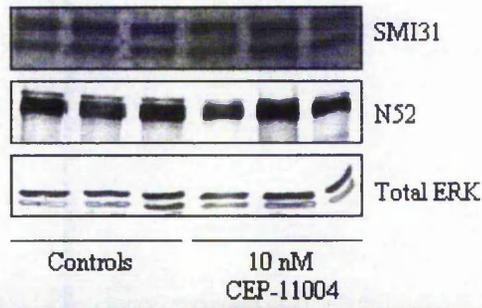
B. Quantification of NF-H protein levels
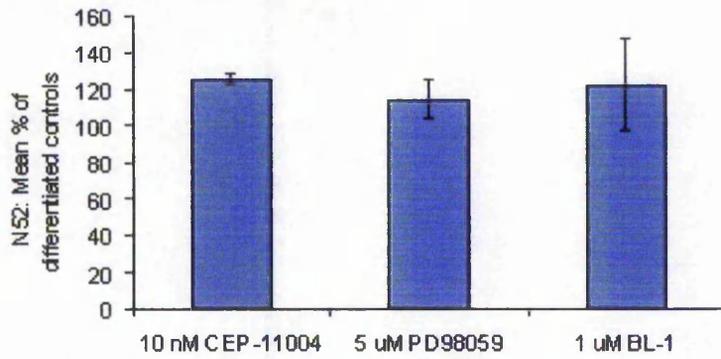
C. Quantification of NF-H/NF-M phosphorylation
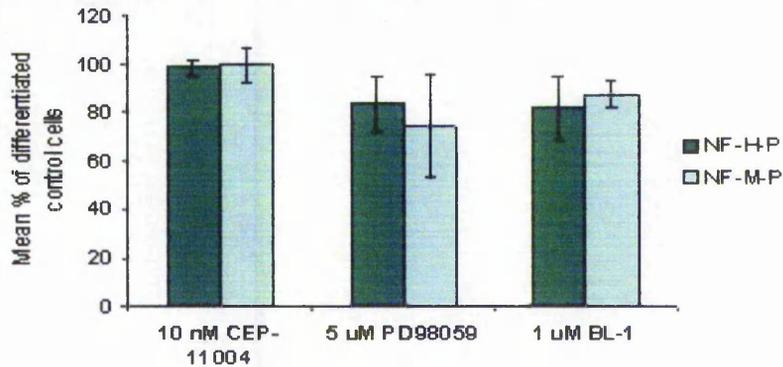
Figure 3.9 Assessment of total NF-H levels and specific NF phosphorylation status following 7 days retinoic acid induced differentiation in the presence/absence of MAPK/ CDK-5 inhibitors.

ECACC clone SH-SY5Y cells were seeded at 400,000 cells / T25 flask and allowed to recover overnight. Medium was removed and replaced with differentiating medium (1 % FBS, 10 µM retinoic acid) ± inhibitors of MEK (PD98059), JNK (mixed lineage kinase inhibitor CEP-11004) or CDK-5 (BL-1). Medium was exchanged on day 4. On day 7 cells were extracted as detailed in methods section 2.2.5.1. 50 µg protein was loaded/lane and separated on acrylamide gels by SDS-PAGE. Protein was transferred to nitrocellulose membrane by Western blotting. NF proteins were probed with SMI31 antibody (1:1000), stripped and re-probed with N52 (1:500). Panel A shows representative blots. Primary antibody binding was detected by alkaline phosphatase and ECL methods (detailed in methods sections 2.2.8.2.3 and 2.2.8.2.4, respectively). Band intensity was quantified and N52 and SMI31 bands were corrected for differences in protein loading against corresponding total ERK bands. Panel B represents quantification of NF-H protein levels. Panel C represents quantification of NF-H and NF-M phosphorylation. Results represent the mean data of inhibitor treated cells from two independent experiments (incorporating 5 flasks of cells) expressed as mean % of corresponding differentiated controls. The range of mean data is shown.
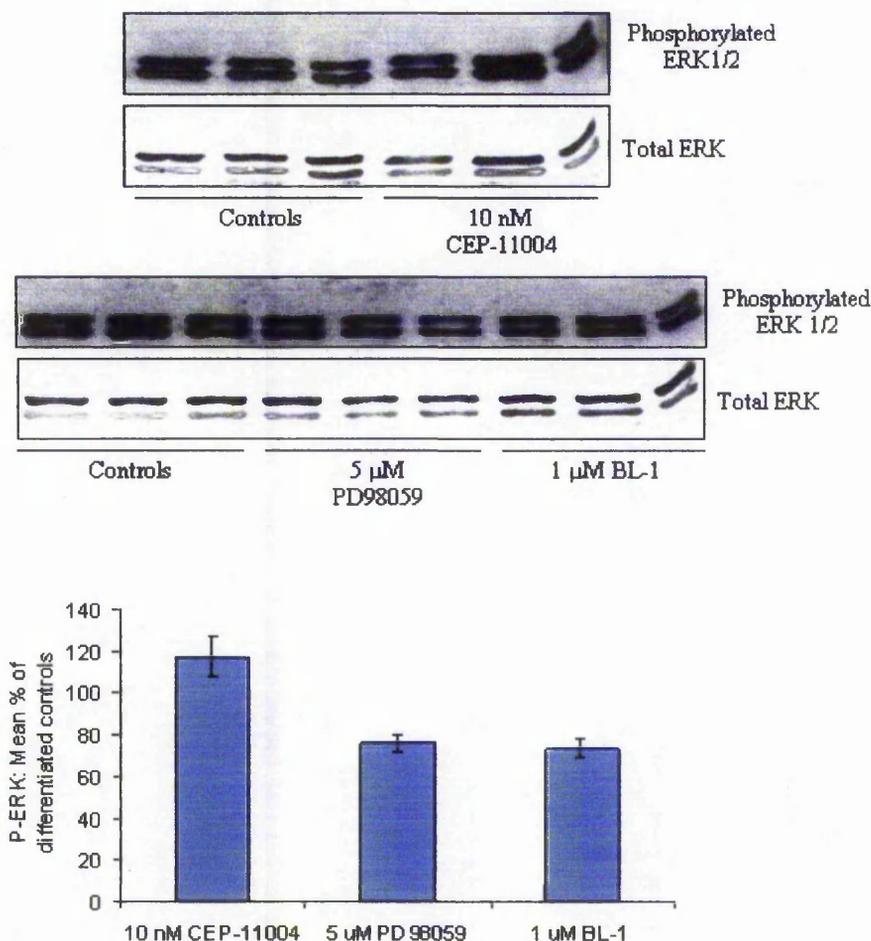
Figure 3.10 Assessment of ERK phosphorylation status following 7 days retinoic acid induced differentiation in the presence/absence of MAPK/CDK-5 inhibitors.
ECACC clone SH-SY5Y cells were seeded at 400,000 cells / T25 flask and allowed to recover overnight. Medium was removed and replaced with differentiating medium (1 % FBS, 10 µM retinoic acid) ± inhibitors of MEK (PD 98059), JNK (mixed lineage kinase inhibitor CEP-11004) or CDK-5 (BL-1). On day 7 cells were extracted as detailed in methods section 2.2.5.1. 50 µg protein was loaded/lane and separated on acrylamide gels by SDS-PAGE. Protein was transferred to nitrocellulose membrane by Western blotting and probed with anti-phosphorylated ERK 1/2 antibody (1:500), then stripped and re-probed with total ERK 1/2 antibody (1:1000). Primary antibody binding was detected by ECL (phospho-ERK) and alkaline phosphatase (total ERK) methods (detailed in methods sections 2.2.8.2.4 and 2.2.8.2.3, respectively). Band intensity was quantified. Phosphorylated ERK bands were corrected for differences in protein loading against corresponding total ERK bands. Results from triplicate flasks extracted on the same day were expressed as mean % of corresponding differentiated control ± SEM.

3.2.2.5.3   Effects of retinoic acid on tTG and Bcl-2 expression

Figures 3.11 shows a representative Western blot analysis of tTG expression at 48 h intervals over the 7-day differentiation time course in 10 μM retinoic acid and 1 % FBS, with corresponding quantification of band intensity. In mitotic cells tTG was scarcely detectable over the 7-day differentiation period but tTG expression was increased markedly (approximately 70 fold). It should be noted that whilst tTG expression was always found to increase following retinoic acid treatment (three independent experiments), the extent of this increase varied. In addition, tTG expression is often easily detected on Western blots of mitotic SH-SY5Y cells. Preliminary assessment of the expression of the anti-apoptotic protein Bcl-2 was reduced by retinoic acid treatment; by day 7, expression was approximately 55 % compared to mitotic controls (see Fig 3.12).

A. tTG

B. Total ERK 1/2

C. Quantitative analysis
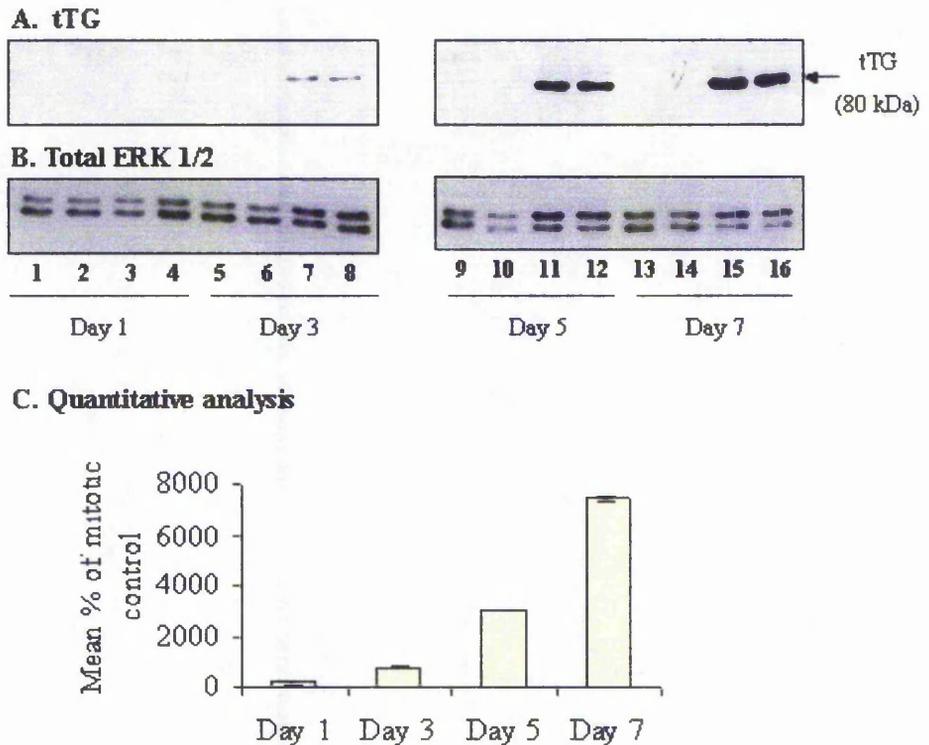
**Figure 3.11 Assessment of tTG expression over a retinoic acid induced differentiation time course in ECACC clone SH-SY5Y cells.**
Cells were induced to differentiate as detailed in methods section 2.2.1.6 or allowed to remain mitotic (controls). On day 1, 3, 5 and 7 of the time course cells were extracted in duplicate as detailed in methods section 2.2.5.1. 30 μg protein was loaded /lane and separated on acrylamide gels by SDS-PAGE. Protein was transferred to nitrocellulose membrane by Western blotting and probed with anti-tissue transgluaminase II (clone CUB-7402) (1:1000). Primary antibody binding was detected by ECL as detailed in methods section 2.2.8.2.4. Band intensity was quantified as detailed in methods section 2.2.8.2.6. Results from duplicate flasks were corrected for loading differences against corresponding total ERK bands and expressed as mean % of mitotic control. The range of data is shown. Lanes 1-16 represent the following; lanes 1 and 2, 5 and 6, 9 and 10 and 13 and 14 – mitotic controls: lanes 3 and 4, 7 and 8, 11 and 12 and 15 and 16 – 10 μM retinoic acid/1 % FBS treated. Results are representative of three independent experiments as detailed in the text.
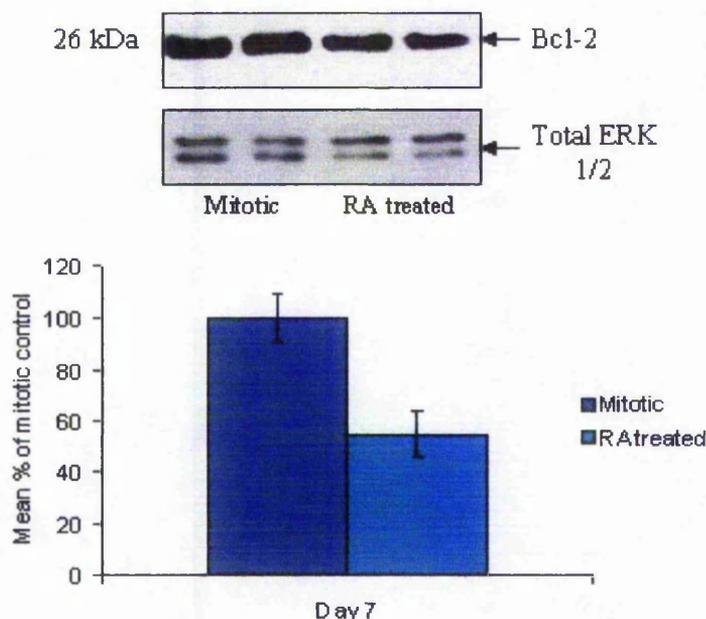
Figure 3.12 Assessment of Bcl-2 expression following retinoic acid induced differentiation in ECACC clone SH-SY5Y cells.
Cells were induced to differentiate as detailed in methods section 2.2.1.6 or allowed to remain mitotic (controls). This figure shows Bcl-2 expression levels on day 7 of the time course, following extraction of cells in duplicate as detailed in methods section 2.2.5.1. 30 µg protein was loaded /lane and separated on acrylamide gels by SDS-PAGE. Protein was transferred to nitrocellulose membrane by Western blotting and probed with anti-Bcl-2 (1:250) Primary antibody binding was detected by ECL as detailed in methods section 2.2.8.2.4. Band intensity was quantified as detailed in methods section 2.2.8.2.6. Results from duplicate flasks were corrected for loading differences against corresponding total ERK bands and expressed as mean % of mitotic control. The range of the data is shown.

3.2.2.5.4   Immunocytochemical analysis of markers of differentiation.

Employing retinoic acid, the ECACC clone became morphologically differentiated over 7 days. To further assess this status, the distribution of proposed markers of differentiation were investigated by immunocytochemical staining and analysis via confocal laser microscopy.

Since phosphorylated NF-H levels did not follow the hypothesised pattern upon retinoic acid treatment, immunocytochemistry was performed on day 7, at which point the cells appeared to be differentiated when assessed morphologically. This was to validate the differentiation protocol and to establish whether processes extending from the cell bodies were indeed axonal in nature and that phosphorylated NF protein was correctly distributed along the processes. Figure 3.13 shows mitotic (A) and 7-day differentiated cells (B) probed with N52 (panel a) and SMI31 (panel b) antibodies to represent distribution of total NF-H and phosphorylated NF-H/NF-M, respectively. Results indicate that following treatment with retinoic acid, NFs become re-distributed from the cell body along the axon-like processes, but in particular phosphorylated NF-H/NF-M implying that cells were indeed differentiated to a neuronal phenotype (compare Fig 3.13A and 3.13B, panel b). Following differentiation, a pool of phosphorylated NF-H/NF-M remains in the cell body, distinctly localising either in the growth cone, apparently in preparation to travel down the axon-like processs, or opposite at the distal end of the cell body (see Fig 3.13B, panel b). A punctate staining pattern could be observed throughout the cell body, and surrounding the nucleus when cells were probed with SMI31 that was not observed following staining with N52.

tTG expression was easily detected in mitotic cells despite the fact that it was detected at low levels in cell extracts following Western blotting (Figure 3.13A, panel c). Punctate staining was observed in the cell body, appearing to concentrate around the periphery and within small neuritic processes extending from mitotic cells. Retinoic acid markedly increased tissue transglutaminase expression, consistent with expression studies in cell extracts, as demonstrated by highly intense staining of cell bodies and also axon-like processes (see Figure 3.13B, panel c).

FITC   FITC + propidium iodide
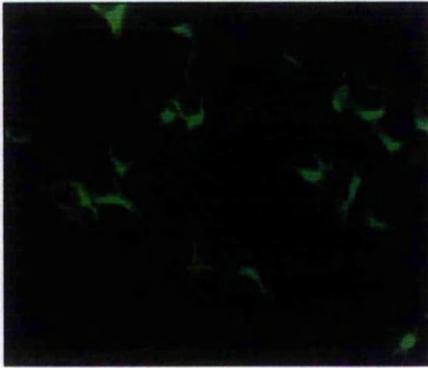
a. N52

b. SMI31

c. CUB-7402

A. Mitotic cells

FITC   FITC + propidium iodide
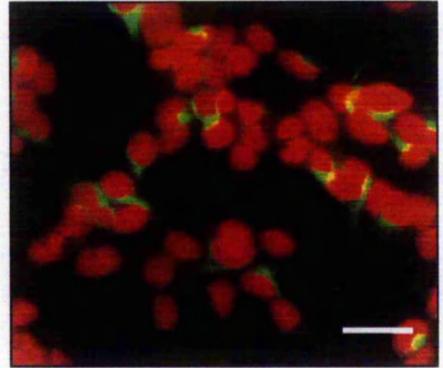
a. N52
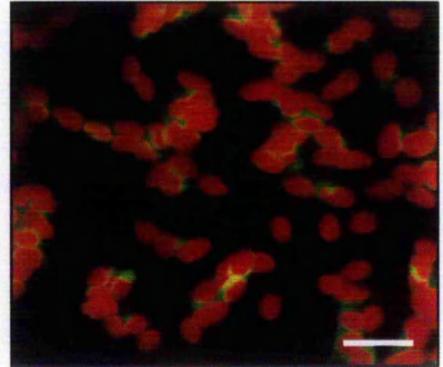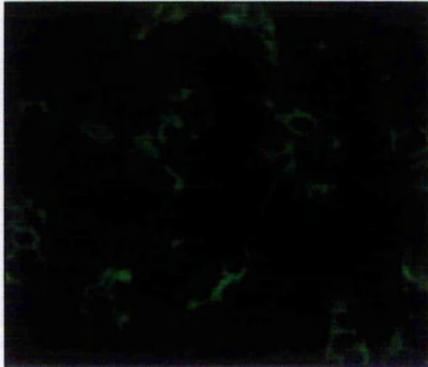
b. SMI31
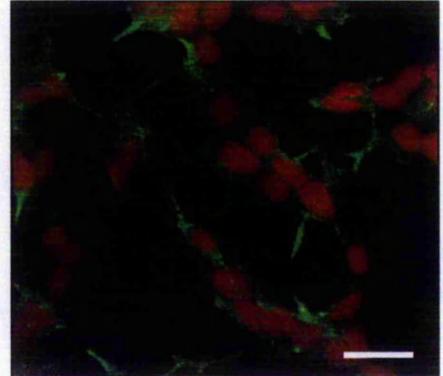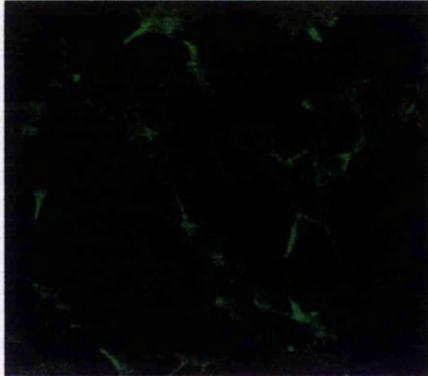
c. CUB-7402
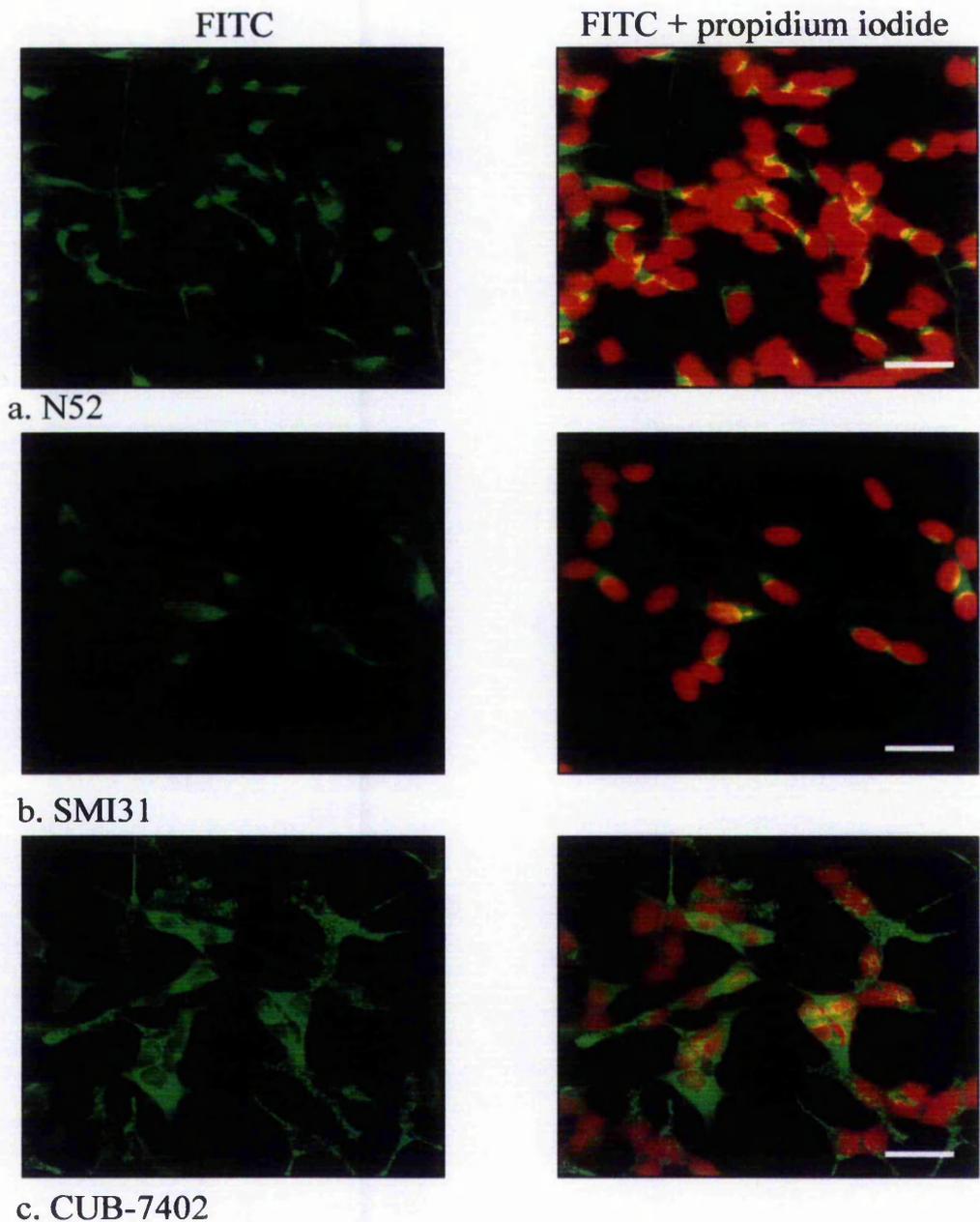
B. Retinoic acid treated cells

Figure 3.13 Immunocytochemical analysis of biochemical markers of differentiation in ECACC clone SH-SY5Y cells following treatment with retinoic acid.

Fig 3.13A represents confocal laser microscopy analysis of mitotic cells. Fig 3.13B represents cells induced to differentiate over 7 days by treatment with 10 µM retinoic acid. Cells to remain mitotic were seeded at 4000 cells/chamber whilst cells to be differentiated were seeded at 10000 cells/chamber. On day 7 cells were fixed, permeabilised and immunocytochemistry performed as detailed in methods section 2.2.9 using (a) N52 (1:200); (b) SMI31 (1:500); (c) CUB 7402 (1:20). Cells were protected using Vectorshield mounting medium containing propidium iodide (propidium iodide stains the nuclei red, shown to the right of each panel). Scale bar represents 20 µm.

3.2.3 Characterisation of retinoic acid induced differentiation in the Johnson SH-SY5Y clone.

3.2.3.1 Morphological studies

Given the apparent clonal differences between the Leicester and ECACC SH-SY5Y clones, a third clone was donated to further clarify the characteristics of this cell line. The Johnson clone had been successfully employed in differentiation studies using retinoic acid and specifically the involvement of tTG in this process (Tucholski *et al.,* 2001). To characterise the differentiation process of this clone in our hands, studies commenced with morphological analysis of retinoic acid induced differentiation over a 7-day protocol. Cells were seeded in growth medium as detailed in methods section 2.2.1.1. The following day medium was exchanged for differentiation medium containing 10 μM retinoic acid and 1 % FBS / 4 % heat inactivated horse serum (see methods section 2.2.1.6). This medium was exchanged on day 3 of the time course. Figure 3.14 demonstrates the morphological transition of mitotic cells (left panel) to differentiating cells (right panel) at 48 h intervals during retinoic acid treatment. The general appearance of the Johnson clone cells can be likened to the ECACC clone but not the Leicester clone. That said, it can be noted that the differences in morphology between mitotic and differentiating cells during retinoic acid treatment are considerably less pronounced in this clone compared to the ECACC clone, with mitotic cells exhibiting a significant number of axon-like extensions. Treatment with retinoic acid does, however, increase the number of axon-like extensions and also reduces cell proliferation (observation). The Johnson clone was obtained at passage 14. In contrast to the ECACC clone, differentiation of the Johnson clone was not dependent on passage number.
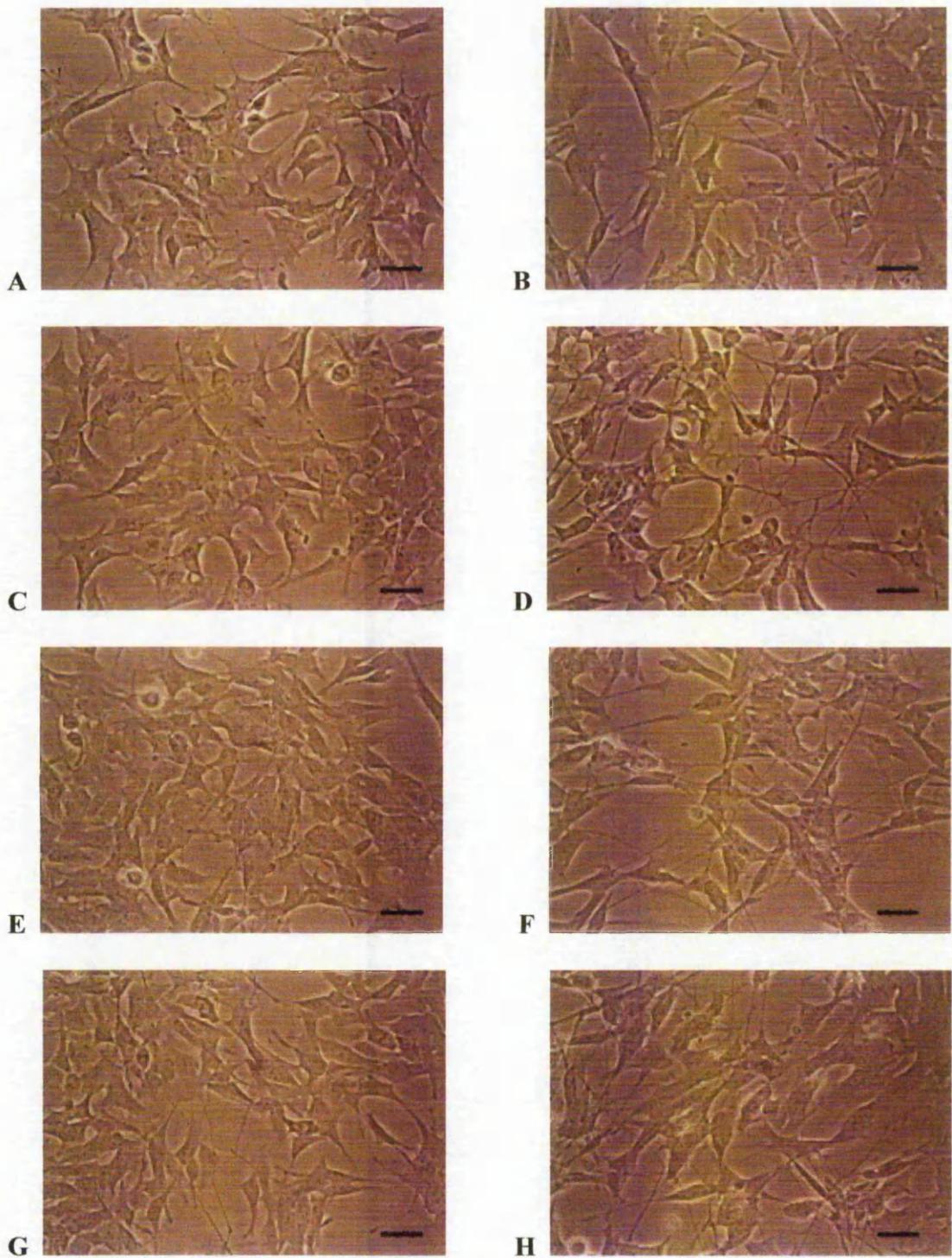
Figure 3.14 Morphological assessment of retinoic acid induced differentiation of the Johnson SH-SY5Y clone.

A, C, E and G represent mitotic cells at day 1, 3, 5 and 7 respectively. B, D, F and H represent differentiating cells at corresponding time points. Cells were seeded in growth media at a density of 80,000 cells/ml approximately 24 h prior to replacement of medium for differentiating medium (1 % FBS/4 % horse serum, 10 μM retinoic acid) and then incubated in 95 % (v/v) air/5 % (v/v) CO_2 at 37 °C in the dark. Media was changed on day 3. Cells were visualised using phase contrast microscopy at x 200 magnification. Scale bar represents 20 μm.

3.2.3.2   Assessment of biochemical markers of retinoic acid induced differentiation

Preliminary assessment of biochemical markers of retinoic acid induced differentiation in the Johnson clone was performed. On day 7, total NF-H status was increased compared to controls (Fig 3.15A). NF-H phosphorylation was reduced as detected by SMI31 and RT97 antibodies, whilst NF-M phosphorylation was reduced but to a lesser extent (Fig 3.15B and C). The ratio of NF-M:NF-H phosphorylation in mitotic versus retinoic acid treated cells was increased 1.3 fold by day 7 (Fig 3.15D). Figure 3.16 demonstrates an increase in tTG (>13 fold) and Bcl-2 (1.4 fold) expression following 7 days treatment with retinoic acid respectively.

3.2.3.3   Immunocytochemical analysis of markers of differentiation.

In accordance with the ECACC clone, retinoic acid treatment of the Johnson clone did not increase NF phosphorylation. Immunocytochemical analysis of 7-day differentiated cells using N52 and SMI31 antibodies to detect total and phosphorylated NFs respectively, revealed that axon-like processes were more intensely stained for phoshorylated epitopes following retinoic acid treatment compared to mitotic controls where staining was predominately located in cell bodies (compare Fig 3.17A and B; panels a and b). tTG was again highly stained in mitotic cells. tTG expression appeared to be elevated in retinoic acid treated cells but in accordance with Western blotting results this increase was not as pronounced as in ECACC the clone (Fig 3.17B, panel c).

A. N52

← Total NF-H
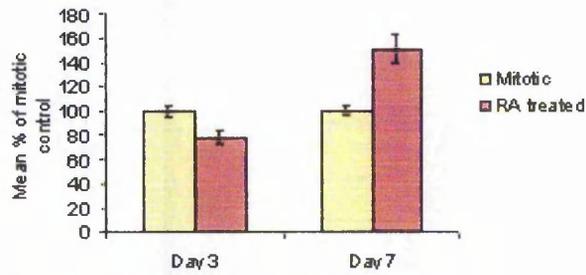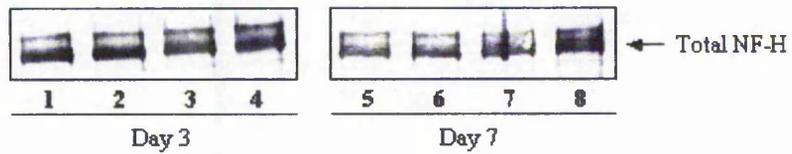
B. RT97
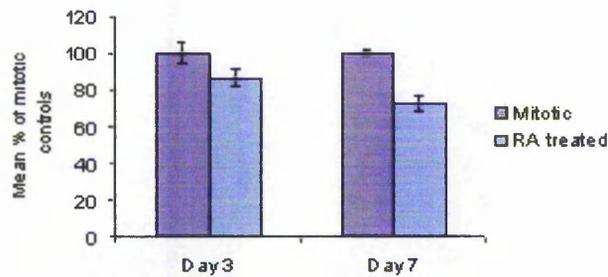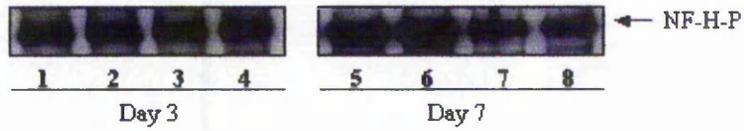
← NF-H-P

C. SMI31
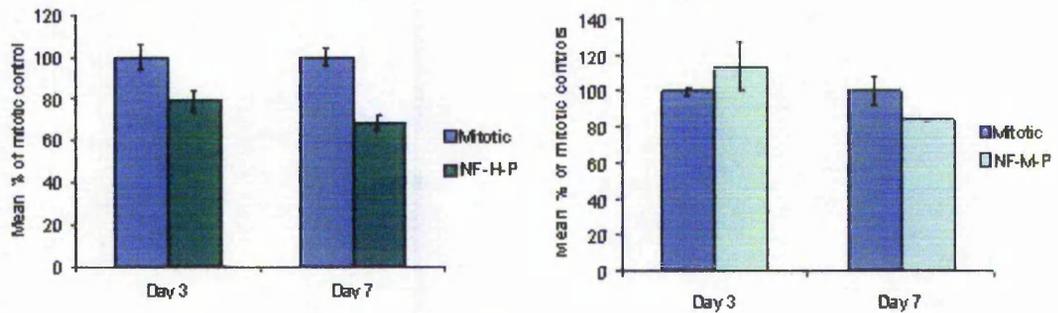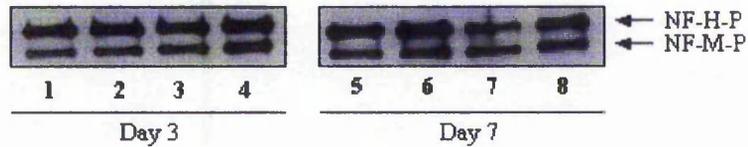
← NF-H-P
← NF-M-P

D. Ratio of NF-M:NF-H phosphorylation in mitotic and retinoic acid treated cells

NF-M:NF-H phosphorylation ratio	Mitotic cells	RA treated cells
Day 3	0.5037 ± 0.017	0.7182 ± 0.037
Day 7	0.5917 ± 0.020	0.7947 ± 0.032

Figure 3.15 Assessment of NF (total and phosphorylation) status of the Johnson clone following retinoic acid induced differentiation.

Cells were induced to differentiate as detailed in methods section 2.2.1.6 or allowed to remain mitotic (controls). On day 3 and 7 of the time course, cells were extracted in duplicate as detailed in methods section 2.2.5.1. 30 μg protein was loaded /lane and separated on acrylamide gels by SDS-PAGE. Protein was transferred to nitrocellulose membrane by Western blotting and probed with N52 (1:500) (panel A), anti-phosphorylated NF-H antibody, RT97 (1:500) (panel B) or with anti-phosphorylated NF-H/NF-M antibody, SMI31 (1:1000) (panel C). Primary antibody binding was detected by alkaline phosphatase (A) or enhanced chemiluminescence (B, C) as detailed in methods sections 2.2.8.2.3 and 2.2.8.2.4, respectively. Band intensity was quantified and corrected against corresponding total ERK bands to account for differences in protein loading. Results were expressed as mean % of mitotic control from duplicate flasks. The range of the data is shown. Lanes 1,2 and 5,6 represent mitotic cells whilst lanes 3,4 and 7,8 represent 10 μM retinoic acid /1 % FBS treatment. The ratio of NF-M:NF-H phosphorylation was calculated (panel D).
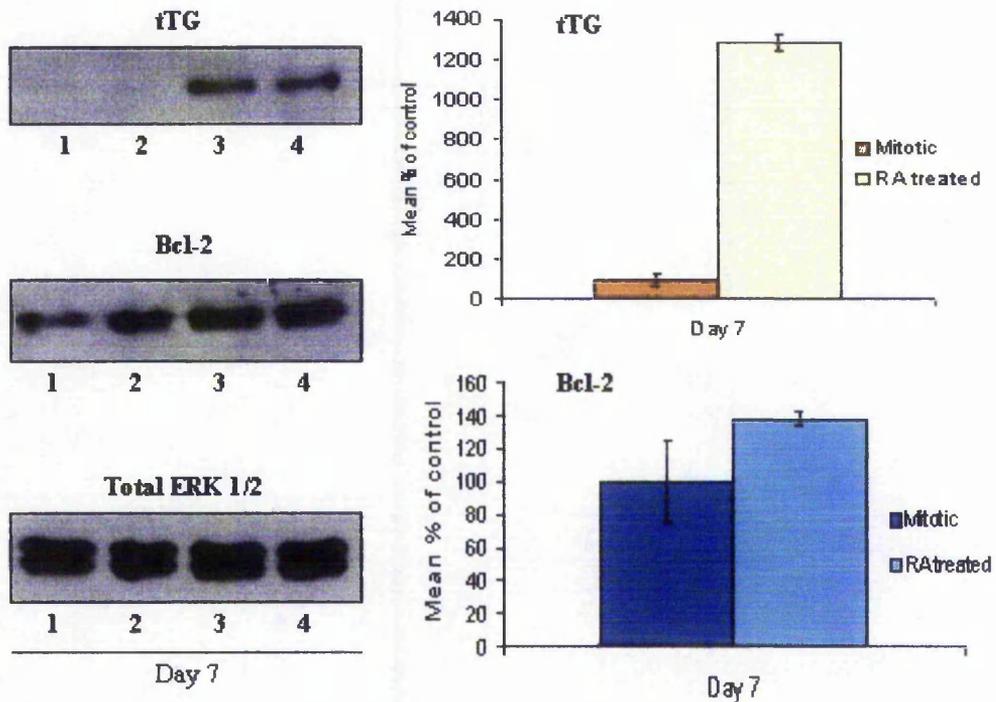
Figure 3.16 Assessment of tissue transglutaminase and Bcl-2 expression in Johnson clone SH-SY5Y cells following retinoic acid induced differentiation.
Cells were induced to differentiate as detailed in methods section 2.2.1.6 or allowed to remain mitotic (controls). 7 days post retinoic acid treatment cells were extracted in duplicate as detailed in methods section 2.2.5.1. 30 μg protein was loaded /lane and separated by SDS-PAGE on a 12 % acrylamide gel. Protein was transferred to nitrocellulose membrane by Western blotting and probed with anti-transglutaminase II (clone CUB-7402) (1:1000) or anti-Bcl-2 (1:250). Primary antibody binding was detected by ECL as detailed in methods section 2.2.8.2.4. Band intensity was quantified as detailed in methods section 2.2.8.2.6. Results were corrected for loading differences against corresponding total ERK bands and expressed as mean % of mitotic control from duplicate flasks. Lanes 1,2 and 3,4 represent mitotic and 7 day differentiated cells, respectively. The range of the data is shown.

FITC   FITC + propidium iodide
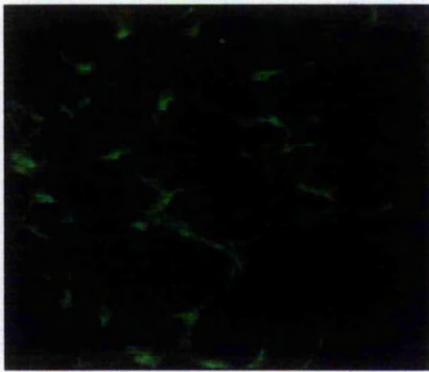
a. N52

b. SMI31

c. CUB-7402

A. Mitotic cells

FITC   FITC + propidium iodide
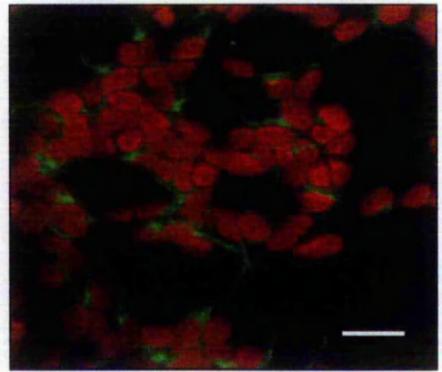
a. N52
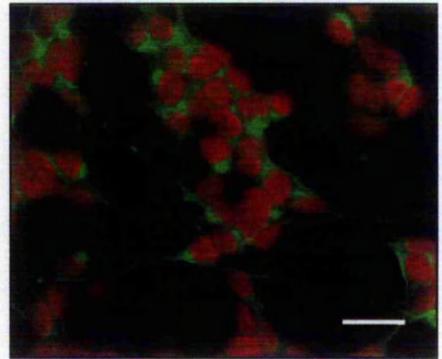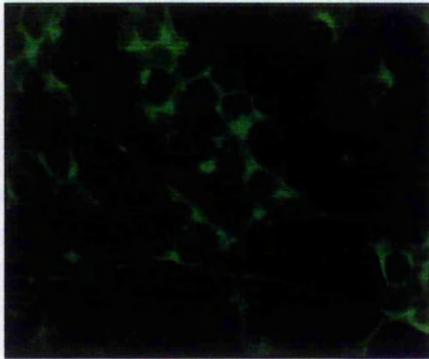
b. SMI31
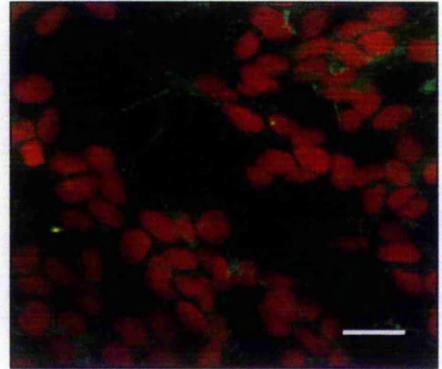
c. CUB-7402
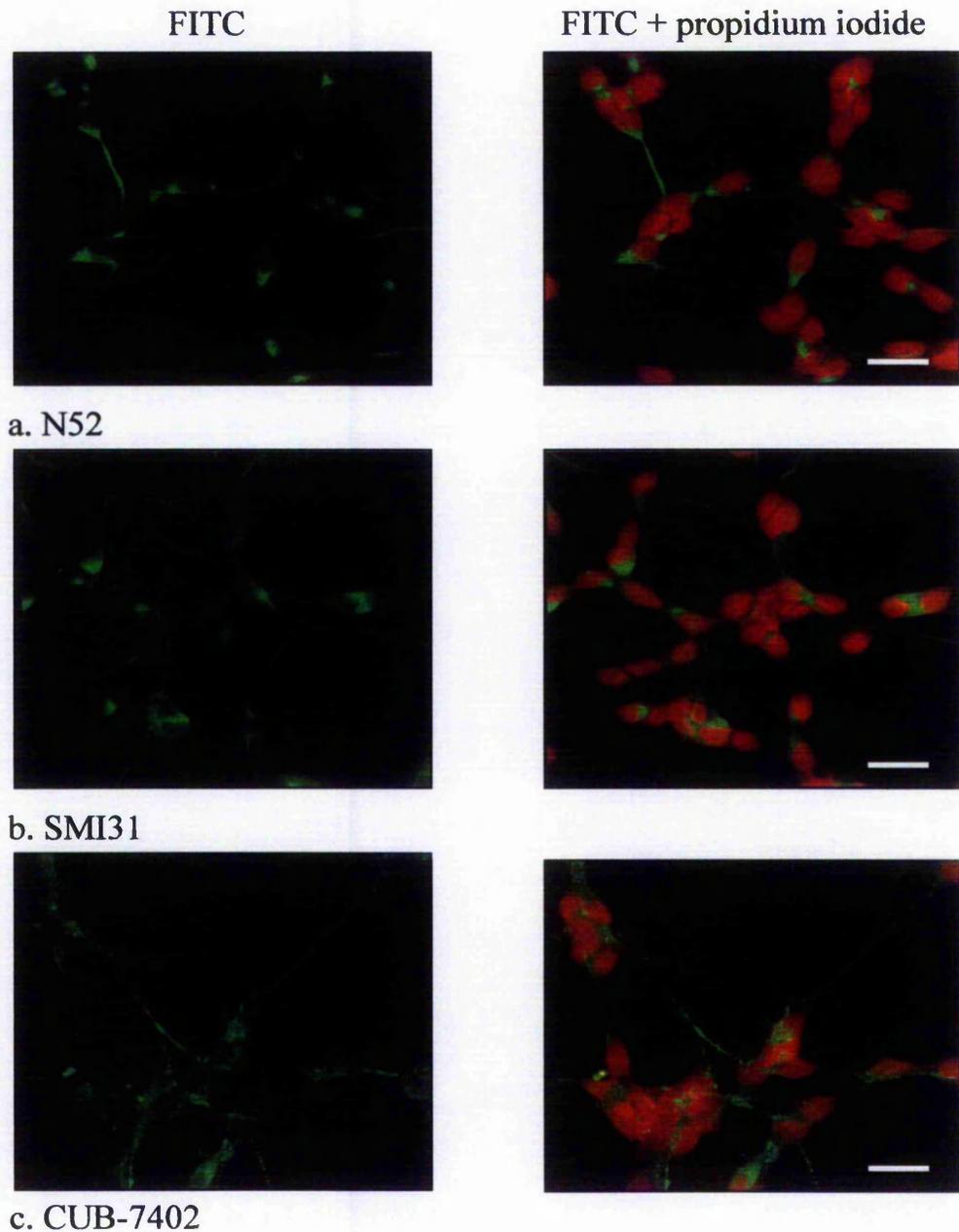
B. Retinoic acid treated cells

Figure 3.17 Immunocytochemical analysis of biochemical markers of differentiation in Johnson clone SH-SY5Y cells following treatment with retinoic acid.
Fig 3.17A represents confocal laser microscopy analysis of mitotic cells. Fig 3.17B represents cells induced to differentiate over 7 days by treatment with 10 μM retinoic acid. Cells to remain mitotic were seeded at 4000 cells/chamber whilst cells to be differentiated were seeded at 10000 cells/chamber. On day 7 cells were fixed, permeabilised and immunocytochemistry performed as detailed in methods section 2.2.9 using (a) N52 (1:200); (b) SMI31 (1:500); (c) CUB 7402 (1:20). Cells were protected using Vectorshield mounting medium containing propidium iodide (propidium iodide stains the nuclei red, shown to the right of each panel). Scale bar represents 20 μm.

3.3 DISCUSSION

3.3.1 Clonal differences in the morphology of the SH-SY5Y cell line

This work sought to establish a pre-differentiated human neuroblastoma model to use in MPP^+ toxicity studies. Three clones of the SH-SY5Y cell line were characterised in terms of neuronal differentiation with respect to morphological changes and proposed biochemical markers of the differentiation process. The differentiation afforded by retinoic acid and staurosporine has been compared (staurosporine data are not shown). A concentration of 10 μM retinoic acid was chosen in accordance with the literature and based on viability and morphological studies as detailed in results section 3.2.2.2. Staurosporine was employed at a concentration of 10 nM, again chosen from viability and morphology studies (results not shown) and published work. Indeed Jalava *et al.*, (1992) state that 10 nM staurosporine used over 72 h caused total inhibition of DNA synthesis in SH-SY5Y cells indicative of terminal differentiation.

A most significant observation was the apparent differences between the three clones. Morphologically, all clones differentiated to a neuronal phenotype, extending axon-like processes. However the morphology of the Leicester clone differed markedly from the ECACC and Johnson clones in that cells exhibited significant homogeneity and appeared smaller with long, sweeping axon-like processes. The absence of detectable NFs in the Leicester clone despite extensive investigation made it unsuitable for further study. The uncharacteristic properties displayed were not predicted, given that this clone had been previously employed in extended differentiation protocols (Hartley *et al.*, 1996). In such studies cells were differentiated with 10 μM retinoic acid in the presence of 1 % FBS over a month. After this time a population of retinoic acid independent, terminally differentiated cells were reported. NF-H phosphorylation was shown to increase during retinoic acid induced differentiation as detected by Western blotting using RT97 and SMI31 antibodies. The passage number of cells used in the study by Hartley *et al.*, (1996) was 84. As previously noted, ECACC recommend that their clone not be used beyond passage 20, due to loss of neuronal markers. The Leicester clone used in this project had been obtained at an unknown passage number, but, through ensuing

communication with their donor, was proposed to be high. If even higher than passage 84, it may be that neuronal markers had become scarce. Despite this, axon-like processes were observed, but their structural composition remains unknown.

In contrast, despite morphological differentiation, the ECACC and Johnson clones were more heterogeneous in terms of cell shape and extent of differentiation. The most extensive work was carried out using the ECACC clone primarily due to its commercial availability, an important factor when considering a cell line for continued studies. Secondly the Johnson clone was not made available until a late stage of the project. Having initiated differentiation studies with the ECACC clone, observing ECACC guidelines regarding the upper passage limit, it became apparent that cells would not differentiate morphologically to a mature neuronal phenotype until reaching passage 18 and on occasions a high percentage of cells would never differentiate to this phenotype. Although the exact reason for this is not known, it is worth noting observations made in SH-SY5Y cells in earlier reports. As previously detailed, early characterisation of the SK-N-SH cell line by Ross *et al*, (1983) and Ciccarone *et al*, (1989) suggested that it consisted of three morphologically distinct cell types. Research indicated that cells could undergo spontaneous bi-directional phenotypic and biochemical inter-conversion between neuroblast-like and fibroblast-like types. For example, the neuroblast SH-SY5Y clone appeared homogeneous at time of seeding but after twenty weeks cultivation 0.3% of colonies had inter-converted to an epithelial phenotype. The percentage of the latter phenotype increased further over time suggesting that, despite being an isolated neuroblast clone, a percentage of S-type (substrate adherent) cells are retained. Encinas *et al.*, (2000) address the nature of transdifferentiation in the SH-SY5Y cell line during retinoic acid induced differentiation suggesting that extended treatments with retinoic acid did not produce a homogeneous population of cells due to increasing proliferation of retained S-type cells. It was proposed that this may be particularly true during culture where cells were not routinely passaged, since this process may act to select against substrate adherent cells (Encinas *et al.*, 2000 and references therein). However, it should be observed that in said study, cells were treated with retinoic acid in the presence of 15 % FBS, which could be expected to support extensive proliferation of S-type cells that were non-responsive to retinoic acid. Therefore it could be proposed that treatment with retinoic acid in the presence of a

much reduced serum level, as demonstrated in this project, would reduce the likelihood of this phenomenon. Indeed in my hands, even when cells were responsive to retinoic acid, there was a population of cells which did not differentiate, but their prevalence did not appear to increase following extended retinoic acid treatments of up to 21 days. These early observations determined that in this project ECACC cells were only used between passage 18 and 20. Where a whole population of cells appeared unresponsive to retinoic acid following 48 h exposure to the drug, the experiment was abandoned. This ensured that all experiments were carried out using a high percentage of pre-differentiated cells of neuronal phenotype. This phenomenon was only observed with the ECACC clone. Johnson clone cells were obtained at passage 14. Whilst experience with this clone was limited, differentiation proved reproducible and was not dependent upon passage number. Mitotic cells, however, did exhibit a more pronounced neuronal morphology than observed in the ECACC SH-SY5Y clone.

3.3.2 Proliferation and viability of differentiated cells

A reduction in serum levels and addition of chemical agents has potential to induce stress to cells that may result in death. According to Macleod et al., (2001), serum withdrawal induced a significant proportion of differentiated SH-SY5Y cells to undergo apoptosis. As previously described, staurosporine can induce both differentiation and apoptosis in a concentration dependent manner, whilst retinoic acid was shown at a concentration of 20 μM to induce apoptosis in the Leicester SH-SY5Y clone. Observation of cells suggested that retinoic acid treatment was not detrimental to cell viability but was assessed in a single trial for its effects on viability as determined by trypan blue exclusion and MTT reduction assays in ECACC SH-SY5Y cells. 10 μM retinoic acid did not affect cell viability following 7 days treatment, and an increase in MTT reduction/cell following retinoic acid treatment was noted. This result may represent a cellular response to addition of an external agent. Whilst investigating use of the MTT assay for studying toxicity in primary astrocyte and C_6 glioma cell cultures, Cookson et al., (1995) reported an increase in MTT reduction to formazan product in response to twelve different compounds tested. Increased MTT conversion may result from alterations in co-factor levels, enzyme activities i.e. cytosolic and mitochondrial dehydrogenases and

other NADH/NADPH linked enzymes (Cookson *et al.,* 1995). As hypothesised, retinoic acid treatment caused a reduction in cell proliferation, consistent with removal of cells from the cell cycle into G_0 phase and terminal differentiation.

3.3.3 Biochemical markers of differentiation

Whilst differences in morphological response to differentiating agents were apparent between clones, so too was the expression of biochemical markers. Table 3.1 summarises the expression of neuronal markers compared to mitotic controls at day 7 of the differentiation process allowing a preliminary comparison of the SH-SY5Y clones to be made.

Neuronal marker	ECACC clone retinoic acid differentiation	Johnson clone retinoic acid differentiation
Tissue transglutaminase expression	↑↑↑	↑↑↑
Total NF-H level	↓	↑↑↑
Phosphorylated NF-H level	↓↓↓ Sub-cellular redistribution	↓↓↓ Sub-cellular redistribution
Phosphorylated NF-M level	↓↓ Sub-cellular redistribution	↓ Sub-cellular redistribution
Fold increase in ratio of NF-M:NF-H phosphorylation	1.9	1.3
Bcl-2 expression	↓↓	↑↑

Table 3.1. Summary of expression of biochemical markers following 7 days differentiation in SH-SY5Y cells.
Results of assessment of biochemical markers of retinoic acid induced differentiation in ECACC and Johnson clones are summarised in Table 3.1. The Leicester clone was not included as it had been deemed unsuitable for proposed work. Elevation or reduction in expression of markers compared to mitotic controls were graded;

↑ > 10 % elevation; ↑↑ >20% elevation; ↑↑↑ > 50 % elevation
↓ > 10 % reduction; ↓↓ > 20 % reduction; ↓↓↓ > 50 % reduction

Sub-cellular redistribution – determines where the distribution of the marker was shown to change in differentiated cells indicative of a neuronal phenotype.

3.3.3.1 *Retinoic acid and staurosporine cause an elevation in tTG expression.*

tTG expression was greatly elevated in a time dependent manner by retinoic acid treatment in both ECACC and Johnson clones, indicative of a neuronal phenotype in accordance with Tucholski *et al.,* (2001) and Singh *et al.,* (2003). Interestingly the observed increase was most pronounced in the ECACC clone following retinoic acid treatment, as shown by Western blot analysis and immunocytochemistry, possibly due to the mitotic Johnson clone appearing more neuronal-like. Staurosporine treatment (results not shown) also induced a large increase in tTG expression in the ECACC clone; this observation has not previously been documented and may suggest a role for tTG in staurosporine-induced differentiation. The mechanism by which staurosporine may increase tTG expression and the downstream consequences of this in terms of neuritogenesis and cell survival, or indeed cell death are as yet unknown. Further trials are required to confirm this observation. However a role for tTG has been reported in staurosporine induced apoptosis in SK-N-BE cells whereby tTG over-expression was shown to prime cells for apoptosis via modification of mitochondrial homeostasis in an event independent from, and preceding release of cytochrome c and apoptosis inducing factor (AIF) (Piacentini *et al.,* 2002). It should be noted, however, that Tucholski *et al.,* (2001) show that retinoic acid induced tTG expression, culminating in neuronal differentiation in SH-SY5Y cells, did not increase the rate of apoptosis. Following retinoic acid treatment it is documented that tTG expression and activity is increased, and leads to, via activation of RhoA, induction of MAPK pathways that result in cytoskeletal reorganisation (Singh *et al.,* 2003).

3.3.3.2 *The role of Bcl-2 in differentiation*

The Bcl-2 family of proteins are key players in the control of apoptosis, incorporating both pro - and anti-apoptotic members that localise to the mitochondria and endoplasmic reticulum, controlling calcium stores and cytochrome c release. Expression of anti-apoptotic Bcl-2 is said to protect against cell death during development when apoptotic and survival pathways converge (Farlie *et al.,* 1995). It has been reported that retinoic acid increases Bcl-2 expression whilst, conversely, staurosporine reduces Bcl-2 expression (Tieu *et al.,* 1999). This differential

expression was shown to impose differential vulnerabilities to toxin treatment, a phenomenon also described by Lombet *et al.,* (2001). In the ECACC SH-SY5Y clone, staurosporine treatment did indeed drastically reduce Bcl-2 expression levels (27.6 % of mitotic control) in agreement with fore-mentioned studies (results not shown). Retinoic acid induced differentiation of the Johnson clone caused a 40 % increase in Bcl-2 expression at day 7 of the time course; again in agreement with previous studies and indicative of neuronal differentiation. In contrast, following retinoic acid treatment of the ECACC clone for 7 days, Bcl-2 level was reduced to 60 % of mitotic controls. This result was unexpected but was obtained from duplicate flasks and therefore warrants further clarification; however morphological and viability assays carried out over the same time course showed cells to be healthy and viable. It should also be appreciated that clonal differences in SH-SY5Y cells have definitely been shown to be apparent in this project, which may account for this anomaly. Indeed, Yuste *et al.,* (2002) reported that over expression of anti-apoptotic Bcl-X$_L$, rather than Bcl-2 played a predominant role in protection from staurosporine induced caspase activation, cytochrome c release and apoptotic changes in SH-SY5Y cells. The authors suggest that pro-apoptotic members of the Bcl-2 family that are bound by Bcl-X$_L$ may be better neutralised than those bound by Bcl-2 in the SH-SY5Y system. This serves to prove that Bcl-2 itself may be less important than other anti-apoptotic Bcl-2 family members in certain SH-SY5Y clones.

3.3.3.3   *NF status and specific phosphorylation during differentiation*

NF phosphorylation is considered an integral process in axonal development in which NFs interact with one another and other cytoskeletal elements providing strength and stability to the axon and increasing axonal calibre (Shea *et al.,* 2003). Increased NF-H and NF-M phosphorylation has been described in differentiation studies, correlating with neurite outgrowth following retinoic acid treatment in SH-SY5Y cells (Sharma *et al.,* 1999c; Encinas *et al.,* 2000; Li *et al.,* 2000; Singh *et al.,* 2003). This project has shown that following retinoic acid treatment, NF-H phosphorylation was reduced compared to mitotic control cells in both the ECACC and Johnson clones. This result was unexpected but reproducible using numerous extraction techniques and various NF-specific antibodies. However it should be noted that in the ECACC clone, following a small reduction in the first 24 h, NF-M

phosphorylation levels were better maintained over the 7-day time course, suggesting that NF-M phosphorylation may be of greater importance in maintaining axon-like structures in this particular SH-SY5Y clone. Interestingly, irrespective of the source of the SH-SY5Y clone, the ratio of NF-M:NF-H phosphorylation increased following retinoic acid treatment. Since the retinoic acid concentration used in this project was consistent with the literature, observed differences in NF phosphorylation status may be in part due to clonal variations and in part to differences in culture conditions such as tissue culture plastic ware, frequency of media changes and components of the basal medium. Studies with the ECACC clone gave the same reduction in NF-H phosphorylation when cells were treated with retinoic acid in the presence of 10 % FBS (results not shown), suggesting that reduced serum conditions were not the cause. Immunocytochemical analysis of retinoic acid treated cells showed phosphorylated NF epitopes to be correctly distributed along the length of the axon-like processes suggesting that retinoic acid treated cells exhibit a neuronal phenotype that can be maintained by the levels of phosphorylated NF proteins present. An important observation was that a phosphorylated pool of NFs was always present in the cell body of differentiated SH-SY5Y cells in addition to axonal staining. Previous studies reveal a Triton-soluble pool of phosphorylated NF-H residing in the perikaryon of differentiated NB2a/d1 mouse neuroblastoma cells (Shea *et al.,* 1988; 1990) a proportion of which were subsequently shown to incorporate into the existing Triton-insoluble cytoskeleton (reviewed by Shea *et al.,* 1997b). Poltorak and Freed, (1989) identified phosphorylated NFs in the perikarya of fresh, unfixed rodent brain sections and neuroblastoma cells, and concluded that phosphorylation of NFs in the perikaryon is a normal process *in-vivo*.

3.3.3.4 The role of MAPK and CDK-5 pathways in NF phosphorylation and neuritogenesis.

Several kinases have a potential role in NF phosphorylation during neuronal differentiation including ERK 1/2 (Veeranna *et al.,* 1998), JNK (Giasson and Mushynski, 1996; Brownlees *et al.,* 2000) and CDK-5 (Li *et al.,* 2000; Grant *et al.,* 2001; Sharma *et al.,* 1999c). The contribution of a particular kinase to NF phosphorylation may be dependant on the species origin of cells and indeed the stimuli inducing phosphorylation (O'Ferrall *et al.,* 2000). In differentiating SH-

119

SY5Y cells, CDK-5 has been proposed to be an important kinase in phosphorylating NF-H and NF-M given the high number of KSPXK motifs present which are preferentially phosphorylated by this kinase (Sun *et al.,* 1996). However, ERK 1/2 are able to phosphorylate all KSP motifs in NF proteins (Veeranna *et al.,* 1998) and therefore warrant due consideration in this cell line. In order to investigate the role of MAPKs and CDK-5 in NF-H/NF-M phosphorylation in the ECACC SH-SY5Y clone during retinoic acid induced differentiation, specific inhibitors to each of the fore-mentioned kinases were added to differentiation medium and incubated with cells over a 7-day time course. The effects of kinase inhibition on total NF status and NF phosphorylation were analysed in two independent experiments. In addition, neuritogenesis was assessed following treatment with retinoic acid alone and in conjunction with inhibitors in a single preliminary trial. PD98059 and BL-1 (inhibitors of ERK 1/2 and CDK-5 respectively) each reduced NF-H and NF-M phosphorylation in the presence of retinoic acid suggesting a role for these kinases. However, further trials would be required to confirm the significance of this finding. Interestingly, following incubation with all kinase inhibitors, total NF protein levels, were increased. At the concentration tested (5 μM), PD98059 caused only 25 % inhibition of ERK phosphorylation. However this was sufficient to reduce neuritogenesis and also to reduce NF phosphorylation. This is in agreement with Encinas *et al.,* (1999) who report that the Ras/MAPK pathway was necessary for BDNF induced neuritogenesis in retinoic acid pre-treated SH-SY5Y cells. However other published studies propose that the ERKs play no role in neuritogenesis of SH-SY5Y cells (Singh *et al.,* 2003; Miloso *et al.,* 2004). The results presented in my study are contrary to Singh *et al,* (2003) who reported that 50 μM PD98059 had no effect on retinoic acid induced neuritogenesis in SH-SY5Y cells. However clonal differences may account for this anomaly since the cells used by Singh *et al,* (2003) originate from Professor G. Johnson of the University of Alabama (Johnson clone). Miloso *et al,* (2004) report that despite persistent ERK activation following retinoic acid treatment, PKC rather than ERK was important in early neuritogenesis. Additionally, this study proposed retinoic acid-induced ERK activation to occur via PKC or PI3-K pathways as opposed to the Raf-kinase dependant pathway, a finding supported by López-Carballo *et al,* (2002). Hence, whilst further characterisation of the ECACC clone may benefit from clarification of the role of PI3-K pathway in

differentiation, this study suggests a role for the ERK pathway in retinoic acid-induced neuritogenesis.

Whilst having potential to phosphorylate NFs in this system, JNK is most usually associated with stress induced NF-phosphorylation (Brownlees *et al.,* 2000). That said, using dorsal root ganglion O'Ferrall *et al,* (2000) report that CEP-1347, an alternative compound to CEP-11004, also found to inhibit JNK (Maroney *et al.,* 1998), lowered constitutive NF-H phosphorylation in non-stressed cells. Results in the current study suggest that the presence of the JNK inhibitor CEP-11004 had no effect on NF phosphorylation during differentiation but increased neuritogenesis. A hypothesis for these findings is discussed below.

CDK-5 was proposed to play an important role in NF phosphorylation in this cell line. However, whilst results suggest that treatment with the CDK-5 inhibitor, BL-1, attenuated NF phosphorylation, no effect on neuritogenesis was observed. It may be possible to relate the differential effects of inhibitors on NF phosphorylation and neuritogenesis to differences in ERK phosphorylation. Thus CEP-11004, increased ERK phosphorylation levels, and also increased neurite outgrowth. On the other hand, PD98059 and BL-1 both reduced ERK phosphorylation compared to controls and cause a reduction, or no change in neuritogenesis respectively. The mechanism by which CEP-11004 induced ERK phosphorylation is unknown and this result requires further clarification. It may have arisen from two scenarios; a response to MLK inhibition i.e. cross-talk between pathways or a secondary response arising from CEP-11004 treatment that is unrelated to MLK inhibition.

In a study using PC12 cells, Sharma *et al,* (2002), propose that CDK-5/p35 can phosphorylate active MEK 1, resulting in reduced MEK 1 activity and reduced ERK 2 phosphorylation. Conversely treatment of cells with CDK-5 inhibitor, rescovitine, significantly increased ERK 1/2 phosphorylation indicating that CDK-5 may provide feedback regulation of MAPK pathways. In the current study it was noted that BL-1 reduced ERK phosphorylation and had no effect on neuritogenesis. The concentration of BL-1 employed may not have been high enough. It has to be noted, however, that according to data provided by the supplier of BL-1, MAPK is approximately 100 fold less sensitive to BL-1 than CDK-5. Hence the reduction in

ERK phosphorylation following BL-1 treatment in the current work may be a result of alternative cross-talk between MAPK pathways or indeed a previously uncharacterised effect of the inhibitor, independent of CDK-5 inhibition.

In conclusion a marked variation in morphology and expression of biochemical markers of differentiation was observed between three clones of the SH-SY5Y cell line, highlighting the importance of cell characterisation. The ECACC clone was chosen to pursue further toxicological studies primarily due to its commercial availability and therefore more precise definition of origin and employment guidelines. In addition the clone differentiates to a stable neuronal phenotype using retinoic acid, allowing toxicity studies to be undertaken over extended time periods. Biochemical markers have been identified that support and maintain the retinoic acid induced neuronal phenotype.

CHAPTER IV

CHARACTERISATION OF EFFECTS OF MPP$^+$ AND PROTEASOME INHIBITION ON CYTOSKELETAL PROTEINS

4.1 INTRODUCTION

4.1.1 MPP$^+$ induced toxicity and its assessment in SH-SY5Y cells

This project investigates the effects of the Parkinsonian mimetic MPP$^+$ on human (SH-SY5Y) neuroblastoma cells. The effects of MPP$^+$ on a pre-differentiated human cell line may provide data with significant clinical and research implications. For example, a human cell culture model may be useful for neuroprotective screening and thus identifying therapeutic agents that prevent or revoke MPP$^+$ induced neuronal degeneration.

The pre-differentiated SH-SY5Y cell line is potentially an ideal model for the investigation of markers of MPP$^+$ toxicity. As previously detailed this cell line expresses the DA uptake system required for MPP$^+$ uptake into cells (Song and Ehrich, 1998). The primary insult in PD and MPP$^+$ toxicity is complex I inhibition with resultant ROS production contributing to oxidative stress. Importantly, MPP$^+$ toxicity in SH-SY5Y cells has been correlated with increased ROS and lactate production, both indicative of impaired electron transport and preceding irreversible commitment to apoptosis, during which, a collapse of ROS production and mitochondrial membrane potential was observed (Fall and Bennett, 1999). Anti-oxidant enzyme activities are reportedly elevated in MPP$^+$ treated SH-SY5Y cells suggestive of compensatory mechanisms to protect against oxidative stress (Cassarino *et al.*, 1997). Additionally, SH-SY5Y cells can produce DA from tyrosine since they express tyrosine hydroxylase activity augmenting the potential for ROS production (Biedler *et al.*, 1978).

Before commencing MPP$^+$ studies concentrations of the toxin that were cytotoxic and sub-cytotoxic to pre-differentiated ECACC SH-SY5Y cells over a range of time points were established using the MTT reduction assay. This assay has been previously used to investigate MPP$^+$ toxicity in SH-SY5Y cells (Gómez *et al.*, 2001; Gómez-Santos *et al.*, 2002; Joyce *et al.*, 2003). Also, previously in my laboratory, a comparison of MTT reduction, lactate dehydrogenase release and Trypan blue exclusion assays yielded comparable data with respect to cell viability measurements following MPTP treatment of N2a mouse neuroblastoma cells, despite measuring

slightly different parameters (De Girolamo, 2000, PhD thesis, The Nottingham Trent University). A significant decrease in MTT reduction in toxin treated cells compared to the control group was regarded as evidence of cytotoxicity. Conversely a sub-cytotoxic concentration may cause changes in cell morphology but does not cause a significant reduction in viability compared to controls. In order to further validate the MTT assay in SH-SY5Y cells, viability was also determined by ATP concentration. In contrast to MPP$^+$, MPTP is taken up into cells via passive diffusion. In order to fully characterise the SH-SY5Y cell line in our hands, a comparison of MPTP and MPP$^+$ induced toxicity was made, both in mitotic and pre-differentiated cells.

Most studies with MPP$^+$ in SH-SY5Y cells have used mitotic cells (Song *et al.,* 1997; Gómez *et al.,* 2001; Brill II and Bennett Jr, 2003; Gómez-Santos *et al.,* 2002; Halvorsen *et al.,* 2002), with fewer studies using differentiated cells, with exposure to toxin for a relatively short time (24-96 h) (Joyce *et al.,* 2003; Mathiasen *et al.,* 2004). Whether a treatment is considered to be "short-term" or "long-term" depends on the system used; for example a 4-day exposure in mitotic cells may be considered long-term, but in differentiated cells this would represent a relatively short-term exposure. Likewise *in-vivo* animal models may define a chronic exposure in terms of months. Indeed Petroske *et al,* (2001) describe a chronic mouse model of combined MPTP/probenecid administration resulting in sustained alterations in the nigrostriatal pathway for 6 months after cessation of treatment. This would be unrealistic using *in-vitro* cell culture models, where an equivalent chronic exposure may be considerably shorter. The aim of this study was to investigate MPP$^+$ toxicity in differentiated SH-SY5Y cells over a range of time points. Hence experiments carried out over 24-72 h were considered "short-term" whilst investigations extending over 14 days were termed "chronic".

4.1.2 The effect of neurotoxin treatment on the neuronal cytoskeleton

Abnormal cytoskeletal element expression and post-translational modification events are extensively documented as being characteristic of neurodegenerative disorders. Hartley *et al.,* (1997) review that NF accumulation is present in giant axonal neuropathies and amyotrophic lateral sclerosis, whilst accumulation of phosphorylated NFs associated with Lewy bodies are accepted characteristics of the

125

Parkinsonian brain. Most *in-vitro* cell culture studies investigating Lewy body-like inclusions have focussed on the aggregation of α-synuclein (Gómez-Santos *et al.,* 2002; Matsuzaki *et al.,* 2004) and more recently, parkin (Zhao *et al.,* 2003; Muqit *et al.,* 2004; for review see Imai and Takahashi, 2004). Whilst these proteins can undoubtedly play a pivotal role in inclusion formation, significantly less work has focussed on aberrant NF accumulation and phosphorylation in *in-vitro* PD models.

In-vitro studies have, however, revealed the presence of abnormal NF accumulation and phosphorylation following treatment with certain toxic agents. For example, Hartley *et al.,* (1997) report the filamentous perikaryal accumulation of NFs in differentiated and non-differentiated SH-SY5Y cells in response to acrylamide and 2,5-hexanedione. Shea *et al.,* (1995) found extensive NF-H phosphorylation in neuronal cells following aluminium treatment, and in a later study, reported that these phosphorylated NFs were retained in the cell perikarya where they formed filamentous inclusions (Shea *et al.,* 1997a). The first studies to focus on the effects of MPTP on NF phosphorylation investigated the effects of sub-cytotoxic MPTP concentrations on NF-H phosphorylation. (De Girolamo *et al.,* 1997, 2001). It was found that in differentiating and differentiated N2a cells, NF-H were hyper-phosphorylated and subsequently localised to the cell perikaryon. This correlated with inhibition of axon outgrowth and axon retraction in the differentiating and differentiated models respectively. Recent research showed that NF phosphorylation was increased following proteasome inhibition in PC12 cells, concomitant with increased JNK activity but with no change in CDK-5 activity, suggesting that the proteasome-ubiquitin system may be involved in NF degradation (Masaki *et al.,* 2000).

A potential role for changes in tubulin expression/dynamics following MPTP/MPP⁺ exposure has been investigated but not in SH-SY5Y cells. The MT system may be an important contributor to MPP⁺ toxicity for a number of reasons. Firstly tubulin epitopes have been detected in Lewy bodies (Galloway *et al.,* 1988). Secondly the MT plays a major role in intracellular transport in cells. Notably it was found by Muchowski *et al.,* (2002) that an intact microtubule cytoskeleton was required for aggregation and inclusion body formation induced by a mutant huntingtin aggregate in cellular models for Huntington's disease. Ren *et al,* (2003) also provide evidence

that Parkin is a tubulin binding protein that prevents the accumulation of misfolded protein by increasing tubulin ubiquitination and degradation through the proteasome. Cappelletti *et al.,* (1995) found a change in ratio of α and β tubulin sub-units following MPP$^+$ treatment of NGF-differentiated PC12 cells and later reported that MPP$^+$ reduced tubulin polymerisation both in intact cells and when incubated with MT proteins directly in a test tube (Cappelletti *et al.,* 1999, 2001). It should be noted that cytoskeletal changes observed in cultured cells have occurred using sub-cytotoxic concentrations of toxins (De Girolamo *et al.,* 2000; Song *et al.,* 1997; Cappelletti *et al.,* 1995).

4.1.3   Aims of chapter

Since neurodegeneration is a chronic process, this project sought to develop a pre-differentiated human neuroblastoma model in which sub-cytotoxic concentrations of MPP$^+$ were employed over extended time periods (14 days), to more closely mimic the *in-vivo* situation. Studies used the active metabolite of MPTP, (MPP$^+$), since the SH-SY5Y cell line was shown to express a dopamine uptake system (Song and Ehrich, 1998), as utilised by MPP$^+$ in dopaminergic cells *in-vivo.* The aim of this chapter was firstly to propose suitable sub-cytotoxic and cytotoxic concentrations of MPP$^+$ over a range of time points.

On the basis of previous work by De Girolamo *et al,* (2000) and Cappelletti *et al.,* (1995), the effects of MPP$^+$ on expression and post-translational modification of cytoskeletal proteins were first analysed using Western blotting. Whilst cytoskeletal proteins are components of the aggresome structure (Johnston *et al.,* 1998; Ardley *et al.,* 2003; Muqit *et al.,* 2004), the potential role of NF proteins in the formation of aggresomes remains to be investigated. In light of this research, the distribution of cytoskeletal proteins following MPP$^+$ treatment was subsequently assessed using immunocytochemistry. In general immunocytochemical analysis of cytoskeletal proteins was conducted on pre-fixed cells. However by using a permeabilisation step prior to fixation in some experiments [based on a method by Ito *et al.,* (2002), with some modifications], it was anticipated that soluble proteins would be removed allowing insoluble proteins (associated with protein aggregation), to be visualised more readily.

Inhibition of the proteasome is implicated in neurodegenerative disease and is reportedly a consequence of MPP$^+$ toxicity in cultured cells (Höglinger *et al.*, 2003). It has also been proposed that the ubiquitin - proteasome system be involved in degradation of NF and tubulin proteins (Masaki *et al.*, 2000; Ren *et al.*, 2003). Thus the role of proteasomal inhibition in degradation of cytoskeletal elements in the pre-differentiated SH-SY5Y system was also assessed.

4.2 RESULTS

4.2.1 Assessment of cell viability following MPP$^+$/ MPTP exposure in mitotic and differentiated cells

4.2.1.1 Comparison of MPTP/MPP$^+$ toxicity in mitotic and differentiated cells

In an initial dose-ranging trial, the comparative effects of MPTP and MPP$^+$ were assessed in mitotic and pre-differentiated cells over 72 h. In all experiments MTT reduction was linear during the assay, indicating that initial rates of enzyme activity were being measured. Results indicated that both mitotic and differentiated cells were more sensitive to MPP$^+$ than to MPTP at all time points (see Figs 4.1 and 4.2). Differentiated cells were less sensitive to toxin treatment than mitotic cells. The EC$_{50}$ values for mitotic and differentiated cells following MPTP and MPP$^+$ treatment are listed in table 4.1. Toxicity was achieved by 1 mM MPP$^+$ at 48 and 72 h exposures in differentiated cells (refer to section 4.2.1.3).

EC$_{50}$ values (μM)			
Cell type	Time (h)	MPP$^+$	MPTP
Mitotic	24	1800	3600
	48	400	2200
	72	300	2400
Differentiated	24	>5000*	>5000*
	48	2600	4750
	72	2200	4000

Table 4.1 EC$_{50}$ values for mitotic and differentiated cells in a single experiment following treatment with MPTP or MPP$^+$.
(*) values were approximate since they were beyond the range of toxin concentrations tested.
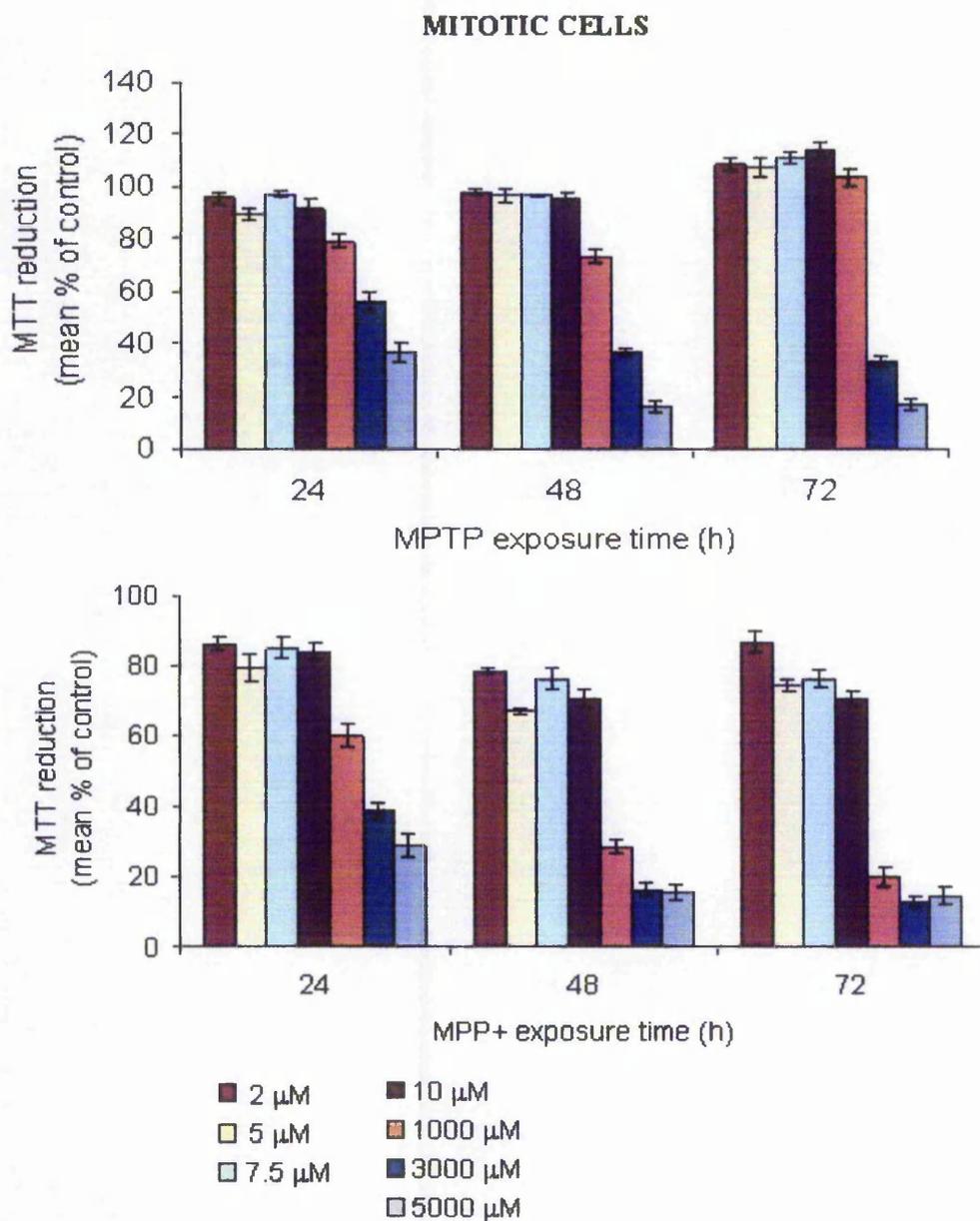
MITOTIC CELLS

Figure 4.1 Viability of mitotic cells following exposure to MPTP/MPP[+].
Cells were seeded in 96 well plates at 10,000 cells / well and allowed to recover overnight. Medium was removed and replaced with fresh growth medium supplemented with MPTP or MPP[+] as detailed in above. Following 24, 48 and 72 h exposure to toxins, cell viability was assessed using the MTT reduction assay as described in methods section 2.2.3.1. Results are expressed as mean percentage MTT reduction ± SEM of toxin treated cells compared to non-toxin treated control cells (assigned 100 %) (based on 6 replicate wells).
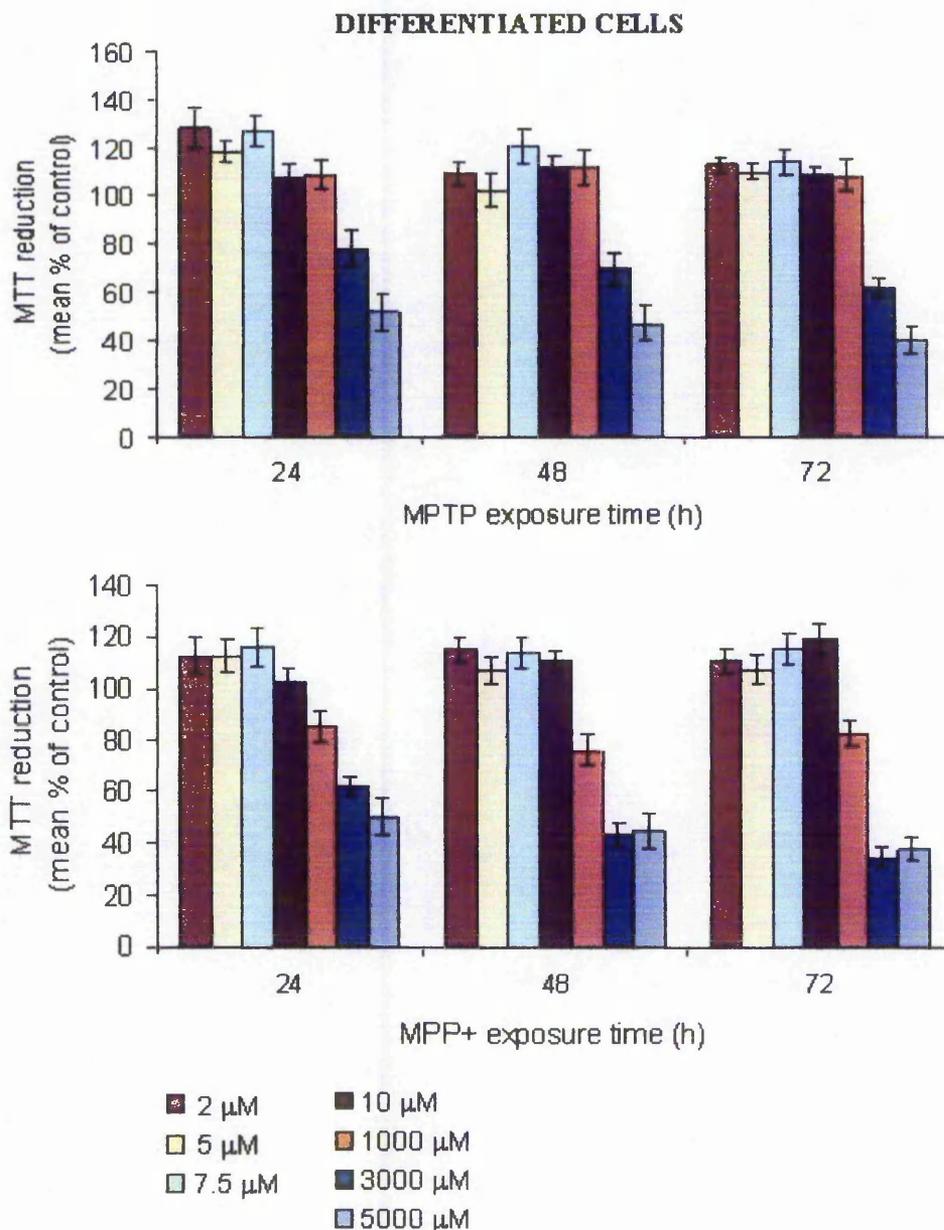
Figure 4.2 Viability of differentiated cells following exposure to MPTP/MPP⁺.
Cells were seeded in 96 well plates at 5,000 cells / well and differentiated over 7 days as detailed in methods section 2.2.1.6. Medium was removed and replaced with fresh differentiation medium supplemented with MPTP or MPP⁺ as detailed in above. Following 24, 48 and 72 h exposure to toxins, cell viability was assessed using the MTT reduction assay as described in methods section 2.2.3.1. Results are expressed as mean percentage MTT reduction ± SEM of toxin treated cells compared to non-toxin treated control cells (assigned 100 %) (based on 6 replicate wells).

4.2.1.2 Validation of MTT studies – comparison of MTT reduction and ATP concentration assays

For chronic studies, cell viability of differentiated cells was also assayed over 14 days of MPP$^+$ exposure. EC$_{50}$ values using the MTT reduction assay were determined as: 7 days, 375 μM; 10 days, 250 μM; 14 days, 100 μM MPP$^+$. To validate the MTT assay, viability was also determined by measuring ATP concentration. Overall MTT reduction and ATP concentration assays were found to show high comparability (compare Fig 4.3 A and B).
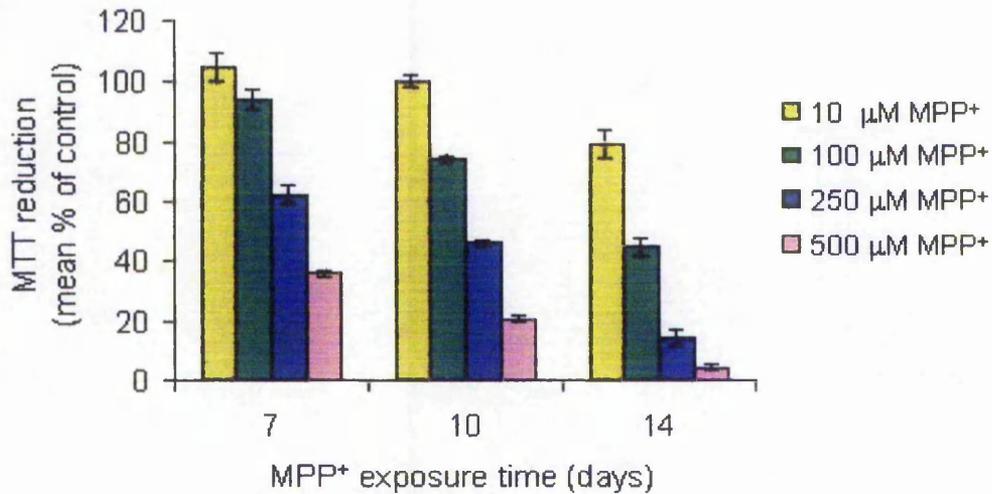
A.
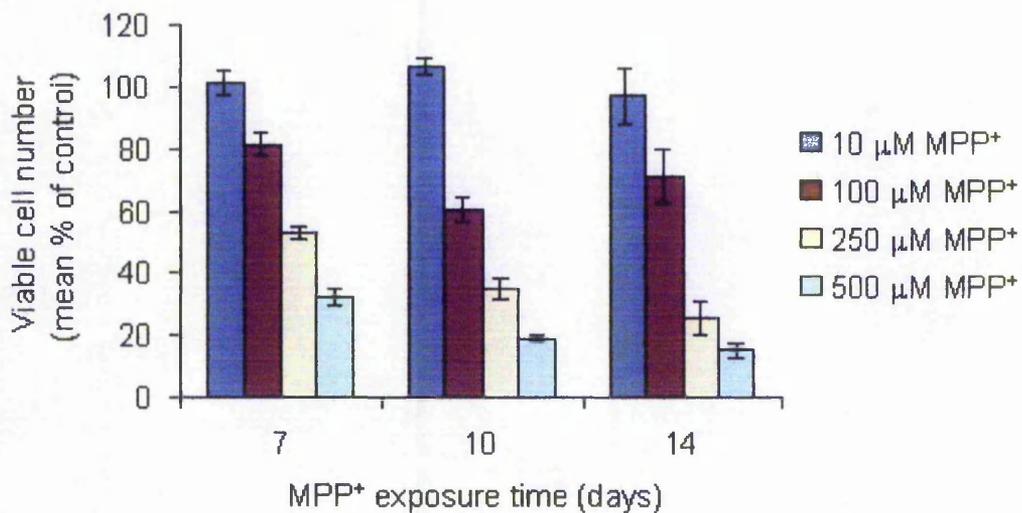
B.

Figure 4.3 Cell viability following chronic MPP$^+$ exposure – comparison of MTT reduction and ATP concentration assays.
Cells were seeded in 96 well plates at 5000 cells / well and differentiated for 7 days as detailed in methods section 2.2.1.6. Medium was removed and replaced with fresh medium supplemented with MPP$^+$. Following MPP$^+$ exposure cell viability assays were performed. A and B, represent cell viability determined over 14 day exposures to MPP$^+$ using the MTT reduction assay and ATP concentration assay (methods sections 2.2.3.1 and 2.2.3.3) respectively. Results are expressed as mean percentage MTT reduction or viable cell number ± SEM (for MTT assay and ATP assay, respectively) of MPP$^+$ treated cells compared to non-toxin treated control cells (assigned 100 %). (A = 6 replicate wells), (B = 5 replicate wells)

4.2.1.3 Determination of working MPP⁺ concentrations

Cytotoxic and sub-cytotoxic concentrations of MPP$^+$ were both time and concentration dependent (Figs 4.2 and 4.3) and chosen on the basis of viability assay data together with consideration of morphological observations and the nature of the experiment in which they were to be used (as summarised in table 4.2). It should be noted that variations in toxicity were observed between experiments and as such, working concentrations are indicated as guidance but are not conclusive as demonstrated in subsequent MTT assays performed throughout chapter V. Cells treated with cytotoxic concentrations of MPP$^+$ appeared abnormally shaped and suffered some degree of process retraction. The morphology of cells exposed to cytotoxic and sub-cytotoxic concentrations of MPP$^+$ over 48 h is shown in Fig 4.4.

MPP$^+$ exposure time	Sub-cytotoxic concentration (μM)	Cytotoxic concentration (μM)
24 h	≤ 1000	≥ 3000
48 h	≤ 10	≥ 1000
72 h	≤ 10	≥ 1000
14 days	< 10	≥ 100

Table 4.2 Summary of MPP$^+$ toxicity in differentiated SH-SY5Y cells
Results of MTT reduction assays shown in Figures 4.2 and 4.3 are summarised to show working sub-cytotoxic and cytotoxic concentrations of MPP$^+$ in differentiated cells over a range of time points as determined from an initial dose ranging trial. It should be noted that using sub-cytotoxic concentrations of MPP$^+$ cells maintained a differentiated morphology, whilst exposure to cytotoxic concentrations of MPP$^+$ induces an abnormal morphology and some process retraction with eventual rounding and cell death.

A. 24 h exposure

a. Differentiated control cells
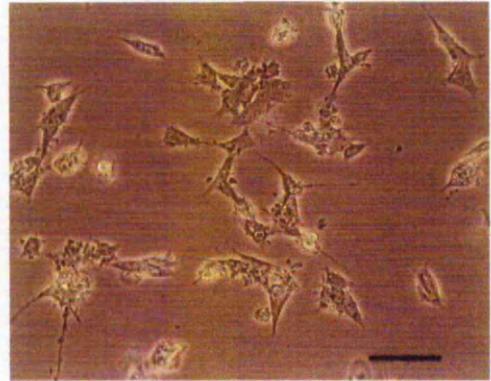
b. 5 mM MPP$^+$

B. 48 h exposure

a. Differentiated control cells
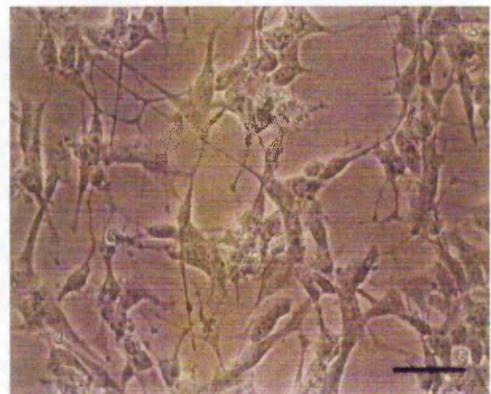
b. 100 µM MPP$^+$
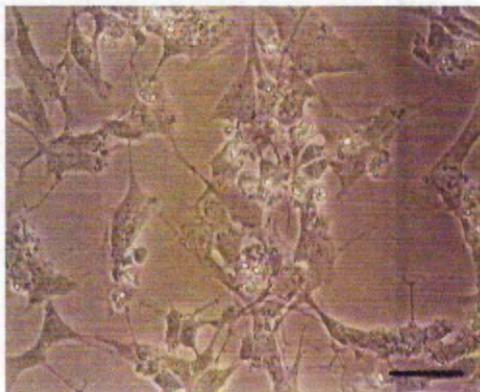
c. 500 µM MPP$^+$
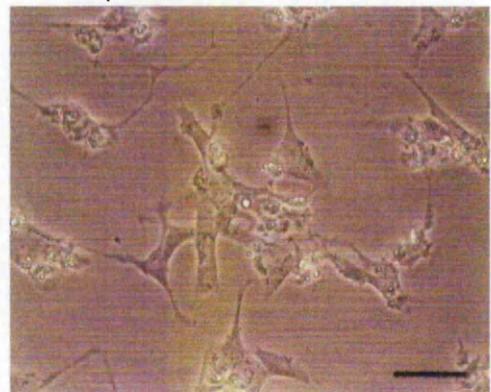
d. 1 mM MPP$^+$

Figure 4.4 Morphological assessment of MPP$^+$ treated cells
Panel A and B represent pre-differentiated cells (see methods section 2.2.1.6) treated with MPP$^+$ at concentrations stated, for 24 and 48 h, respectively. Cells were visualised using phase contrast microscopy at x 200 magnification. Scale bar represents 40 µm.

4.2.2 Changes in cytoskeletal and related proteins following exposure to MPP$^+$: analysis using Western blotting

In this section the effects of MPP$^+$ on the expression and post-translational modification of cytoskeletal proteins are analysed. Western blotting/immunoprobing and imunocytochemical techniques were employed to provide both quantitative analysis of protein expression and distributional changes in proteins. Results are sectioned to represent short-term exposure to cytotoxic concentrations of MPP$^+$ and longer exposures to sub-cytotoxic concentrations that may provide greater analogy to neurodegeneration *in-vivo*.

4.2.2.1 *Cytotoxic concentrations of MPP$^+$*

4.2.2.1.1 *Specific NF phosphorylation status following 24 h exposure to cytotoxic concentrations of MPP$^+$*

Figure 4.5 shows that total NF-H and phosphorylated NF-H / NF-M levels increase following exposure to 5 mM MPP$^+$ over 24 h, accompanied by an increase (approximately 1.6 fold) in the ratio of phosphorylated NF-M to phosphorylated NF-H following MPP$^+$ treatment. Preliminary investigation suggested that the CDK-5 inhibitor, BL-1, partially reversed the increase in phosphorylated NF-M:NF-H ratio observed following exposure to 5 mM MPP$^+$; the ratio of phosphorylated NF-M to phosphorylated NF-H was increased 2.6 fold following MPP$^+$ treatment but was reduced to 1.7 fold following 5 mM MPP$^+$ plus 1 µM BL-1 (see Fig 4.6).
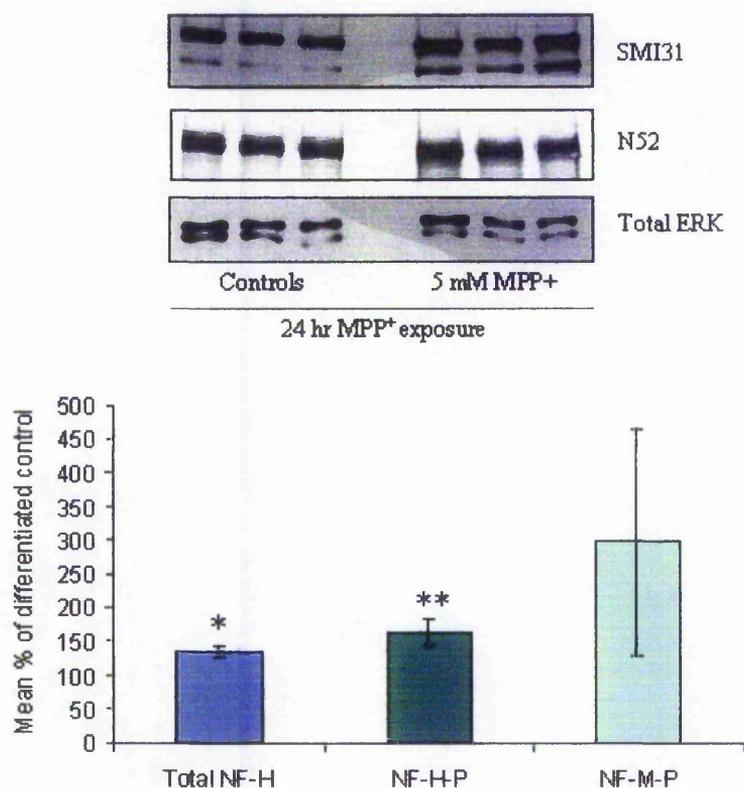
Figure 4.5 NF phosphorylation following 24 h exposure to 5 mM MPP⁺.
Cells were seeded into T25 flasks and differentiated for 7 days as detailed in methods section 2.2.1.6 prior to treatment with fresh differentiation medium alone (controls) or supplemented with 5 mM MPP⁺. Cells were extracted following 24 h exposure to the toxin as detailed in methods section 2.2.5.1 and proteins separated by SDS-PAGE. Protein was transferred to nitrocellulose by Western blotting and probed with SMI31 (1:1000), N52 (1:500) and anti-total ERK 1/2 (1:500). Bands were corrected against total ERK for differences in protein loading. Results are presented as mean % of control (assigned 100 %) ± SEM. Data presented is combined from 3 independent experiments (n = 3). Statistical analysis of control versus toxin treated cells was carried out using two-tailed t-Tests where statistical significance was accepted at p < 0.05 (*) and p < 0.01 (**).

SMI31

NF-H-P →

NF-M-P →

| | Control | 1 µM BL-1 | | 5 mM MPP+ | 5 mM MPP+/ 1 µM BL-1 |
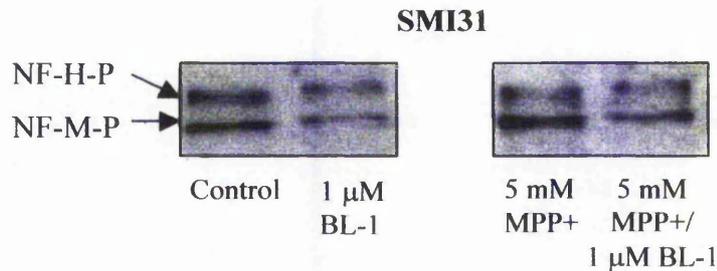
Ratio of NF-M-P:NF-H-P	Control	0.778 ± 0.300
	1 µM BL-1	0.808 ± 0.120
	5 mM MPP⁺	1.992 ± 0.210
	5 mM MPP⁺/1 µM BL-1	1.354 ± 0.120

Figure 4.6 Ratio of phosphorylated NF-M: NF-H following MPP⁺ ± BL-1
Cells were seeded into T25 flasks and differentiated for 7 days as detailed in methods section 2.2.1.6 prior to treatment with fresh differentiation medium alone (controls) or supplemented with 1 µM BL-1, 5 mM MPP⁺ or 5 mM MPP⁺ plus 1 µM BL-1. Duplicate flasks were extracted following 24 h exposure to the toxin as detailed in methods section 2.2.5.1 and proteins separated by SDS-PAGE. Protein was transferred to nitrocellulose by Western blotting and probed with SMI31 (1:1000). The ratio of NF-M phosphorylation to NF-H phosphorylation was calculated. The range of the data is indicated.

4.2.2.1.2 Activation of MAPK pathways following MPP$^+$ exposure

To determine whether ERK or JNK activity were accountable for the increase in NF-H/NF-M phosphorylation following treatment with 5 mM MPP$^+$, cell extracts were immunoprobed using phosphorylation specific ERK and JNK antibodies as shown in Figure 4.7. Phosphorylated JNK levels were significantly reduced compared to differentiated control extracts following a 24 h exposure to MPP$^+$. Phosphorylated ERK levels were also reduced but not significantly.

Changes in the activation patterns of JNK and ERK over a 16 h period were also studied, using cytotoxic (5 mM) and sub-cytotoxic (10 µM) MPP$^+$ for comparison. A transient increase in both JNK and ERK phosphorylation was observed at early time points (30 min), with ERK activation (Fig 4.8A) appearing to be greater than JNK activation (Fig 4.8B) for both MPP$^+$ concentrations. Following a 2 h exposure to 5 mM MPP$^+$, a sustained reduction in ERK activity was observed, followed by a reduction in JNK activity 6 h later. Attempts to analyse p38 MAPK phosphorylation were unsuccessful despite using a variety of commercial antibodies.
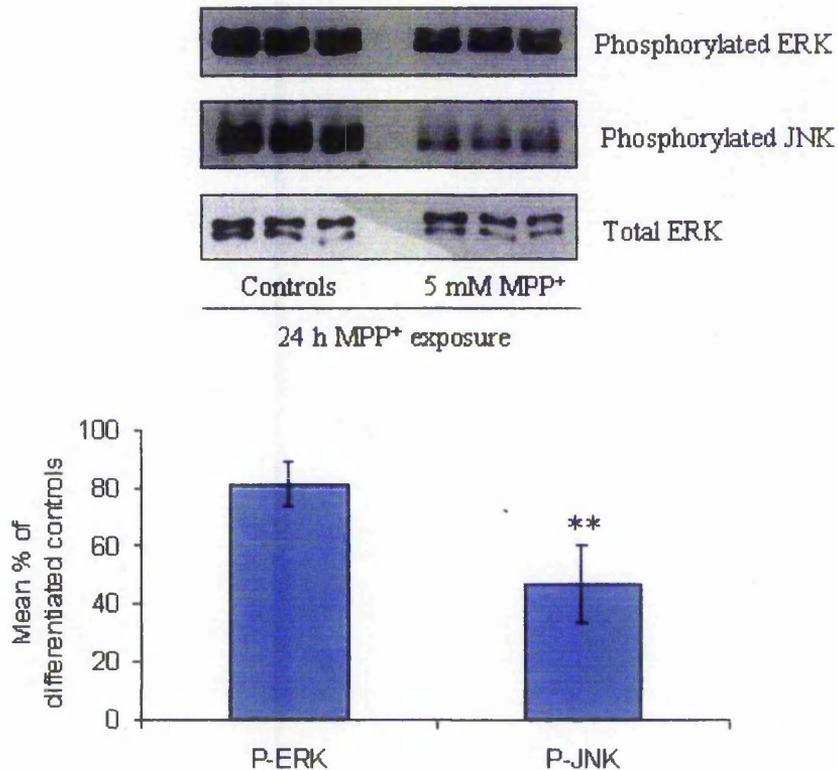
Figure 4.7   ERK and JNK phosphorylation following 24 h exposure to 5 mM MPP$^+$.
Cells were seeded into T25 flasks and differentiated for 7 days as detailed in methods section 2.2.1.6 prior to treatment with fresh differentiation medium alone (controls) or supplemented with 5 mM MPP$^+$. Cells were extracted following 24 h exposure to the toxin as detailed in methods section 2.2.5.1 and proteins separated by SDS-PAGE. Protein was transferred to nitrocellulose by Western blotting and probed with anti-phosphorylated ERK 1/2 (1:500) or anti phosphorylated JNK (1:100). Bands were corrected against total ERK for differences in protein loading. Results are presented as mean % of control (assigned 100 %) ± SEM. Data is derived from three independent experiments (n = 3). Statistical analysis of control versus toxin treated cells was carried out using two-tailed t-Tests where statistical significance was accepted at p<0.01 (**).
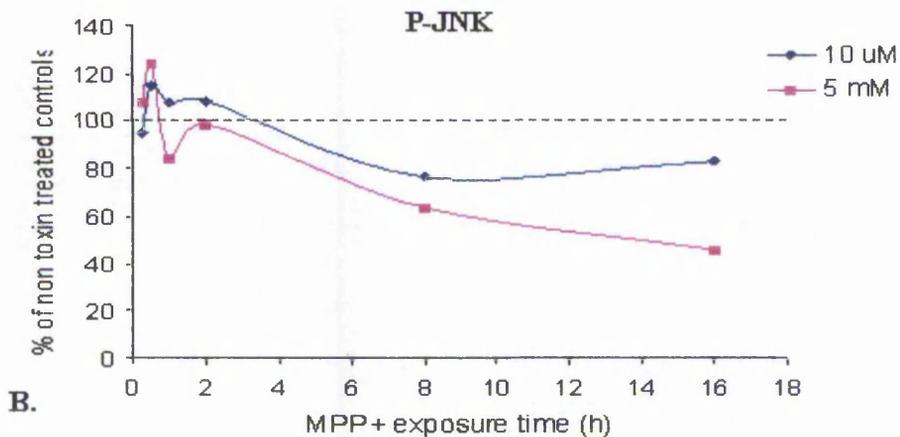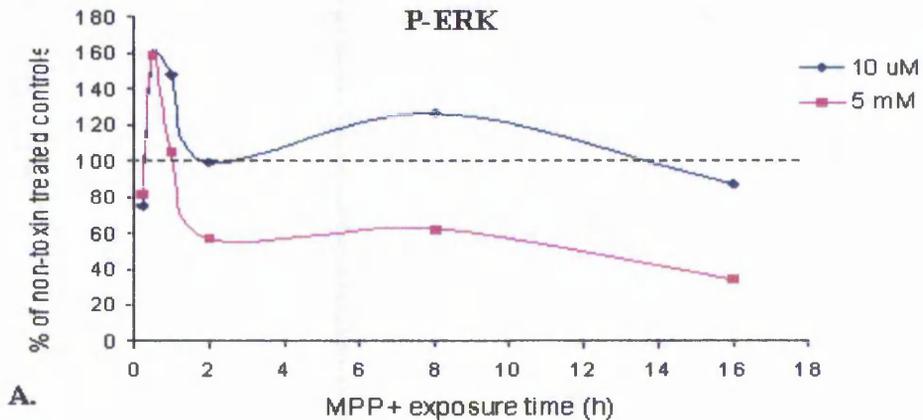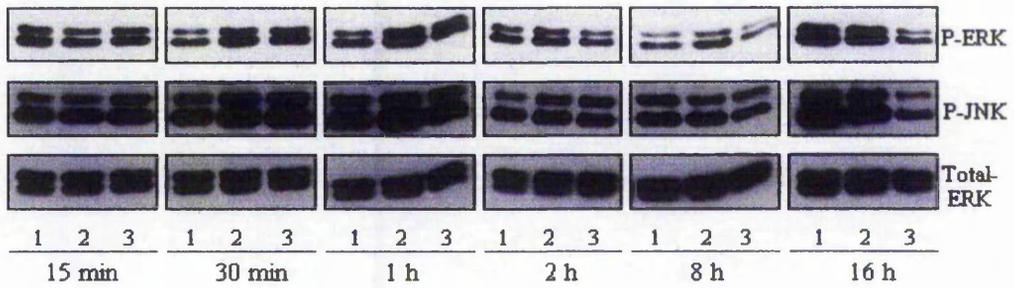
Figure 4.8 Activation of ERK and JNK pathways over 16 h exposure to MPP⁺.
Cells were seeded into 6 well plates at 80,000 cells/well and allowed to differentiate over 7 days as detailed in methods section 2.2.1.6. On day 7, medium was replaced with fresh medium supplemented with MPP⁺. Cells were extracted over a 16 h time course as detailed in methods section 2.2.5.2. 100 μg protein was separated by SDS-PAGE and transferred to nitrocellulose membrane by Western blotting. Nitrocellulose was probed with antibodies against (A) phosphorylated ERK (1:500) and (B) phosphorylated JNK (1:100). Membranes were stripped and re-probed with anti-total ERK 1/2 antibody (1:1000) to correct for differences in protein loading. Band intensity was quantified as detailed in methods section 2.2.8.2.6. Representative blots are shown. Results are presented as mean percentage of differentiated control cells (assigned 100 %). Lanes 1, 2 and 3 represent control, 10 μM MPP⁺ and 5 mM MPP⁺ respectively.

4.2.2.1.3   α-tubulin expression following 24 h exposure to 5 mM MPP⁺

Western blot analyses suggest that α-tubulin expression was not affected by a 24 h exposure to a cytotoxic (5 mM) concentration of MPP⁺ (Fig 4.9).
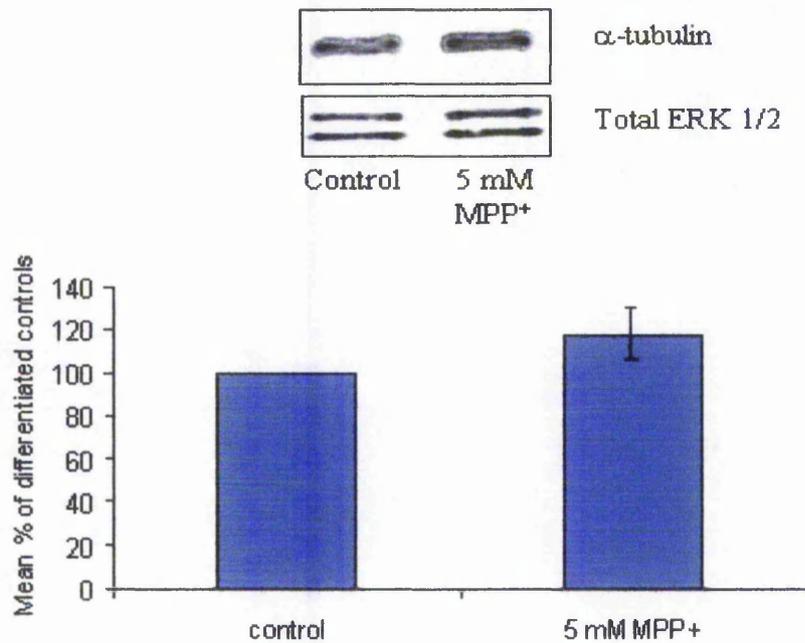
Figure 4.9 Expression of α-tubulin in cells following 24 h exposure to 5 mM MPP⁺.
Cells were seeded into T25 flasks and differentiated for 7 days as detailed in methods section 2.2.1.6 prior to treatment with fresh differentiation medium alone (controls) or supplemented with 5 mM MPP⁺. Cells were extracted following 24 h exposure to the toxin as detailed in methods section 2.2.5.1 and proteins separated by SDS-PAGE. Proteins were transferred to nitrocellulose and probed with anti α-tubulin (B512) (1:500) and anti-ERK 1/2 (1:500) Bands were corrected against total ERK for differences in protein loading. Results are combined from two independent experiments (triplicate flasks in each experiment), presented as mean % of control (assigned 100 %). The range of the mean data is shown.

4.2.2.1.4   Assessment of ubiquitinated proteins following 24 h exposure to 5 mM
MPP⁺

Western blot analyses and immunoprobing using anti-ubiquitin-protein conjugate antibody (UG9510) suggested that the level of ubiquitinated proteins in MPP⁺ treated cells were higher than in non-toxin treated controls (Fig 4.10). In both control and toxin treated cells, ubiquitinated proteins were of high molecular weight (approx 200 kDa).
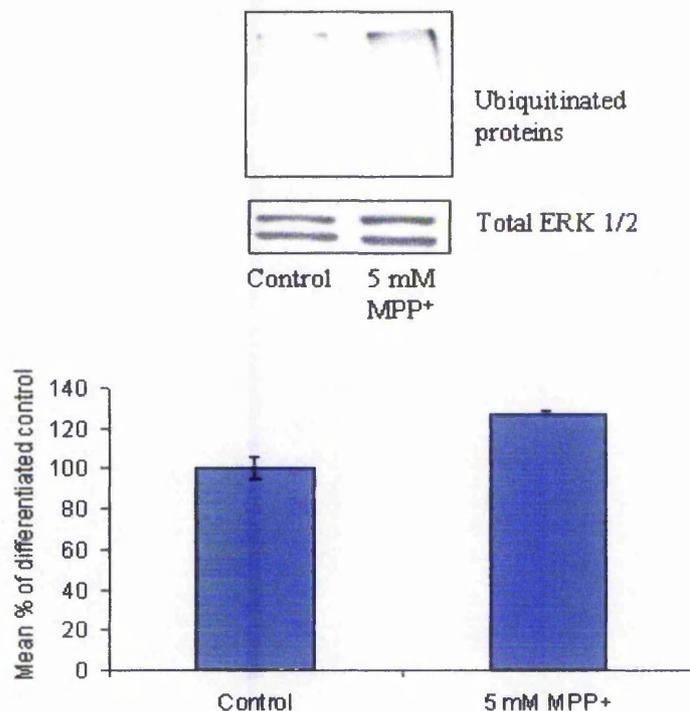
Figure 4.10 Assessment of the level of ubiquitin-protein conjugates in cells following 24 h exposure to 5 mM MPP⁺.
Cells were seeded into T25 flasks and differentiated for 7 days as detailed in methods section 2.2.1.6 prior to treatment with fresh differentiation medium alone (controls) or supplemented with 5 mM MPP⁺. Cells were extracted following 24 h exposure to the toxin as detailed in methods section 2.2.5.1 and proteins separated by SDS-PAGE. Protein was transferred to nitrocellulose by Western blotting and probed with anti-ubiquitin-protein conjugates (1:1000) and anti-ERK 1/2 (1:500). Bands were corrected against total ERK for differences in protein loading. Results from triplicate flasks extracted on the same day are presented as mean % of control (assigned 100 %) ± SEM.

4.2.2.2   72 h exposure to sub-cytotoxic and cytotoxic concentrations of MPP$^+$

4.2.2.2.1   Exposure to sub-cytotoxic and cytotoxic concentrations of MPP$^+$ over 72 h time periods: effects on NF status and α-tubulin

In accordance with previous studies (De Girolamo *et al.,* 2000; Song *et al.,* 1997; Cappelletti *et al.,* 1995), effects of exposure to a sub-cytotoxic and a cytotoxic concentration of MPP$^+$ (10 μM and 500 μM, respectively) were investigated over 72 h. Immunoprobing of Western blots revealed no significant change in NF-H protein levels (Fig 4.11). The total levels of phosphorylated NF-H/NF-M epitopes remained unchanged over the 72 h time course (Fig 4.12). Levels of α-tubulin sub-units were unaffected by both concentrations of MPP$^+$ (Fig 4.13).
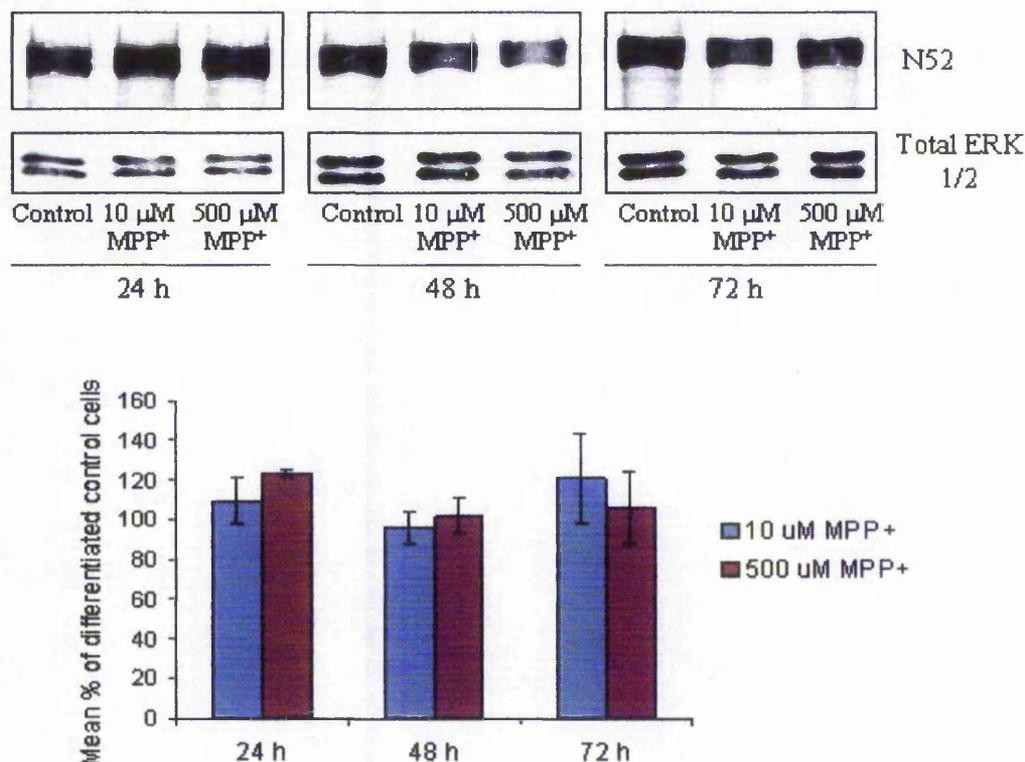
Figure 4.11 Assessment of total NF-H protein levels following MPP+ exposure over 72 h
Cells were seeded into T25 flasks and differentiated for 7 days as detailed in methods section 2.2.1.6 prior to treatment with fresh differentiation medium alone (controls) or supplemented with 10 μM or 500 μM MPP+. Cells were extracted following 24, 48 and 72 h exposure to the toxin as detailed in methods section 2.2.5.1 and proteins separated by SDS-PAGE. Protein was transferred to nitrocellulose by Western blotting and probed with N52 (1:500) and anti-total ERK 1/2 (1:500). Bands were quantified and corrected against total ERK for differences in protein loading and expressed as % of control (assigned 100 %). Results presented are combined data from 3 independent experiments (n = 3) ± SEM. Statistical analysis of control versus toxin treated cells was carried out using two-tailed t-Tests.

Specific NF-H and NF-M phosphorylation status
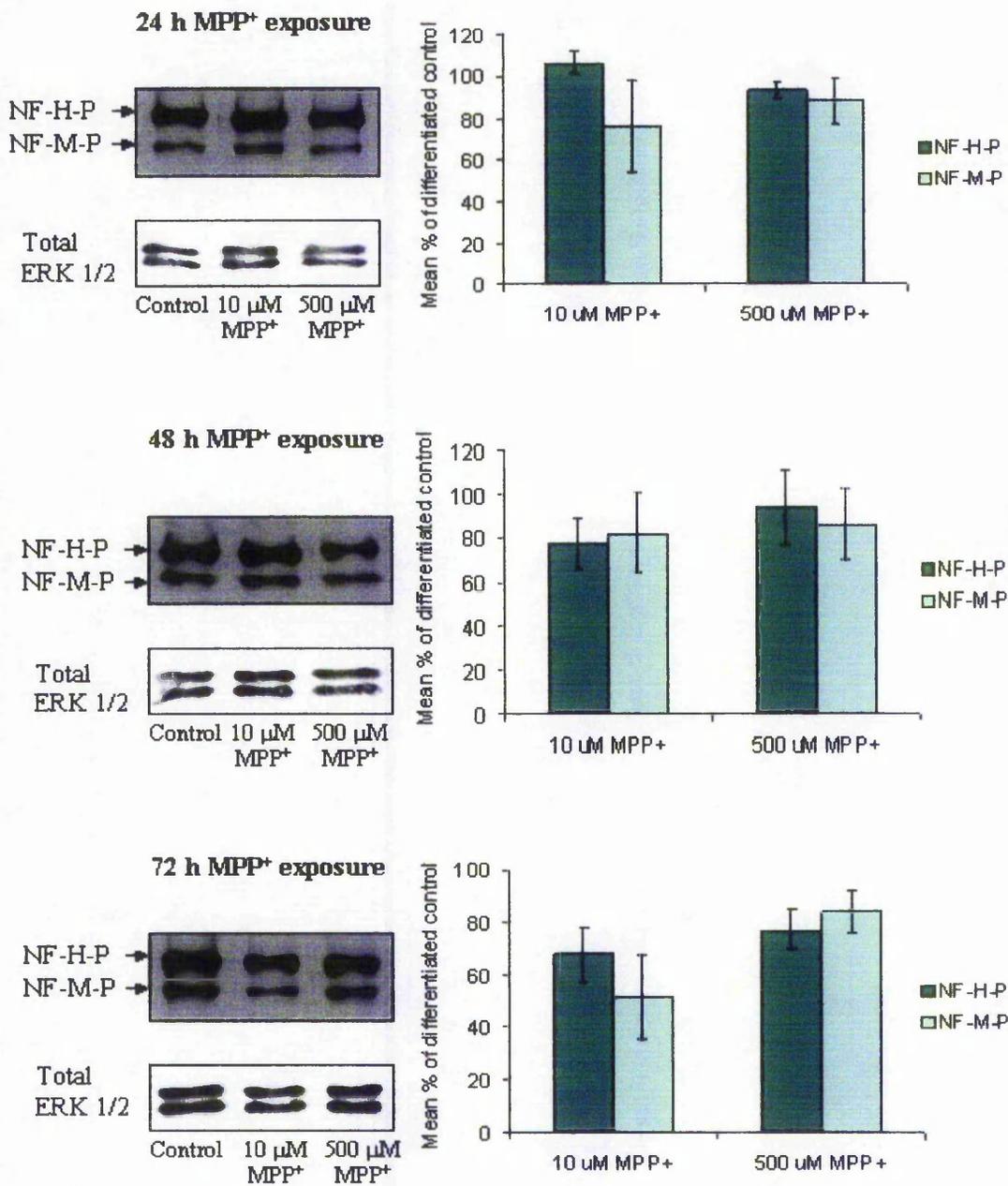
Figure 4.12 NF phosphorylation status following MPP$^+$ exposure over 72 h.
Cells were seeded in T25 flasks at 400,000 cells/flask and induced to differentiate over 7 days as detailed in methods section 2.2.1.6. On day 7 medium was removed and replaced with fresh differentiation medium supplemented with MPP$^+$ as detailed above. At 24, 48 and 72 h time points, duplicate flasks of cells were extracted as detailed in methods section 2.2.5.1. Extracts were subjected to SDS-PAGE and Western blotting. Representative blots probed with SMI31 (1:1000) (for NF-H-P and NF-M-P) and Total ERK 1/2 (1:500) are shown in. Bands were quantified and corrected against total ERK for differences in protein loading and expressed as % of control (assigned 100 %). Results presented are combined data from 3 independent experiments (n = 3) ± SEM. Statistical analysis of control versus toxin treated cells was carried out using two-tailed t-Tests.
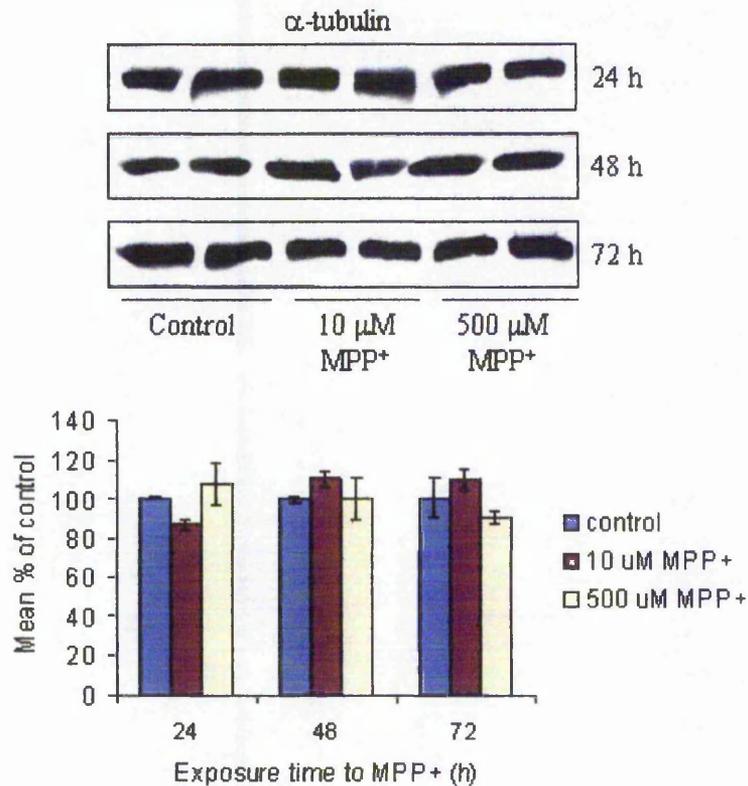
Figure 4.13 α-tubulin expression following 72 h MPP$^+$ exposure.
Cells were seeded in T25 flasks at 400,000 cells/flask and induced to differentiate over 7 days as detailed in methods section 2.2.1.6. On day 7 medium was removed and replaced with fresh differentiation medium supplemented with MPP$^+$ as detailed above. At 24, 48 and 72 h time points, duplicate flasks of cells were extracted as detailed in methods section 2.2.5.1. Extracts were subjected to SDS-PAGE and Western blotting and probed with B512 (1:500). Bands were quantified and corrected against total ERK to account for any differences in protein loading. Results are expressed as % of control (assigned 100 %). The range of the data is shown.

*4.2.2.2.2   Exposure to sub-cytotoxic concentrations of MPP$^+$ over 14 days: effects
on NF status and α-tubulin*

Following 14 days exposure of pre-differentiated cells to 10 μM MPP$^+$ there was a
30 % increase in total NF-H compared to controls (see Fig 4.14A). Specific NF-H
and NF-M phosphorylation was also significantly increased (1.8-fold and 2.4-fold
respectively; see Fig 4.14B). Additionally the ratio of NF-M:NF-H phosphorylation
was increased approximately 1.3 fold in cells treated with 10 μM MPP$^+$ at day 14
(Fig 4.14C). None of these changes were observed following 7 days exposure.
Significantly ERK and JNK phosphorylation at the 14-day time point was similar in
control and MPP$^+$ treated cells (results not shown). Over a 14-day period, α-tubulin
expression was not affected by MPP$^+$ (Fig 4.15).

A. Total NF-H protein levels
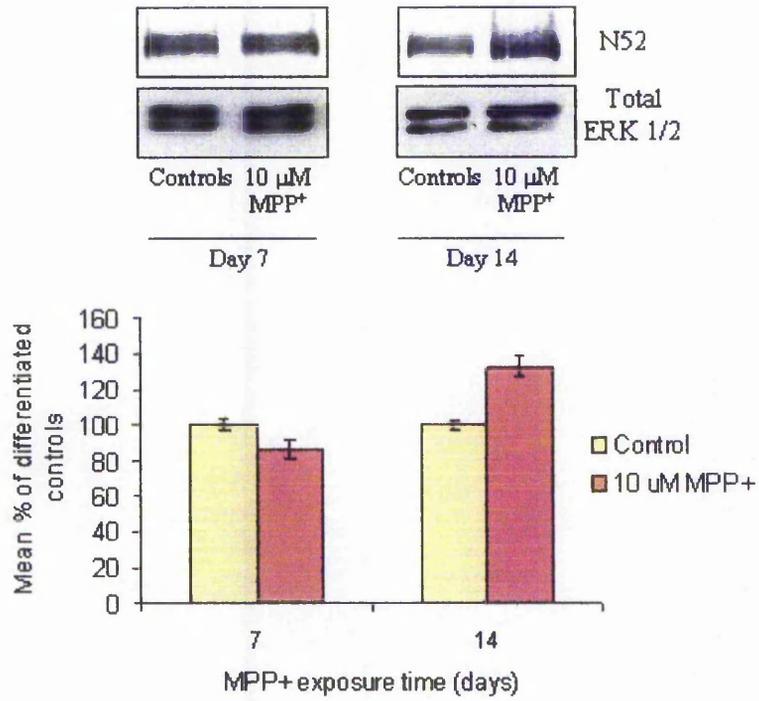
B. Specific NF-H and NF-M phosphorylation
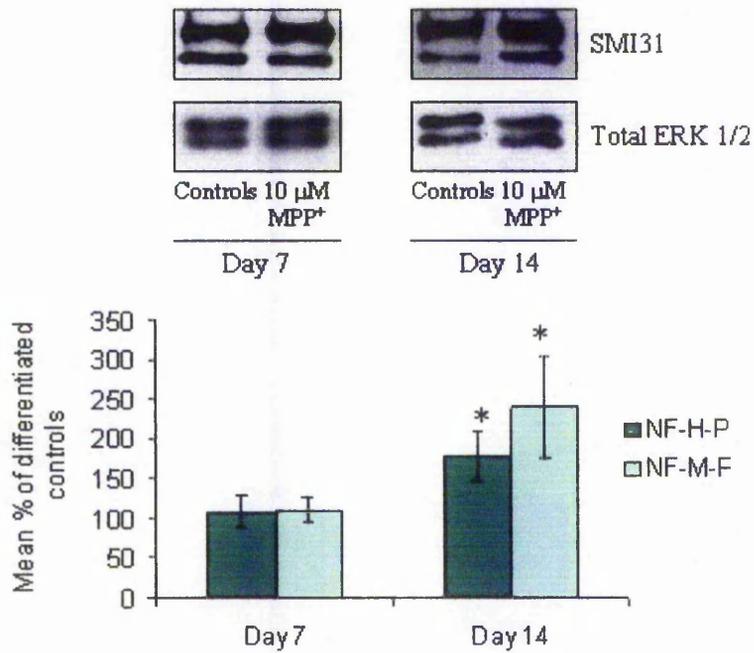
C. Ratio of NF-M:NF-H phosphorylation

MPP$^+$ exposure (days)	Non-toxin treated control	10 µM MPP$^+$
7	1.207 ± 0.534	1.180 ± 0.436
14	1.223 ± 0.724	1.643 ± 1.092

Figure 4.14 Total NF-H level and specific NF-H/NF-M phosphorylation status following chronic MPP$^+$ exposure.
Cells were seeded into T25 flasks at 400,000 cells/flask and differentiated for 7 days as detailed in methods section 2.2.1.6. Medium was exchanged for fresh differentiation medium alone (controls) or supplemented with 10 µM MPP$^+$ then changed twice weekly. Control and toxin treated cells were extracted in triplicate following 7 and 14 day exposures to the toxin as detailed in methods section 2.2.5.1 and proteins separated by SDS-PAGE. Protein was transferred to nitrocellulose by Western blotting and probed with (A), N52 (1:500) and (B), SMI31 (1:1000). Bands were quantified and corrected for differences in protein loading against corresponding total ERK bands. Results are presented as mean % of differentiated control cells. For experiment A (total NF-H), results are derived from triplicate flasks extracted on the same day (± SEM). For experiment B (phosphorylated NF-H/NF-M) mean data is combined from 3 independent experiments (± SEM) (n = 3). Statistical analysis of control versus toxin treated cells was carried out using two-tailed t-Tests where statistical significance was accepted at $p<0.05$ (*). The mean ratio of NF-M:NF-H phosphorylation was calculated ± SEM (C).
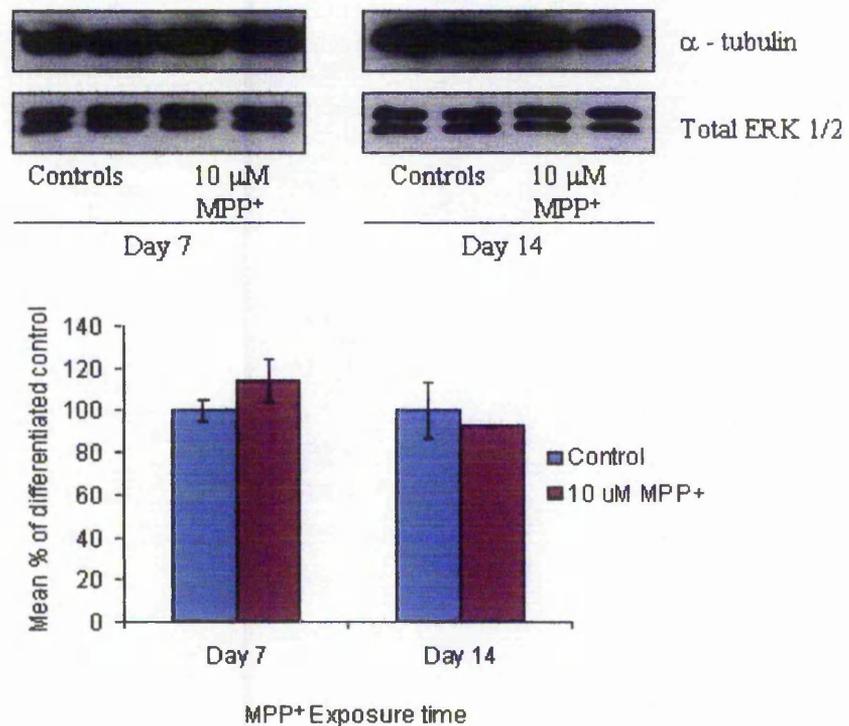
Figure 4.15   Expression of α-tubulin following chronic MPP⁺ exposure
Cells were seeded in T25 flasks at 400,000 cells/flask and induced to differentiate over 7 days as detailed in methods section 2.2.1.6. On day 7 medium was removed and replaced with fresh differentiation medium supplemented with MPP⁺ as detailed above. Medium was then exchanged twice weekly. At day 7 and day 14 time points, duplicate flasks of cells were extracted as detailed in methods section 2.2.5.1. Extracts were subjected to SD-PAGE and Western blotting and probed with B512 (1:500). Bands were quantified and corrected against total ERK to account for any differences in protein loading. Results are expressed as % of control (assigned 100 %). The range of the data is shown.

4.2.3   Immunocytochemical analyses

4.2.3.1   NF proteins

Immunocytochemistry was performed on controls and MPP$^+$ treated cells fixed in methanol and then permeabilised using Triton X-100 as detailed in methods section 2.2.9.2. The distribution of phosphorylated NF proteins was visualised by probing with SMI31 and total NF-H using N52.

Figure 4.16 shows the effect of treatment for 24 h with a cytotoxic (5 mM) concentration of MPP$^+$. As described in chapter III, section 3.2.2.5.4, SMI31 staining in control cells was observed in axon-like processes, as a discrete mass in the perikaryon, and also punctate staining throughout the cell body (see Fig 4.16A, panel a) suggesting the presence of a pool of unassembled phosphorylated NFs. Following exposure to 5 mM MPP$^+$, phosphorylated NF-H/NF-M staining was intensified and restricted to the cell body and was concentrated in a perinuclear fashion (see staining of NF protein in conjunction with propidium iodide staining of nuclei Fig 4.16A panel b, indicated by white arrow). The distribution of total NF-H was monitored using N52 and was found to be different from SMI31 staining. Control cells exhibited diffuse staining throughout the cell body and axon with little or no punctate staining. MPP$^+$ treated cells showed a similar diffuse staining pattern but without axonal staining (see Fig 4.16B).

Figure 4.17 shows the distribution of phosphorylated NF-H/NF-M in cells treated with 10 µM and 500 µM concentrations of MPP$^+$ for 72 h. There was no large difference between control cells and cells treated with 10 µM MPP$^+$ except that a number of toxin treated cells showed greater staining in the cell body that formed a halo of immunoreactivity around the nucleus. This perinuclear staining occurred in cells with and without axon-like processes. Staining of 10 µM MPP$^+$ treated cells was also more intense. Following exposure to 500 µM MPP$^+$, phosphorylated NF-H/NF-M staining was largely (but not exclusively) absent from axonal processes and localised in the cell body particularly in the perinuclear region (Fig 4.17c i and ii). Exposure of cells over 14 days to 10 µM MPP$^+$ showed no difference between

153

control and toxin treated cells in the distribution of phosphorylated NF-H/NF-M but relative staining intensity was greater in toxin treated cells, particularly within the cell body (Fig 4.18, compare panel a and panel b).

FITC   FITC + propidium iodide

a. Control

b. 5 mM MPP$^+$

A. SMI31 (phosphorylated NF-H/NF-M)

FITC   FITC + propidium iodide

a. Control

b. 5 mM MPP⁺

B. N52 (NF-H phosphorylation independent)

Figure 4.16   Immunocytochemical analysis of total NF-H and phosphorylated NF-H/ NF-M following 24 h exposure to 5 mM MPP⁺

Cells were differentiated in permanox chamber slides over 7 days. Medium was removed and replaced with fresh differentiating medium or medium supplemented with 5 mM MPP⁺. After 24 h cells were fixed then permeabilised and immunocytochemistry performed as detailed in methods section 2.2.9. Cells were probed with (A) SMI31 antibody (1:500) or (B) N52 antibody (1:200). Analysis was performed by confocal microscopy at x 400 magnification. Scale bar represents 20 μm. Results are representative of 2 independent experiments.

FITC   FITC + propidium iodide

a. Control

b. 10 μM MPP$^+$

i   ii   iii

c. 500 μM MPP$^+$

Figure 4.17   Immunocytochemical analysis of phosphorylated NF-H and NF-M following 72 h exposure to 10 μM and 500 μM MPP$^+$

Cells were differentiated in permanox chamber slides over 7 days. Medium was removed and replaced with fresh differentiating medium supplemented with 10 μM or 500 μM MPP$^+$. After 72 h cells were fixed then permeabilised and immunocytochemistry performed as detailed in methods section 2.2.9. Cells were probed with SMI31 antibody (1:500). Analysis was performed by confocal microscopy at x 400 magnification.   Scale bar represents 20 μm. Results are representative of 3 independent experiments.

FITC   FITC + propidium iodide

a. Control

b. 10 μM MPP⁺
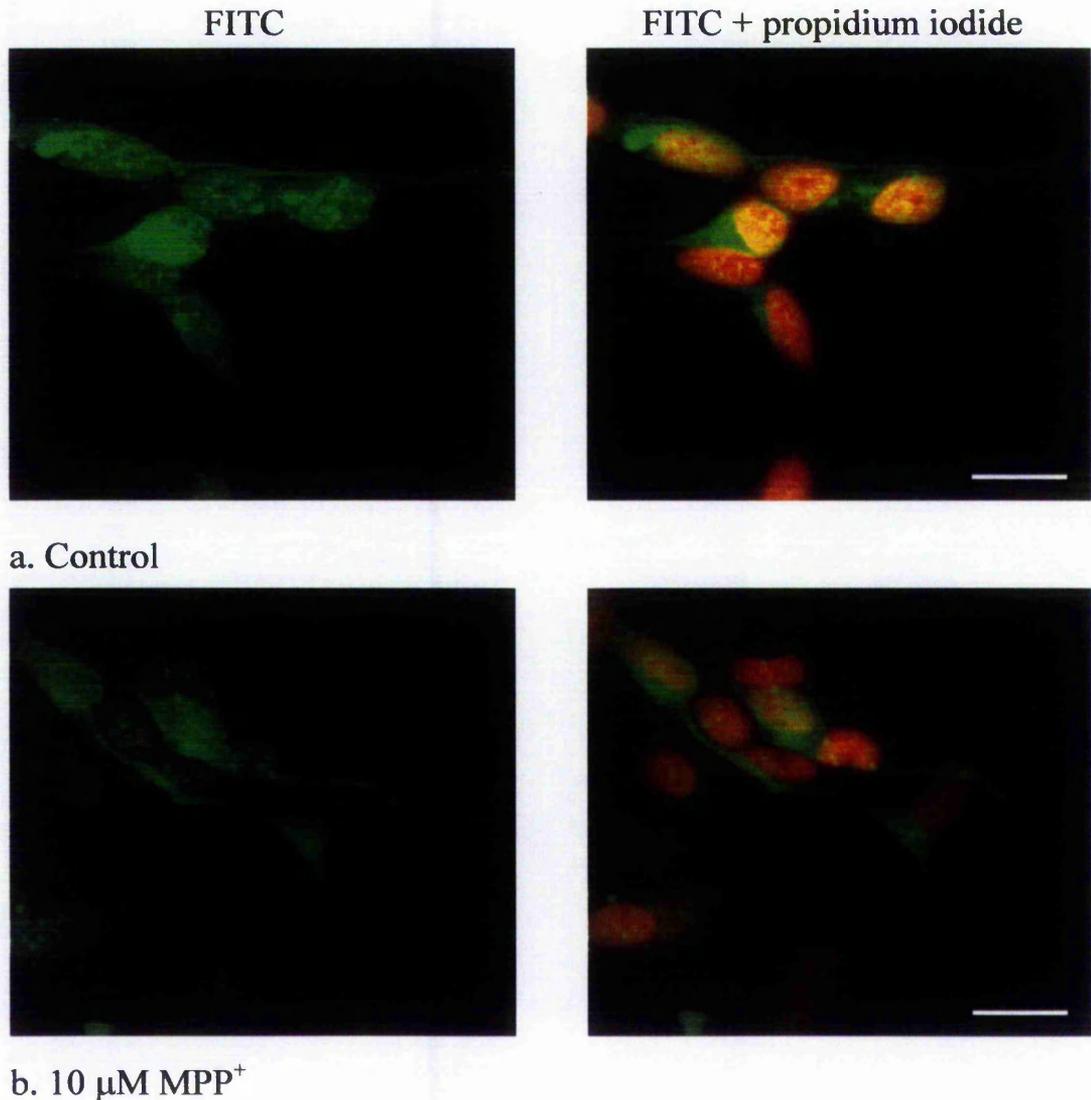
Figure 4.18   Immunocytochemical analysis of phosphorylated NF-H and NF-M following a 14-day exposure to 10 μM MPP⁺

Cells were differentiated in permanox chamber slides over 7 days. Medium was removed and replaced with fresh differentiating medium supplemented with 10 μM MPP⁺. Medium was changed twice weekly. After 14 days cells were fixed then permeabilised and immunocytochemistry performed as detailed in methods section 2.2.9. Cells were probed with SMI31 antibody (1:500). Analysis was performed by confocal microscopy at x 400 magnification. Scale bar represents 20 μm. Results are representative of 2 independent experiments.

4.2.3.2 α-tubulin

Figure 4.19 shows α-tubulin distribution following exposure to 5 mM MPP$^+$ for 24 h. Staining in control (non-toxin treated) cells was cytoplasmic and punctate along axon-like processes. Following exposure to 5 mM MPP$^+$ staining was more intense within the cell body. No change in α-tubulin distribution was observed following 72 h exposure to 10 μM and 500 μM MPP$^+$ (results not shown).
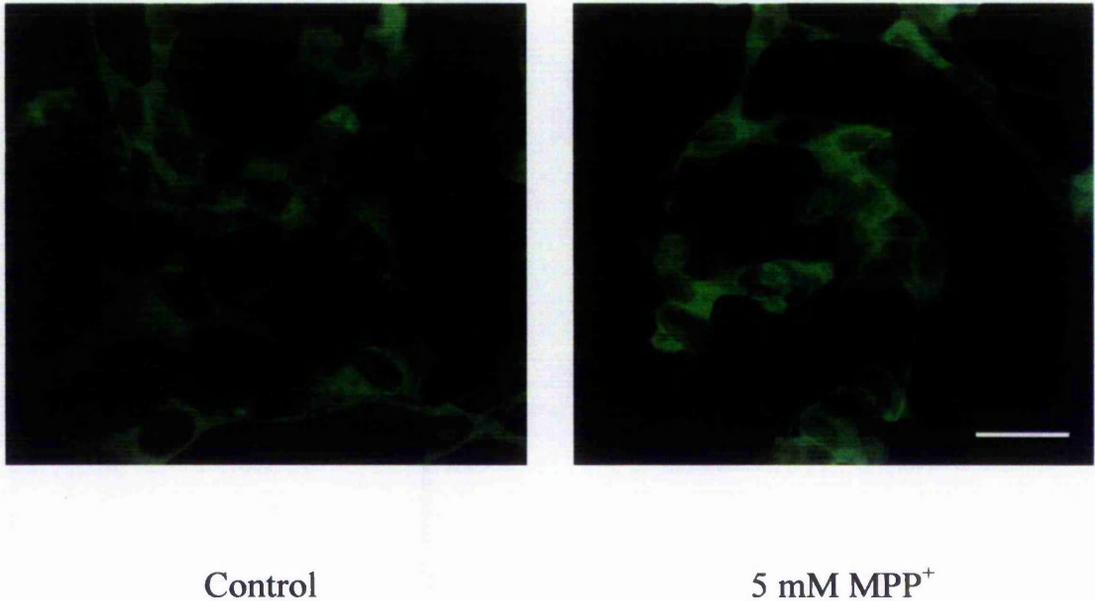
Control   5 mM MPP$^+$

Figure 4.19 α - tubulin expression following 24 h exposure to 5 mM MPP$^+$
Cells were differentiated in permanox chamber slides over 7 days. Medium was removed and replaced with fresh differentiating medium supplemented with 5 mM MPP$^+$. After 24 h cells were fixed and permeabilised and immunocytochemistry performed as detailed in methods section 2.2.9. Cells were probed with B512 antibody (1:500). Analysis was performed by confocal microscopy at x 400 magnification. Scale bar represents 20 μm. Results represent a single experiment.

4.2.4 Preliminary investigation of the effects of proteasome inhibition on the cytoskeleton of pre-differentiated SH-SY5Y cells.

In order to achieve proteasomal inhibition, a commercially available chemical proteasome inhibitor (MG132) was employed at 0.1 µM, a concentration which has been shown in our laboratory to inhibit proteasomal activity in mitotic SH-SY5Y cells within 24 h (Begoñã Caneda-Ferron, unpublished results). Cells were induced to differentiate in permanox chamber slides before incubation with 0.1 µM MG132 over 72 h. Slides were fixed at 24, 48 and 72 h time points and probed with SMI31 and B512 antibodies recognising phosphorylated NF-H/NF-M and α-tubulin proteins respectively.

In the presence of MG132, phosphorylated NF proteins appeared to accumulate in both the cell body and axons within 24 h, compared to controls (see Fig 4.20) and this trend remained over 72 h (results not shown). Probing of cells with B512 revealed no accumulation of α-tubulin at 24 and 48 h time points. However following 72 h exposure to MG132, α-tubulin staining was greater than in control cells in both the cell body and the axons (see Fig 4.21).
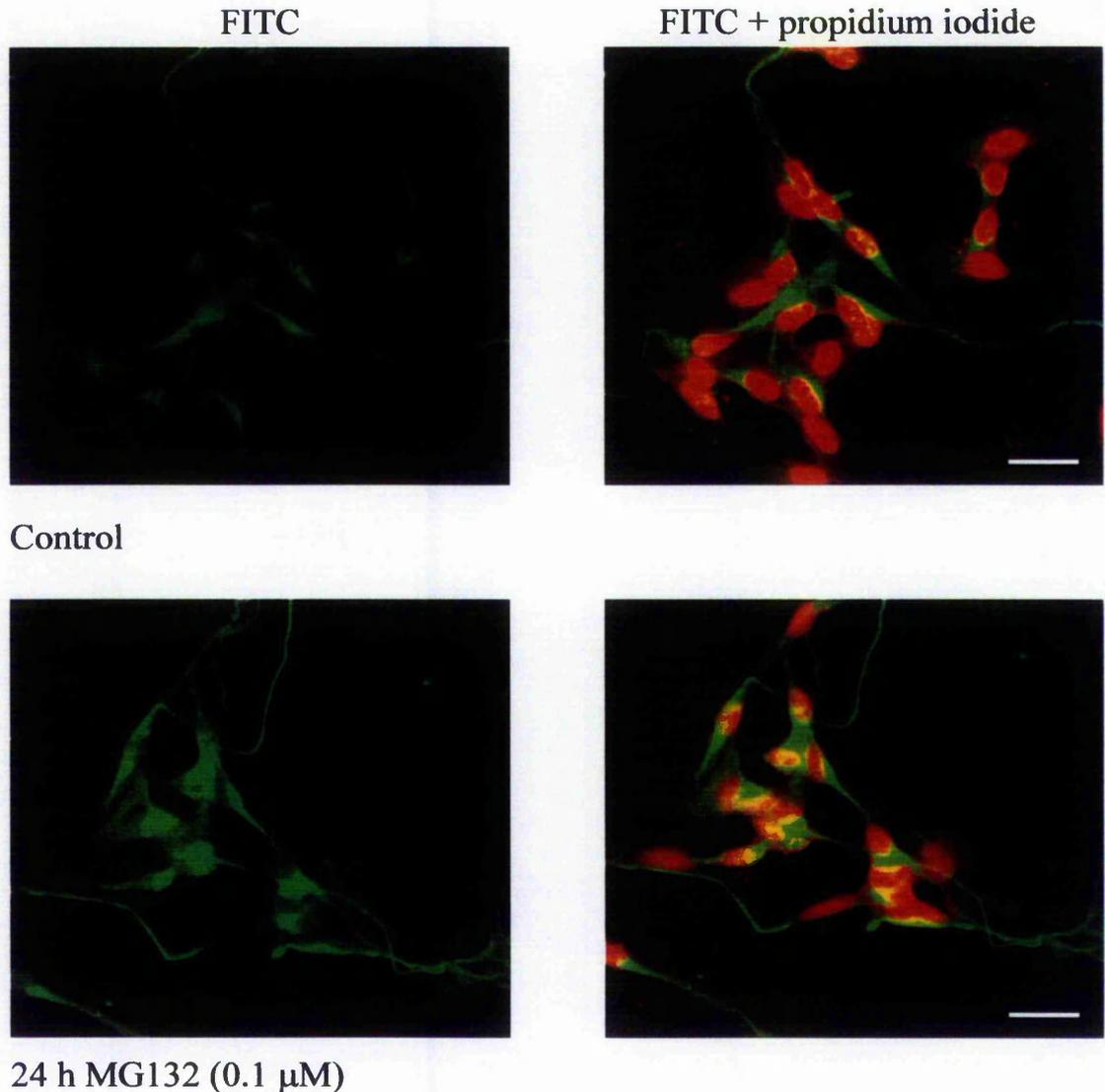
Figure 4.20 Accumulation of phosphorylated NF proteins following proteasomal inhibition.
Cells were differentiated in permanox chamber slides over 7 days. Medium was removed and replaced with fresh differentiating medium supplemented with 0.1 μM MG132. After 24 h cells were fixed and permeabilised and immunocytochemistry performed as detailed in methods section 2.2.9. Cells were probed with SMI31 antibody (1:500). Cells were protected using Vectorshield mounting medium containing propidium iodide that stained the nuclei red (shown overlaid with the FITC stain to the right of each panel). Analysis was performed by confocal microscopy at x 400 magnification. Scale bar represents 20 μm. Results are representative of 2 independent experiments.

FITC   FITC + propidium iodide
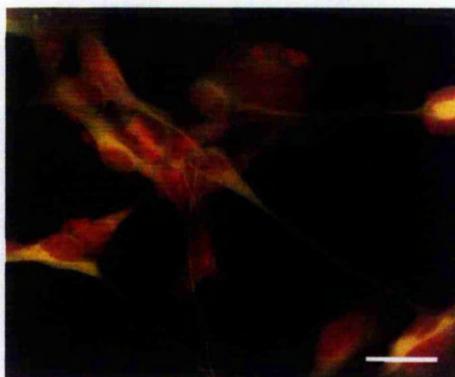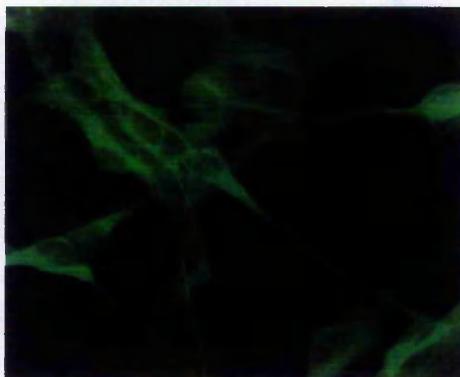
Control
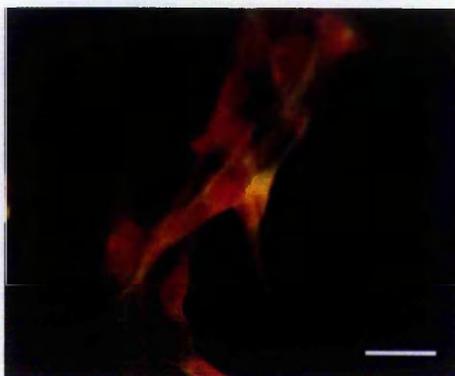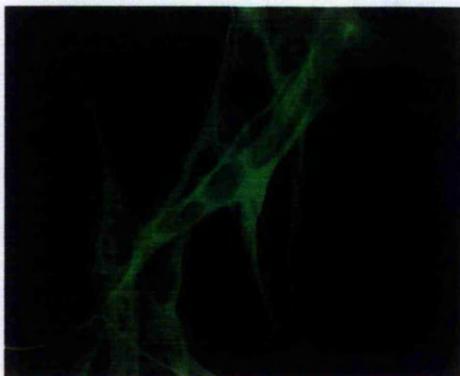
24 h 0.1µM MG132
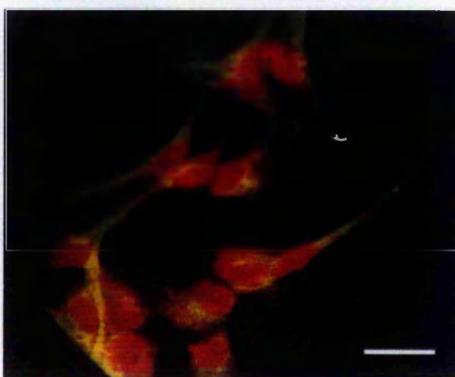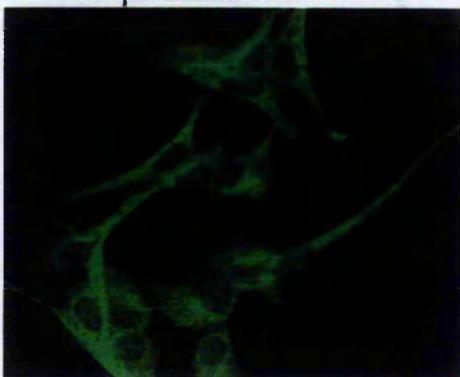
Control
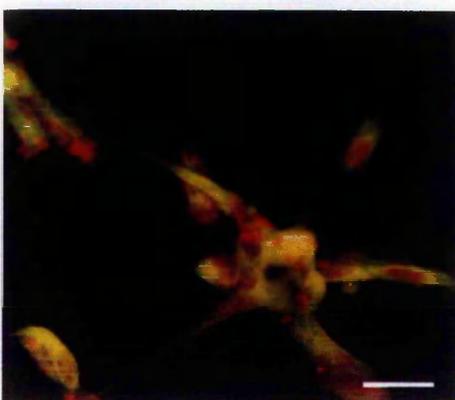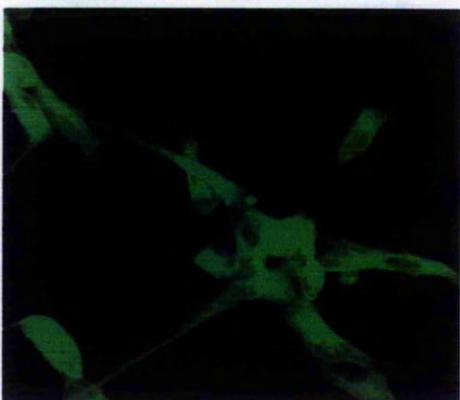
72 h 0.1µM MG132

Figure 4.21   Accumulation of α-tubulin following proteasomal inhibition
Cells were differentiated in permanox chamber slides over 7 days. Medium was removed and replaced with fresh differentiating medium supplemented with 0.1 μM MG132. After 24 and 72 h cells were fixed and permeabilised and immunocytochemistry performed as detailed in methods section 2.2.9. Cells were probed with B512 (1:200). Cells were protected using Vectorshield mounting medium containing propidium iodide that stained the nuclei red (shown overlaid with the FITC stain to the right of each panel). Analysis was performed by confocal microscopy at x 400 magnification.   Scale bar represents 20 μm.   Results are representative of 2 independent experiments.

4.2.5 Modification of fixing procedures for visualisation of protein aggregates: NF and α-tubulin distribution

By permabilising cells prior to fixation it was anticipated that soluble proteins would be removed and insoluble proteins might be visualised more effectively. Experiments investigating phosphorylated NF and α-tubulin distribution following MPP$^+$ exposures were repeated using this alternative method.

4.2.5.1 Cytotoxic concentration of MPP$^+$

When exposed to a cytotoxic concentration of MPP$^+$, cells showed very similar staining profiles independent of the fixing/permabilisation protocol. For example, Figure 4.22 shows the distribution of insoluble phosphorylated NF-H/NF-M and total NF-H in cells permabilised prior to fixing (probing with SMI31 and N52 respectively) following 24 h exposure to 5 mM MPP$^+$. As expected, results suggest the majority of phosphorylated NF proteins in differentiated cells to be insoluble. In control cells, the majority of staining was present in axon-like extensions and in the perikaryal region whilst following 5 mM MPP$^+$ treatment, phosphorylated NF-H/NF-M was restricted to the perinuclear region. Punctate staining was again evident throughout the cytoplasm, particularly in MPP$^+$ treated cells, therefore presumably detecting assembled and insoluble, phosphorylated NFs (Fig 4.22A). Total NF-H staining remained diffuse throughout the cytoplasm and axons in control cells but was restricted to the cell body following 5 mM MPP$^+$ (Fig 4.22B). Control cells pemeabilised prior to fixation, displayed a clearly visible, insoluble α-tubulin network (Fig 4.23, left panel). Following MPP$^+$ treatment, α-tubulin remained distributed throughout the cytoplasm with no obvious change in staining intensity; however the staining was diffuse rather than filamentous.

4.2.5.2 Sub-cytotoxic concentration of MPP$^+$

Treatment with sub-cytotoxic concentrations of MPP$^+$ revealed differences in phosphorylated NF-H/NF-M distribution independent of the fixing/permabilisation protocol but these were more clearly revealed at lower concentrations of MPP$^+$ and at

earlier time points when cells were permeabilised prior to fixation. Figure 4.24 shows the staining pattern that could be observed following 72 h exposure to 10 μM MPP$^+$ when cells were pre- permeabilised; a halo of immunoreactivity was again observed around the periphery of the nucleus in a greater number of MPP$^+$ treated cells (Fig 4.24b). 10 μM MPP$^+$ treated cells stained with greater intensity. The number of cells exhibiting perinuclear "halo's" were counted in a total of 1800 cells (from 8 random fields, with a mean of 225 cells / field) either fixed or permeabilised first (expressed as mean number of halo's / field ± SEM). In cells fixed before permeabilisation, the number of halo's was 4.1 ± 0.58 in 10 μM MPP$^+$ treated cells compared to 1.8 ± 0.49 in control cells. In cells permeabilised prior to fixing, the number of halo's in 10 μM MPP$^+$ treated cells was 9.4 ± 1.52 compared to 3.6 ± 0.89 in corresponding control cells. This halo of reactivity occurred in cells with and without additional axonal staining and also occurred in a proportion of cells which had axons that were not stained but that were observed by light microscopy (see Fig 4.24, panel b, i and ii). Importantly cells permeabilised prior to fixation showed no change in α-tubulin distribution following 10 μM MPP$^+$ treatment compared to control cells, suggesting that the MT system was generally not de-stabilised (Fig 4.25). A similar phosphorylated NF-H/NF-M pattern was observed when cells were treated with 10 μM or 500 μM MPP$^+$ for 24 h; pre-permeabilisation revealed changes that prior fixing did not. However 72 h exposure to 500 μM MPP$^+$ revealed perinuclear immunoreactivity regardless of whether cells were prior fixed or permeabilised (results not shown).
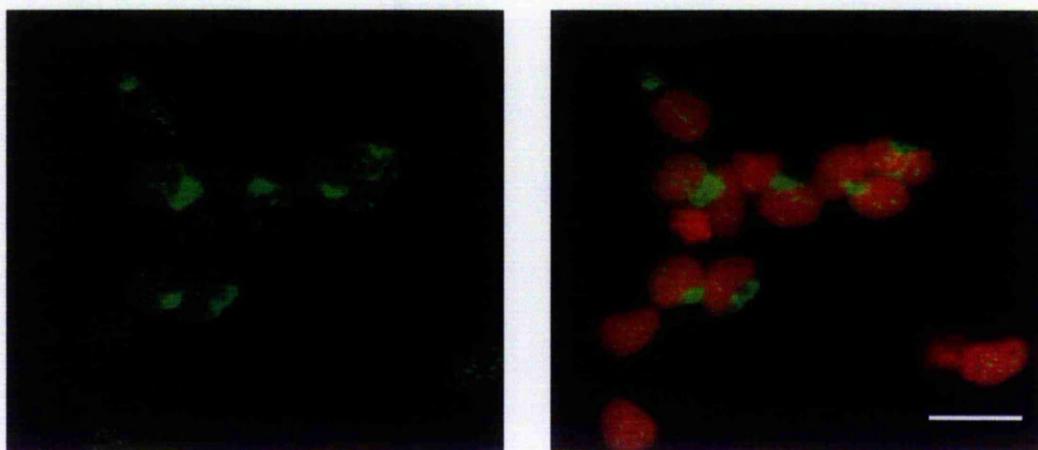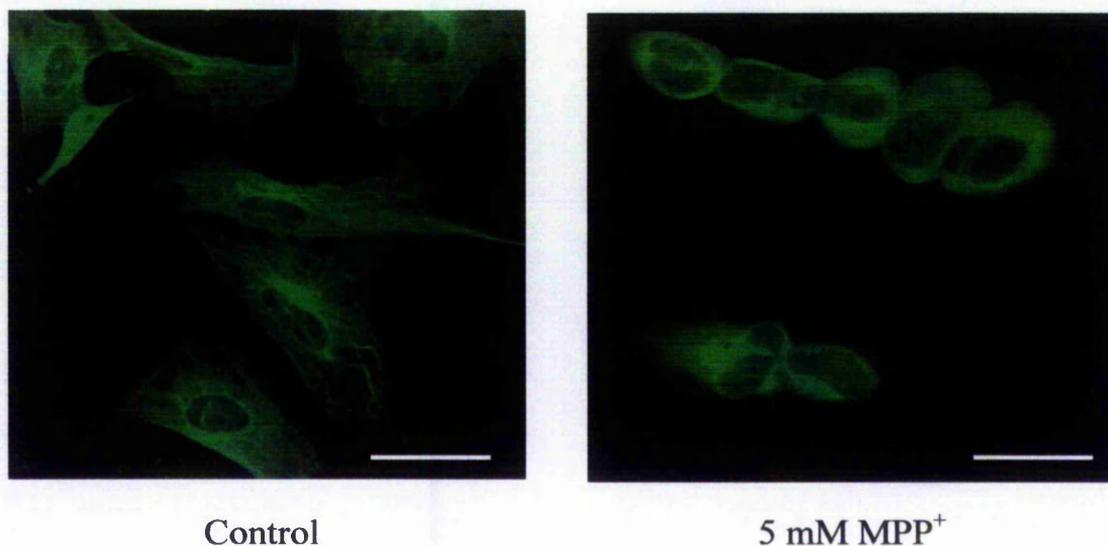
FITC   FITC + propidium iodide

a. Control

b. 5 mM MPP$^+$

A. SMI31 (phosphorylated NF-H/NF-M)

FITC   FITC + propidium iodide

a. Control

b. 5 mM MPP$^+$

B. N52 (NF-H phosphorylation independent)

Figure 4.22   Immunocytochemical analysis of total NF-H and phosphorylated NF-H/ NF-M following 24 h exposure to 5 mM MPP$^+$
Cells were differentiated in permanox chamber slides over 7 days. Medium was removed and replaced with fresh differentiating medium or medium supplemented with 5 mM MPP$^+$. After 24 h cells were permeabilised then fixed and immunocytochemistry performed as detailed in methods section 2.2.9. Cells were probed with (A) SMI31 antibody (1:500) or (B) N52 antibody (1:200). Analysis was performed by confocal microscopy at x 400 magnification. Scale bar represents 20 μm. Results represent a single experiment.

Control   5 mM MPP$^+$

Figure 4.23 α - tubulin expression following 24 h exposure to MPP$^+$
Cells were differentiated in permanox chamber slides over 7 days. Medium was removed and replaced with fresh differentiating medium supplemented with 5 mM MPP$^+$. After 24 h cells were permeabilised then fixed and immunocytochemistry performed as detailed in methods section 2.2.9. Cells were probed with B512 antibody (1:500). Analysis was performed by confocal microscopy at x 400 magnification. Scale bar represents 20 μm. Results represent a single experiment.

Fixed first | Permeabilised first

a. Control

Fixed first | Permeabilised first

i | ii
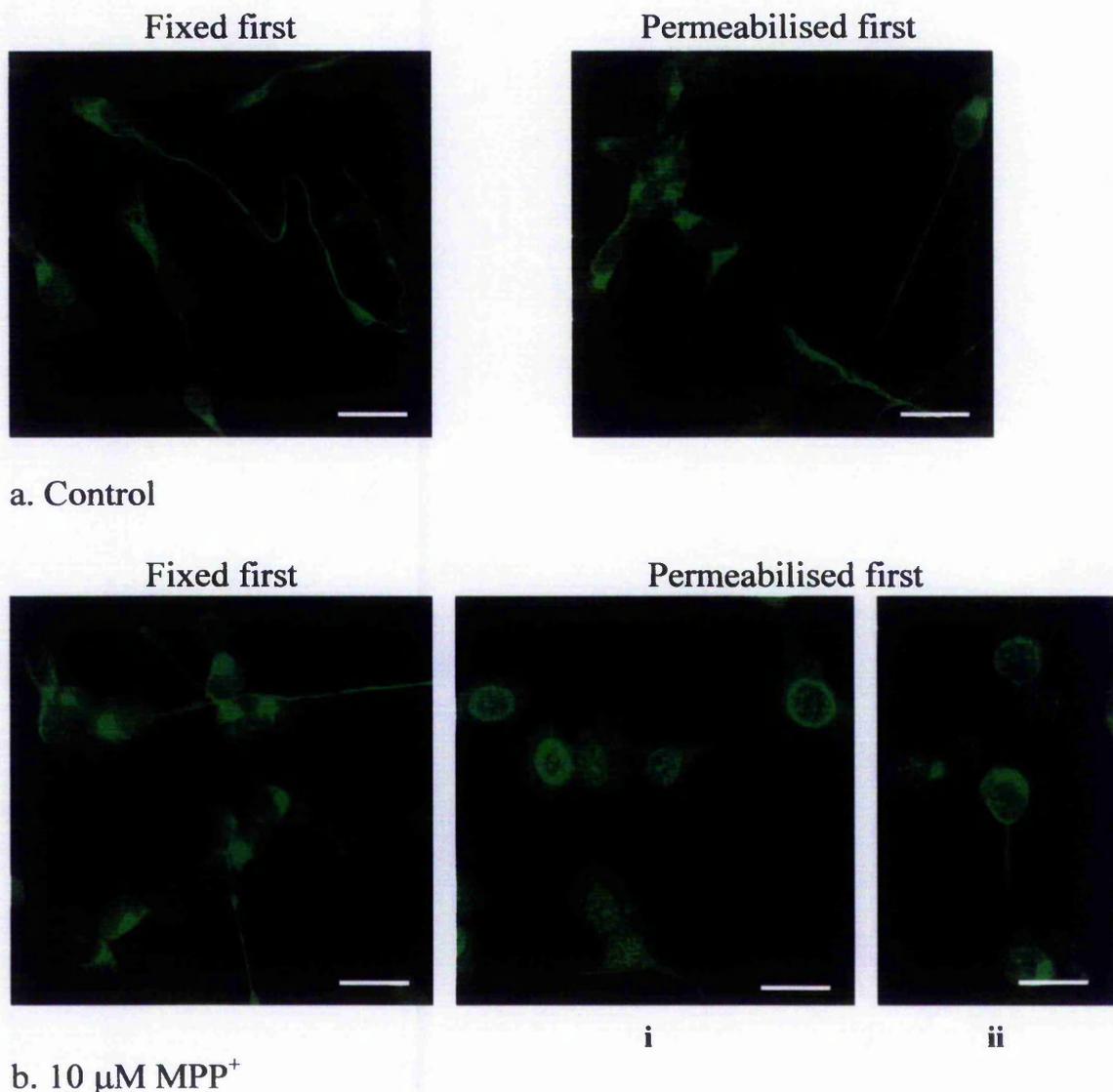
b. 10 μM MPP⁺

Figure 4.24 Comparison of phosphorylated NF-H and NF-M distribution following 72 h exposure to 10 μM MPP⁺ in cells fixed or permeabilised first
Cells were differentiated in permanox chamber slides over 7 days. Medium was removed and replaced with fresh differentiating medium supplemented with MPP⁺. Cells were fixed in methanol and permeabilised in Triton X-100 (left panel) or permeabilised in igepal/MgCl₂ then fixed in methanol (right panel) as detailed in methods section 2.2.9.2. Immunocytochemistry was performed using SMI31 antibody (1:500) as detailed in methods section 2.2.9.3. Analysis was performed by confocal microscopy at x 400 magnification. Scale bar represents 20 μm. Results are representative of 2 independent experiments.

Fixed first   Permeabilised first

a. Control

b. 10 μM MPP$^+$

Figure 4.25 Comparison of α-tubulin distribution following 72 h exposure to 10 μM MPP$^+$ in cells fixed or permeabilised first
Cells were differentiated in permanox chamber slides over 7 days. Medium was removed and replaced with fresh differentiating medium supplemented with MPP$^+$. Cells were fixed in methanol and permeabilised in Triton X-100 (left panel) or permeabilised in igepal/MgCl$_2$ then fixed in methanol (right panel) as detailed in methods section 2.2.9.2. Immunocytochemistry was performed using B512 antibody (1:500) as detailed in methods section 2.2.9.3. Analysis was performed by confocal microscopy at x 400 magnification. Scale bar represents 20 μm. Results are representative of two independent experiments (fixed first) and a single experiment (permeabilised first).

4.3 DISCUSSION

4.3.1 MPTP/MPP$^+$ toxicity in mitotic and differentiated cells

The comparative toxic effects of MPP$^+$ and MPTP have been previously investigated in the mitotic SH-SY5Y system (Song *et al.,* 1997). In this chapter, toxicity induced by MPTP and MPP$^+$ was compared in mitotic and pre-differentiated SH-SY5Y cells in an initial dose ranging trial. In accordance with previous studies, mitotic cells exhibited greater sensitivity to MPP$^+$ than MPTP (Song *et al.,* 1997). This finding was also apparent in pre-differentiated SH-SY5Y cells. The presence of a DA transport system in the SH-SY5Y cell line was confirmed by Song and Ehrich, (1998) using the DA uptake inhibitor, nomifensine, which blocked MPP$^+$ transport into cells. Hence the results of this initial study are compatible with the presence of the DA uptake system in the ECACC clone, and therefore its suitability for MPP$^+$ studies. Pre-differentiated cells were less sensitive to MPP$^+$ than mitotic cells at a given time point. The increased sensitivity of mitotic cells may be attributable to the greater energy demand of dividing cells, rendering them less able to withstand complex I inhibition. Tieu *et al,* (1999) demonstrated that mitotic cells were more sensitive to a range of toxic paradigms than retinoic acid treated cells, proposed to be linked to an up-regulation in Bcl-2 associated with retinoic acid treatment in their study. Since retinoic acid treatment decreased the sensitivity of ECACC SH-SY5Y cells with no concurrent up-regulation of Bcl-2, it would again appear that Bcl-2 is less important for cell survival in this clone than in the clone used by Tieu *et al,* (1999).

Initial dose ranging trials suggested that MPP$^+$ induces cell death in a time and concentration dependent manor. Using the MTT reduction assay or measuring ATP concentration, 10 μM MPP$^+$ remained sub-cytotoxic to cells over 14 days. The aim of this study was to establish a differentiated cell model that could mimic dopaminergic neurones *in-vivo*. It can be noted that the pre-differentiated SH-SY5Y cells used in this study exhibited considerably lower sensitivity when compared to primary dopaminergic neurones, where 10 μM MPP$^+$ reduced cell viability by almost 50 % in 48 h (Bilsland *et al.,* 2002). In a study by Lotharius *et al,* (1999), also using

170

mouse dopaminergic neurones, 5 μM MPP$^+$ completely abolished tyrosine hydroxylase-positive neurones within 48 h. The results presented in this thesis are however, consistent with Mathiasen *et al*, (2004) who determined that 3 mM MPP$^+$ was required to significantly increase lactate dehydrogenase release following 48 h exposure in pre-differentiated SH-SY5Y cells. The reduced sensitivity of SH-SY5Y cells to MPP$^+$ may occur due to a reduced rate of uptake into cells on the DA transporter. Indeed Pifl *et al*, (1993) propose that sensitivity to the effects of MPP$^+$ be partly dependent on the level of expression of the DA transporter. Alternatively, the ability to concentrate MPP$^+$ into the mitochondria may be reduced in this cell line. The complexity with this situation is that the mechanisms that result in cell death may differ, or at least the contribution of different mechanisms may differ, between dopaminergic neurones and SH-SY5Y cells. For example Figure 1.4 (chapter I) details the proposed mechanisms of MPP$^+$ toxicity. Indeed the primary insult to cells following MPP$^+$ exposure is considered to be complex I inhibition. However, oxidative stress can be induced through alternative mechanisms. If SH-SY5Y cells do have a lesser ability to concentrate MPP$^+$ into the mitochondria, then alternative death pathways may be employed. Hence it becomes more difficult to compare MPP$^+$ toxicity between cell systems and highlights a potential disadvantage of this cell line.

4.3.2 Effects of MPP$^+$ and proteasomal inhibition on the neuronal cytoskeleton in differentiated SH-SY5Y cells

4.3.2.1 The NF system

This study sought to investigate the effects of cytotoxic and sub-cytotoxic concentrations of MPP$^+$ on the expression and distribution of NFs and tubulin in differentiated SH-SY5Y cells. Aberrant NF phosphorylation is found in response to several toxins *in-vitro* (De Girolamo *et al.*, 2000; Hartley *et al.*, 1997; Shea *et al.*, 1995, 1997a) and importantly, *in-vivo* in Lewy bodies (Forno *et al.*, 1986) and was therefore an additional key consideration. Results in the present study showed that following 24 h exposure to a cytototoxic (5 mM) concentration, or 14 days exposure to a sub-cytotoxic (10 μM) MPP$^+$ concentration, NF-H and NF-M phosphorylation were increased. Total NF-H levels were also increased following exposure to MPP$^+$

at these time points. This was in agreement with De Girolamo *et al,* (2000) where increased NF-H phosphorylation was reported in differentiated N2a cells treated with a sub-cytotoxic concentration of MPTP. Importantly the ratio of NF-M phosphorylation to NF-H phosphorylation was increased in MPP$^+$ treated cells at the 24 h and 14 day time points.

Immunocytochemical analysis of the sub-cellular distribution of phosphorylated NF-M/NF-H epitopes was performed following MPP$^+$ treatments. Following exposure to a cytotoxic concentration of MPP$^+$ for 24 h, phosphorylated NF-H/NF-M staining was intense and restricted to the cell body, observed as a discrete mass of staining residing next to, and indenting upon, the nucleus. As previously noted a sub-cytotoxic concentration (10 μM) MPP$^+$ increased NF phosphorylation after 14 days, detected by Western blotting. In accordance with this finding, immunocytochemistry revealed that a greater phosphorylated NF-H/NF-M reactivity was observed in toxin treated cells.

An alternative method (Ito *et al.,* 2002) for cell preparation prior to confocal analysis was tested whereby cells were permeabilised prior to fixation and compared with the more traditional method of fixation followed by a permeabilisation step. The aim was to help determine whether MPP$^+$ causes inclusions of insoluble NF proteins, masked by the presence of soluble NFs. This method did not change the distribution of phosphorylated NFs following exposure to a cytotoxic concentration of MPP$^+$. Additionally the staining pattern in control, non-toxin treated cells was not affected. This would suggest that phosphorylated NFs within the perikaryon of control cells, including punctate cytoplasmic staining, were predominantly insoluble. Indeed, Shea *et al,* (1998) review that whilst NF subunits can be transported into axons and rapidly become incorporated into the Triton-insoluble cytoskeleton, a population of NF subunits may become incorporated into Triton-insoluble structures within the perikaryon, prior to transport into axons. However, the permeabilisation step may not have been sufficient to completely remove all soluble proteins. Alternatively, cytotoxic concentrations of MPP$^+$ may affect membrane permeability *per se* so that differences between the two methods are less evident.

Permeabilising cells prior to fixation better revealed a unique staining pattern that was more prominent in cells treated with a sub-cytotoxic concentration of MPP$^+$ (10 µM). In these cells the majority of immunoreactivity within the cell body formed a "halo" around the nucleus. 10 µM MPP$^+$ does not reduce cell viability after 72 h. Indeed cells appear viable and well differentiated following 10 µM MPP$^+$. It should be noted that a role for ERK was proposed in neuritogenesis in SH-SY5Y cells in chapter I of this thesis, whilst 10 µM MPP$^+$ was found to transiently activate ERK (Fig 4.8). Therefore the change in distribution of phosphorylated NF-H/NF-M may represent early cytoskeletal changes that occur following sub-cytotoxic MPP$^+$ exposure. This staining pattern was more frequently observed in toxin treated cells, both with and without axons. The implications of this observation and also the perinuclear mass of phosphorylated NFs observed following cytotoxic MPP$^+$ treatment are uncertain. However it is interesting for a number of reasons, principally because of the recent discovery of aggresomes, proposed to provide a cellular response to mis-folded proteins that may be prone to aggregation when the capacity of the cell to degrade proteins through the proteasome is exceeded or the proteasome is impaired (Johnston *et al.,* 1998; Wigley *et al.,* 1999). Staurosporine, proteasome inhibition and DA can induce parkin-containing aggresomes in mitotic SH-SY5Y cells (Muqit *et al.,* 2003). Additionally Hasegawa *et al,* (2004) reported the formation of large aggresome-like perinuclear inclusion bodies that contained α-synuclein, γ-tubulin and dynein, in α-synuclein over-expressing SH-SY5Y cells that were induced to differentiate in the presence of ferrous iron. Significantly, the vast majority of aggresome related studies employ cells into which proteins i.e. parkin, and α-synuclein have been over-expressed. Whilst such systems provide important information, it is equally imperative to study the ability of endogenous levels of proteins to form inclusions. Indeed Muquit *et al,* (2004) reported that SH-SY5Y cells transfected with parkin form fewer aggresomes than wild-type cells whilst observing that the composition of aggresomes is dependent on the stress applied to the cell. The potential for MPP$^+$ to produce aggresome like structures has also not yet been investigated despite the fact that MPP$^+$ has been reported to inhibit the proteasome (Höglinger *et al.,* 2003). Indeed 5 mM MPP$^+$ significantly increased ubiquitin-protein conjugates in the study presented in this thesis, indicative of impaired

proteasomal function and which could potentiate formation of aggresome like structures.

Vimentin is a major intermediate filament protein shown to undergo reorganisation to the aggresome (Johnston *et al.,* 1998; Ardley *et al.,* 2003; Muqit *et al.,* 2004). It was proposed by Johnston *et al.,* (1998) that the mesh-like structure of intermediate filaments encapsulating the aggresome might offer stabilisation and act to retain aggregated protein within the structure. (Johnston *et al.,* 1998; Muqit *et al.,* 2003). The potential role for NFs, (also a member of the family of intermediate filaments) in stabilising the aggresome structure has not yet been investigated, despite its prominence in both Lewy bodies and cellular inclusions formed by toxic agents. Of significance is that the aggresome structure has been described as juxtanuclear and has been found to impinge upon the nuclear envelope, an observation that also appears to apply to phosphorylated NFs following cytotoxic MPP$^+$ treatment. However the immunoreactive "halo" observed following sub-cytotoxic MPP$^+$ treatment might represent an early event in the formation of the perinuclear mass of phosphorylated NFs observed following 5 mM MPP$^+$ exposure. Indeed, Kopito, (2000) proposed that aggresome formation involved transport of smaller aggregates, formed at the cell periphery, to the MTOC on MT associated motor proteins (see Fig 4.26). This retrograde transport is proposed to involve dynein motor proteins (García-Mata *et al.,* 1999) and dynein is detected within aggresome-like structures (Hasegawa *et al.,* 2004). In support of this theory, Shea and Flannagan, (2001) review that NFs exhibit bi-directional transport within the axon and can undergo retrograde transport in association with dynein. The perinuclear inclusions staining patterns of phosphorylated NFs presented in this thesis share definite similarities to aggresomes stained for other proteins, including parkin (Muquit *et al.,* 2004), γ-tubulin, chaperone proteins, proteasome sub-units (Wigley *et al.,* 1999) and vimentin (Johnston *et al.,* 1998). Results presented in this thesis show that α-tubulin did not accumulate following cytotoxic or sub-cytotoxic exposure to MPP$^+$ (refer to section 4.3.2.2). This is consistent with Johnston *et al,* (1998) who reported recruitment of γ-tubulin (located at the centrosome), but not α-tubulin to the aggresome structure and also reported the requirement of an intact MT network for the formation, but not the stability of an aggresome.
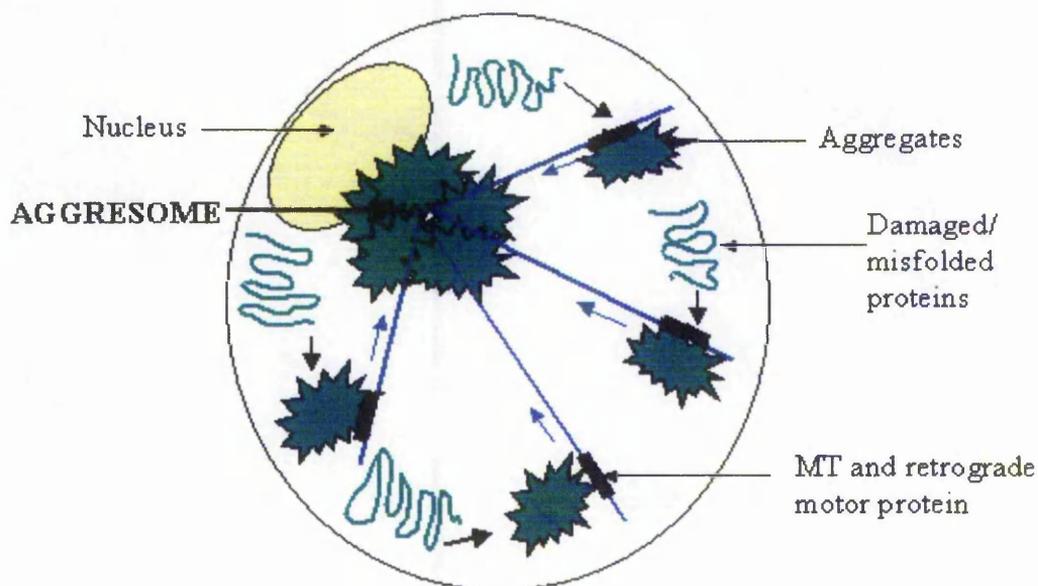
Figure 4.26   Proposed model for aggresome formation (taken from Kapito, 2000).
It is proposed that small aggregates of damaged/misfolded protein nucleate within the cell periphery then undergo retrograde transport along MTs in association with dynein motors towards the aggresome, forming at the MTOC.

The finding that NF-M phosphorylation, and phosphorylated NF-M:NF-H ratio both increase following MPP$^+$ treatment suggest that this sub-unit is important in MPP$^+$ toxicity. Indeed, that NF-M may also represent a down-stream marker of MPP$^+$ toxicity in the SH-SY5Y cell line is significant. Immunoreactivity to non-phosphorylated and phosphorylated NF-M has been extensively reported as a major component of PD Lewy bodies and diffuse Lewy body disease (Forno *et al.*, 1986; Pollanen *et al.*, 1993). The potential significance of NF-M gene mutations in PD has been investigated. Lavedan *et al*, (2002) reported a Gly336Ser substitution in the NF-M protein rod-domain in a case of familial, early onset PD. However further research characterising the effects of a mammalian expression vector encoding the mutated NF-M cDNA in cell lines revealed that this substitution had no effect on the assembly of IF networks (Perez-Olle *et al.*, 2004). Furthermore, in an extensive

mutation analysis of the NF-M gene in sporadic and familial PD cases, no patients showed the Gly336Ser mutation (Kruger *et al.,* 2003). Kruger *et al,* (2003) reported four mutations, occurring in a highly conserved region of the NF-M gene, encoding the tail domain. This domain, as noted by the authors, functions to form cross-bridges between filaments and control longitudinal elongation of filaments, (Nakagawa *et al.,* 1995). However it was concluded that mutations in the NF-M gene are unlikely to play a major role in PD, but that rare gene variants may increase susceptibility to the disease.

4.3.2.1.1 *The role of intracellular kinases in aberrant NF phosphorylation*

The kinase(s) responsible for aberrant NF phosphorylation in the present study is currently unidentified. The NF-H/NF-M phosphorylation at the time points investigated occurred in the absence of increased ERK or JNK phosphorylation. However, transient JNK and ERK phosphorylation were observed within 30 min of exposure to sub-cytotoxic and cytotoxic concentrations of MPP⁺. In the N2a system, JNK is proposed to be responsible for MPTP-induced NF-H hyperphosphorylation (De Girolamo and Billett, manuscript submitted). Similarly, O'Ferrall *et al,* (2000) established that elevated JNK activity caused by MG132 and calpain inhibitor I, induced NF-H/NF-M hyperphosphorylation in differentiated PC12 cells and dorsal root ganglion neurones respectively. However, CDK-5 has been implicated in constitutive NF-H phosphorylation in SH-SY5Y cells (Sharma *et al.,* 1999; Li *et al.,* 2000). Shea *et al,* (2004a) also report that CDK-5 is also involved in normal NF distribution/phosphorylation in chicken dorsal root ganglion neurones; overexpression of CDK-5 increased NF phosphorylation and gave rise to bundles of phosphorylated NFs in the perikarya, whilst reducing NF transport. There is now compelling evidence that CDK-5 can phosphorylate cytoskeletal proteins including NFs in response to cell stress (Ahlijanian *et al.,* 2000; Nguyen *et al.,* 2001). Preliminary evidence was presented in this thesis to suggest that in the pre-differentiated SH-SY5Y cell line, treatment with MPP⁺ in conjunction with CDK-5 inhibitor, BL-1, partially reverses the increase in phosphorylated NF-M-NF-H ratio observed following MPP⁺ treatment. In a recent study, Shea *et al,* (2004b) use both chicken dorsal root ganglion neurones and differentiated NB2a/d1 cells transfected with green fluorescent protein-tagged NF-M, to assess the role of CDK-5 on NF

phosphorylation following oxidative stress induced by H_2O_2. The study showed that H_2O_2 caused ROS elevation, increased perikaryal NF levels and specific NF phosphorylation, associated with impaired NF transport. This was reportedly attributable to CDK-5, since treatment with H_2O_2 in conjunction with the CDK-5 inhibitor rescovitine prevented the increase in aberrant perikaryal NF phosphorylation. The role of CDK-5 was confirmed by transfection of NB2a/d1 cells with an endogenous CDK-5 inhibitor protein (CIP), which also reduced perikaryal NF phosphorylation.

4.3.2.2 The MT system

The effect of MPP$^+$ on tubulin expression/distribution is warranted since tubulin sub-units have been found in Lewy bodies (Galloway et al., 1988) and MPP$^+$ has been proposed to de-stabilise MTs (Cappelletti et al., 1999). Additionally the MT network is required for neuronal transport and indeed the formation of aggresomes (discussed in section 4.3.2.1). Following 24 h exposure to 5 mM MPP$^+$ or following cytotoxic or sub-cytotoxic MPP$^+$ treatments over 14 days, Western blot analysis suggested no change in α-tubulin expression. However, further trials are required to confirm the significance of these observations. Published data regarding a role for tubulin in MPP$^+$ toxicity is a little ambiguous. MPP$^+$ has previously been shown to evoke an imbalance in tubulin sub-unit pools in differentiated PC12 cells (Cappelletti et al., 1995). Indeed it was reported that expression levels of α and β-tubulin sub-units were increased and decreased respectively in MPP$^+$ treated differentiated PC12 cells. MPP$^+$ induced effects on calcium homeostasis and ATP depletion were hypothesised to be attributable to these findings, but do not explain the differential effects of MPP$^+$ on the α/β subunit pools. Cappelletti et al, (1999) found that sub-cytotoxic concentrations of MPP$^+$ influenced polymerisation of α-tubulin, increasing the soluble pool and decreasing the insoluble pool. Through [^{35}S] methionine labelling and immunoprecipitation, the synthesis of α and β-tubulin sub-units were reportedly reduced by MPP$^+$. In-vitro studies confirmed that at high concentrations, MPP$^+$ could directly affect MT assembly (Cappelletti et al., 1999; 2001). In this thesis, Western blot data were in agreement with immunocytochemical analyses, suggesting that 5 mM MPP$^+$ treated cells, fixed and then permeabilised prior to confocal microscopy,

did not show an increase in the total α-tubulin pool. However when 5 mM MPP$^+$ treated cells were permeabilised prior to fixation, the MT network could be observed as disorganised compared to non-toxin treated control cells. Further trials would confirm such observations. Distribution of total or insoluble α-tubulin pools were not affected by treatment with sub-cytotoxic concentrations of MPP$^+$ (results were not shown).

4.3.2.3   Inhibition of the proteasome

Impaired proteasomal function within the substantia nigra pars compacta has been reported in sporadiac and familial PD (McNaught et al., 2003) whilst aged brains have a lower proteasomal activity (reviewed by Shoesmith Berke and Paulson, 2003). Inhibition of the ubiquitin-proteasome system is shown to cause accumulation and aggregation of mutant proteins in-vitro (Johnston et al., 1998; Zhao et al., 2003; Ardley et al., 2003; Muqit et al., 2003). Preliminary results presented in this thesis suggested that exposure of cells to 5 mM MPP$^+$ for 24 h caused an increase in ubiquitin – protein conjugates, suggestive of proteasome impairment. It has been demonstrated in my laboratory using mitotic SH-SY5Y cells that 100 μM MPP$^+$ significantly reduces glutathione levels prior to causing a reduction in activity of the 20S proteasome (Begonã Caneda-Ferron, unpublished observations). On the basis of these data, preliminary investigation into the effects of proteasome inhibition on distribution/expression of phosphorylated NFs and α-tubulin was performed in pre-differentiated SH-SY5Y cells. MG132, a reversible synthetic peptide inhibitor (as detailed by Ardley et al., 2003) was used at a concentration that had previously been shown to inhibit the proteasome in SH-SY5Y cells in my laboratory.

Preliminary results suggested that MG132 induced accumulation of phosphorylated NF-H/NF-M within 24 h and this accumulation was still evident at 72 h. In a study by Masaki et al, (2000), treatment with the non-reversible proteasome inhibitor Lactacystin, caused an accumulation of phosphorylated NFs in the perikaryia of non-differentiated PC12 cells. Lactacystin increased JNK activity, which was attributed to the increase in NF phosphorylation described. Also in this study neither CDK-5 protein (assessed by Western blotting), nor activity, (using Histone 1 as a substrate

following immunoprecipitation of CDK-5), were affected by Lactacystin treatment. However, one may question whether this was due to the use of a rodent, non-differentiated cell line. Therefore the results presented in this project firstly suggest accumulation of phosphorylated NF protein in response to MG132, an alternative proteasome inhibitor to Lactacystin, supporting the belief that NFs are degraded through the proteasome. Secondly results show that this occurs in a human, pre-differentiated, wild-type (non-transfected) system, which has greater analogy to neurones *in-vivo*.

Immunocytochemical studies revealed an accumulation of α-tubulin following 72 h MG132 treatment as observed by an intense staining pattern in treated cells compared to controls. Previous studies using mitotic SH-SY5Y cells have shown that degradation of the MAP, tau, to be blocked by Lactacystin (David *et al.*, 2002). Using rat brain lysates and HEK293 cells, parkin was found tightly bound to MTs, resulting in ubiquitination and degradation of tubulin sub-units (Ren *et al.*, 2003). Over-expression of Parkin in HEK293 cells increased polyubiquitination of tubulin, a further increase noted following treatment with Lactacystin (Ren *et al.*, 2003). Hence results shown here support the view that tubulin is degraded through the proteasome and demonstrate this finding in a human, differentiated system.

This preliminary data is particularly interesting since a recent study by Biasini *et al*, (2004) highlighted the importance of studying proteasome inhibition in wild-type (non-transfected) cell systems. In this study the authors compared the effects of proteasomal inhibition on α-synuclein and parkin in transfected and non-transfected PC12 cells finding differing results. Endogenous levels of parkin and synuclein were not increased following proteasomal inhibition. This directly contrasted with results using the cells transfected with parkin and synuclein under the control of a cytomegalovirus (CMV) promoter. In transfected cells, parkin and synuclein were found to accumulate. However it was noted that the accumulation of these proteins was a consequence of increased protein synthesis rather than proteasome inhibition since inhibition of protein synthesis removed this effect. In turn the authors concluded that inhibition of the proteasome might have caused up-regulation of CMV driven transcription accounting for spurious results. Hence wild type cell

systems may prove more reliable to investigate the effects of proteasomal inhibition in cell culture systems.

In conclusion, this chapter has provided important information regarding the involvement of MPP$^+$ toxicity on the cytoskeleton in the pre-differentiated SH-SY5Y system. Results suggest that NF-H and NF-M phosphorylation status *per se* may be useful as a quantitative molecular downstream marker of short term and chronic MPP$^+$ toxicity in the SH-SY5Y system. Importantly, its sub-cellular redistribution may be a useful ultrastructural marker and might represent the formation/stabilisation of an aggresome-like structure in this system, in response to MPP$^+$ toxicity. The role of NFs in aggresome formation has not yet been investigated. An exciting possibility may be that NFs, like vimentin, play a role in stabilising aggresomes by encapsulating the accumulated protein. Further research should focus on identification of proteins that may co-localise with phosphorylated NFs in this system including ubiquitin and α-synuclein in order to determine whether protein inclusions in this pre-differentiated culture system might correlate with pathological processes *in-vivo*. Additionally it was demonstrated that cytotoxic concentrations of MPP$^+$ might impair proteasomal function and that inhibition of the proteasome induced phosphorylated NFs and α-tubulin to accumulate in differentiated cells.

CHAPTER V

NEUROPROTECTIVE EFFECTS OF INHIBITORS OF MAPK AND CDK-5 PATHWAYS FOLLOWING MPP$^+$ EXPOSURE

5.1   INTRODUCTION

5.1.1   Neuroprotective strategies in MPP$^+$ toxicity

5.1.1.1   General approaches

An important reason for investigating MPP$^+$ toxicity, as a model for PD, is to establish neuroprotective strategies that may become applicable to the disease state. No protective therapy is yet available, probably because PD pathology is not yet fully understood; thus further research is warranted. To date, agents suggested to confer some degree of neuroprotection from MPP$^+$ toxicity in neuronal cell culture systems have been diverse and include oestradiol (De Girolamo *et al.*, 2001; Callier *et al.*, 2002), caspase inhibition (Bilsland *et al.*, 2002; Gómez *et al.*, 2001), MAO inhibition (De Girolamo *et al.*, 2001), DA agonists (Joyce *et al.*, 2003) and antioxidant compounds (Stull *et al.*, 2002). A major line of investigation into MPP$^+$ toxicity has however, focussed on the role of the MAPK signalling pathways in cell death and survival and studies using specific inhibitors to these pathways, as discussed in section 5.1.1.2.

5.1.1.2   Neuroprotection afforded by MAPK Inhibitors

The role of MAPK pathways in MPP$^+$ toxicity is complicated, given that activation patterns, their role in cell death and any neuroprotection conferred by subsequent inhibition can vary between cell systems. MPP$^+$ induces activation of both pro and anti-apoptotic pathways (Cassarino *et al.*, 2000), dependant on toxin concentration, time of exposure and the cell line. ERK 1/2 pathways are traditionally considered to be activated in response to external signals that promote survival and proliferation /differentiation of cells, and phosphorylated ERK can activate many down-stream, pro-survival targets (Grewal *et al.*, 1999; Kaplan and Miller, 2000). Alternatively in conditions of cellular stress that result in apoptosis, ERK activity has been reportedly suppressed (Wang *et al.*, 1998). In support of this view, studies have correlated inhibition of the ERK pathway with induction/exacerbation of neurotoxicity (Xia *et al.*, 1995; Halvorsen *et al.*, 2002; Crossthwaite *et al.*, 2002). Indeed, in a study of H$_2$O$_2$ induced oxidative stress in HeLa (human cervical carcinoma) cells (Wang *et*

al., 1998), ERK 2 activity was initially elevated and pre-treatment with the MEK inhibitor, PD98059, induced a significant increase in apoptosis compared to control cells, suggesting that early ERK activation was a survival signal. In a mitotic SH-SY5Y model Halvorsen *et al,* (2002) also report that pre-treatment with the ERK inhibitor U0126 reduced cell viability and exacerbated toxicity induced by 24 h exposure to 5 mM MPP$^+$, again suggesting that ERK activation is anti-apoptotic in this system. However contrary to these reports, several studies using neuronal cell lines and primary neuronal cultures have shown that cellular stress does not only activate ERK, but that inhibition of this pathway promotes cell survival, following focal cerebral ischemia (Alessandrini *et al.,* 1999); oxidative stress induced by glutamate (Satoh *et al.,* 2000; Stanciu *et al.,* 2000, 2002) and H$_2$O$_2$ (Ruffels *et al.,* 2004), endoplasmic reticulum stress induced by thapsigargin (Arai *et al.,* 2004) and MPP$^+$ (Gómez-Santos *et al.,* 2002). Thus it is generally accepted that the regulation of cell survival may depend on a dynamic balance between survival and apoptosis promoting pathways.

JNK has been shown to undergo biphasic activation in SH-SY5Y cells when induced by 5 mM MPP$^+$ over 24 h (Cassarino *et al.,* 2000). Early JNK activation (15-30 min) in response to MPP$^+$ exposure was reportedly dependent on mitochondrial adenine nucleotide translocator activity (ANT). Pre-incubation of cells with an ANT antagonist blocked the early activation but not the late (12 h) activation of JNK. The JNK pathway is generally considered to be pro-apoptotic although this theory is not unequivocal. As reviewed by Tibbles and Woodgett, (1999), activation of the JNK pathway can be "graded and adaptive" and as such the overall cellular response can vary dramatically from apoptosis to repair. Certainly in the context of *in-vivo* and *in-vitro* cell culture models of MPTP/MPP$^+$ toxicity, the JNK pathway is proposed to be pro-apoptotic (Xia *et al.,* 2001; Saporito *et al.,* 1999, 2000; Wang *et al.,* 2004). Inhibition of MLK3/JNK using the inhibitor CEP-1347 has been very recently shown to attenuate MPP$^+$ induced apoptosis and loss of morphology in differentiated SH-SY5Y cells (Mathiasen *et al.,* 2004). It should be noted that the duration of this study was only 4 days. DA also induces JNK activation through an apoptotic death programme induced by oxidative stress in primary neuronal cultures (Luo *et al.,* 1998). This is significant since DA auto-oxidation and subsequent generation of reactive oxygen species and neuromelanin are inherently linked to PD (reviewed in

chapter 1, section 1.3), thus strengthening the hypothesis that JNK inhibition may be a potential therapeutic target for PD.

The role of the p38 pathway in cell death/survival is less understood and can again be dependent upon the cell model and the nature of external stressors. As was discussed in chapter III, neuronal differentiation induced by retinoic acid is proposed to induce Myocyte enhancing factor 2 (MEF-2), a transcription factor believed, via p38α activation, to prevent apoptosis during neuronal development (Okamoto *et al.*, 2000). In many studies, however, the p38 pathway is implicated in orchestrating cell death. In accordance with this theory, viability was increased in SH-SY5Y cells exposed to oxidative stress induced by the peroxynitrite donor, 3-morpholino-sydonimine (SIN-1), when treated in the presence of the p38 inhibitor SB202190 (Oh-hashi *et al.*, 1999), following detection of p38 phosphorylation. Similarly in this cell line, DA induced p38 phosphorylation was reduced by the inhibitor, SB203580, with subsequent attenuation of apoptosis (Junn *et al.*, 2001). In a differentiating mouse N2a neuroblastoma model, SB202190 protected cells against the effects of sub-cytotoxic concentrations of MPTP on cell morphology, but could not maintain viability at high MPTP concentrations (De Girolamo *et al.*, 2001). In contrast, Halvorsen *et al.*, (2002) showed short term MPP^+ toxicity induced by 5 mM to be exacerbated by the p38 inhibitor, SB203580, in SH-SY5Y cells.

5.1.2 CDK-5 and neurotoxicity

5.1.2.1 Activation of CDK-5

CDK-5 has been aptly described as a "Jekyll and Hyde" kinase (Cruz and Tsai, 2004). This is because it plays many key roles in maturation and maintenance of the CNS but it has more recently been demonstrated that uncontrolled CDK-5 activity is linked to several neurodegenerative diseases. A mechanism by which CDK-5 activity becomes harmful to the cell is thought to be due to the regulatory partners that control its activation. There is now compelling evidence that p35, the most widespread of such activators, along with p39, can become truncated under some pathological conditions to form p25 and p29 proteins respectively (Patrick *et al.*, 1999; Patzke and Tsai, 2002). Cleavage occurs 10 amino acids from the amino-

terminus of the p35 protein yielding p25 and a resultant p10 species (Patrick *et al.,* 1999). Lee *et al,* (2000) provide evidence that this conversion is mediated by calpains (calcium dependent cysteine proteases) that can become activated in response to raised intracellular calcium levels, induced in cell culture systems by oxidative stress and excitotoxins. Notably, conversion of p35 to p25 was prevented by calpain inhibition (Lee, *et al.,* 2000). Resultant p25 can still activate CDK-5 but this differs from the normal, beneficial, p35-induced activation. Firstly, p35 is bound to peripheral membranes controlled by a conserved myristoylation signal. However this signal is absent in p25 which becomes mis-localised to the cytosol, specifically, to nuclear and perinuclear regions, hence priming CDK-5 for abnormal phosphorylating activities. Secondly, p25 has greater stability than p35. p35 is tightly regulated and rapidly degraded through the ubiquitin proteasome system, following phosphorylation upon activating CDK-5 (Patrick *et al.,* 1998, 1999) (refer to chapter I, section 1.5.2). Therefore the CDK-5/p25 complex is hyperactive and deregulated as summarised in Figure 5.1.
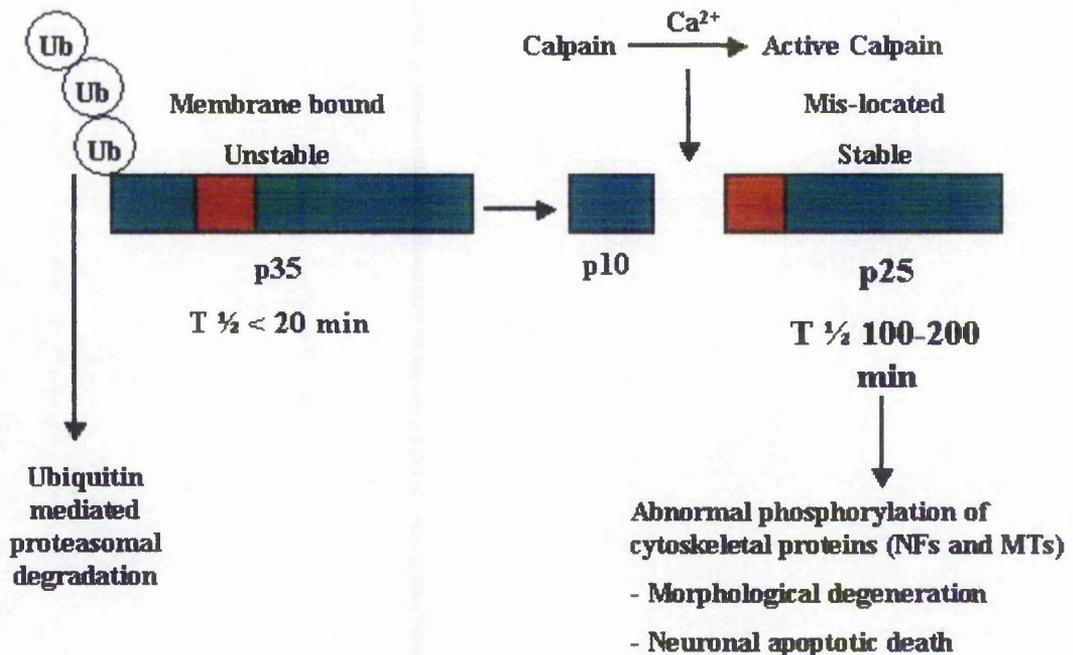
Figure 5.1 Conversion of p35 to p25 by calpains (taken from Patrick *et al.*, 1999 and Lee, *et al.*, 2000 with modifications).
In the presence of raised intracellular calcium levels p35 is cleaved by activated calpains within a proline rich region to yield p10 and a stable, mis-localised p25 moiety, capable of inducing CDK-5 hyperactivity.

5.1.2.2   *CDK-5 and neurodegenerative disease – potential neuroprotective strategies via CDK-5 inhibition*

Numerous studies suggest p25 to be neurotoxic. The implications of uncontrolled CDK-5 activity are associated with cellular pathogenicity and neurodegenerative disease, by virtue of resultant effects on, for example, cytoskeletal regulation, which have been demonstrated both *in-vivo* and in cultured cells. The most compelling evidence for the disruptive influence of CDK-5/p25 has been presented in Alzheimer's disease, where CDK-5/p25 hyperphosphorylates tau *in-vivo*, reducing the ability of this MAP to associate with MTs (Patrick *et al.*, 1999). Interestingly, this study also showed p25 to localise within neurones containing neurofibrillary tangles, an interneuronal pathological feature of the disease. The ratio of p25 to p35 was shown to be higher in post mortem brains of Alzheimer's disease patients

compared to age matched controls (Tseng *et al.*, 2002). It should be noted that there are conflicting data concerning the role of CDK/p35/p25 in Alzheimer's disease (see Shelton and Johnson, 2004 for review) but a general consensus is that CDK-5 deregulation can evoke harmful effects on the MT network and this has been proposed to induce more widespread cytoskeletal disruption (Ahlijanian *et al.*, 2000). By virtue of its role in NF phosphorylation, CDK-5 activity has been implicated in Amyotrophic Lateral Sclerosis where accumulation of NFs in cell bodies and proximal axons of the spinal cord have been reported (Bajaj, 2000). CDK-5 has been shown to inhibit NF axonal transport and to increase perikaryal NF phosphorylation in cultured cells following H_2O_2 treatment (Shea *et al.*, 2004b). NF protein was shown to be hyperphosphorylated in transgenic mice expressing human p25 (Ahlijanian *et al.*, 2000). By the same token, CDK-5 has been implicated in dopaminergic cell death in PD. Henchcliffe and Burke, (1997) show that, following apoptosis in dopaminergic cells of rat pups, induced by excitotoxic lesion, high levels of CDK-5 protein was present in apoptotic cells. Despite the finding that active CDK-5 is found in PD Lewy bodies (Brion and Couck, 1995), very little research has focussed on the role of CDK-5 in MPTP/MPP$^+$ induced neurotoxicity. One interesting *in-vivo* study using mice has shown CDK-5 expression and activity to be elevated following MPTP treatment (Smith *et al.*, 2003). In the same study treatment with flavopiridol, a general CDK inhibitor, or the expression of dominant-negative CDK-5 attenuated dopaminergic neurone cell death induced by MPTP.

5.1.3 Aims of chapter

Current literature demonstrates a role for MAPK signalling in pro and anti-apoptotic responses to MPP$^+$ toxicity in cultured cells. However there is no current understanding of longer-term contributions of such pathways to MPP$^+$ toxicity and many studies still employ mitotic cell systems. Hence the aim of this chapter was to re-visit the effects of MAPK (ERK, JNK and p38) inhibitors on cell viability following short-term MPP$^+$ exposures and, more importantly, to extend these investigations to the effects of chronic treatments of differentiated SH-SY5Y cells with MPP$^+$. Finally, since the effects of CDK-5 inhibition on MPP$^+$ toxicity in a human cell culture system have not previously been investigated, this chapter sought

to determine the effects of a specific CDK-5 inhibitor on cell viability following short-term and chronic MPP$^+$ treatments.

5.2 RESULTS

5.2.1 Neuroprotection conferred by inhibitors to MAPK pathways

5.2.1.1 MAPK inhibitors

A range of commercial inhibitors to MAPK pathways were used in this work; see section 2.1.4 in chapter II for sources. PD98059 (2'-Amino-3'-methoxyflavone) is a selective, cell permeable inhibitor of MAP kinase kinase (MEK), which acts to inhibit the activation of MAP kinase (ERK) by Raf or MEK kinase and subsequent phosphorylation of MAPK sub-units (Alessi *et al.*, 1995). It was previously found that 5 μM PD98059 completely inhibited ERK phosphorylation in differentiated SH-SY5Y cells following MPP^+ treatment (results not shown). SB202190, (4-(4-Fluorophenyl)-2-(4-hydroxyphenyl)-5-(4-pyridyl) 1 H-imidazole) is a cell permeable, potent inhibitor of p38 (Carvalho *et al.*, 2004). 1 μM SB202190 was found to completely inhibit staurosporine-induced p38 phosphorylation in mitotic SH-SY5Y cells in my laboratory (Julia Fitzgerald, unpublished observations). CEP-11004 was used with prior permission from Cephalon Inc. This compound is reported to promote survival *in-vivo* and *in-vitro* by inhibiting upstream of JNK, at the level of mixed lineage kinases (Hidding *et al.*, 2002; Murakata *et al.*, 2002). 1 μM CEP-11004 is used to inhibit MPTP-induced JNK phosphorylation in mouse neuroblastoma cells in my laboratory (De Girolamo *et al.*, 2004, manuscript submitted). This compound has not been used previously in SH-SY5Y cells but a related compound, CEP-1347 significantly inhibited MPP^+-induced JNK phosphorylation when employed at a concentration of 10 nM (Mathiasen *et al.*, 2004).

5.2.1.2 The effects of MAPK inhibition on viability of differentiated cells

To enable detailed interpretation of the effects of MAPK inhibition on MPP^+ toxicity, the effects of the inhibitors alone on cells were also analysed. Firstly this enabled their role in cell survival *per se* to be established. Secondly suitable

concentrations of inhibitors to use in toxicity studies were determined by titration, to check whether or not effective concentrations of inhibitors effected cell viability.

Figure 5.2A shows that increasing the concentration of the MEK inhibitor, PD98059, above 1 µM reduced cell viability in a concentration-dependent manner over a 24 h time period. Over 14 days exposure to PD98059 both 0.1 and 1 µM induced a degree of toxicity to cells (Fig 5.2B). In accordance with these results, morphological analysis showed that PD98059 induced retraction of axon-like processes, particularly at higher (20 µM) concentrations (see Fig 5.3). This would suggest that ERK is a pro-survival pathway in SH-SY5Y cells.

Investigations with the p38 inhibitor, SB202190, showed that short-term exposures of 2 and 4 days had no effect on cell viability at the concentrations tested. However following 7 days and beyond, exposure to SB202190 can induce variable effects on the viability of cells as indicated by the range of data from 2 independent experiments (see Fig 5.4). Where SB202190 increased MTT reduction compared to controls, morphological analysis supported these results; qualitative analysis revealed that SB202190 treatment appeared to increase both cell number and the number of axon-like extensions. (see Fig 5.5). Analysis of involvement of MAPK inhibitors alone on cell viability is therefore vital for independent trials.

Titration of the mixed lineage kinase inhibitor, CEP-11004 was performed over 72 h and over 14 days for chronic studies using 1 and 10 nM concentrations Figure 5.6 shows that over 72 h and 14 days, CEP-11004 did induce an increase in MTT reduction. CEP-11004 had no effect at the concentrations tested on cell morphology.
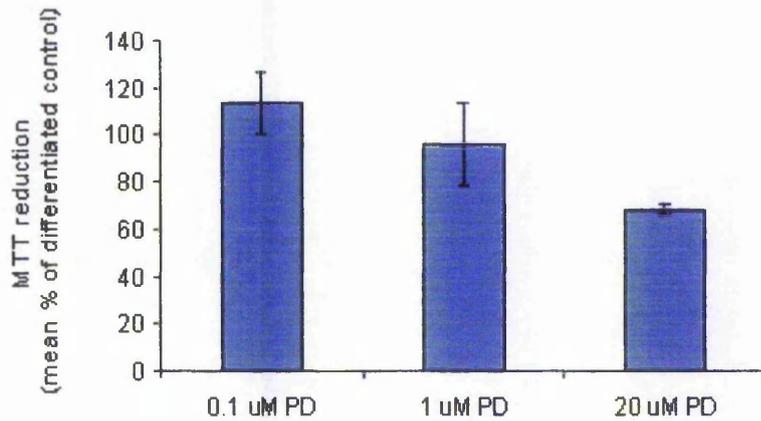
A.
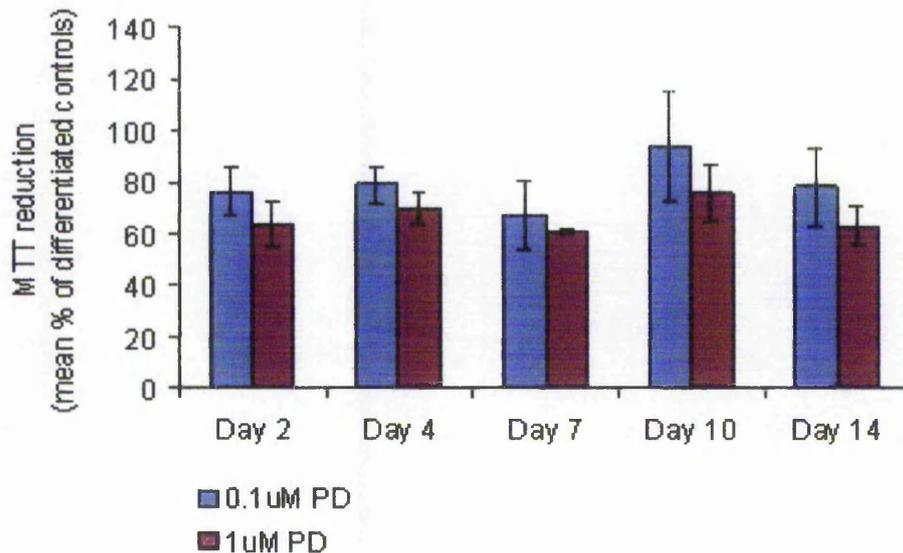
B.

Figure 5.2 Titration of PD98059 in differentiated cells.
Cells were seeded into 96 well plates at a density of 5000 cells/well and induced to differentiate over 7 days as detailed in methods section 2.2.1.6. Medium was removed and replaced with fresh differentiating medium supplemented with PD98059 to give the final concentrations shown above. After incubation for 24 h (A) and over 14 days (B), cells were assayed for viability using the MTT reduction assay as detailed in methods section 2.2.3.1. Results are expressed as the mean percentage of differentiated control cells and are combined data from 2 independent experiments (5 replicate wells/treatment in each experiment). The range of the data is shown.

Differentiated control cells   0.1 µM PD98059

1 µM PD98059   20 µM PD98059
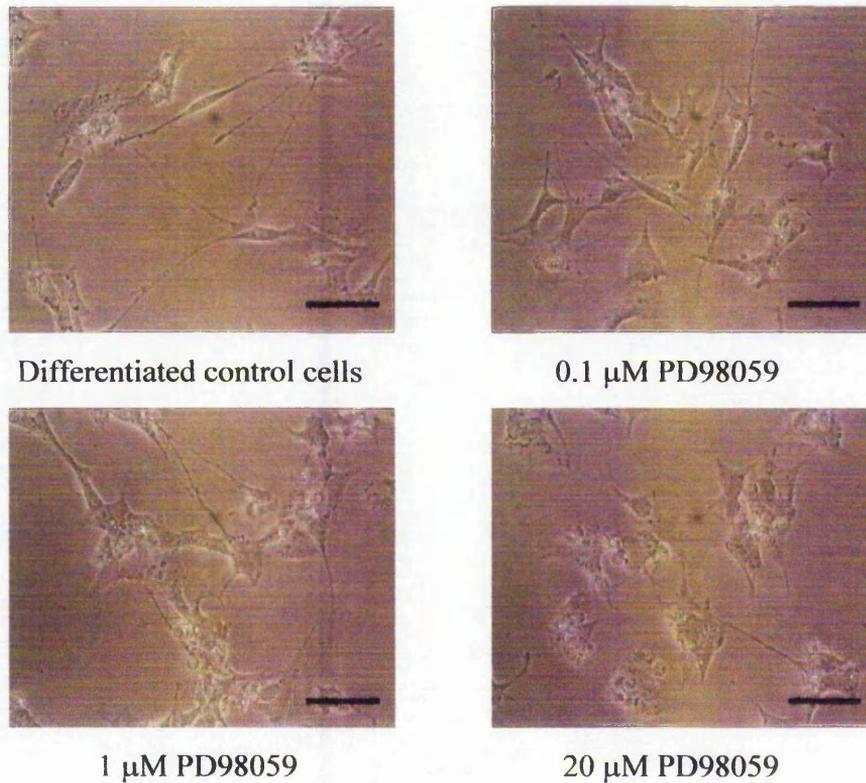
Figure 5.3 Morphological analysis following 24 h exposure to PD98059
Cells were induced to differentiate over 7 days in 96 well plates. On day 7 medium was replaced with fresh differentiating medium supplemented with PD98059 at the concentrations shown above. Cells were observed by phase contrast microscopy at 100 x magnification. Scale bar represents 40 µm.
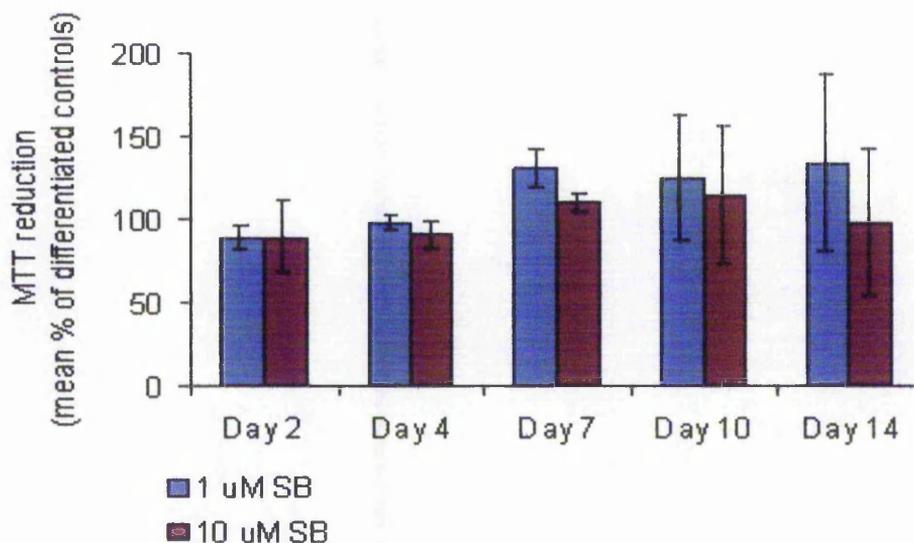
Figure 5.4 Titration of SB202190 in differentiated cells.
Cells were seeded into 96 well plates at a density of 5000 cells/well and induced to differentiate over 7 days as detailed in methods section 2.2.1.6. Medium was removed and replaced with fresh differentiating medium supplemented with SB202190 to give the final concentrations shown above. After incubation periods of up to 14 days, cells were assayed for viability using the MTT reduction assay as detailed in methods section 2.2.3.1. Results are expressed as the mean percentage of differentiated control cells and are combined data from 2 independent experiments (5 replicate wells/treatment in each experiment). The range of the data is shown.

Day 4

Day 10

Differentiated control
Cells

+ 1 µM SB202190

+ 10 µM SB202190
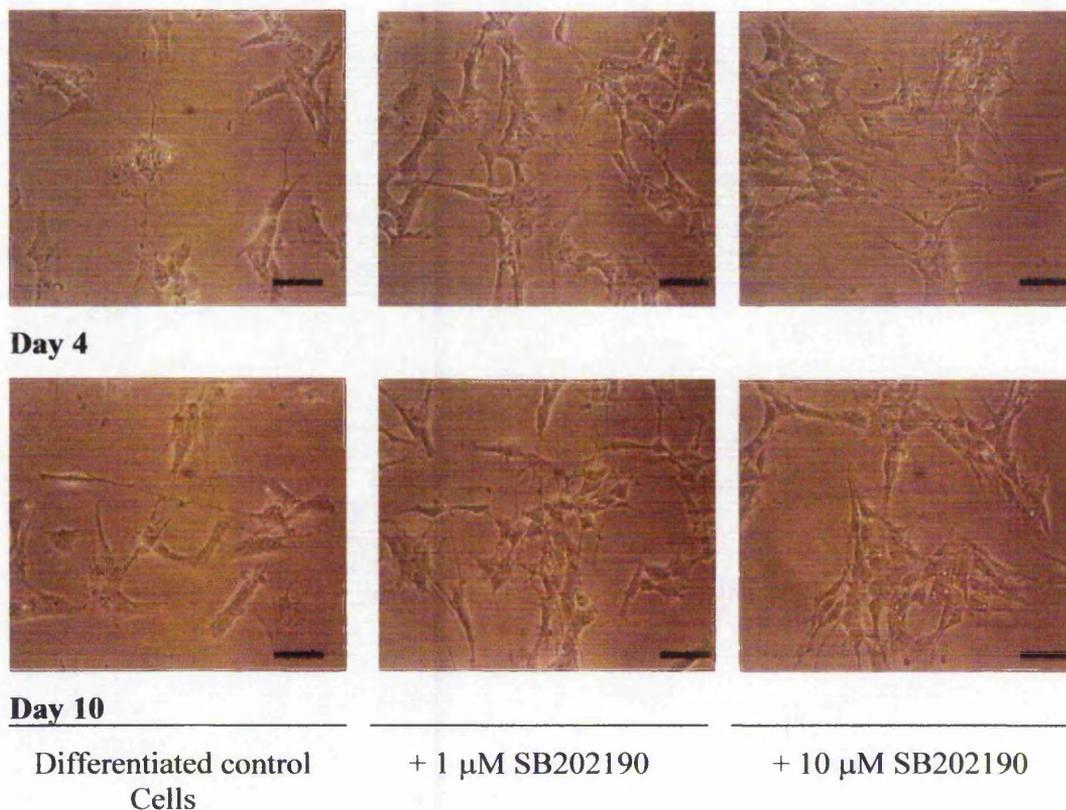
Figure 5.5 Morphological analysis of cells following long-term exposure to SB202190.
Cells were induced to differentiate over 7 days in 96 well plates. On day 7 medium was replaced with fresh differentiating medium supplemented with SB202190 at the concentrations shown above. Cells were observed by phase contrast microscopy at 100 x magnification. Scale bar represents 40 µm.
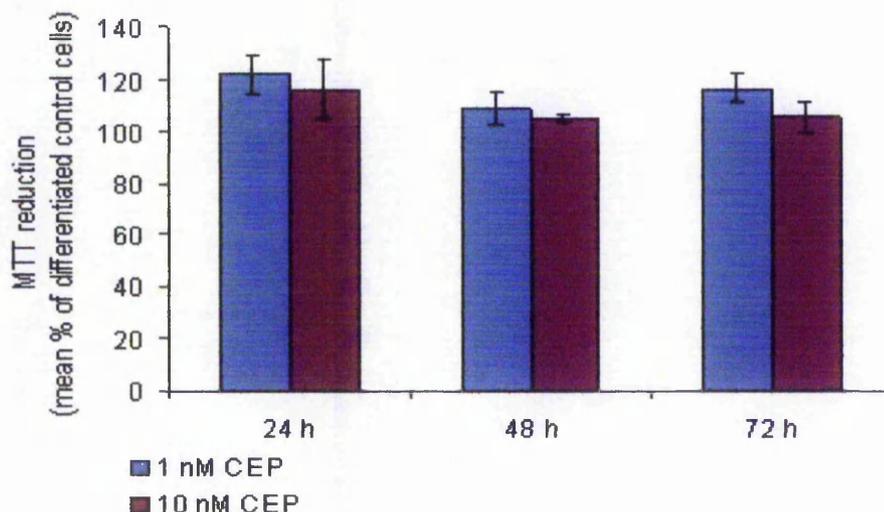
A.
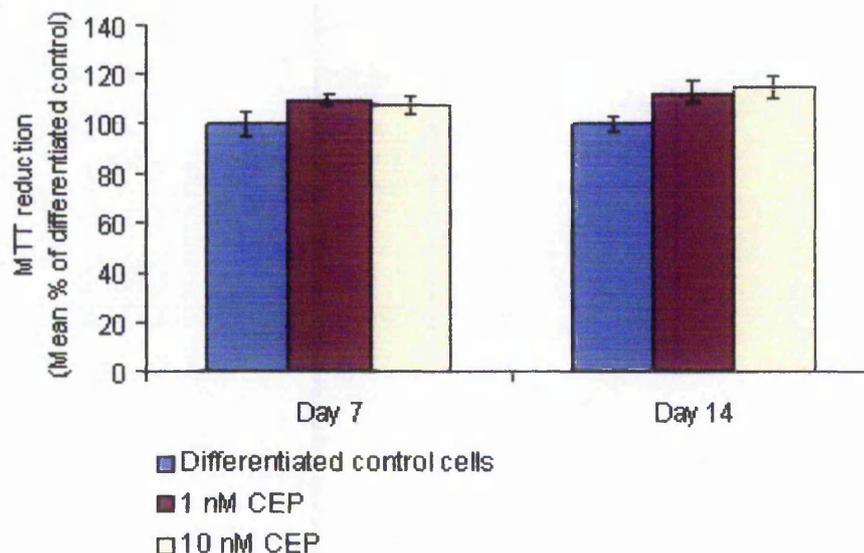
B.

Figure 5.6 Titration of CEP-11004 in differentiated cells.
Cells were seeded into 96 well plates at a density of 5000 cells/well and induced to differentiate over 7 days as detailed in methods section 2.2.1.6. Medium was removed and replaced with fresh differentiating medium supplemented with CEP-11004 to give the final concentrations shown above. After incubation periods of up 72 h (A) and 14 days (B), cells were assayed for viability using the MTT reduction assay as detailed in methods section 2.2.3.1. (A) Results are expressed as the mean percentage of differentiated control cells ± SEM and are combined data from 3 independent experiments (5 replicate wells/treatment in each experiment) (B) Results are expressed as the mean percentage of differentiated control cells ± SEM of 5 replicate wells/treatment and represent preliminary data from a single trial.

5.2.1.3   Effects of MAPK inhibitors on MPP$^+$ toxicity

The effects of MAPK inhibitors on MPP$^+$ toxicity were investigated over a range of time points to encompass short-term and also chronic studies. In all experiments cells were pre-differentiated for 7 days and inhibitors were added to cells at the same time as MPP$^+$. All results were expressed as a percentage of differentiated control cells (assigned a value of 100 %). Results shown are combined data from 2 or 3 independent experiments of 5 or 6 replicate wells/treatment in each experiment as detailed in legends.

5.2.1.3.1   Effects of PD98059 on MPP$^+$ toxicity

Results indicated that cytotoxicity induced by 1 mM MPP$^+$ following 24 h exposure was exacerbated by the presence of PD98059 in a dose-dependent manner. (see Fig 5.7A). Morphological studies shown in Figure 5.8 demonstrate the effects of 1 mM MPP$^+$ in the presence and absence of PD98059. At higher concentrations of PD98059, cells appear rounded compared to toxin treatment alone (compare Fig 5.8B and F), supporting exacerbation of toxicity. However, in contrast, a further experiment suggested both 0.1 and 1 μM PD98059 to confer partial protection to cells following exposure to 1 mM MPP$^+$, albeit the toxicity induced by 1 mM MPP$^+$ was greater in experiment B (71 % as opposed to 37 % toxicity in experiment A).
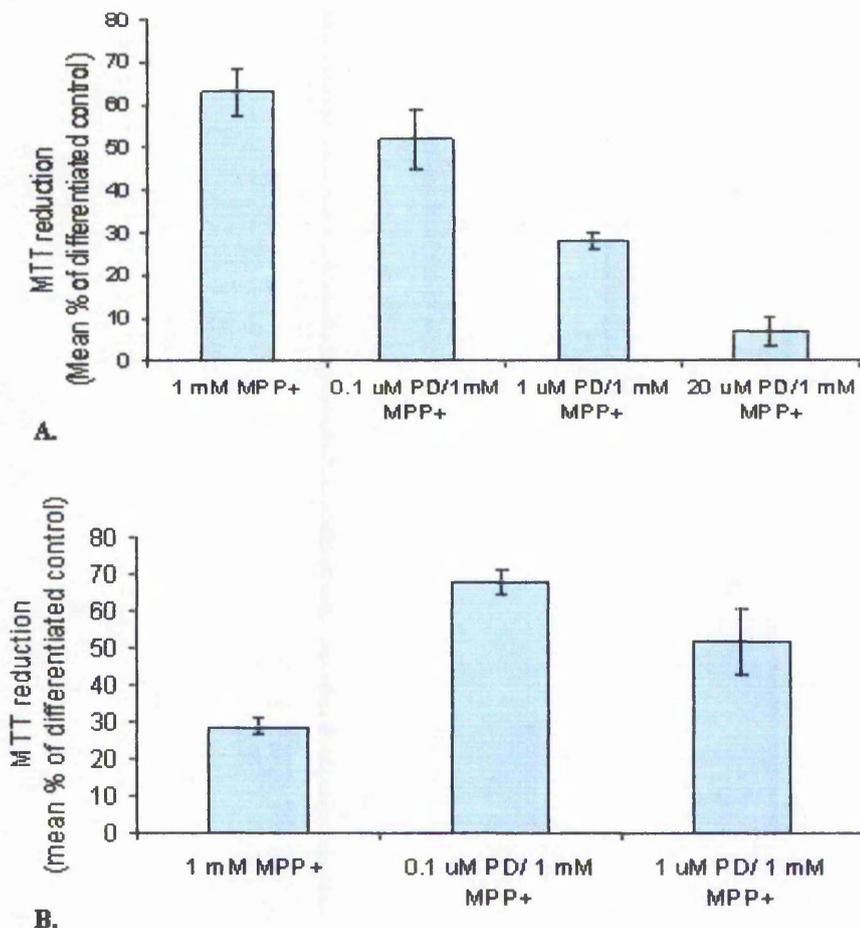
Figure 5.7 Effect of PD98059 on 24 h MPP$^+$ toxicity.
Cells were seeded into 96 well plates at a density of 5000 cells/well and induced to differentiate over 7 days as detailed in methods section 2.2.1.6. Medium was removed and replaced with fresh differentiating medium supplemented 1 mM MPP$^+$ and PD98059 at final concentrations shown above. After incubation for 24 h, cells were assayed for viability using the MTT reduction assay as detailed in methods section 2.2.3.1. Results are expressed as the mean percentage of differentiated control cells ± SEM from 5 replicate wells/treatment. A and B are independent experiments (see text for details).
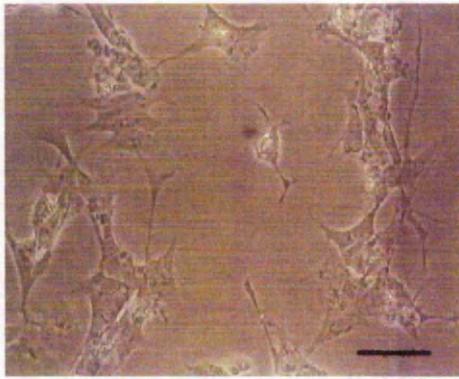
A. Differentiated control cells
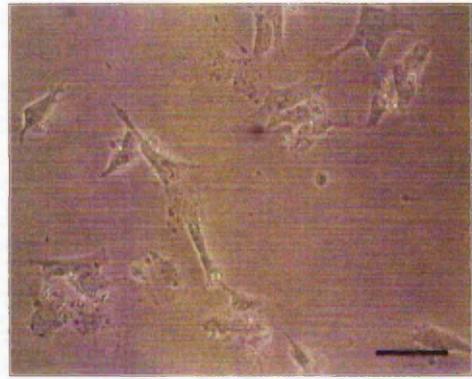
B. 1 mM MPP$^+$
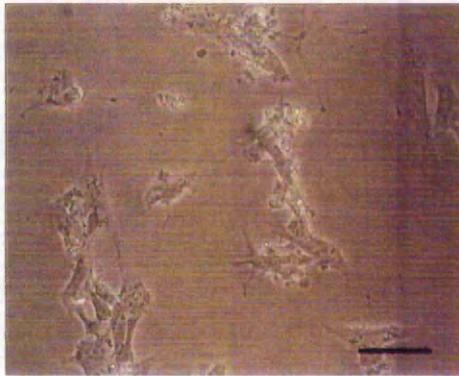
C. 1 mM MPP$^+$ / 0.1 µM PD98059
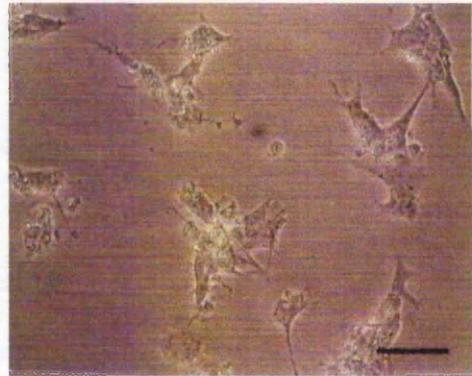
D. 1 mM MPP$^+$ / 1 µM PD98059
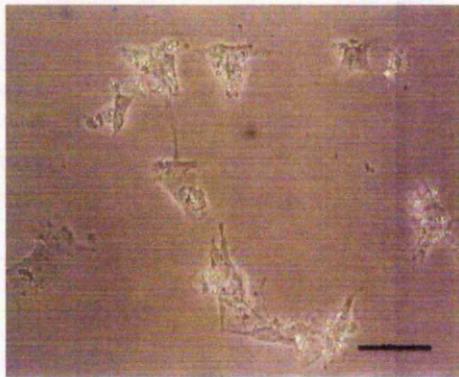
E. 1 mM MPP$^+$ / 10 µM PD98059
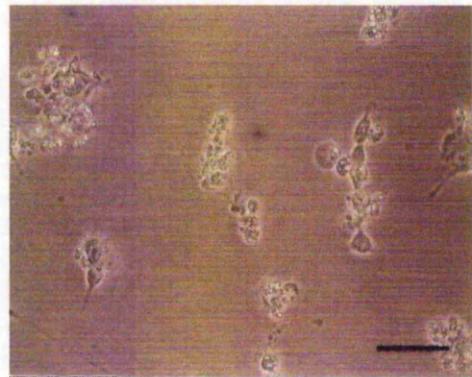
F. 1 mM MPP$^+$ / 20 µM PD98059

Figure 5.8 Morphological analysis of the effects of PD98059 on 24 h MPP$^+$ toxicity.
Cells were induced to differentiate over 7 days in 96 well plates. On day 7 medium was replaced with fresh differentiating medium supplemented with 1 mM MPP$^+$ and PD98059 at the concentrations shown above. Following 24 h incubation, cells were observed by phase contrast microscopy at 200 x magnification. Scale bar represents 40 µm.

The effects of PD98059 on chronic MPP^+ toxicity were also investigated. Differentiated cells were treated with 250 or 500 µM MPP^+ over 14 days in the presence or absence of PD98059 at concentrations of 0.1 and 1 µM. In conjunction with 250 µM MPP^+ exposure, PD98059 again exacerbated MPP^+ toxicity (Fig 5.9A). This was independent of whether MPP^+ alone caused toxicity. Hence these data again indicate that ERK is required for cell survival.

In striking contrast, treatment with PD98059 in conjunction with 500 µM MPP^+ caused attenuation of MPP^+ toxicity (Fig 5.9B). At each time point both 0.1 and 1 µM PD98059 conferred protection against MPP^+ toxicity. These results suggest that the concentration of toxin, and therefore the degree of insult to the cells, is a crucial determinant of the effect of MEK inhibitor treatment. This concept is supported by results presented in Fig 5.7 where PD98059 conferred differential effects on cell viability in 2 independent experiments where the degree of toxicity induced by 1 mM MPP^+ differed after a 24 h exposure.

A.

B.
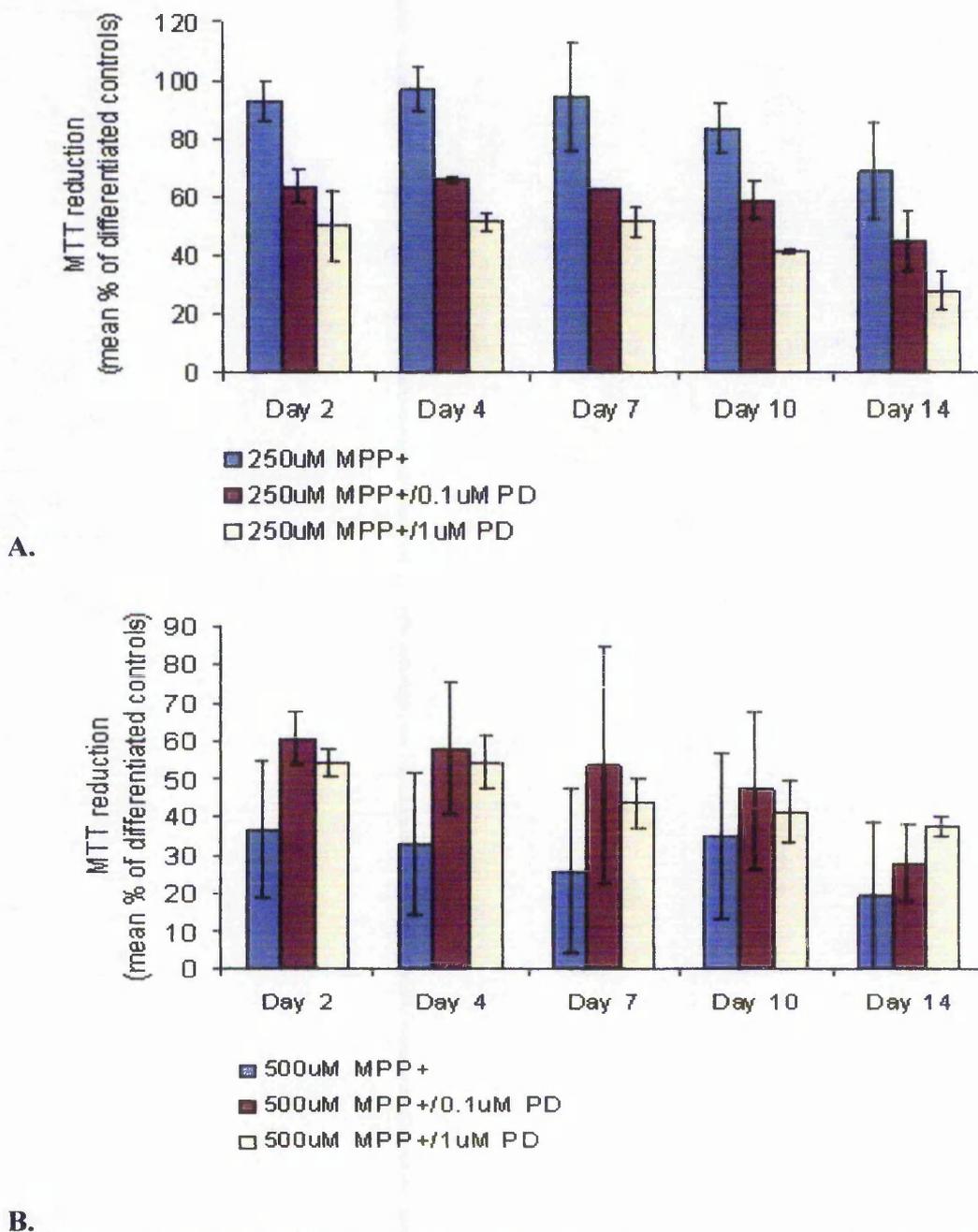
Figure 5.9 Effect of PD98059 on chronic MPP⁺ exposure.

Cells were seeded into 96 well plates at a density of 5000 cells/well and induced to differentiate over 7 days as detailed in methods section 2.2.1.6. Medium was removed and replaced with fresh differentiating medium supplemented with 250 μM MPP⁺ (A) or 500 μM MPP⁺ (B) and PD98059 at final concentrations shown above. At time points indicated, cells were assayed for viability using the MTT reduction assay as detailed in methods section 2.2.3.1. Results are expressed as the mean percentage of differentiated control cells and are combined data from 2 independent experiments (5 replicate wells/treatment in each experiment). The range of the data is shown.

5.2.1.3.2   Effect of SB202190 on MPP$^+$ toxicity

As with PD98059, treatment of cells with 1 mM MPP$^+$ in conjunction with the p38 inhibitor, SB202190, exacerbated MPP$^+$ toxicity when compared with either differentiated controls or toxin treated cells (see Fig 5.10). Since the inhibitor alone was not toxic over this time course (Fig 5.4), results suggest that p38 is required for cell survival whilst its inhibition in the presence of MPP$^+$ promotes cell death.
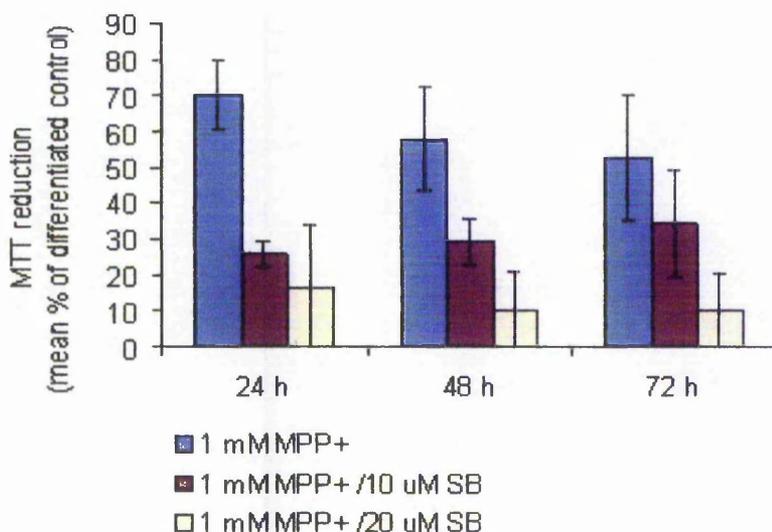
Figure 5.10 Effect of SB202190 on MPP$^+$ toxicity over 72 h.
Cells were seeded into 96 well plates at a density of 5000 cells/well and induced to differentiate over 7 days as detailed in methods section 2.2.1.6. Medium was removed and replaced with fresh differentiating medium supplemented 1 mM MPP$^+$ and SB202190 at final concentrations shown above. After incubation for 24, 48 and 72 h, cells were assayed for viability using the MTT reduction assay as detailed in methods section 2.2.3.1. Results are expressed as the mean percentage of differentiated control cells and are combined data from 2 independent experiments (5 replicate wells/treatment in each experiment). The range of the data is shown.

A similar trend to that observed following chronic exposure to PD98059 was also found when cells were exposed chronically to MPP^+ with SB202190. The role of the p38 inhibitor depended on the degree of insult to which the cells were exposed. Indeed following exposure to 250 µM MPP^+, 10 µM SB202190 exacerbated toxicity in a time-dependent manor (see Fig 5.11A). At days 4, 7, 10 and 14, 1 µM SB202190 did confer a degree of protection to cells against 250 µM MPP^+ toxicity.

In the presence of 500 µM MPP^+, both 1 µM and 10 µM SB202190 protected cells against MPP^+ toxicity at all time points (see Fig 5.11B), a greater effect again conferred by 1 µM SB202190. The protection afforded by SB202190 was reflected in morphological analyses of cells treated with MPP^+, particularly in conjunction with 500 µM MPP^+ treatment (Fig 5.12).

A.

B.
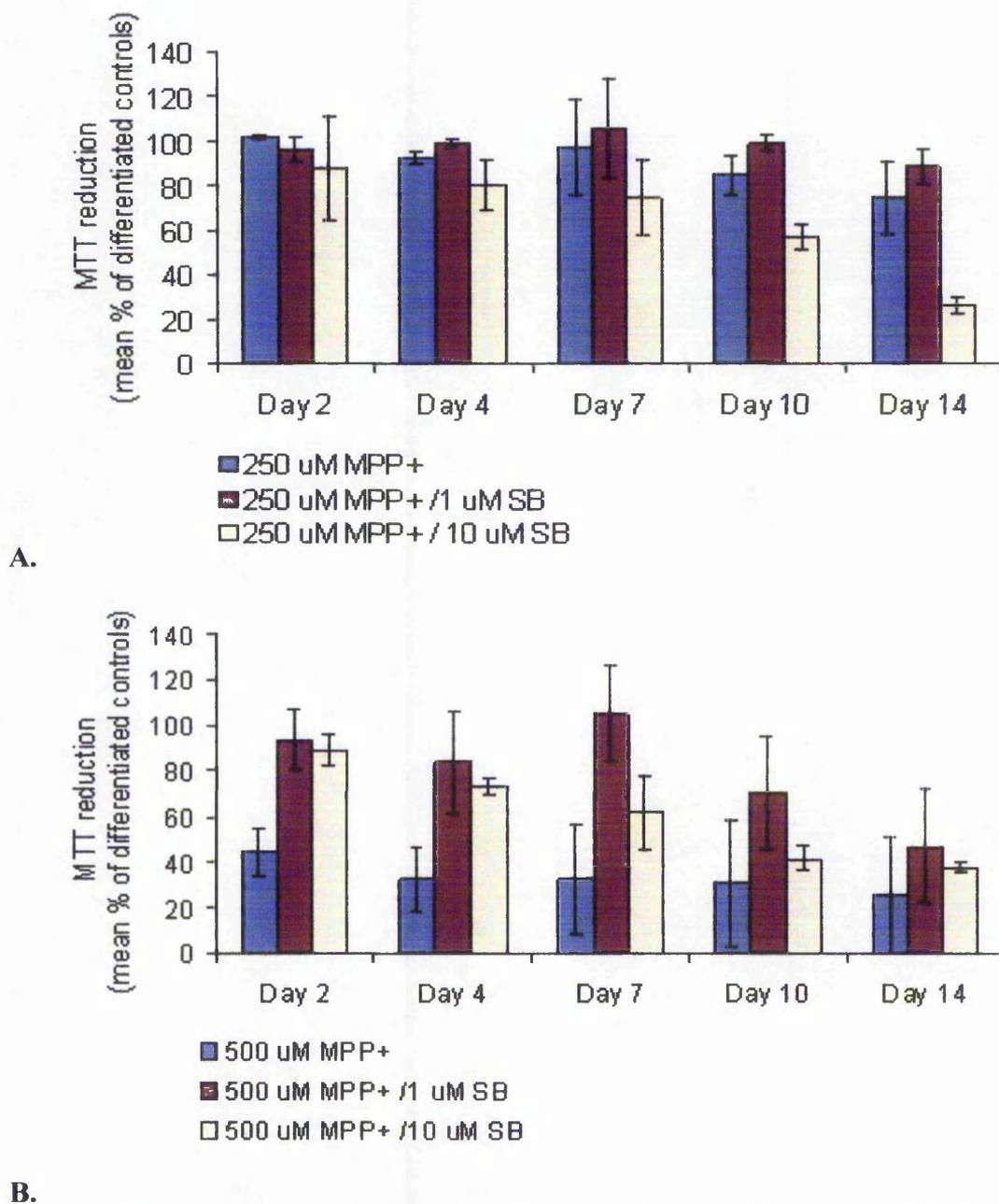
Figure 5.11 Effect of SB202190 on chronic MPP$^+$ exposure.
Cells were seeded into 96 well plates at a density of 5000 cells/well and induced to differentiate over 7 days as detailed in methods section 2.2.1.6. Medium was removed and replaced with fresh differentiating medium supplemented with 250 μM MPP$^+$ (A) or 500 μM MPP$^+$ (B) and SB202190 at final concentrations shown above. At time points indicated, cells were assayed for viability using the MTT reduction assay as detailed in methods section 2.2.3.1. Results are expressed as the mean percentage of differentiated control cells and are combined data from 2 independent experiments (5 replicate wells/treatment in each experiment). The range of the data is shown.

Control

250 μM MPP⁺   250 μM MPP⁺/ 1 μM SB   250 μM MPP⁺/ 10 μM SB

500 μM MPP⁺   500 μM MPP⁺/ 1 μM SB   500 μM MPP⁺/ 10 μM SB

Figure 5.12A Morphological analysis of the effects of SB202190 on 4-day MPP⁺ toxicity.
Cells were induced to differentiate over 7 days in 96 well plates. On day 7 medium was replaced with fresh differentiating medium supplemented with MPP⁺ and SB202190 at the concentrations shown above. Cells were observed by phase contrast microscopy at 200 x magnification. Scale bar represents 40 μm.

Control

250 µM MPP⁺   250 µM MPP⁺/ 1 µM SB   250 µM MPP⁺/ 10 µM SB

500 µM MPP⁺   500 µM MPP⁺/ 1 µM SB   500 µM MPP⁺/ 10 µM SB
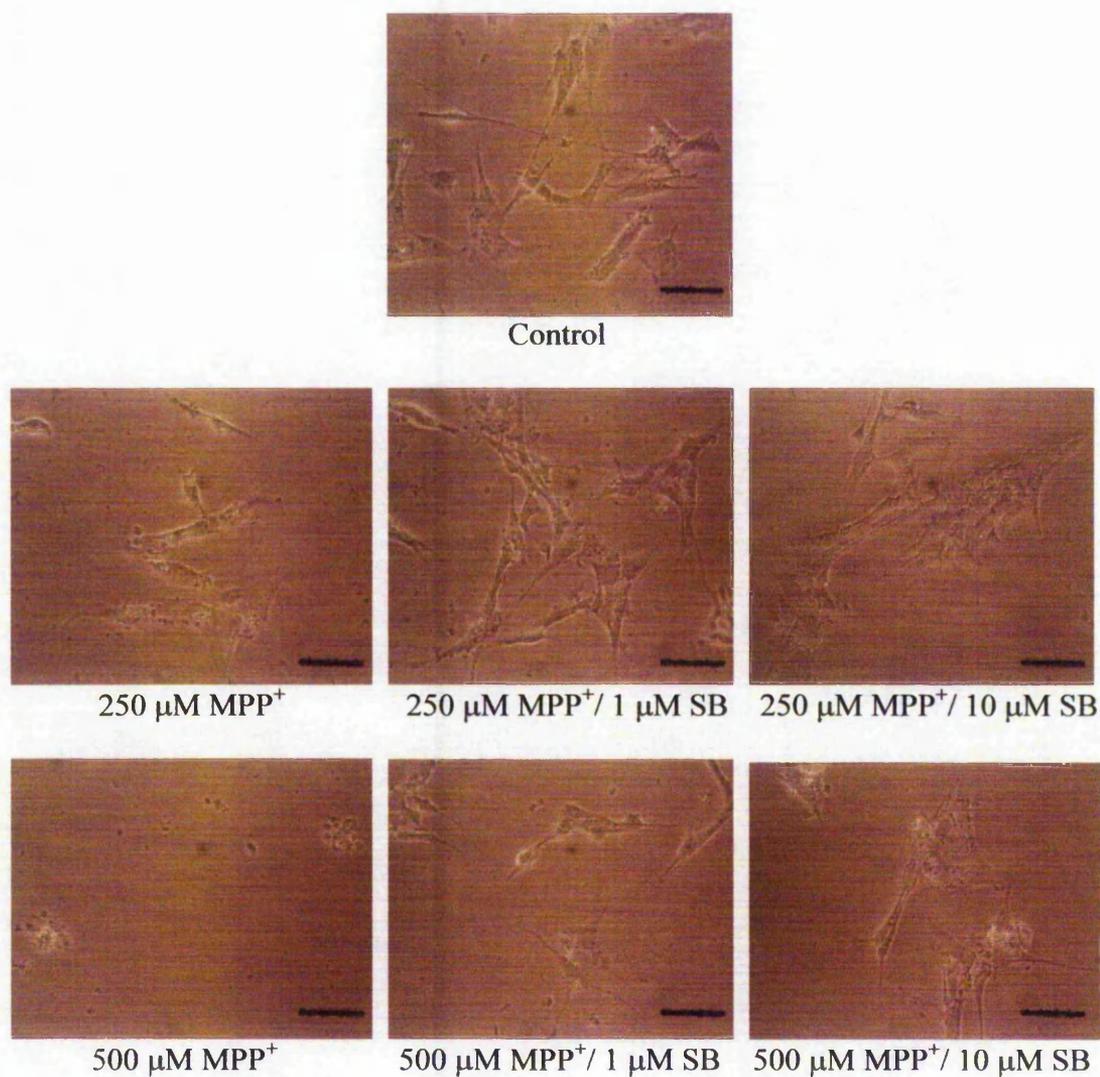
Figure 5.12B Morphological analysis of the effects of SB202190 on 10-day MPP⁺ toxicity.
Cells were induced to differentiate over 7 days in 96 well plates. On day 7 medium was replaced with fresh differentiating medium supplemented with MPP⁺ and SB202190 at the concentrations shown above. Cells were observed by phase contrast microscopy at 200 x magnification. Scale bar represents 40 µm.

5.2.1.3.3   Effect of CEP-11004 on MPP$^+$ toxicity

The presence of CEP-11004 attenuated the cytotoxic effects of 1 mM MPP$^+$ over a 72 h exposure although this was not proven statistically. It should be noted that inhibitor treatment of control cells increased viability by between 5 and 22 % over the range of concentrations tested (Fig 5.6A). However, when corrected for the effect of the inhibitor alone, 1 nM CEP-11004 increased MTT reduction by 20 and 32 % when compared to MPP$^+$ treated cells (assigned a value of 100 %) at 48 and 72 h, respectively.

Following chronic exposure to both 250 and 500 μM MPP$^+$, a preliminary trial suggested that CEP-11004, used at 1 and 10 nM conferred partial protection against MPP$^+$ toxicity as shown in Figure 5.14 when MTT reduction in the presence of the inhibitor was compared to MPP$^+$ treated cells (assigned 100 %) and corrected for the effect of the inhibitor on control cell alone (Fig 5.6B).
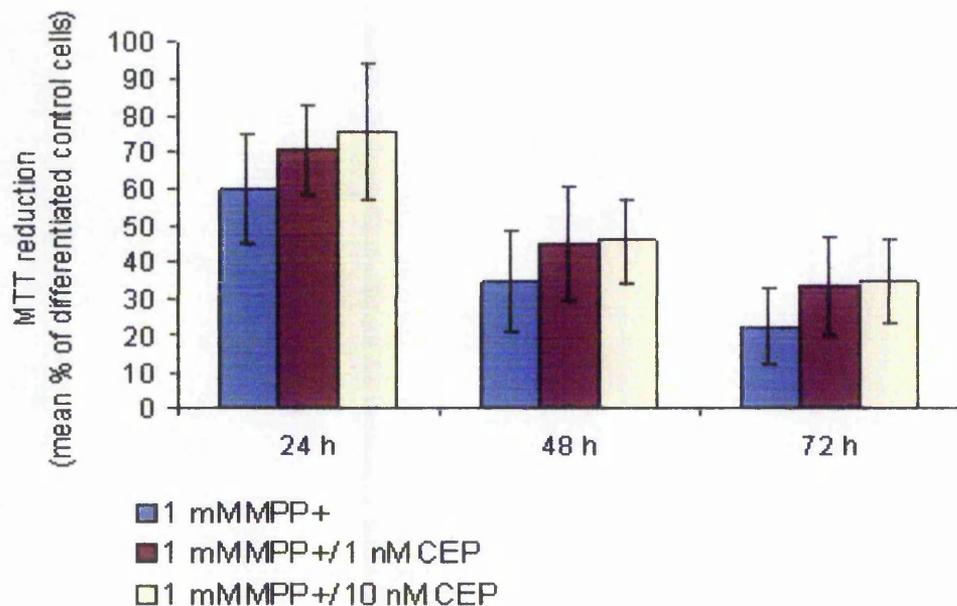
Figure 5.13 Effect of CEP-11004 on MPP$^+$ toxicity over 72 h.
Cells were seeded into 96 well plates at a density of 5000 cells/well and induced to differentiate over 7 days as detailed in methods section 2.2.1.6. Medium was removed and replaced with fresh differentiating medium supplemented 1 mM MPP$^+$ and CEP-11004 at final concentrations shown above. After incubation over 72 h, cells were assayed for viability using the MTT reduction assay as detailed in methods section 2.2.3.1. Results are expressed as the mean percentage of differentiated control cells ± SEM and are combined data from 3 independent experiments (5 replicate wells/treatment in each experiment).

A.

B.
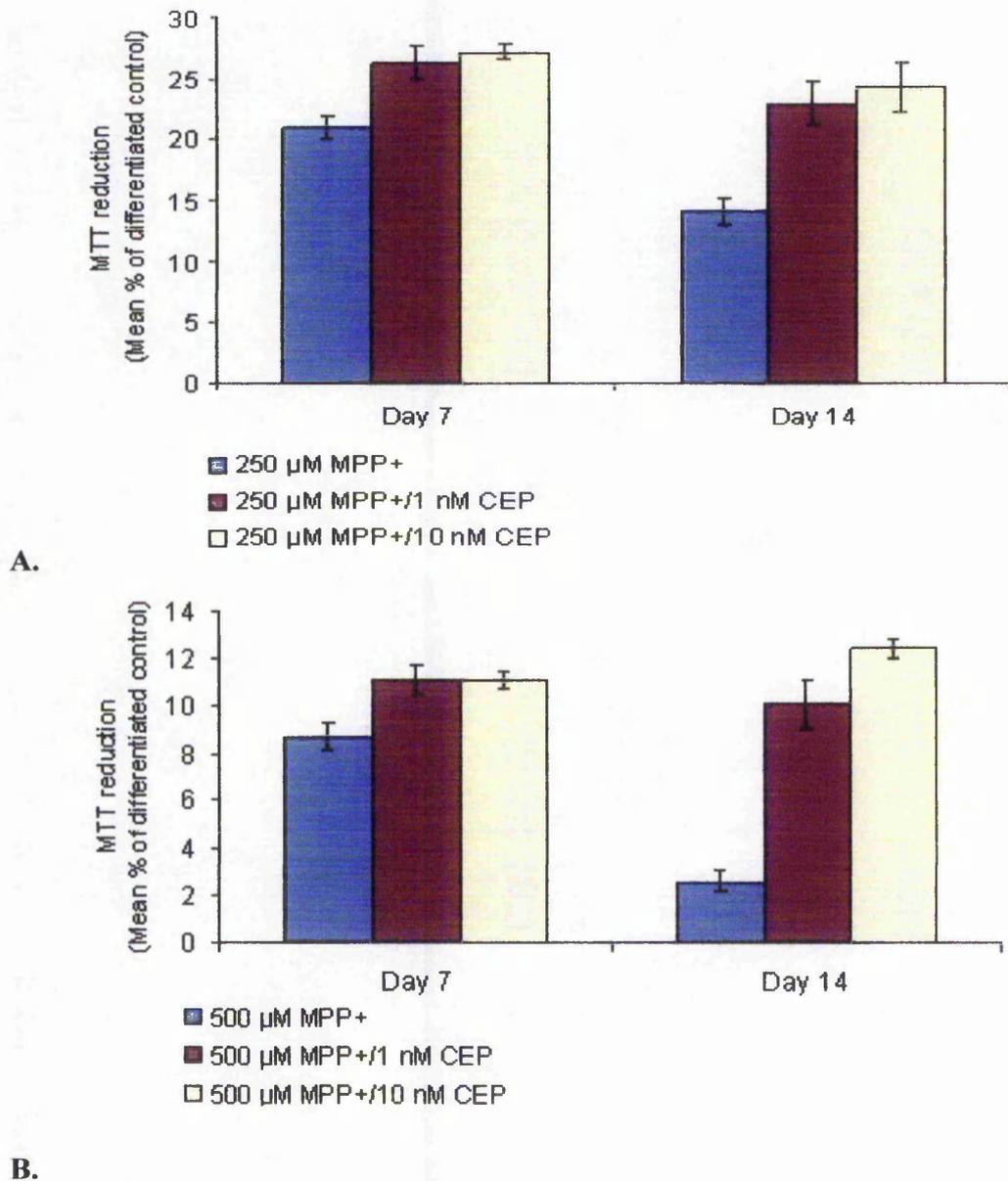
Figure 5.14 Effect of CEP-11004 on chronic MPP$^+$ exposure.
Cells were seeded into 96 well plates at a density of 5000 cells/well and induced to differentiate over 7 days as detailed in methods section 2.2.1.6. Medium was removed and replaced with fresh differentiating medium supplemented with 250 μM MPP$^+$ (A) or 500 μM MPP$^+$ (B) and CEP-11004 at final concentrations shown above. At time points indicated, cells were assayed for viability using the MTT reduction assay as detailed in methods section 2.2.3.1. Results are expressed as the mean percentage of differentiated control cells ± SEM of 5 replicate wells from a single plate.

5.2.2 Effects of a CDK-5 Inhibitor on MPP$^+$ toxicity

A cell permeable, chemical inhibitor of CDK-5, butyrolactone I (BL-1), was used to investigate the effect of CDK-5 inhibition on cells in the presence and absence of MPP$^+$ toxicity. 10 μM BL-1 was reported to significantly reduce laminin-induced CDK-5 activity in differentiated SH-SY5Y cells (Li *et al.,* 2000). Figure 5.15 shows that 1 μM and 10 μM BL-1 induced a dose dependant increase in MTT reduction over 72 h of between 9 and 39 %. Conversely, when titrated over 14 days, 1 μM BL-1 did not increase MTT reduction compared to control cells.

Results suggested that in the presence of 1 mM MPP$^+$, BL-1 conferred protection to cells, although this was not proven statistically. At 24, 48 and 72 h, 1 μM and 10 μM BL-1 attenuated MPP$^+$ toxicity. However, some of this protection was attributable to the effect of BL-1 alone on cells. For example, once the effect of BL-1 alone was corrected for, the increase in viability of 1 mM MPP$^+$ treated cells in the presence of 1 μM BL-1 at 48 and 72 h was from 45 to 71 % and 45 to 65 % of differentiated control cells, respectively. If 1 mM MPP$^+$ is assigned the value of 100 %, the protection afforded by 1 μM BL-1 after correction for the effect of BL-1 alone equates to 87 % and 56 % at 48 and 72 h, respectively. Protection by BL-1 is confirmed by morphological studies in Figure 5.17. Cells are found to be clustering and rounding following MPP$^+$ treatment alone; however, in the presence of BL-1, are healthier and also maintain the axon-like processes.

A differential response to inhibitor treatment, apparently dependent on the degree of MPP$^+$ toxicity, was again observed with 250 and 500 μM MPP$^+$ (see Fig 5.18). BL-1 did not protect cells treated with 250 μM MPP$^+$; indeed 1 μM BL-1 exacerbated toxicity. In contrast, results suggested that 1 μM BL-1 attenuated toxicity induced by 500 μM MPP$^+$ at the day 7 and day 10 time points. However even at 14 days, morphology studies showed that cells appeared healthier when treated with BL-1 in conjunction with 500 μM MPP$^+$ (Fig 5.19).
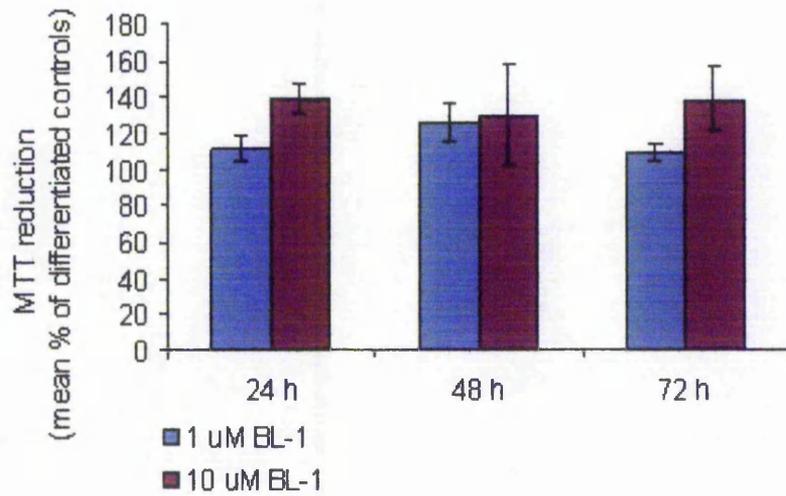
A.
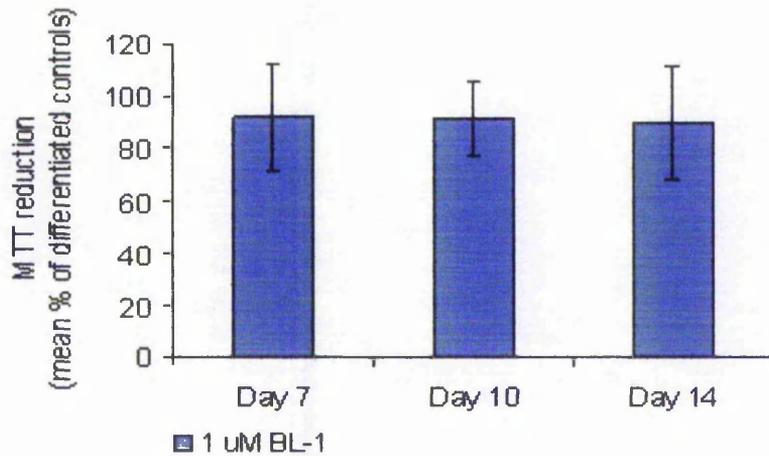
B.

Figure 5.15 Titration of BL-1 in differentiated cells
Cells were seeded into 96 well plates at a density of 5000 cells/well and induced to differentiate over 7 days as detailed in methods section 2.2.1.6. Medium was removed and replaced with fresh differentiating medium supplemented BL-1 at final concentrations shown above. Cells were assayed for viability using the MTT reduction assay as detailed in methods section 2.2.3.1. Results are expressed as the mean percentage of differentiated control cells ± SEM and are combined data from 3 independent experiments (5 replicate wells/treatment in each experiment) (1 µM BL-1) and 2 independent experiments (10 µM BL-1; the range of the data is shown).
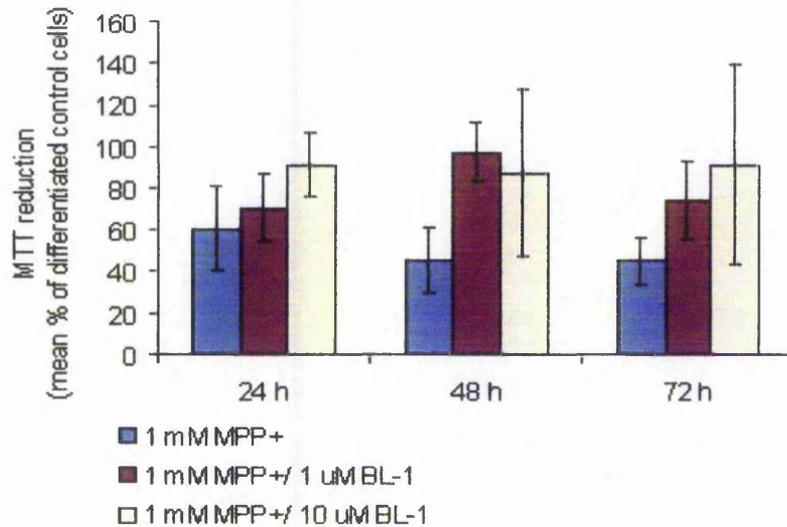
Figure 5.16 Effect of BL-1 on MPP$^+$ toxicity over 72 h.
Cells were seeded into 96 well plates at a density of 5000 cells/well and induced to differentiate over 7 days as detailed in methods section 2.2.1.6. Medium was removed and replaced with fresh differentiating medium supplemented 1 mM MPP$^+$ and BL-1 at final concentrations shown above. After incubation for 24, 48 and 72 h, cells were assayed for viability using the MTT reduction assay as detailed in methods section 2.2.3.1. Results are expressed as the mean percentage of differentiated control cells ± SEM and are combined data from 3 independent experiments (5 replicate wells/treatment in each experiment) (1 µM BL-1) and 2 independent experiments (10 µM BL-1; the range of the data is shown).

48 h

72 h

| Differentiated control cells | 1 mM MPP$^+$ | 1 mM MPP$^+$/ 1µM BL-1 |
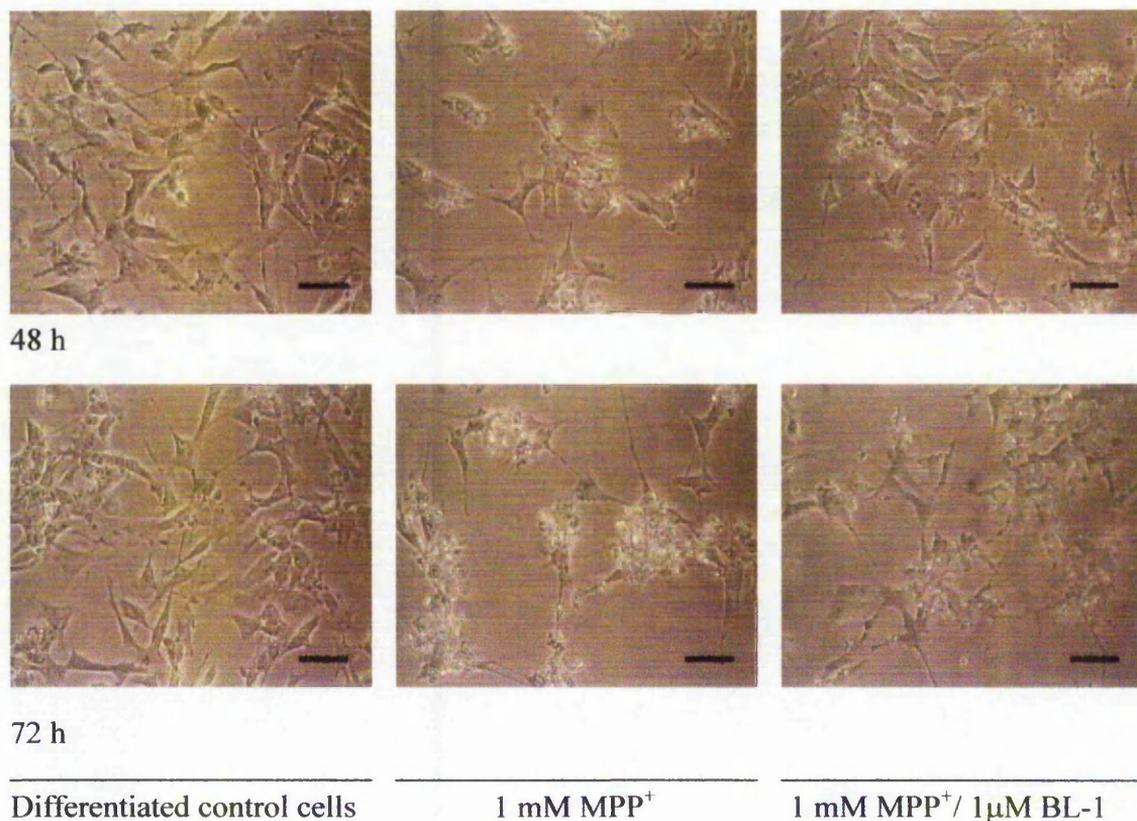
Figure 5.17 Morphological analysis of the effects of BL-1 on short-term MPP$^+$ toxicity.
Cells were induced to differentiate over 7 days in 96 well plates. On day 7 medium was replaced with fresh differentiating medium supplemented with 1 mM MPP$^+$ and 1 µM BL-1. Cells were observed by phase contrast microscopy at 200x magnification. Scale bar represents 40 µm.

A.

B.
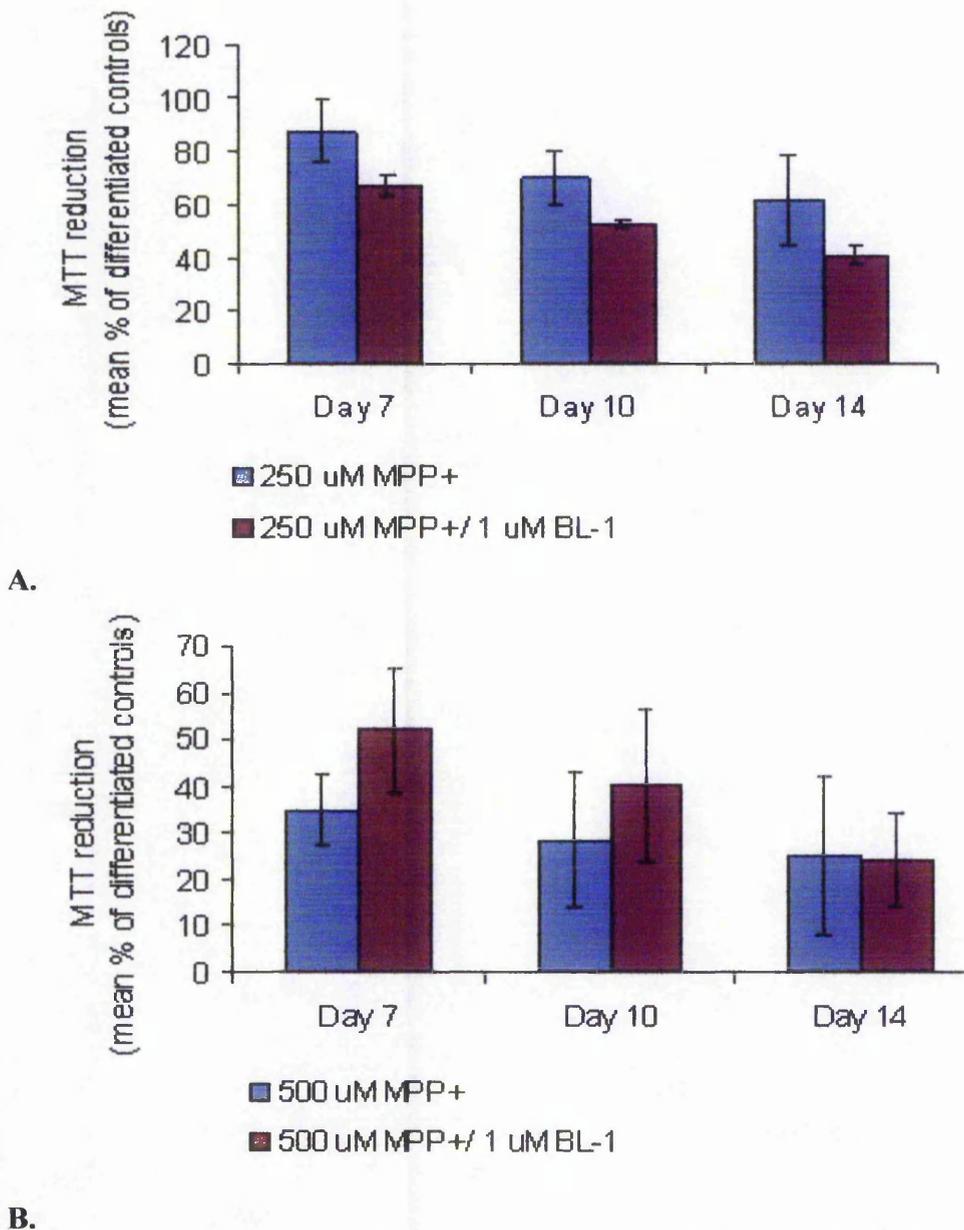
Figure 5.18 Effect of BL-1 on long-term MPP$^+$ exposure.
Cells were seeded into 96 well plates at a density of 5000 cells/well and induced to differentiate over 7 days as detailed in methods section 2.2.1.6. Medium was removed and replaced with fresh differentiating medium supplemented with 250 μM MPP$^+$ or 500 μM MPP$^+$ and BL-1 at final concentrations shown above. At time points indicated, cells were assayed for viability using the MTT reduction assay as detailed in methods section 2.2.3.1. Results are expressed as the mean percentage of differentiated control cells $\pm$ SEM and are combined data from 3 independent experiments (5 replicate wells/treatment in each experiment).

14 days

Differentiated control cells   500 μM MPP⁺   500 μM MPP⁺/ 1 μM BL-1

Figure 5.19   Morphological analysis of the effects of BL-1 on chronic MPP⁺ toxicity.
Cells were induced to differentiate over 7 days in 96 well plates. On day 7 medium was replaced with fresh differentiating medium supplemented with 500 μM MPP⁺ and 1 μM BL-1. Cells were observed by phase contrast microscopy at 200x magnification. Scale bar represents 40 μm.

5.2.2.1 Expression of p35/p25 in differentiated SH-SY5Y cells and following MPP$^+$ exposure

In order to determine the levels of p35 in cells and to investigate whether p35 cleavage had occurred, an antibody raised against the carboxy terminal domain of p35/p25 was used. Attempts to detect p35/p25 were made using cells treated with varying concentrations of MPP$^+$ and separating up to 100 µg protein using SDS-PAGE prior to Western blotting. An example is shown in Figure 5.20. Since exposure to 5 mM MPP$^+$ over 24 h has been found to reduce tTG protein levels, and that this may be attributable to elevated calpain activity (refer to chapter VI, section 6.2.1), it was logical to use this concentration of MPP$^+$ to investigate whether p35 could be cleaved to p25 in this system. However, results repeatedly showed p35 and p25 to be undetectable in both control and MPP$^+$ treated cells. p35/p25 were detectable in a pig brain cytosolic fraction and therefore may suggest that p35 is expressed at a very low level in SH-SY5Y cells.
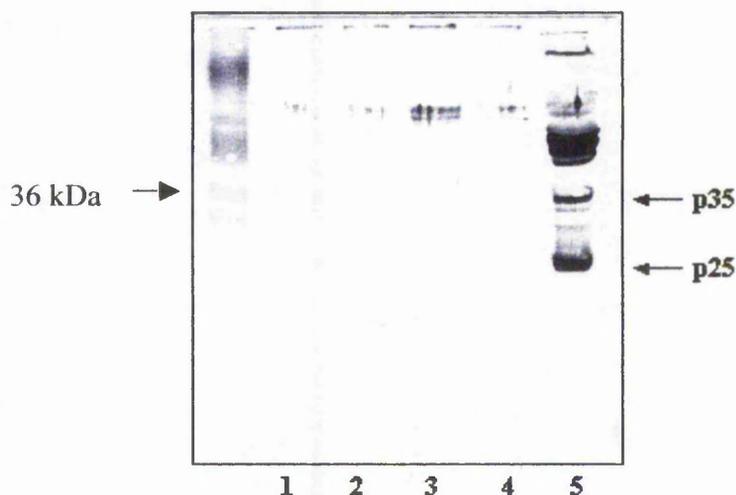
Figure 5.20   Attempts to detect p35/p25 in differentiated and MPP⁺ treated SH-SY5Y cells

Cells were seeded into T25 flasks at 400,000 cells/flask and induced to differentiate over 7 days as detailed in methods section 2.2.1.6. On day 7 medium was removed and replaced with fresh differentiating medium supplemented 1 μM BL-1, 5 mM MPP⁺ or 1 μM BL-1 plus 5 mM MPP⁺. After 24 h cells were extracted as detailed in methods section 2.2.5.1. 100 μg protein was separated on a 12 % acrylamide gel by SDS-PAGE and transferred to nitrocellulose by Western blotting. The nitrocellulose was probed with anti-p35 antibody (1:100) and developed using the alkaline phosphatase method (see methods section 2.2.8.2.3).

Lane 1, differentiated control cells; lane 2, 1 μM BL-1; lane 3, 5 mM MPP⁺; lane 4, 1 μM BL-1 plus 5 mM MPP⁺; lane 5, 100μg pig brain cytosolic fraction.

5.2.2.2   Sub-cellular distribution of p35/p25 proteins following MPP⁺ and proteasome inhibitor treatment

MPP^+ has been shown to raise intracellular calcium levels and to reduce proteasomal activity (Chen *et al.,* 1995; Höglinger *et al.,* 2003). Such effects may induce (a) cleavage of p35 to p25 (Lee *et al.,* 2002) and as a consequence, altered distribution of proteins and (b) accumulation of p35/p25 which would normally be degraded through the proteasome (Patrick *et al.,* 1998, 1999). Since Western blotting and immunoprobing had proven unsuccessful in detecting p35/p25 in SH-SY5Y cells, the anti-p35/p25 antibody was used in conjunction with immunocytochemistry to determine the sub-cellular distribution of p35/p25 proteins following treatment with 1 mM MPP^+, 0.1 μM MG132 or 1 mM MPP^+ in the presence of 0.1 μM MG132.

p35/p25 was detected in cells using immunocytochemistry. In control cells the location of p35/p25 staining appeared mainly within the cytoplasm, extending into axon-like structures, with some being membrane bound. Preliminary results did not suggest that p35/p25 protein was accumulating in response to the treatments of 1 mM MPP^+, 0.1 μM MG132 or following combined MPP^+ plus MG132 treatment over 48 h (see Fig 5.21b, c and d).

FITC   FITC + propidium iodide
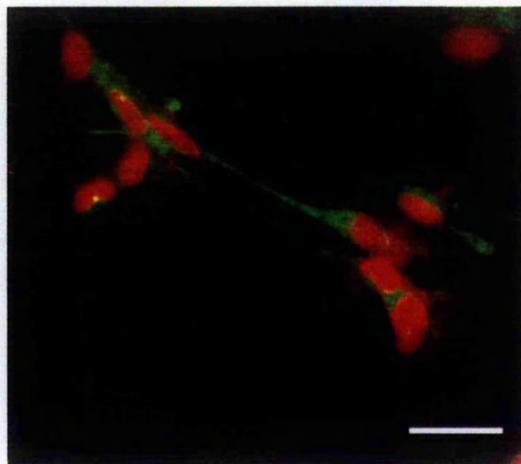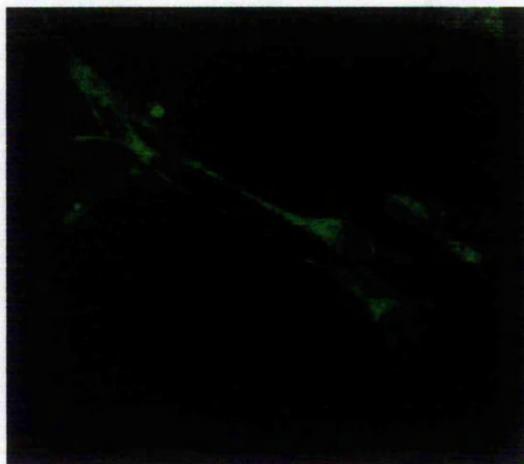
a.   Differentiated cells

b.   0.1 μM MG132

Figure 5.21

FITC   FITC + propidium iodide

c. 1 mM MPP$^+$

d. 1 mM MPP$^+$ plus 0.1 μM MG132

Figure 5.21 Distribution of p35 protein following 48 h exposure to 1 mM MPP$^+$ ± proteasomal inhibitor.
Cells were differentiated in permanox chamber slides over 7 days. Medium was removed and replaced with fresh differentiating medium or medium supplemented with 1 mM MPP$^+$, 0.1 μM MG132 or 1mM MPP$^+$ plus 0.1 μM MG132. After 48 h cells were fixed and permeabilised and immunocytochemistry performed as detailed in methods section 2.2.9. Cells were probed with anti-p35 antibody (1:20). Cells were protected using Vectorshield mounting medium containing propidium iodide (shown overlaid with the FITC stain on the right of each panel). Analysis was performed by confocal microscopy at x 400 magnification. Scale bar represents 20 μm.

5.3   DISCUSSION

5.3.1   Conflicting roles of MEK and p38 inhibitors against MPP$^+$ toxicity

In this study, treatment of pre-differentiated SH-SY5Y cells with the MEK inhibitor, PD98059, induced cell death in a concentration dependent manner, suggesting that the ERK pathway is indeed required for cell survival. However, following MPP$^+$ exposure, cell viability was differentially affected by co-treatment with PD98059. This trend was observed in 2 independent experiments and combined data was presented in Fig 5.9. The extent of toxicity induced by MPP$^+$ appeared to determine whether PD98059 conferred protection to cells. This is an important observation since differences in the effects of MAPK inhibitors on MPP$^+$ toxicity are observed between studies as detailed in the introduction to this chapter (section 5.1). These findings suggest that a threshold exists whereby the ERK pathway, most likely in conjunction with other pathways, changes its influence on cell survival.

It can be noted that in Fig 5.7A the toxicity induced by 1 mM MPP$^+$ over 24 h is comparable to that induced by 250 µM MPP$^+$ over 14 days (up to 40 % reduction in cell viability), where ERK is likely to be pro-survival in both cases. ERK was also a pro-survival signal in the study by Halvorsen *et al*, (2002) where 5 mM MPP$^+$ reduced cell viability by 25 %. Conversely the toxicity induced by 1 mM MPP$^+$ in Fig 5.7B, and following exposure to 500 µM MPP$^+$ over 14 days, was greater (between 60 and 100 % reduction in cell viability). This suggests that the degree of toxicity induced by MPP$^+$, irrespective of the exposure time, may have been an important factor in determining the role of ERK in this toxin paradigm. The variability of SH-SY5Y cells to MPP$^+$ toxicity has been discussed. It is interesting that whilst 2 independent experiments were performed where the same trend was noted, cells were less sensitive to MPP$^+$ in the second experiment, which caused approximately 10 % and 50 % reduction in viability following exposure to 250 and 500 µM, respectively. In both instances described, the difference in viability of cells protected by the inhibitor and cells in which the presence of the inhibitor was detrimental was approximately 40 %. Hence it may be hypothesised that within this window, the inhibitor would have no effect on cell viability. This is demonstrated

when the results from the 2 independent experiments are combined and presented as a scatter plot (Fig 5.22). Further trials would confirm this concept. In support of this hypothesis, Crossthwaite *et al,* (2002) demonstrate that stimulus strength (concentration of H_2O_2) in primary cortical neurones was important in determining the outcome of MAPK signal activation. Stanciu *et al,* (2002) provide evidence in HT22 mouse hippocampal cells, that glutamate induced oxidative stress and MG132-mediated proteasome inhibition induce ERK activation, inhibition of which promotes cell survival. Of interest was that activated ERK was persistently retained in the nucleus. The study proposed that changes in compartmentalisation of activated ERK, possibly via effects on an anchor protein for ERK or inactivation of a phosphatase otherwise required for de-phosphorylation of ERK and removal from the nucleus, could establish ERK as pro-apoptotic signal.

Correlation coefficients

	MPP+	0.1 uM PD	1 uM PD
MPP+	1		
0.1 uM PD	0.8375	1	
1 uM PD	0.9426	0.9267	1
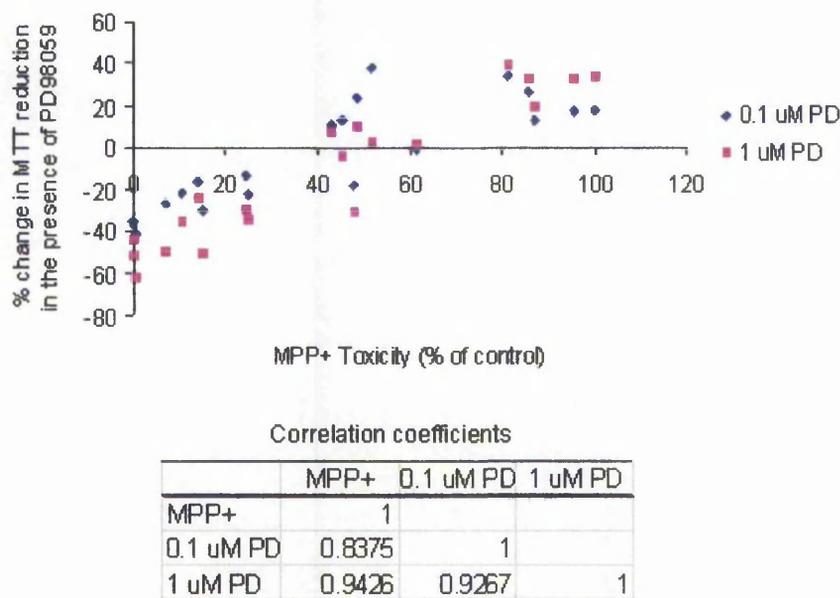
Figure 5.22 Differential effects of PD98059 on cell viability following MPP⁺ exposure.
Viability of cells following exposure to MPP⁺ (250 and 500 µM) and MPP⁺ plus PD98059 (0.1 and 1 µM) was assessed at 5 time points over 14 days using the MTT reduction assay. Results shown are pooled data from 2 independent experiments. The viability of cells in the presence of MPP⁺ and MPP⁺ plus PD98059 was expressed as a % of differentiated control cells (assigned 100 %). Results are plotted as a scatter plot to show degree of toxicity versus % change in MTT reduction (as a % of differentiated control) in the presence of PD98059. Correlation coefficients were performed to indicate correlation between treatments.

There is conflicting evidence regarding the role of the p38 pathway following cellular stress (Mielke and Herdegen, 2000). Incubation of cells with MPP$^+$ in the presence of the SB202190 evoked differential effects on cell viability. The same trend was observed as for PD98059 whereby 2 independent experiments demonstrated that the presence of the inhibitor exacerbated short-term toxicity induced by 1 mM or chronic toxicity following 250 μM MPP$^+$. However SB202190 conferred protection to cells treated with 500 μM MPP$^+$ for 2 days and beyond. This differential effect of SB202190 depending on the degree of MPP$^+$ toxicity is presented as scatter plot in Fig 5.23. Halvorsen *et al*, (2002) demonstrated that treatment with SB203580 alone reduced viability of cells and exacerbated toxicity in the presence of 5 mM MPP$^+$. Of interest is again the observation that the apparent pro-survival role of the p38 pathway in the study by Halvorsen *et al*, (2002) occurs at a level of MPP$^+$ toxicity that correlates with the study presented in this thesis.

An important point to note is that in this study, incubation of cells with SB202190 during the differentiation time course resulted in increased ERK phosphorylation correlated with increased neuritogenesis (results not shown). Previous studies with the related compound, SB203580 extensively document this effect (Hall-Jackson *et al.*, 1999; Kalmes *et al.*, 1999). The fore-mentioned studies unanimously propose that SB203580 activates serine/threonine kinase, Raf-1, independent of inhibition of p38. This effect was not prevented by inhibition of MAPK, PKC or PI3-K pathways (Hall-Jackson *et al.*, 1999). An alternative and novel p38α inhibitor, NPC31169 (Ohashi *et al.*, 2004) also induced the same effect in a rat model of renal disease. Whilst an explanation for the differential effects of SB202190 on MPP$^+$- induced toxicity is presently unknown, it seems likely that at least some of the effects exerted by SB202190 were due to effects on the p38 pathway.
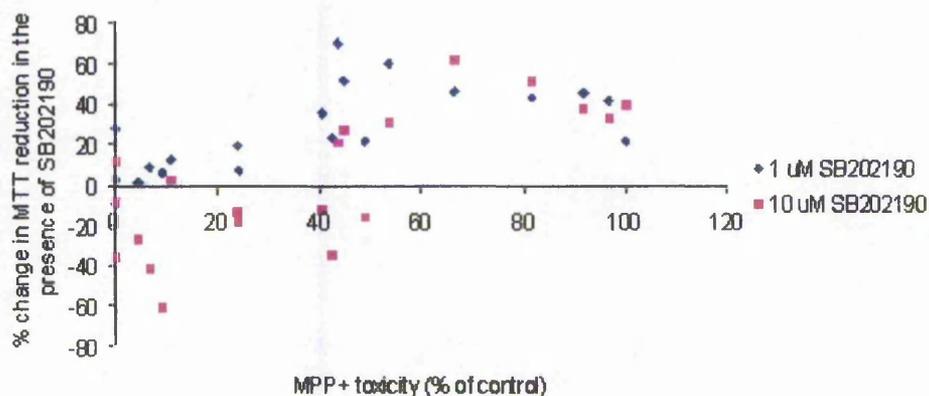
Correlation Coefficients

	MPP+	1 uM SB	10 uM SB
MPP+	1		
1 uM SB	0.6277	1	
10 uM SB	0.7390	0.6831	1

Figure 5.23 Differential effects of SB202190 on cell viability following MPP$^+$ exposure.

Viability of cells following exposure to MPP$^+$ (250 and 500 μM) and MPP$^+$ plus SB202190 (1 and 10 μM) was assessed at 5 time points over 14 days using the MTT reduction assay. Results shown are pooled data from 2 independent experiments. The viability of cells in the presence of MPP$^+$ and MPP$^+$ plus SB202190 was expressed as a % of differentiated control cells (assigned 100 %). Results are plotted as a scatter plot to show degree of toxicity versus % change in MTT reduction (as a % of differentiated control) in the presence of SB202190. Correlation coefficients were performed to indicate correlation between treatments.

5.3.2 CEP-11004 confers protection against short-term and chronic exposures to MPP$^+$

MPTP activates mitogen activated protein kinase kinase 4 (MKK4) and JNK in the substantia nigra and striatum of mice (Saporito *et al.*, 2000). Inhibition of JNK has been unanimously reported to attenuate MPTP/MPP$^+$ toxicity (Saporito *et al.*, 1999, 2000; Xia *et al.*, 2001; Wang *et al.*, 2004; Mathiasen *et al.*, 2004), and was also the case in this thesis where a compound related to CEP-1347, (CEP-11004, KT8138, also reported to inhibit JNK at the level of MLKs [Hidding *et al.*, 2002; Fu *et al.*, 2003]) was employed. CEP-11004 alone had no detrimental effect on the viability of

pre-differentiated SH-SY5Y cells. Over a short time course of 72 h CEP-11004 attenuated MPP$^+$ toxicity, further trials are required to confirm that this attenuation of toxicity was significant. Over an extended MPP$^+$ exposure of up to 14 days, preliminary studies also suggested that CEP-11004 might confer protection. Further trials would confirm this effect. Whilst a recent study has shown that CEP-1347 attenuated MPP$^+$ toxicity in differentiated SH-SY5Y cells, the concentration of MPP$^+$ was relatively high (3 mM) and duration of exposure to MPP$^+$ was only 48 h (Mathiasen *et al.,* 2004). Additionally, although cells were pre-differentiated, retinoic acid was removed from the media prior to treatment with MPP$^+$. Also cells were pre-incubated with CEP-1347 before addition of MPP$^+$. The data presented here are therefore novel given that cells were pre-differentiated and maintained in differentiation media whilst being exposed to MPP$^+$ and CEP-11004 simultaneously. Additionally the time course over which the effects of CEP-11004 on MPP$^+$ induced toxicity were investigated was greatly extended.

The mechanism by which CEP-11004 attenuated MPP$^+$ toxicity was most likely via inhibition of MLK. It has been reported that CEP-1347 plays no role in prevention of MPP$^+$ mediated inhibition of mitochondrial complex I in SH-SY5Y cells (Mathiasen *et al.,* 2004). According to Maroney *et al,* (1998) CEP-1347 had no effect on ERK 1 activity in rat motorneurones. Similarly it was reported that CEP-1347 did not activate PI3-K or ERK pathways in primary sympathetic neurones deprived of NGF, despite preservation of neurones (Harris *et al.,* 2002). In my laboratory, no effect of CEP-11004 was observed on ERK phosphorylation using N2a cells (De Girolamo, personal communication). On the contrary there is some evidence that CEP-11004 additionally activates ERK. Indeed it was noted in results chapter III (Figure 3.10) of this study, that cells induced to differentiate in the presence of CEP-11004 exhibited increased neuritogenesis compared to control cells and that ERK phosphorylation, at the same time point, was also elevated. Additionally Roux *et al,* (2002), reported that CEP-1347 phosphorylates Akt and ERK in primary mouse cortical neurones under conditions where MLK 3 was inhibited, via a MLK 3 independent, Src dependant mechanism since treatment with CEP-1347 in the presence of PP1, a Src family inhibitor, blocked ERK activation. Interestingly the authors noted that maintaining cells in low serum enhanced ERK phosphorylation by CEP-1347.

5.3.3 Selective CDK-5 inhibitor (Butyrolactone I) confers protection against MPP$^+$ toxicity

The effect of BL-1 (CDK-5 inhibitor) on the viability of cells treated with MPP$^+$ was assessed over short-term (72 h) and chronic (14-day) exposures. CDK-5 has been found to mediate loss of dopaminergic neurones in an *in-vivo* mouse MPTP model (Smith *et al.,* 2003). In addition, MPTP was reported to increase both CDK-5 expression and also activity, as measured by tau phosphorylation and *in-vitro* kinase assays following CDK-5 immunoprecipitation. CDK-5 activity, but not expression, was attenuated by treatment with flavopiridol, (a general CDK inhibitor). The data presented in this thesis is the first to utilise a human *in-vitro* model with a more selective CDK-5 inhibitor to study neuroprotective effects in the presence of MPP$^+$. Over 72 h, BL-1 conferred protection against treatment of cells with 1 mM MPP$^+$ although further trials are required to confirm that this attenuation of toxicity is significant. In addition, 1 µM BL-1 conferred a degree of protection to cells treated with 500 µM MPP$^+$ over 10 days. Furthermore the morphology of cells treated with 500 µM MPP$^+$ was improved following BL-1 treatment over 14 days.

The mechanism by which a CDK-5 inhibitor may promote survival in an *in-vitro* MPP$^+$ model remains to be deciphered. However a number of credible hypotheses exist. De-regulation of nuclear CDK-5 is particularly significant since CDK-5 has access to a host of transcription factors that can influence neuronal survival and development, an important example of which is Myocyte enhancer factor 2 (MEF-2). MEF-2 (encoded by four genes; MEF-2A, MEF-2B, MEF-2C and MEF-2D) is a member of the MADS (MCM1-agamous-deficiens-serum response factor) family of transcription factors. All four genes are expressed in neuronal cells giving rise to alternatively spliced transcripts (reviewed by Okamoto *et al.,* 2000; Li *et al.,* 2001; Gong *et al.,* 2003). Neuronal differentiation and survival is associated with phosphorylation/activation of the MEF-2 carboxy-terminal transactivation domain by kinases including p38 (Okamoto *et al.,* 2000) and ERK 5 (Kato *et al.,* 1997). However reports show that hyperphosphorylation of MEF-2 at distinct sites by alternative kinases can reduce MEF-2 activity. Significantly, Gong *et al,* (2003) show that both oxidative stress induced by H_2O_2 and excitotoxicity induced by

225

glutamate in cortical neurones increased CDK-5 activity causing CDK-5 dependant phosphorylation of MEF-2 isoforms at distinct, identified serine residues. This resulted in reduction in MEF-2 activity, causing cell death. Effects were blocked by the CDK-5 inhibitor, rescovitine and by co-transfection with CDK-5/p25 and a constitutively active form of MEF-2. The down-stream consequences of aberrant MEF-2 phosphorylation that promote cell death remain to be fully resolved but may involve caspases (Gong et al., 2003; Li et al., 2001). Hence it may be hypothesised that MPP^+, through mechanisms of oxidative stress and excitotoxicity may activate CDK-5 resulting in MEF-2 phosphorylation (and potentially other survival factors) and disruption of survival pathways.

As previously described, conversion of p35 to p25 results in an inappropriate "gain of function" of the CDK-5/p25 complex, causing disruption and hyper-phosphorylation of numerous substrates, including cytoskeletal proteins that have been linked to neurodegenerative disease (Patrick et al., 1999; Nguyen et al., 2001; Hashiguchi et al., 2002). Smith et al, (2003) reported that increased levels of p25 were found in the substantia nigra of mice following MPTP treatment. Studies show that both the CDK inhibitor, flavopiridol (Smith et al., 2003) and calpain inhibition (Crocker et al., 2003) significantly improved the hypo-locomotive state induced by MPTP in mice and also prevented degeneration of nigral DA neurones. These observations were not associated with improved striatal DA levels or DA turnover but were found to improve existing striatal circuitry; expression of the early intermediate gene, encoding delta FosB, (a marker of basal ganglion circuitry that is up-regulated by MPTP in response to dopaminergic denervation) was attenuated. Also calpain inhibition was found to prevent MPTP induced up-regulation of neurotensin, a neuropeptide suggested to antagonise DA neurotransmission (reviewed by Crocker et al., 2003). These findings are particularly significant given that CDK-5 levels and calpain activity are elevated in the PD brain (Brion and Couck, 1995; Crocker et al., 2003).

Preliminary investigations have found that p35 could not be detected in SH-SY5Y cells by Western blotting; it is as yet unclear why p35 protein could however be detected using immunocytochemistry. Detection of this protein may benefit from immunoprecipitation methods. 1 mM MPP^+ did not induce accumulation of p35 in

pre-differentiated cells. Gong *et al,* (2003) report that H_2O_2 induced oxidative stress in rat cortical neurones increased CDK-5 activity but did not affect p35 expression levels. Hence low protein levels in control cells may not be up-regulated following MPP^+ treatment. It has been shown in my laboratory using mitotic SH-SY5Y cells that 1 mM MPP^+ inhibits the proteasome by only 10-20 % over 48 h. Hence the concentration of MPP^+ may not have been high enough to detect p35 accumulation due to insufficient proteasomal inhibition. However, MG132, employed at a concentration that was shown to inhibit the proteasome, also failed to induce accumulation of p35. Clearly, further work is required to establish the effects of MPP^+ on p35/p25 expression/activity in this system.

An overview of the potential effects of MPP^+ on CDK-5 and subsequent downstream *in-vitro* neurotoxic events is given in Figure 5.24 whilst a summary of the effects of MAPK and CDK-5 inhibitors on MPP^+ toxicity is given in table 5.1.
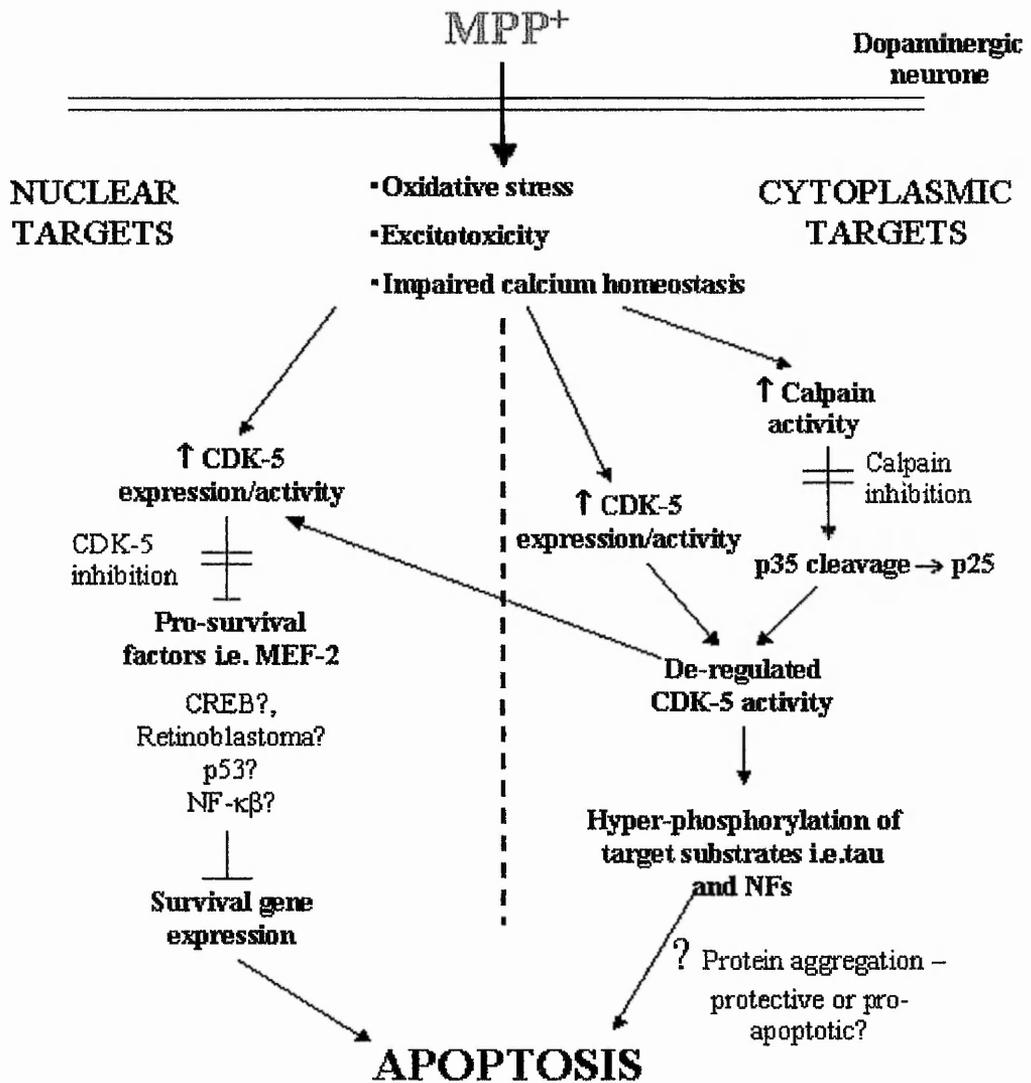
Figure 5.24   Proposed mechanism of CDK-5 mediated neurotoxicity following MPP$^+$ treatment (taken from Gong *et al.*, 2003, with modifications).

MPP$^+$ may mediate neurotoxicity via increased/de-regulated CDK-5 activity through nuclear and cytoplasmic pathways culminating in suppression of survival genes and hyper-phosphorylation of target protein substrates.

	Concentration of MPP$^+$ / exposure time		
Inhibitor	1 mM MPP$^+$, 72h	250 μM MPP$^+$, 14 days	500 μM MPP$^+$, 14 days
PD98059	Pro-death	Pro-death	Pro-survival
SB202190	Pro-death	Pro-death	Pro-survival
CEP-11004	Pro-survival	Pro-survival?	Pro-survival?
BL-1	Pro-survival	Pro-death	Pro-survival?

Table 5.1 Summary of the pro-survival or pro-death effects of MAPK/CDK-5 inhibitors when used in conjunction with MPP$^+$ over a short time course (72 h) or 14 days.

In conclusion, inhibitors of MLK and CDK-5 confer protection to MPP$^+$ treated cells. Inhibitors of p38 and MEK can reduce MPP$^+$ toxicity but in a manner that is dependent on the degree of toxicity that is exerted on cells; hence their role in cell survival in this system is more difficult to ascertain. Also many potential differences between cell culture systems, for example whether mitotic or differentiated, the nature of the stress and time of exposure to that stress, may to some extent, account for anomalies between studies. The fact that no one inhibitor can fully rescue cells from MPP$^+$ toxicity supports the concept that signalling pathways operate in complex manner to determine the ultimate fate of a cell. It should be noted that the degree of toxicity induced by a particular concentration of MPP$^+$ was variable between experiments. It light of the results presented in this thesis suggesting that the degree of toxicity is an important determinant in MAPK signalling, it is therefore particularly important to analyse individual data sets with due care. Significantly this is the first study to demonstrate protection in pre-differentiated SH-SY5Y cells using MAPK inhibitors following an extended MPP$^+$ time course of up to 14 days. Likewise, this study is the first to investigate the effects of a more selective CDK-5 inhibitor in a human cell system. These results provide a platform on which to further investigate the neuroprotective mechanisms of MAPK/CDK-5 inhibitors in a pre-differentiated cell system over a chronic MPP$^+$ time course, which may provide greater analogy to neurones *in-vivo*.

CHAPTER VI

INVESTIGATING THE ROLE OF TISSUE TRANSGLUTAMINASE IN MPP$^+$ TOXICITY

6.1 INTRODUCTION

6.1.1 The role of tTG expression/activity in cell survival/death

tTG is endogenously expressed in the CNS where it contributes to neural development, function and regeneration (for review see Lesort *et al.,* 2000a). The multi-functionality of tTG no doubt contributes to its complex involvement in cellular function. As such, a major line of investigation relates to the role of tTG in cell survival and death pathways. As described in chapter III, tTG activity is necessary and sufficient to differentiate SH-SY5Y cells (Tucholski *et al.,* 2001) and tTG is evidently pro-survival in this process given its activation by PI3-K (Antonyak *et al.,* 2002). Indeed studies suggest that tTG confers a protective effect during retinoic acid induced differentiation (Antonyak *et al.,* 2001; 2002). Several studies implicate tTG expression/activity following neuronal insult both *in-vivo* and *in-vitro* but the role of tTG in terms of cell death or survival is not easy to decipher. tTG expression is elevated following spinal cord injury (Festoff *et al.,* 2002), and traumatic brain injury (Tolentino *et al.,* 2002). Interestingly both fore-mentioned studies report up-regulated expression of the normal long tTG (L) isoform and also a short non-GTP regulated tTG (S) transcript, proposed to contribute to apoptotic pathways via its ability to be activated at lower Ca^{2+} concentrations. Significantly tTG(S) mRNA levels were found to exceed tTG(L) levels in extracts from Alzheimer's disease brains (Citron *et al.,* 2001). Over-expression of tTG in SK-N-BE cells was sufficient to increase spontaneous apoptosis and also to prime cells for subsequent apoptotic stimuli (Piredda *et al.,* 1999). Furthermore tTG over-expression was shown to disrupt mitochondrial homeostasis by inducing hyper-polarisation of the inner membrane, in the absence of changes in ATP levels, thus promoting commitment of cells to apoptosis (Piacentini *et al.,* 2002). Importantly, the ability of tTG to modulate apoptotic pathways reportedly depends greatly on the type of stimulus and, more specifically, its transamidating activity, which was shown to modulate apoptosis in the absence of changes in tTG expression (Tucholski and Johnson, 2002).

6.1.2   The role of tTG in neurodegeneration

The ability of tTG to catalyse the formation of insoluble protein-protein cross-links has led to its implication in neurodegenerative conditions where insoluble inclusions characterise disease pathology, including Alzheimer's Disease (Tucholski *et al.,* 1999), Huntington's Disease (Chun *et al.,* 2001) and Parkinson's Disease (Junn *et al.,* 2003). Of significance is that many proteins found to contribute to such aggregates are substrates for tTG. tTG is up-regulated in Alzheimer's Disease brains and localises with tau proteins in neurofibrillary tangles, which are highly insoluble intra-cytoplasmic inclusions (Tucholski *et al.,* 1999). Grierson *et al.,* (2001) reported that three human tau isoforms and NF-L, -M and -H chain proteins were cellular substrates for tTG. Junn *et al.,* (2003) reported that tTG can mediate α-synuclein aggregation *in-vitro* and, significantly, tTG catalysed ε(γ-glutamyl)-lysine cross-links were found in the halo of Lewy bodies, co-localised with α- synuclein, in Parkinson's disease and dementia with Lewy bodies. Since very few studies have explored the link between tTG and Parkinson's disease, further investigation into the role of this enzyme in death pathways in models of this disease may prove useful.

The role of tTG in neurodegeneration is augmented by its dependence on calcium for activation. Raised intracellular calcium levels and oxidative stress are contributory factors of neurodegenerative disease and MPP$^+$ toxicity (discussed in chapter I, section 1.3). In Swiss 3T3 fibroblasts, ROS production (in response to lysophosphatidic acid and transforming growth factor-β) was essential for the induction of tTG activity, which was consequently inhibited by ROS scavengers (Lee *et al.,* 2003). Additionally it was proposed that ROS induced activation of tTG in this system was mediated by an increase in intracellular calcium. Conversely Piacentini *et al.,* (2002) demonstrate in SK-N-BE cells that tTG over-expression resulted in increased ROS formation.

6.1.3   *In-vitro* methods employed to measure tTG activity

Consideration was given to a suitable methodology for measuring tTG activity in cells. *Zhang et al.,* (1998a) employ three different methods, none of which are specific for tTG since they measure overall TG activity. The first, and most commonly used method is an *in-vitro* radioactive incorporation assay in which [^{3}H] putrescine becomes incorporated into protein by TG. Proteins incorporating [^{3}H] putrescine are then precipitated from cell extracts; the extent of incorporation, which reflects the level of TG activity, is determined by liquid scintillation counting. An alternative assay involves *in-situ* incorporation of 5-(biotinamido) pentylamine, a pseudo-substrate for TG, which can be determined by an Enzyme Linked Immunosorbant Assay (ELISA). Following incubation with 5-(biotinamido) pentylamine, cells are harvested, lysed and homogenate protein coated onto plates. Proteins into which 5-(biotinamido) pentylamine had been incorporated are revealed by addition of HRP-conjugated streptavidin followed by HRP substrate and measurement of product spectrophotometrically. Both *in-vitro* and *in-situ* assays offer an advantage in that TG activity can be easily quantified using either method. The third method (which has subsequently been used in this project, with modifications) also involves *in-situ* incorporation of 5-(biotinamido) pentylamine, followed by electrophoretic separation and subsequent detection of individual proteins into which 5-(biotinamido) pentylamine has become incorporated.

6.1.4   Aims of chapter

The purpose of this chapter was to establish whether tTG has a role in MPP⁺ toxicity. Expression/distribution of tTG protein was analysed using Western blotting and immunoprobing and imunocytochemical techniques. TG activity in response to MPP⁺ toxicity was subsequently assessed. Finally, TG and tTG-specific inhibitors were employed in conjunction with viability assays in an attempt to establish the role of tTG in MPP⁺ mediated toxicity.

6.2   RESULTS

6.2.1   Changes in tTG expression following MPP$^+$ exposure

Changes in tTG expression were analysed following MPP$^+$ treatment over 24 h. This work employed the anti-transglutaminase II (clone CUB-7402) antibody. Figure 6.1 indicates that a 24 h exposure to 1 mM and 5 mM concentrations of MPP$^+$ caused a significant reduction in tTG expression. Immunocytochemistry was performed to confirm this change in expression and to determine the sub-cellular distribution of tTG in MPP$^+$ treated cells. In Figure 6.2 cells were fixed in methanol prior to permeabilisation using Triton. Immunocytochemical analysis shows that tTG staining in differentiated cells was generally punctate and was present throughout the cell body and axon-like processes, whilst low level staining was present in the nucleus (Fig 6.2a). However, the staining pattern of tTG following MPP$^+$ exposure appears to localise predominantly around the nucleus (Fig 6.2 b and c).
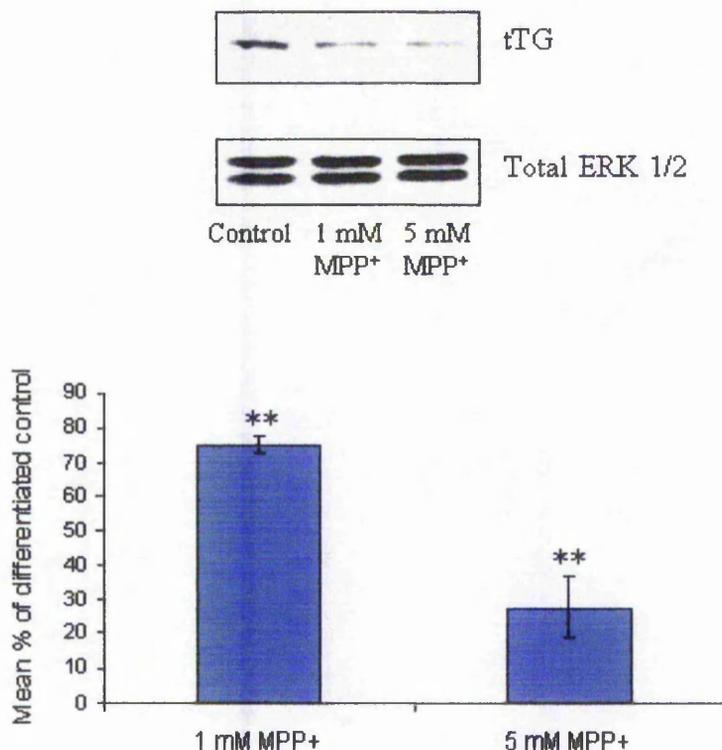
Figure 6.1   Assessment of tTG expression following MPP⁺ treatment.
Cells were seeded into T25 flasks at 400,000 cells / flask and differentiated for 7 days as detailed in methods section 2.2.1.6. On day 7 medium was removed and replaced with fresh differentiating medium supplemented with 1 or 5 mM MPP⁺. Following 24 h cells were extracted as detailed in methods section 2.2.5.1 and proteins separated by SDS-PAGE. Protein was transferred to nitrocellulose by Western blotting and probed with anti-transglutaminase II (clone CUB-7402) (1:1000). Bands were quantified and corrected against total ERK for differences in protein loading. Results are presented as mean % of non-toxin treated control (assigned 100 %) ± SEM for three (1mM MPP⁺) (n = 3) and four (5 mM MPP⁺) (n = 4) independent experiments, respectively. Statistical analysis of control versus toxin treated cells was carried out using two-tailed t-Tests where statistical significance was accepted at p<0.01 (**).

FITC   FITC + propidium iodide

a. Control

b. 1 mM MPP$^+$
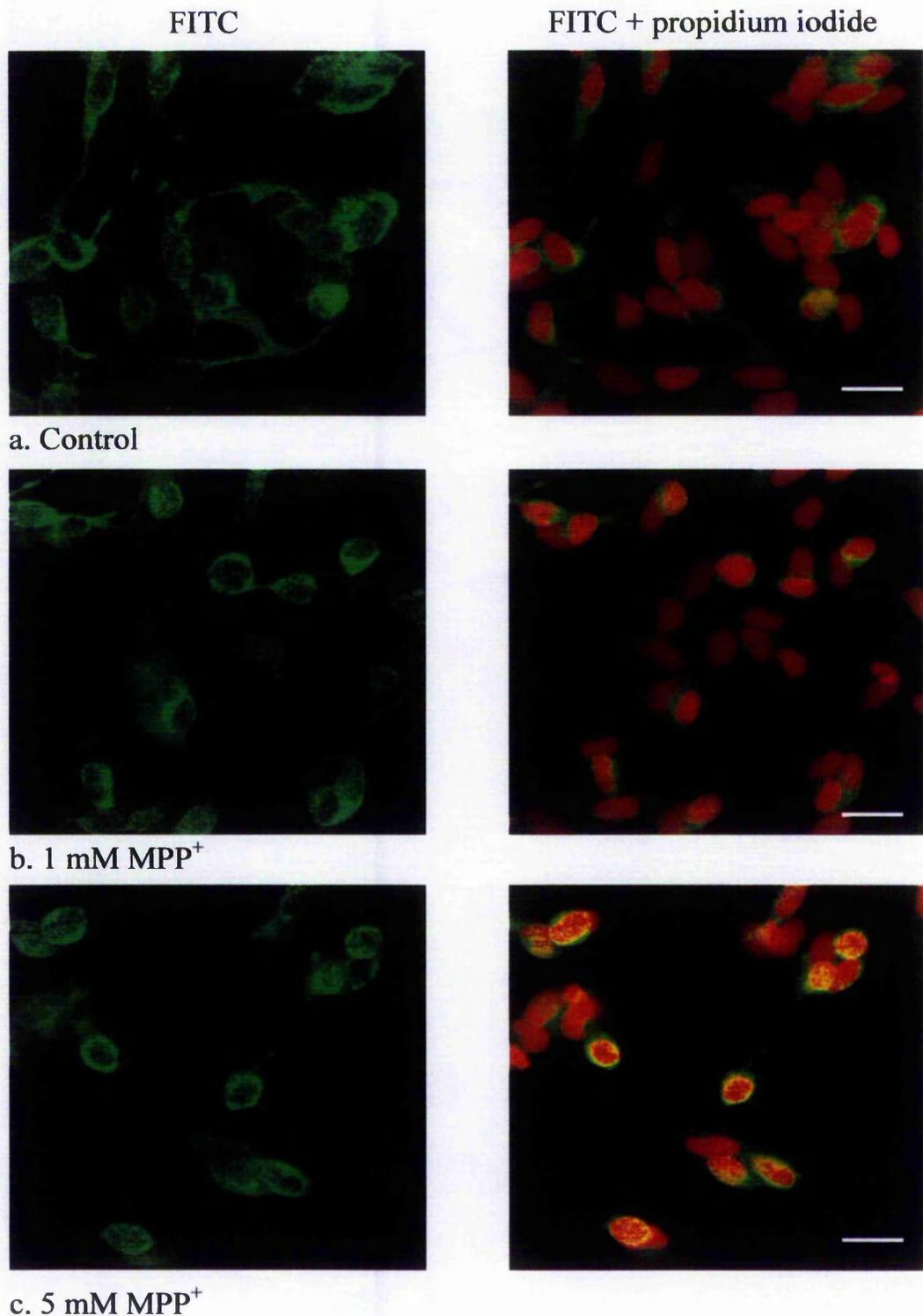
c. 5 mM MPP$^+$

Figure 6.2 Expression and distribution of tTG in MPP$^+$ treated cells
Cells were differentiated in permanox chamber slides over 7 days. Medium was removed and replaced with fresh differentiating medium supplemented with 1 mM or 5 mM MPP$^+$. After 24 h cells were fixed and then permeabilised as detailed in methods section 2.2.9. Cells were probed with anti-tTG antibody (CUB-7402) (1:20). Confocal analysis was performed at x 400 magnification. Scale bar represents 20 μm.

6.2.2 Changes in tTG activity following MPP$^+$ exposure

The ability of TG enzymes to catalyse the incorporation of polypeptides into proteins was exploited to determine whether MPP$^+$ treatment evoked a change in TG activity. This method utilised a polyamine substrate (EZ-link-5-(biotinamido) pentylamine), which was incubated with cells for the final hour of 24 h MPP$^+$ exposure. TG-dependent incorporation of the substrate into proteins was detected using a Neutravidin, HRP conjugated secondary antibody and ECL procedures (see chapter II section 2.2.10). Figure 6.3 shows that TG activity was increased in a dose dependent manner following MPP$^+$ exposure. Significantly this increase in activity occurred despite a reduction in tTG protein with MPP$^+$. Of interest is that the position of phosphorylated NF-H and NF-M proteins were found to coincide with proteins shown to incorporate the pentylamine, albeit not the strongest bands.

To determine whether polyamine incorporation was indeed TG mediated, putrescine, a competitive substrate for TG was added at high concentration (10 mM) to the cells, prior to addition of EZ-link-5-(biotinamido) pentylamine. Results are shown in Figure 6.4. Amine incorporation following MPP$^+$ treatment was reduced by putrescine, suggesting that it be, in part, mediated by TG activity. As a positive control 15 min exposure to the calcium ionophore Ionomycin increased amine incorporation, again attenuated by putrescine (see Fig 6.4, left panel). To substantiate that polyamine incorporation was mediated by tTG, a second, more specific tTG inhibitor, R283. was employed. Polyamine incorporation following MPP$^+$ treatment was dose-dependently reduced by R283 (100 μM and 250 μM) (Figure 6.5). For example, 100 μM R283 (a concentration which does not significantly affect cell viability) (see Fig 6.6) substantially reduced amine incorporation following treatment with 1 mM MPP$^+$ to near control levels.
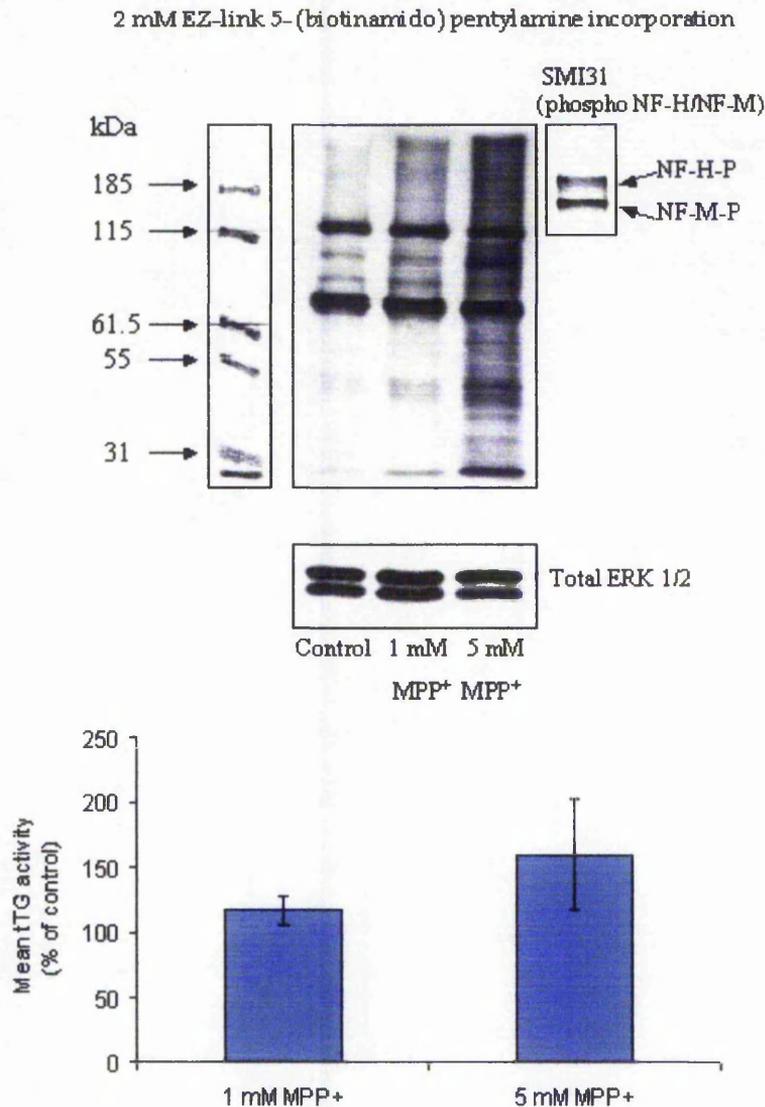
Figure 6.3 Elevated TG activity following 24 h exposure to MPP+.
Cells were seeded into T25 flasks at 400,000 cells / flask and induced to differentiate as detailed in methods section 2.2.1.6. On day 7 medium was removed and replaced with fresh differentiating medium supplemented with MPP+. Cells were exposed to MPP+ for 24 h and with EZ-Link 5-(biotinamido) pentylamine for the final hour, then extracted as detailed in methods section 2.2.10. Proteins were separated on 7.5 % acrylamide gels and transferred to nitrocellulose by Western blotting. EZ-Link 5-(biotinamido) pentylamine incorporation was detected by probing with neutravidin-HRP conjugated secondary antibody (2 μg/ml). Antibody was stripped from the membrane (methods section 2.2.8.2.5) and re-probed with anti-phosphorylated NF-H/NF-M (SMI31) (1:1000) and total anti-ERK 1/2 (1:500) antibodies. Results were corrected against total ERK 1/2 bands to ensure equal protein loading then expressed as a percentage of the differentiated control (assigned 100 %). Results are the mean values of four independent experiments ± SEM (n = 4).
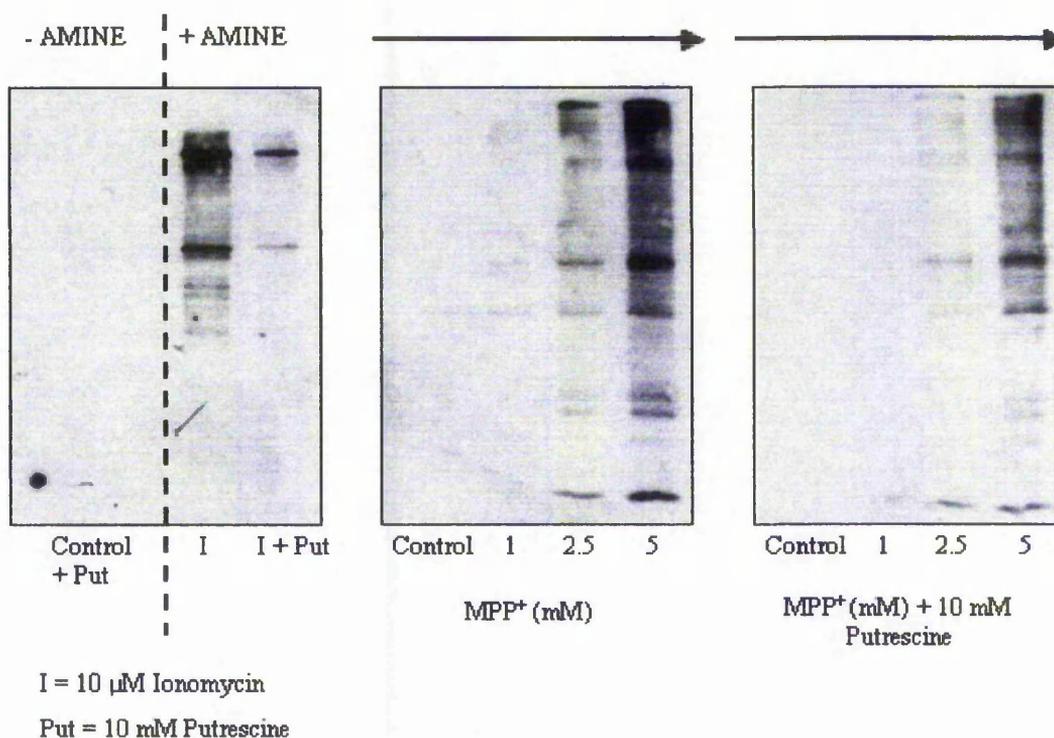
Figure 6.4 EZ-Link 5-(biotinamido) pentylamine incorporation is mediated via transglutaminase.

Cells were seeded into T25 flasks at 400,000 cells / flask and differentiated as detailed in methods section 2.2.1.6. On day 7 medium was removed and replaced with fresh differentiating medium supplemented with MPP⁺ ± putrescine for 24 h. For the final 1 h incubation with treatments, EZ-Link 5-(biotinamido) pentylamine was added to each flask at a final concentration of 2 mM, then cells extracted as detailed in methods section 2.2.10. As a positive control, cells were firstly treated with fresh differentiating medium ± putrescine for 24 h (with 2 mM EZ-Link 5-(biotinamido) pentylamine added for the final hour) ± 10 μM ionomycin for a final 15 min. Proteins were separated on 7.5 % acrylamide gels and transferred to nitrocellulose by Western blotting. EZ-Link 5-(biotinamido) pentylamine incorporation was detected by probing with neutravidin-HRP conjugated secondary antibody (2 μg / ml). Results are representative of 2 independent experiments.
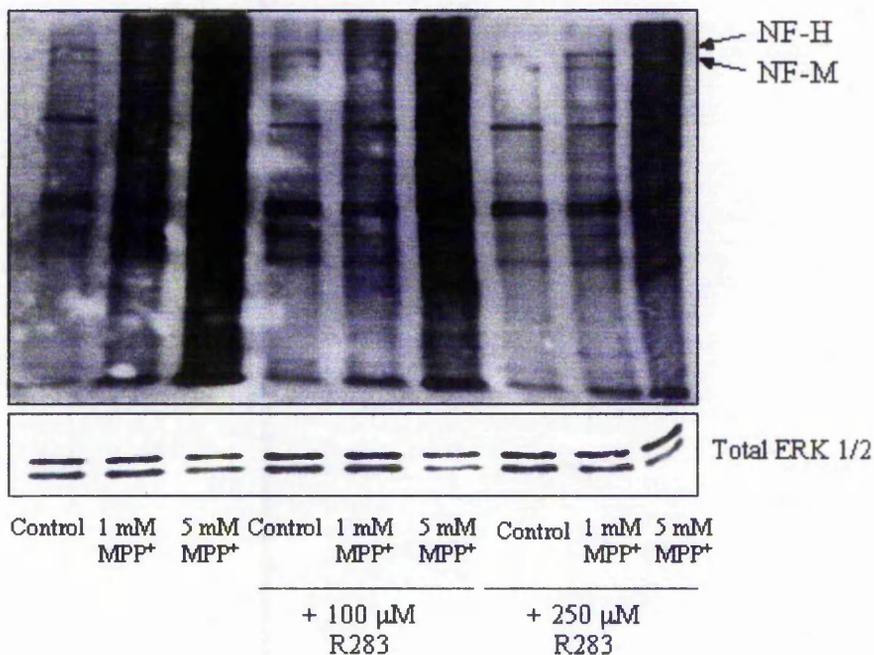
Figure 6.5   Inhibition of EZ-Link 5-(biotinamido) pentylamine incorporation using internal tTG inhibitor, R283.
Cells were seeded into T25 flasks at 400,000 cells / flask and differentiated as detailed in methods section 2.2.1.6. On day 7 medium was removed and replaced with fresh differentiating medium supplemented with MPP+ ± R283 for 24 h. For the final 1 h incubation with treatments, EZ-Link 5-(biotinamido) pentylamine was added to each flask at a final concentration of 2 mM, then cells extracted as detailed in methods section 2.2.10. Proteins from a single experiment were separated on 7.5 % acrylamide gels and transferred to nitrocellulose by Western blotting. EZ-Link 5-(biotinamido) pentylamine incorporation was detected by probing with neutravidin-HRP conjugated secondary antibody (2 µg / ml).

6.2.3 Inhibition of TG exacerbates MPP$^+$ toxicity

Further studies sought to determine the effect of TG inhibition on MPP$^+$ toxicity. Using the MTT reduction assay as a determinant of viability, a titration of R283 was performed to determine concentrations that did not significantly effect viability of control cells (Fig 6.6A). Cells were subsequently treated with MPP$^+$ in conjunction with putrescine (10 mM) or R283 (at concentrations ranging between 50 and 500 µM). Results show that TG inhibition significantly exacerbated MPP$^+$ toxicity (Fig 6.6B and C), suggesting that tTG activation may represent a pro-survival event in this toxic paradigm.
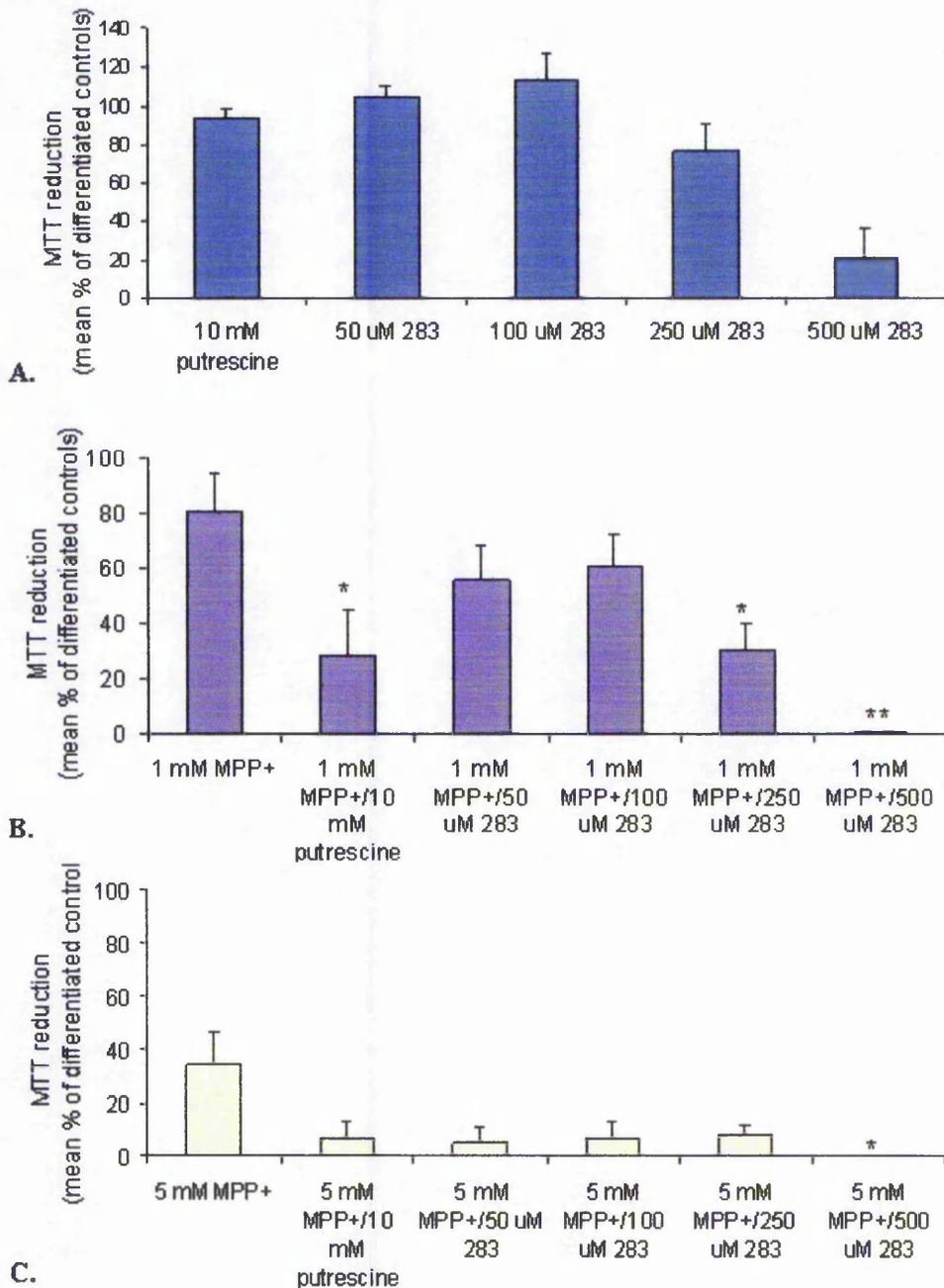
Figure 6.6   Inhibition of tTG exacerbates MPP⁺ toxicity

Cells were seeded into 96 well plates at 5000 cells/well and differentiated for 7 days as detailed in methods section 2.2.1.6. On day 7 medium was exchanged for fresh differentiation medium supplemented with putrescine or R283 (A), 1 mM MPP⁺ ± putrescine or R283 (B), or 5 mM MPP⁺ ± putrescine or R283 (C). After 24 h plates were assayed for viability using the MTT reduction assay as detailed in methods section 2.2.3.1 and data expressed as mean percentage MTT reduction of differentiated controls (assigned 100 %) ± SEM. Data shown is combined from four independent experiments (triplicate wells in each experiment). Statistical analysis of MPP⁺ versus MPP⁺ plus inhibitor treated cells was performed using two-tailed t-Tests where statistical significance was accepted at p< 0.05 (*) or p<0.01 (**).

6.3 DISCUSSION

6.3.1 The role of tTG in MPP$^+$ mediated toxicity

6.3.1.1 MPP$^+$ reduces tTG expression but increases tTG activity

The effects of MPP$^+$ on tTG expression and activity are previously uncharacterised. In this study, following 72 h and 14 days (chronic) exposure to sub-cytotoxic MPP$^+$ concentrations, tTG expression remained unchanged (results not shown). However, tTG expression following cytotoxic MPP$^+$ exposure was significantly reduced; this is likely to be calpain-mediated since tTG is a substrate for calpains (Zhang et al., 1998b). Indeed MPTP/MPP$^+$ has previously been shown to increase cytosolic calcium levels, which would in turn activate calpain (Urani et al., 1994; Kass et al., 1988; Chen et al., 1995). A recent study by Lesort et al, (2000b) further strengthens this hypothesis; treatment of SH-SY5Y cells over-expressing wild type or mutant tTG with 5 mM 3-nitropropionic acid (3-NP; a mitochondrial complex II inhibitor), was reported to significantly increase *in-situ* tTG activity by reducing GTP levels whilst not affecting intracellular Ca^{2+} levels or tTG protein levels. On the other hand, Crocker et al, (2003) have shown that treatment of mice with MPTP leads to increased calpain-mediated proteolysis and that calpain inhibition attenuates MPTP toxicity. It would be of interest to investigate the effects of calpain inhibitors on the MPP$^+$- induced reduction in tTG protein levels in the SH-SY5Y cells.

It is widely accepted that MPP$^+$ depletes cellular ATP levels as a consequence of complex I inhibition. For example, my group has shown that treatment of mitotic SH-SY5Y cells with 2 mM MPP$^+$ significantly reduces ATP levels within 24 h (Begoñã Caneda-Ferron and Luigi De Girolamo, unpublished observations). If a parallel reduction in GTP ensued, tTG activity could increase. Indeed Lesort et al, (2000b) showed that the complex II inhibitor, 3-NP led to a reduction in GTP levels in addition to ATP levels. The latter study also strengthened the association between oxidative stress and tTG activity since treatment with antioxidants attenuated the 3-NP-mediated increase in tTG activity and tTG-induced modification of proteins. In the current study, TG activity was markedly increased following exposure to a cytotoxic concentration of MPP$^+$. This is particularly significant given that at the

243

same time point tTG expression was reduced. In the presence of R283, a tTG-specific inhibitor, TG activity was reduced signifying that the increase in TG activity in the presence of MPP⁺ was, at least in part, mediated by tTG. It was also interesting to note that the banding pattern observed following MPP⁺ treatment differed to that induced by ionomycin, suggesting that TG may preferentially affect different substrates depending on the insult (reviewed by Griffin *et al.*, 2002). This may be a very important consideration *in-vivo*.

6.3.1.2 *Inhibition of tTG exacerbates MPP⁺ toxicity*

The implications of elevated TG activity in MPP⁺ toxicity are as yet unclear. Tucholski and Johnson, (2002) reported a pro-apoptotic role for tTG when transamidating activity was elevated. This would agree with work by Piacentini *et al.*, (2002) who suggest that tTG may sensitise cells to apoptosis by affecting mitochondrial function, poignant given that MPP⁺ is itself an inhibitor of mitochondrial complex I (Nicklas *et al.*, 1985). MPP⁺ has the potential to up-regulate tTG activity via a number of mechanisms. For example, MPP⁺ has been reported to increase ROS production (Höglinger *et al.*, 2003) and increase intracellular calcium levels, both factors that would increase tTG activity (Zhang *et al.*, 1998a). However, in the current study, TG inhibitors in combination with MPP⁺ significantly exacerbated MPP⁺ toxicity, suggesting that tTG activity has a pro-survival role in this instance. This is in line with Antonyak *et al*, (2002) who noted that the pro-survival, PI3-K pathway was necessary for retinoic acid induced tTG expression and activity in NIH3T3 cells. Furthermore, inhibition of tTG caused retinoic acid to activate apoptosis rather than differentiate the cells. It should be noted that whilst the cell culture system used in the current project employs retinoic acid as a differentiation agent, TG inhibitors, at concentrations that exacerbated MPP⁺ toxicity, had no effect on the viability of control cells. Antonyak *et al*, (2001) also reported that pre-treatment with retinoic acid protected human leukaemia cells (HL60) from synthetic retinoid (N-(4-hydroxyphenyl retinamide)-induced cell death which correlated with the ability of retinoic acid to mediate expression of active tTG. An *in-vivo* study whereby tTG expression was ubiquitously inactivated in mice produced animals that were viable. However dexamethasone treated thymocytes from tTG knock-out mice showed reduced viability, whilst fibroblast cells showed

reduced adherence (Nanda *et al.*, 2001). Finally, Tucholski and Johnson, (2003) reported that tTG, by facilitating adenylyl cyclase activation and cAMP production, enhanced the activation of CREB, which can act as a survival signal.

6.3.1.3 *Immunocytochemical analysis of tTG distribution in MPP$^+$ treated cells*

Lesort *et al*, (1998) investigated the distribution of tTG in SH-SY5Y cells and reported that the majority (93 %) was localised within the cytoplasm with the remainder found in the nucleus. A very similar distribution was observed in pre-differentiated cells in this thesis. Treatment with 1 nM maitotoxin, which increased intracellular Ca^{2+} but did not affect cell viability, induced nuclear translocation of tTG, which co-localised with tTG activity (Lesort *et al.*, 1998). In contrast, treatment with 5 mM MPP$^+$ did not increase tTG protein levels in the nucleus but interestingly caused an intense halo of tTG immunoreactivity to form around the nucleus. This may be significant, since within the nucleus tTG might transamidate or activate specific substrates in its role as a signal transducing G protein. Of significance is that tTG cross-links have been identified in the halo of Lewy bodies, where they co-localise with α-synuclein (Junn *et al.*, 2003). In the current study, visualisation of proteins into which EZ-Link 5-(biotinamido) pentylamine had been incorporated following MPP$^+$ treatment, revealed bands that appeared to have migrated to the same position as phosphorylated NF-H/NF-M proteins. This requires further clarification but is interesting given that intense phosphorylated NF immunoreactivity was also observed as a discrete mass or a halo structure, consistently in the perinuclear region following MPP$^+$ exposure. In a study by Grierson *et al*, (2001), COS cells were co-expressed with NF-L, NF-M and NF-H and either wild type or mutant tTG and incubated with 5-(biotinamido) pentylamine prior to treatment with the calcium mobilising agent, maitotoxin, for 15 min. Results revealed that tTG catalysed incorporation of 5-(biotinamido) pentylamine into each NF subunit. Additionally, immunoprobing of blots with NF-H-, NF-M- and NF-L-specific antibodies revealed that tTG induced cross-linking of the NF proteins which gave rise to higher molecular mass species.

Though the role of inclusion bodies is not yet firmly established, one could postulate that if such inclusions were indeed pro-survival, tTG may contribute to cell survival

via inclusion formation. Whether tTG colocalises with NF proteins and other cytoskeletal elements in MPP$^+$ treated SH-SY5Y cells, and the subsequent role of tTG, warrants further investigation. Such investigations would require further immunocytochemical, and also immunoprecipitation studies and would benefit from use of an antibody directed to the tTG cross-link.

CHAPTER VII

GENERAL DISCUSSION AND FUTURE WORK

CHAPTER VII. GENERAL DISCUSSION AND FUTURE WORK

7.1 Establishment of a pre-differentiated human neuroblastoma model

Given that the biochemical and pathological basis of PD remains elusive, research must continue to strive to determine exactly how and why dopaminergic neurones die. The MPTP parkinsonian model continues to offer the most valuable PD model to date and induces many comparable pathological features *in-vivo* and in cell culture systems. The latter are advantageous since they afford homogenous systems in which to investigate, at the sub-cellular level, the biochemical basis of MPP^+ induced cell death. Given that species differences in sensitivity to MPP^+ exist, a human cell system is advantageous. Three clones of the SH-SY5Y cell line were initially characterised in terms of neuronal differentiation with respect to morphological changes and proposed biochemical markers of the differentiation process. Clonal differences were revealed highlighting the importance of characterisation of the cell system. A clone originating from ECACC was used in subsequent studies. Following a 7-day retinoic acid-mediated differentiation time course, cells were morphologically and biochemically differentiated; Total NF-H and phosphorylated NF-H/NF-M was located within axon-like processes. ERK was suggested to play a prominent role in neuritogenesis in SH-SY5Y cells. tTG protein levels were elevated, indicative of differentiation. Retinoic acid-mediated differentiated SH-SY5Y cells have previously been used in MPP^+ investigations but the exposure has been short (Joyce *et al.*, 2003; Mathiasen *et al.*, 2004). However the current study was unique in that it used pre-differentiated cells that were viable, and remained morphologically and biochemically differentiated, for up to 14 days. Thus the window for toxicity studies was greatly extended and permitted the effects of sub-cytotoxic concentrations of MPP^+ to be investigated. A pre-differentiated human model that can be used over extended time periods may also be useful for investigation of other chronic, neurodegenerative disorders. Indeed SH-SY5Y cells are used in models of Huntingtons disease (Lesort *et al.*, 2000; Chun *et al.*, 2001), and Alzheimer's disease (Wei *et al.*, 2002; Liu *et al.*, 2003). However future work should incorporate determination of the effect of MPP^+ on mitochondrial complex I in this system, firstly to establish whether investigated markers of toxicity manifest upstream or downstream of complex I inhibition, and secondly, to determine how comparable the

toxicity induced in SH-SY5Y cells is to that of dopaminergic neurones and in turn, how useful this model is.

7.2 Employment of a pre-differentiated SH-SY5Y system for MPP$^+$ investigations

This thesis has focussed on 3 main areas of research with respect to MPP$^+$ toxicity; cytoskeletal changes, the involvement of MAPK and CDK-5 signalling pathways and the protection afforded by specific inhibitors of these pathways and a potential role for tTG in MPP$^+$ mediated toxicity, which are discussed in sections 7.2.1 – 7.2.3.

7.2.1 Neuroprotection strategies using MAPK/CDK-5 inhibitiors

It has been demonstrated for the first time in this thesis that a more specific CDK-5 inhibitor can confer a degree protection against MPP$^+$ toxicity over short term and chronic time courses in a cell culture system. This finding is in agreement with Smith et al, (2003) who demonstrated that MPTP increases CDK-5 protein levels and activity in-vivo. Furthermore the fore-mentioned study showed that CDK inhibition improved locomotive state and prevented loss of dopaminergic neurones. A cell culture system as demonstrated in this thesis will permit further investigation of the role of CDK-5 in MPP$^+$ toxicity at the sub-cellular level. Indeed it will be important to establish CDK-5 activation levels in the SH-SY5Y system following MPP$^+$ exposure (and to ascertain whether p25/CDK-5 plays a role) and, in line with Gong et al, (2003) to investigate the effects of CDK-5 on pro-survival signals in this system so that the protective effect of BL-1 be exacted.

Using specific MAPK inhibitors, results demonstrated that inhibition of JNK attenuated short-term (72 h) exposures to MPP$^+$ whilst preliminary data suggested that CEP-11004 might also reduce toxicity following chronic MPP$^+$ exposure. However the role of ERK and p38 pathways were more difficult to determine; both exerted a pro-survival role in response to lower level toxicity (up to 40 % kill) but exacerbated toxicity when 60 – 100 % of cells were killed, suggesting that the level of MPP$^+$ toxicity altered the balance of MAPK pathways. Since the effect of MPP$^+$ on mitochondrial respiration was not determined in this study it was not possible to

in turn determine the effects of neuroprotective agents on cellular ATP levels. This may have provided information regarding the mechanism of neuroprotection conferred and would be an important aspect of future work. Such agents may have reduced the cellular requirement for ATP thereby increasing cellular ATP levels in the face of MPP^+ toxicity. It should be noted that other signalling pathways would contribute to the decision of a cell to survive or to die. For example, Crossthwaite *et al,* (2002) demonstrate that the pro-survival pathway PI-3K-Akt was involved in influencing the outcome of MAPK signal activation in H_2O_2 treated primary cortical neurones. MPP^+ can induce cytochrome c release and thereby induce caspase-mediated apoptotic cell death (Casarino *et al.,* 1999; Fall and Bennett, 1999; Gómez *et al.,* 2001). Indeed it has been demonstrated in my laboratory using mitotic SH-SY5Y cells that effector caspase 3 activation is elevated following 10 h exposure to 1 mM MPP^+ (Julia Fitzgerald, unpublished observations) whilst caspase 3 inhibition attenuated MPP^+ toxicity in primary dopaminergic neurones (Bisland *et al.,* 2002) Moreover, cell cultures obtained from transgenic mice over-expressing Bcl-2 showed resistance to MPP^+-mediated toxicity (Offen *et al.,* 1998).

It must be appreciated that MAPK and CDK-5 pathways are activated as a consequence of normal cell function, in addition to stressful scenarios; thus the employment of such inhibitors as neuroprotective strategies requires due care. Having said this JNK inhibitors are currently being used in clinical trials for PD. A desirable therapy for PD might combine a number of drugs tested for efficacy and may incorporate multiple antioxidants as proposed by Prasad *et al,* (1999). Alternative therapeutic approaches to neuroprotection involve the employment of adeno-associated viruses (AAV) that may target genes to specific brain areas. Indeed striatal delivery of a recombinant AAV containing the caspase recruitment domain of Apaf-1 (which recruits and activates pro-caspase 9 causing dominant negative inhibition of the Apaf-1-procaspase 9 complex), prevented MPTP mediated-nigrostriatal degeneration (Mochizuki *et al.,* 2001). In another study, SH-SY5Y cells were infected with adenoviral vectors encoding the JNK binding domain (JBD) of JNK interacting protein 1 (JIP 1) (AdV-JBD). JIP 1 is a scaffold protein that binds to JNK causing it to remain in the cytoplasm, thus inhibiting its translocation to the nucleus to activate gene expression (Xia *et al.,* 2001). In SH-SY5Y cells, AdV-JBD inhibited JNK and c-jun phosphorylation mediated by 5 mM MPP^+ and protected

cells from apoptotic death. Additionally inhibition of JNK by AdV-JBD blocked the activation of caspases and dopaminergic cell death in MPTP treated mice (Xia *et al.,* 2001).

7.2.2 Cytoskeletal changes induced by MPP^+

A focus of this project was to investigate the effects of MPP^+ toxicity on the NF and MT systems. Specific NF-H and NF-M phosphorylation was increased by MPP^+, accompanied by a change in the phosphorylated NF-M:NF-H ratio, following short term and chronic exposures. The reason for the change in ratio of NF-H and NF-M sub-units is not known but was also observed following the differentiation time course of the cells. Results therefore implicate that NF-M phosphorylation is important in both differentiation and the response to stress in SH-SY5Y cells. Use of an antibody specific for total NF-M protein (phosphorylation independent) would further ascertain the seemingly predominant role for NF-M. Further studies would determine the kinase(s) responsible for elevated NF phosphorylation following MPP^+ treatment. ERK and JNK activation were found to transiently increase following exposure to cytotoxic and sub-cytotoxic concentrations of MPP^+ but were reduced compared to control cells within 16 h. An interesting hypothesis would be the involvement of CDK-5, since it has recently been shown that H_2O_2-mediated oxidative stress could induce CDK-5 activity, which in turn increased perikaryal NF phosphorylation and slowed NF transport (Shea *et al.,* 2004b). Of significance is that data presented in this thesis show a CDK-5 inhibitor, BL-1 to attenuate MPP^+ toxicity (discussed in section 7.2.1). Preliminary data also suggested that treatment with MPP^+ plus BL-1 partially reversed the increase in ratio of phosphorylated NF-M to NF-H observed following MPP^+ exposure. α-tubulin subunit protein levels were not affected by MPP^+ at any time point.

Using immunocytochemical analyses, phosphorylated NFs and α-tubulin were suggested to accumulate in response to proteasome inhibitor MG132, indicating that at least a proportion of the degradation of these proteins occurs via the UPP. Further trials would be warranted to confirm these findings. Interestingly, phosphorylated NF levels increased before tubulin perhaps indicating that NFs have a shorter half-life than tubulin. Alternatively, of course it may mean that the proteasomal route of

degradation is more important for NFs than for tubulin. Evidence of impaired proteasomal activity following MPP$^+$ exposure was suggested by an increase in ubiquitinated proteins following exposure to a cytotoxic concentration of MPP$^+$.

In addition to changes in post-translational modification of NFs, MPP$^+$ also induced changes in the distribution of phosphorylated NFs to form structures that are interesting in light of the discovery of aggresomes (Johnston *et al.*, 1998). Importantly, changes in distribution of the NF network following sub-cytotoxic concentrations of MPP$^+$ occurred in the absence of MT disruption, consistent with the hypothesis that an intact MT network is required for the retrograde transport of proteins to the cell body to form protein aggregates and inclusion bodies (Johnston *et al.*, 1998; Zhao *et al.*, 2003; Muchowski *et al.*, 2002). A link between the aggresome structure and NF accumulations observed in this thesis is at this stage tenuous and requires further investigation. For example immunocytochemical co-localisation studies using an anti-vimentin antibody and other aggresome components would be useful determinants. Additionally, exposure to MT depolymerising agents (MPP$^+$ reportedly destabilises MTs but at sub-cytotoxic concentrations of MPP$^+$ used in the current study, this was not observed) would identify aggresomes. The role of NF proteins in aggresome formation has not been investigated despite their prominence in Lewy bodies (Schmidt *et al.*, 1991; Galloway *et al.*, 1992). Nevertheless this project demonstrates that NFs phosphorylation/redistribution are down-stream markers of MPP$^+$ toxicity in the SH-SY5Y system. Further investigation into the formation and characteristics of aggresomes are warranted. Indeed McNaught *et al.*, (2002) relate the formation of a Lewy body to that of an aggresome and determine that events may be similar.

7.2.3   The role of tTG in MPP$^+$ mediated toxicity

Results presented in this thesis propose a novel role for tTG in MPP$^+$ toxicity. The pre-differentiated SH-SY5Y system provides an excellent model for tTG studies since endogenous tTG protein levels have been shown to be greatly up-regulated by retinoic acid (chapter III, section 3.2.2.5.3). MPP$^+$ increased tTG activity whilst significantly reducing tTG protein levels, both in a dose-dependent manner.

Importantly, specific inhibition of tTG exacerbated MPP$^+$ toxicity suggesting a pro-survival role for tTG in this system. This is a novel finding.

In-vivo studies have shown that homozygous deletion of tTG is not lethal and that animals are viable and phenotypically normal (Nanda *et al*, 2001). The possibility remains that compensation due to other TGs occurs (reviewed by Griffin *et al.*, 2002; Lorand and Graham, 2003). However other TG enzymes do not exhibit GTP binding and signal transduction properties and as such tTG knock-out animals do exhibit impaired clearance of apoptotic cells, impaired wound healing and reduced fibroblast adherence (Nanda *et al*, 2001; Fesus and Piacentini, 2002). tTG has been implicated in the morphological changes associated with apoptosis where, due to raised Ca^{2+} levels, tTG acts to cross-link intracellular proteins and thereby stabilise the cell for phagocytosis (reviewed by Lesort *et al.*, 2000; Fesus and Piacentini, 2002). However, results in this thesis demonstrate that both a general TG, and a specific tTG inhibitor exacerbated MPP$^+$ toxicity indicating that tTG activity is pro-survival in this system. It remains to be determined whether the latter involves either transamidating and/or the GTP hydrolysis/signal transduction activities of tTG.

tTG is implicated in the formation of stable and insoluble characteristic inclusions associated with neurodegenerative diseases. Indeed, Citron *et al*, (2002) reported that tTG cross-links were co-localised with α-synuclein and ubiquitin in the substantia nigra of PD brains whilst Junn *et al*, (2003) showed that tTG cross-links did indeed co-localise with α-synuclein in Lewy bodies. tTG activity and protein levels are elevated in Alzheimer's disease brains (Johnson *et al.*, 1997; Citron *et al.*, 2002) whilst tTG is reportedly co-localised with tau in neurofibrillary tangles and found within amyloid plaques (Citron *et al.*, 2001 and references therein); both the Aβ peptide and its β-amyloid precursor protein are *in-vitro* substrates for tTG (reviewed by Lesort *et al.*, 2000). An exciting possibility is that tTG may play a role in stabilisation of the aggresome structure described by Johnston *et al*, (1998) which is reportedly "caged" by the intermediate filament, vimentin (Johnston *et al*, 1998; Muqit *et al.*, 2004), an *in-situ* target for tTG (Singh *et al.*, 2001 and references therein). Thus investigation of the effects of TG inhibitors on aggresome formation may be warranted. NF proteins are substrates for tTG (Grierson *et al.*, 2001) and

results presented this thesis suggest cross-linkage by tTG, thus implicating tTG-mediated transamidation of NFs in the SH-SY5Y system. It may even be possible that NFs replace vimentin in the formation of aggresomes in certain systems. However this requires further clarification. Immunoprecipitation of NFs following treatment with pentylamine and subsequent detection of amine incorporation might provide evidence of a functional role in normal SH-SY5Y cells and following MPP$^+$ treatment. Identification of proteins into which tTG had mediated incorporation of polyamine in MPP$^+$ treated cells would further exact the role of tTG in MPP$^+$ mediated toxicity. Finally, co-localisation studies, using antibodies against tTG, NFs, synuclein, vimentin, tubulin and ubiquitin will need to be conducted in the future.

7.3   Conclusions

Figure 7.1 proposes how the data presented in this thesis might integrate with current literature as reviewed in chapter 1.
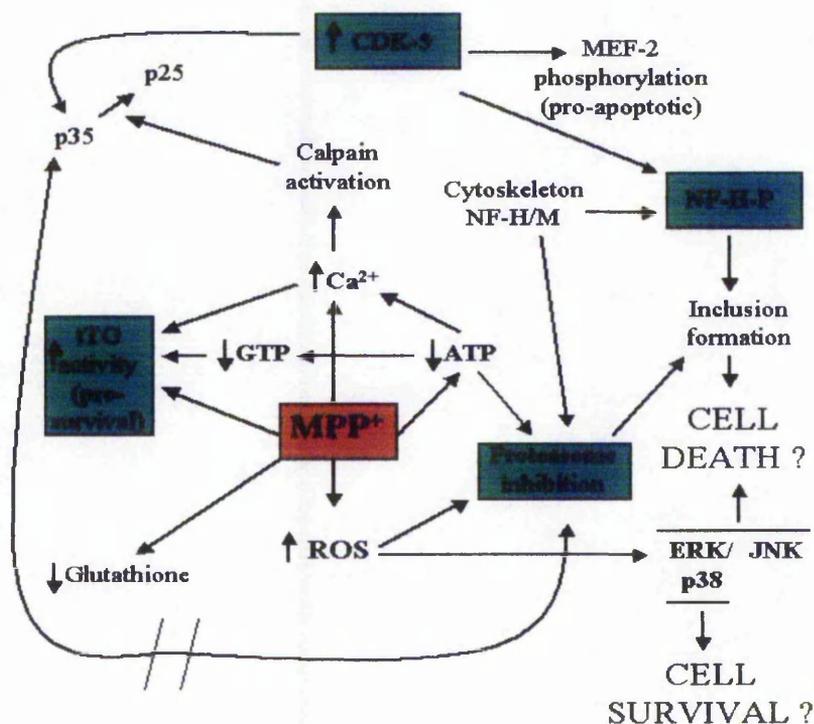
Figure 7.1   Overview of proposed mechanisms of MPP⁺ toxicity as detailed in this thesis and current literature.

(1) MPP$^+$ reduces ATP and glutathione levels but increases ROS. (2) A reduction in GTP levels might follow the reduction in ATP, in turn tTG activity is increased. (3) Raised intracellular Ca^{2+} levels can augment increased tTG activity and also activate calpains, which cleave p35 to p25. (4) p25 is more stable than p35 thus CDK-5 activity is increased. CDK-5 can phosphorylate, and thereby inactivate, nuclear transcription factors that promote cell survival i.e. MEF-2. (5) Reduced cellular ATP and elevated ROS can reduce proteasomal activity causing accumulation of proteins that require UPP-mediated degradation (p35, NFs, tubulin sub-units). (6) Intracellular kinases i.e. JNK and CDK-5, increase NF-H/NF-M phosphorylation which accumulates within the perinuclear region of cells. The controversial role of protein aggregation in cells is discussed in chapter 1, section 1.8.4.2. (7) Elevated ROS activates MAPK pathways, which promote cell survival or death depending on the level of MPP$^+$ toxicity.

In conclusion, the employment of a pre-differentiated SH-SY5Y system has provided a model that can be exploited to investigate MPP^+ toxicity following short term and chronic exposures, the later potentially exhibiting greater analogy to neurones *in-vivo*. Several important findings have been noted:

- MPP^+ induced changes in the post-translational modification and distribution of the NF network that precede changes in the MT network. Evidence of impaired proteasomal activity was noted following MPP^+ exposure. Preliminary studies suggested that proteasomal inhibition caused accumulation of NF proteins and tubulin in this system suggesting that the UPP be at least in part involved in the degradation of these proteins.

- Neuroprotection against MPP^+ toxicity can be afforded using MAPK inhibitors, but is dependent on the relative extent of toxicity. A CDK-5 inhibitor, BL-1 conferred a degree of protection against short term and chronic MPP^+ toxicity.

- A novel role for tTG in MPP^+ was established; MPP^+ induces tTG activity, inhibition of which exacerbates MPP^+-mediated toxicity.

Continued understanding of the mechanisms of MPP^+ toxicity using both *in-vivo* and cell culture models will hopefully further develop the existing knowledge of PD pathology so that more effective neuropreventative and neuroprotective strategies may be determined.

CHAPTER VIII

REFERENCES

CHAPTER VIII. REFERENCES

Ackerley, S., Thornhill, P., Grierson, A.J., Brownlees, J., Anderton, B.H., Leigh, P.N., Shaw, C.E. and Miller, C.C.J. (2003). Neurofilament heavy chain side-arm phosphorylation regulates axonal transport of neurofilaments. *Journal of Cell Biology* **161,** 489-495.

Ahlijanian, M.K., Barrezueta, N.X., Williams, R.D., Jakowski, A., Kowsz, K.P., McCarthy, S., Coskran, T., Carlo, A., Seymour, P.A., Burkhardt, J.E., Nelso, R.B. and McNeish, J.D. (2000). *Proceedings of the National Academy of Science* **97(6),** 2910-2915.

Alberts, B., Bray, D., Lewis, J., Raff, M., Roberts, K. and Watson, J.D. (1994). *Molecular biology of the cell* (3rd ed). New York: Garland Publishing.

Alessandrini, A., Namura, S., Moskowitz, M.A. and Bonventre, J.V. (1999). MEK1 protein kinase inibition protects against damage resulting from focal cerebral ischemia. *Proceedings of the National Academy of Science* **96(22),** 12866-12869.

Alessi, D., Cuenda, A., Cohen, P, Dudley, D.T. and Saltiel, A.R. (1995). PD 098059 is a specific inhibitor of the activation of mitogen-activated protein kinase kinase *in vitro* and *in vivo. The Journal of Biological Chemistry* **270(46),** 27489-27494.

Alves-Rodrigues, A., Gregori, L., Figueiredo-Pereira, M.E. (1998). Ubiquitin, cellular inclusions and their role in neurodegeneration. *Trends in Neurosciences* **21(12),** 516-520.

Antonyak, M.A., Boehm, J.E. and Cerione, R.A. (2002). Phosphoinosistide 3-kinase activity is required for retinoic acid-induced expression and activation of the tissue transglutaminase. *Journal of Biological Chemistry* **277(17),** 14712-14716.

Antonyak, M.A., Singh, U.S., Lee, D.A., Boehm, J.E., Combs, C., Zgola, M.M., Page, R.L. and Cerione, R.A. (2001). Effects of tissue transglutaminase on retinoic acid-induced cellular differentiation and protection against apoptosis. *Journal of Biological Chemistry* **273(36),** 33582-33587.

Arai, K., Lee, S., Leyen, K., Kurose, H. and Lo, E. (2004). Involvement of ERK MAP kinase in endoplasmic reticulum stress in SH-SY5Y human neuroblastoma cells. *Journal of Neurochemistry* **89,** 232-239.

Ardley, H.C., Scott, G.B., Rose, S.A, Tan, N.G.S., Markham, A.F. and Robinson, P.A. (2003). Inhibition of proteasomal activity causes inclusion formation in neuronal and non-neuronal cells overexpressing Parkin. *Molecular Biology of the Cell* **14,** 4541-4556.

Arrasate, M., Mitra, S., Schweitzer, E.S., Segal, M.R. and Finkbeiner, S. (2004). Inclusion body formation reduces levels of mutant huntingtin and the risk of neuronal death. *Nature* **431,** 805-810.

Bajaj. (2000). Cyclin-dependent kinase-5 (CDK-5) and amyotrophic lateral sclerosis. *ALS and Other Motor Neuron Disorders* **1,** 319-327.

Barzilai, A. and Melamed, E. (2004). Molecular mechanisms of selective dopaminergic neuronal death in Parkinson's disease. *Trends in Molecular Medicine* **9(3),** 126-131.

Bennett, M.C., Bishop, J.F., Leng, Y., Chock, P.B., Chase, T.N. and Mouradian, M.M. (1999). Degradation of α-synuclein by proteasome. *Journal of Biological Chemistry* **274(48),** 33855-33858.

Betarbet, R. (2000). Chronic systemic pesticide exposure reproduces features of Parkinson's disease. *Nature Neuroscience* **3,** 1301-1306.

Biasini, E., Fioriti, L., Ceglia, I., Invernizzi, R., Bertoli, A., Chiesa, R. and Forloni, G. (2004). Proteasome inhibition and aggregation in Parkinson's disease: a comparative study in untransfected and transfected cells. *Journal of Neurochemistry* **88,** 545-553.

Bibb, .A., Nishi, A., O'Callaghan, J.P., Ule, J., Lan, M., Snyder, G.L., Horiuchi, A., Saito, T., Hisanaga, S., Czernik., Nairn, A.C. and Greengard, . (2001a). Phosphorylation of protein phosphatase inhibitor-1 by Cdk5. *Journal of Biological Chemistry* **276(17),** 14490-14497.

Bibb, J.A., Chen, J., Taylor, J.R., Svenningsson, P., Nishi, A., Snyder, G.L., Yan, Z., Sagawa, Z.K., Ouimet, C.C., Nairn, A.C., Nestler, E.J. and Greengard, P. (2001b). Effects of chronic exposure to cocaine are regulated by the neuronal protein Cdk5. *Nature* **410,** 376-380.

Biedler, J.L., Foffler-Tarlov, S., Schachner, M. and Freedman, L.S. (1978). Multiple neurotransmitter synthesis by human neuroblastoma cell lines and clones. *Cancer Research* **38,** 3751-3757.

Biedler, J.L., Helson, L. and Spengler, B.A. (1973). Morphology and growth, tumorigenicity, and cytogenetics of human neuroblastoma cells in continuous culture. *Cancer Research* **33,** 2643-2652.

Bisland, J., Roy, S., Xanthoudakis, S., Nicholson, D.W., Han, Y., Grimm, E., Hefti, F. and Harper, S.J. (2002). Caspase inhibitors attenuate 1-methyl-4-phenylpyridinium toxicity in primary cultures of mesencephalic dopaminergic neurones. *Journal of Neuroscience* **22(7),** 2637-2649.

Blum, D., Torch, S., Lambeng, N., Nissou, M., Benabid, A., Sadoul, R., Verna, J. (2001). Molecular pathways involved in the neurotoxicity of 6-OHDA, dopamine and MPTP: contribution to the apoptotic theory in Parkinson's disease. *Progress in Neurobiology* **65.** 135-172.

Bogoyevitch, M.A. and Court, N.W. (2004). Counting on mitogen-activated protein kinases-ERKs 3,4,5,6,7 and 8. *Cellular Signalling* **16,** 1345-1354.

Brazil, D.P., Yang, Z. and Hemmings, B.A. (2004). Advances in protein kinase B signalling: AKTion on multiple fronts. *Trends in Biochemical Sciences* **29(5),** 233-242.

Brill II, L.B. and Bennett Jr, J.P. (2003). Dependence on electron transport chain function and intracellular signalling of genomic responses in SH-SY5Y cells to the mitochondrial neurotoxin MPP^+. *Experimental Neurology* **181,** 25-38.

Brion, J.P. and Couck A.M. (1995). Cortical and brainstem-type Lewy bodies are immunoreactive for the cyclin-dependent kinase 5. *American Journal of Pathology* **147,** 1465-1476.

Brownlees, J., Yates, A., Bajaj, N.P., Anderton, B.H., Leigh, P.N., Shaw, C.E. and Miller, C.C.J. (2000). Phosphorylation of neurofilament heavy chain side-arms by stress activated protein kinase-1b/Jun N-terminal kinase-3. *Journal of Cell Science* **113,** 401-407.

Brunet, A., Datta, S.R. and Greenberg, M.E. (2001). Transcriptional-dependent and – independent control of neuronal survival by the PI3K-AKT signalling pathway. *Current Opinion in Neurobiology* **11,** 297-305.

Burns, R.S., Chiueh, C.C., Markey, S.P., Ebert, M.H., Jacobowitz, D.M. and Kopin, I.J. (1983). A primate model of parkinsonism: Selective destruction of dopaminergic neurone in the pars compacta of the substanta nigra by N-methyl-4-phenyl-1,2,3,6-tetrahydropyridine. *Proceedings of the National Academy of Science USA* **80,** 4546-4550.

Callier, S., Le Saux, M., Lhiaubet, A., Di Paolo, T., Rostène, W. and Pelaprat, D. (2002). Evaluation of the protective effect of oestradiol against toxixity induced by 6-hydroxydopamine and 1-methyl-4-phenylpyridinium ion (MPP^+) towards dopaminergic mesencephalic neurones in primary culture. *Journal of Neurochemistry* **80,** 307-316.

Cappelletti, G., Incani, C. and Maci, R. (1995). Involvement of tubulin in MPP+ neurotoxicity on NGF-Differentiated PC12 cells. *Cell Biology International* **19(8),** 687-693.

Cappelletti, G., Maggioni, M.G. and Maci, R. (1999). Influence of MPP+ on the state of tubulin polymerisation in NGF-Differentiated PC12 cells. *Journal of Neuroscience Research* **56,** 28-35.

Cappelletti, G., Pedrotti, B., Maggioni, M.G. and Maci, R. (2001). Microtubule assembly is directly affected by MPP^+ *in-vitro. Cell Biology International* **25(10),** 981-984.

Carlier, M. (1991). Actin: Protein structure and filament dynamics. *Journal of Biological Chemistry* **266(1),** 1-4.

Carvalho, H., Evelson, P., Sigaud, S., Gonzalez-Flecha, B. (2004). Mitogen-activated protein kinases modulate H_2O_2-induced apoptosis in primary rat alveolar epithelial cells. *Journal of Cellular Biochemistry* **92(3),** 502-513.

Cassarino, D.S and Bennett Jr, J.P. (1999). An evaluation of the role of mitochondria in neurodegenerative diseases: mitochondrial mutations and oxidative pathology, protective nuclear responses and cell death in neurodegeneration *Brain Research Reviews* **29,** 1-25.

Cassarino, D.S., Fall, C.P., Swerdlow, R.H., Smith, T.S., Halvorsen, E.M., Miller, S.W., Parks, J.P., Parker Jr, W.D. and Bennett Jr, J.P. (1997). Elevated reactive oxygen species and antioxidant enzyme activities in animal and cellular models of Parkinson's disease. *Biochimica et Biophysica Acta* **1362,** 77-86.

Cassarino, D.S., Halvorsen, E.M., Swerdlow, R.H., Abramova, N., Parker Jr, W.D., Stergill, T.W. and Bennett Jr, J.P. (2000). Interaction among mitochondria, mitogen- activated protein kinases, and nuclear factor-kappaB in cellular models of Parkinson's disease. *Journal of Neurochemistry* **74(4),** 1384-1392.

Cassarino, D.S., Parks, J.K., Davis Parker Jr, W., and Bennett Jr, J.P. (1999). The parkinsonian neurotoxin MPP^+ opens the mitochondrial permeability transition pore and releases cytochrome c in isolated mitochondria via an oxidative mechanism. *Biochimica et Biophysica Acta* **1453,** 49-62.

Castagnoli Jr, N., Chiba, K. and Trevor, A.J. (1985). Potential bio-activation pathways for the neurotoxin MPTP. *Life Sciences* **36(3),** 225-230.

Chambaut-Guérin, A., Hérigault, S., Rouet-Benzineb, P., Rouher, C. and Lafuma, C. (2000). Induction of matrix metallproteinase MMP-9 (92-kDa gelatinase) by retinoic acid in human neuroblastoma SKNBE cells: relevance to neuronal differentiation. *Journal of Neurochemistry* **74,** 508-517.

Chan, P., DeLanney, L.E., Irwin, I., Langston, W. and Di Monte, D. (1991). Rapid ATP loss caused by 1-methyl-4-phenyl-1,2,3,6-tetrahydropyridine in mouse brain. *Journal of Neurochemistry* **57,** 348-351.

Chang, L., Jones, Y., Ellisman, M.H., Goldstein, L.S.B. and Karin, M. (2003). JNK1 is required for maintenance of neuronal microtubules and controls phosphorylation of microtubule-associated proteins. *Developmental Cell* **4(4),** 521-533.

Chen, T.S., Koutsilieri, E. and Rausch, W.D. (1995). MPP+ selectively affects calcium homeostasis in mesencephalic cell cultures from embryonal C57/B16 mice. *Journal of Neural Transmission - General Section* **100(2),** 153-163.

Chergui, K., Svenningsson, P. and Greengard, P. (2004). Cyclin-dependent kinase 5 regulates dopaminergic and glutaminergic transmission in the striatum. *Proceedings of the National Academy of Science* **101(7),** 2191-2196.

Chiba, K., Peterson, L.A., Casagnoli, K.P., Trevor, A.J. and Castagnoli Jr, N. (1985). Studies on the molecular mechanism of bioactivation od the selective nigrostriatal toxin 1-methyl-4-phenyl-1,2,3,6-tetrahdropyridine. *Drug Metabolism and Disposition* **13(3),** 342-347.

Chiba, K., Trevor, A. and Castagnoli Jr, N. (1984). Metabolism of the neurotoxic tertiary amine, MPTP by brain monoamine oxidase. *Biochemical and Biophysical Research Communications* **120,** 574-578.

Chun, W., Lesort, M., Tucholski, J., Ross, C.A. and Johnson, G.V.W. (2001). Tissue transglutaminase does not contribute to the formation of mutant huntingtin aggregates. *Journal of Cell Biology* **153(1),** 25-34.

Chun, W.J., Lesort, M., Tucholski, J., Faber, P.W., MacDonald, M.E., Ross, C.A. and Johnson, G.V.W. (2001). Tissue transglutaminase selectively modifies proteins associated with truncated mutant huntingtin in intact cells. *Neurobiology of Disease* **8(3),** 391-404.

Chung, K.K.K., Dawson, V.L. and Dawson, T.M. (2001). The role of the ubiquitin-proteasomal pathway in parkinson's disease and other neurodegenerative disorders. *Trends in Neurosciences* **24(11 Suppl.),** S7-S14.

Ciccarone, V., Spengler, B.A., Meyers, M.B., Biedler., J.L. and Ross, R.A. (1989). Phenotypic diversification in human neuroblastoma cells: Expression of distinct neural crest lineages. *Cancer Research* **49,** 219-225.

Citron, B.A., SantaCruz, K.S., Davies, P.J.A. and Festoff, B.W. (2001). Intron-exon swapping of transglutaminase mRNA and neuronal tau aggregation in Alzheimer's disease. *Journal of Biological Chemistry* **276(5),** 3295-3301.

Citron, B.A., Suo, Z., SantaCruz, K., Davies, P.J.A., Qin, F. and Festoff, B.W. (2002). Protein crosslinkin, tissue transglutminase, alternative splicing and neurodegeneration. *Neurochemistry International* **40,** 69-78.

Clark, A.R., Dean, J.L.E. and Saklatvala, J. (2003). Post-transcriptional regulation of gene expression by the mitogen-activated protein kinase p38. *FEBS Letters* **546,** 37-44.

Coffey, T.T., Smiciene, G., Hongisto, V., Cao, J., Brecht, S., Herdegen, T. and Courtney, M.J. (2002). C-Jun N-terminal protein kinase (JNK) 2/3 is specifically activated by stress, mediating c-Jun activation, in the presence of constitutive JNK1 activity in cerebellar neurones. *Journal of Neuroscience* **22(11),** 4335-4345.

Cookson, M.R., Mead, C., Austwick, S.M. and Pentreath, V.W. (1995). Use of the MTT assay for estimating toxicity in primary astrocytes and C_6 glial cell cultures. *Toxicolology In Vitro* **9**, 39-48.

Crocker, S.J., Smith, P.D., Jackson-Lewis, V., Lamba, W.R., Hayley, S.P., Grimm, E., Callaghan, S.M., Slack, R.S., Melloni, E., Przedborski, S., Robertson, G.S., Anisman, H., Merali, Z. and Park, D.S. (2003). Inhibiton of calpains prevents neuronal and behavioural deficits in an MPTP mouse model of Parkinson's disease. *Journal of Neuroscience* **23(10)**, 4081-4091.

Crossthwaite, A.J., Hasan, S. and Williams, R.J. (2002). Hydrogen peroxide-mediated phosphorylation of ERK1/2, Akt/PKB and JNK in cortical neurones: dependence on Ca^{2+} and PI3-kinase. *Journal of Neurochemistry* **80**, 24-35.

Cruz, J.C., and Tsai, L. (2004). A Jekyll and Hyde kinase: roles for Cdk-5 in brain development and disease. *Current Opinion in Neurobiology* **14**, 390-394.

D'Amato, R.J., Benham, D.F. and Snyder, S.H. (1987). Characterisation of the binding of N-methyl-4-phenylpyridine, the toxic metabolite of the Parkinsonian neurotoxin N-methyl-4-phenyl-1,2,3,6-tetrahydropyridine to neuromelanin. *Journal of Neurochemistry* **48**, 653-658.

D'Amato, R.J., Lipman, Z.P. and Snyder, S.H. (1986). Selectivity of the parkinsonian neurotoxin MPTP: toxic metabolite MPP^+ binds to neuromelanin. *Science* **231**, 987-989.

Dauer, W., Kholodilov, N., Vila, M., Trillat, A-C., Goodchild, R., Larsen, K.E., Staal, R., Tieu, K., Schmitz, Y., Yuan, C. A., Rocha, M., Jackson-Lewis, V., Hersch, S., Sulzer, D., Prezedborski, S., Burke, R. and Hen, R. (2002). Resistance of α-synuclein null mice to the parkinsonian neurotoxin MPTP. *Proceedings of the National Academy of Science* **99**, 14524-14529.

David, D.C., Layfield, R., Serpell, L., Narain, Y., Goedert, M. and Spillantini, M.G. (2002). Proteasomal degradation of tau protein. *Journal of Neurochemistry* **83**, 176-185.

Davis, G.C., Williams, A.C., Markey, S.P., Ebert, M.H., Caine, E.D., Reichert, C.M. and Kopin, I.J. (1979). Chronic parkinsonism secondary to intravenous injection of meperidine analogues. *Psychiatry Research* **1**, 249-254.

Davis, R.J. (2000). Signal transduction by the JNK group of MAP kinases. *Cell* **103**, 239-252.

De Girolamo, L.A. (2000) PhD thesis, The Nottingham Trent University.

De Girolamo, L.A. and Billett, E.E. (2004). The role of c-jun NH_2 terminal kinase in 1-methyl-4-phenyl-1,2,3,6 tetrahydopyridine induced aberrant neurofilament heavy chain phosphorylation and cell death. Manuscript submitted.

De Girolamo, L.A., Billett, E.E. and Hargreaves, A.J. (2001). Effects of 1-methyl-4-phenyl-1,2,3,6-tetrahydropyridine on differentiating mouse N2a neuroblastoma cells. *Journal of Neurochemistry* **75(1)**, 133-140.

De Girolamo, L.A., Hargreaves, A.J. and Billett, E.E. (1997). Axon outgrowth and neurofilament protein expression in mouse neuroblastoma cells exposed to the neurotoxin MPTP. *Biochemical Society Transactions* **25**, S575.

De Girolamo, L.A., Hargreaves, A.J. and Billett, E.E. (2001). Protection from MPTP-induced neurotoxicity in differentiating mouse N2a neuroblastoma cells. *Journal of Neurochemistry* **76(3),** 650-660.

Del Tredici, K., Rub, U., De Vos, R.A., Bohl, J.R. and Braak, H. (2002). Where does Parkinson's begin? *Journal of Neuropathology and Experimental Neurology* **61,** 413-426.

Dhavan, R and Tsai, L. (2001). A decade of CDK-5. *Nature Reviews Molecular Cell Biology* **2,** 749-759.

Dhavan, R., Greer, P.L., Morabito, M.A., Orlando, L.R. and Tsai, L-H. (2002). The cyclin-dependent kinase 5 activators p35 and p39 interact with the α-subunit of Ca^{2+}/calmodulin-dependent protein kinase II and α-actinin-1 in a calcium dependent manner. *Journal of Neuroscience* **22(18),** 7879-7891.

Ding, Q. and Keller, J.N. (2001). Proteasomes and proteasome inhibition in the central nervous system. *Free Radical Biology and Medicine* **31(5),** 574-584.

Downing, K.H. and Nogales, E. (1998). Tubulin and microtubule structure. *Current Opinion in Cell Biology* **10,** 16-22.

Eberhardt, O., Schulz, J.B. (2003). Apoptotic mechanisms and antiapopotic therapy in the MPTP model of Parkinson's disease. *Toxicology Letters* **00,** 1-17.

Eidelberg, E., Brooks, B.A., Morgan, W.W., Walden, J.G. and Kokemoor, R.H. (1986). Variability and functional recovery in the N-methyl-4-phenyl-1,2,3,6-tetrahydropyridine model of Parkinsonism in monkeys. *Neuroscience* **18,** 817-822.

Encinas, M., Iglesias, M., Liu, Y., Wang, H., Muhaisen, A., Cena, V., Gallego, C. and Comella, J. (2000). Sequential treatment of SH-SY5Y cells with retinoic acid and brain-derived neurotrophic factor gives rise to fully differentiated, neurotrophic factor-dependant, human neuron-like cells. *Journal of Neurochemistry* **75,** 991-1003.

Encinas, M., Iglesias, M., Llecha, N. and Comella, J.X. (1999). Extracellular-regulated kinases and phosphatidylinositol 3-kinase are involved in brain-derived neurotrophic factor-mediated survival and neuritogenesis of the neuroblastoma cell line SH-SY5Y. *Journal of Neurochemistry* **73,** 1409-1421.

Fall, C.P. and Bennett Jr, J.P. (1999). Characterisation and time course of MPP^+ induced apoptosis in human SH-SY5Y neuroblastoma cells. *Journal of Neuroscience Research* **55,** 620-628.

Farlie, P.G., Dringen, R., Rees, S.M., Kannourakis, G. and Bernard, O. (1995). *bcl-2* transgene expression can protect neurons against developmental and induced cell death. *Proceedings of the National Academy of Science USA* **92,** 4397-4401.

Feng, J.F., Rhee, S.G. and Im, M.J. (1996). Evidence that phospholipase delta 1 is the effector in the G(h) (transglutaminase II)-mediated signalling. *Journal of Biological Chemistry* **271(28),** 16451-16454.

Festoff, B.W., SantaCruz, K., Arnold, P.M., Sebastian, C.T., Davies, P.J.A and Citron, B.A. (2002). Injury-induced 'switch' from GTP-regulated to novel GTP-independent isoform of tissue transglutaminase in the rat spinal cord. *Journal of Neurochemistry* **81,** 708-718.

Fesus, L. and Piacentini, M. (2002). Transglutaminase 2: an enigmatic enzyme with diverse functions. *Trends in Biochemical Sciences* **27(10),** 534-539.

Fischer, A., Sananbenesi, F., Schrick, C., Speiss, J. and Radulovic, J. (2002). Cyclin-dependent kinase 5 is required for associative learning. *Journal of Neuroscience* **22(9),** 3700-3707.

Fletcher, A.I., Shuang, R., Giovannucci, D.R., Zhang, L., Bittner, M.A. and Stuenkel, E.L. (1999). Regulation of exocytosis by cyclin-dependent kinase 5 via phosphorylation of Munc18. *Journal of Biological Chemistry* **274,** 4027-4035.

Forno, L.S., De Lanney, L.E., Irwin, I. and Langston, J.W. (1993). Similarities and differences between MPTP - induced Parkinsonism and Parkinson's disease. Neuropathological considerations. *Advances in Neurology* **60,** 600-608.

Forno, L.S., Langston, J.W., De Lanney, L.E. and Irwin, I. (1988). An electron microscope study of MPTP-induced inclusion bodies in old monkey. *Brain Research* **448(1),** 150-157.

Forno, L.S., Sternberger, L.A., Sternberger, N.H., Strefling, A.M., Swanson, K. and Eng, L.F. (1986). Reaction of Lewy bodies with antibodies to phosphorylated and non-phosphorylated neurofilaments. *Neuroscience Letters* **64(3),** 253-258.

Fu, A.K., Fu, W.Y., Cheung, J., Tsim, K.W., Ip, F.C., Wang, J.H. and Ip, N.Y. (2001). Cdk5 is involved in neuroregulin-induced AchR expression at the neuromuscular junction. *Nature Neuroscience* **4,** 374-381.

Fu, H., Hu, Q., Lin, Z., Ren, T., Song, H., Cai, C. and Dong, S. (2003). Aluminium- induced apoptosis in cultured cortical neurones and its effect on SAPK/JNK signal transduction pathway. *Brain Research* **980,** 11-23.

Fu, W-Y., Wang, J.H. and Ip, N.Y. (2002). Expression of Cdk5 and its activators in NT2 cells during neuronal differentiation. *Journal of Neurochemistry* **81,** 646-654.

Funakoshi, T., Takeda, S. and Hirokawa, N. (1996). Active transport of photoactivated tubulin molecules in growing axons revealed by a new electron microscope analysis. *Journal of Cell Biology* **133(6),** 1347-1353.

Gai, W.P., Yuan, H.X., Li, X.Q., Power, J.T., Blumbergs, P.C. and Jensen, P.H. (2000).In situ and in vitro study of colocalisation and segregation of alpha-synuclein, ubiquitin, and lipids in Lewy bodies. *Experimental Neurology* **166,** 324-333.

Gallo, K.A. and Johnson, G.L. (2002). Mixed-Lineage kinase control of JNK and p38 MAPK pathways. *Nature Reviews, Molecular Cell Biology* **3,** 663-672.

Galloway, P.G., Grundkeiqbal, I. and Perry, G. (1988). Lewy bodies contain epitopes both shared and distinct from Alzheimer neurofibrillary tangles. *Journal of Neuropathology and Experimental Neurology* **47(6),** 654-663.

Galloway, P.G., Mulvihill, P. and Perry, G. (1992). Filaments of Lewy bodies contain insoluble cytoskeletal elements. *American Journal of Pathology* **140(4),** 809-822.

Garrington, T.P. and Johnson, G.L. (1999). Organisation and regulation of mitogen-activated protein kinase signalling pathways. *Current Opinion in Cell Biology* **11,** 211-218.

Giasson, B.I. and Mushynski, W.E. (1996). Aberrant stress-induced phosphorylation of perikaryal neurofilaments. *Journal of Biological Chemistry* **271(48),** 30404-30409.

Gómez, C., Reiriz, J., Piqué, M., Gil, J., Ferrer, I. and Ambrosio, S. (2001). Low concentrations of 1-methyl-4-phenylpyridinium ion induce caspase-mediated apoptosis in human SH-SY5Y neuroblastoma cells. *Journal of Neuroscience Research* **63,** 421-428.

Gómez-Santos, C., Ferrer, I., Reiriz, J., Viñals, F., Barrachina, M. and Ambrosio, S. (2002). MPP$^+$ increases α-synuclein expression and ERK/MAP-kinase phosphoryation in human neuroblastoma SH-SY5Y cells. *Brain Research* **935,** 32-39.

Gong, X., Tang, X., Wiedmann, M., Wang, X., Peng, J., Zheng, D., Blair, L., Marshall, J. and Mao, Z. (2003). Cdk-5-mediated inhibition of the protective effects of transcription factor MEF2 in neurotoxicity-induced apoptosis. *Neuron* **38,** 33-46.

Gonzalez-Polo, R.A., Rodriguezmartin, A., Moran, J.M. and Fuentes, J.M. (2004). Protection against MPP$^+$ neurotoxicity in cerebellar granule cells by antioxidants. *Cell Biology International* **28(5),** 373-380.

Gracia-Mata, R., Bebok, Z., Sorscher, E.J. and Sztul, E.S. (1999). Characterisation and dynamics of aggresome formation by a cytosolic GFP-chimera. *Journal of Cell Biology* **146(6),** 1239-1254.

Grant, P., Sharma, P. and Pant, H.C. (2001). Cyclin-dependent protein kinase 5 (Cdk5) and the regulation of neurofilament metabolism. *European Journal of Biochemistry* **268,** 1534-1546.

Greenberg, C.S., Birckbichler. and Rise, R.H. (1991). Transglutaminases: multifunctional cross-linking enzymes that stabilise tissues. *FASEB Journal* **5,** 3071-3077.

Grewal, S.S., York, R.D. and Stork, P.J.S. (1999). Extracellular-signal-related kinase signalling in neurones. *Current Opinion in Neurobiology* **9,** 544-553.

Grierson, A.J., Johnson, V.W. and Miller, C.C.J. (2001). Three different human tau isoforms and rat neurofilament light, middle and heavy chain proteins are cellular substrates for transglutaminase. *Neuroscience Letters* **298,** 9-12.

Griffin, M., Casadio, R. and Bergamini, C.M. (2002). Transglutaminases: Nature's biological glues. *Biochemical Journal* **368,** 277-396.

Guidato, S., Tsai, L., Woodgett, J. and Miller, C.C.J. (1996). Differential cellular phosphorylation of neurofilament heavy side-arms by glycogen synthase kinase-3 and cyclin-dependent kinase-5. *Journal of neurochemistry* **66,** 1698-1706.

Gupta, M., Gupta, B.K., Thomas, R., Bruemmer, V., Sladek, J.R.Jr. and Felton, D.L. (1986). Aged mice are more sensitive to 1-methyl-4-phenyl-1,2,3,6-tetrahydropyridine than young adults. *Neuroscience Letters* **70,** 326-331.

Gupta, S., Barrett, T., Whitmarsh, J., Cavanagh, J., Sluss, H.K., Derijard, B. and Davis, R.J. (1996). Selective interaction of JNK protein kinase isoforms with transcription factors. *EMBO Journal* **15,** 2760-2770.

Hagemann, C and Blank, J.L. (2001). The ups and downs of MEK kinase interactions. *Cellular Signalling* **13,** 863-875.

Halasz, A.S., Palfi, M., Tabi, T., Magyar, K. and Szoko, E. (2004). Altered nitric oxide production in mouse brain after administration of 1-methyl-4-phenyl-1,2,3,6-tetrahydro-pyridin or methamphetamine. *Neurochemistry International* **44(8),** 641-646.

Halliwell, B. and Jenner, P. (1998). Impaired clearance of oxidised proteins in neurodegenerative disease. *Lancet* **351,** 1510.

Hall-Jackson, C.A., Goedert, M., Hedge, P. and Cohen, P. (1999). Effect of SB 203580 on the activity of c-Raf in vitro and in-vivo. *Oncogene* **18(12),** 2047-2054.

Halvorsen, E.M., Dennis, J., Keeney, P.M., Sturgill, T.W., Tuttle, J.B. and Bennett Jr, J.P. (2002).Methylpyridinium (MPP$^+$) – and nerve growth factor-induced changes in pro- and anti-apoptotic signalling pathways in SH-SY5Y neuroblastoma cells. *Brain Research* **952,** 98-110.

Hancock, J.T. (1997). *Cell Signalling*. Essex: Addison Wesley Longman Ltd.

Haroon, Z.A., Hettasch, J.M., Lai, T.S., Dewhirst, M.W. and Greenberg, C.S. (1999). Tissue transglutaminase is expressed, active, and directly involved in rat dermal wound healing and angiogenesis. *FASEB Journal* **13(13),** 1787-1795.

Harper, S.J. and LoGrasso, P. (2001). Signalling for survival and death in neurones. The role of stress-activated kinases, JNK and p38. *Cellular Signalling* **13,** 299-310.

Harris, C.A., Deshmukh, M., Tsui-Pierchala, B., Maroney, A.C. and Johnson Jr, E.M. (2002). Inhibition of the c-jun N-terminal kinase signalling pathway by the mixed lineage kinase inhibitor CEP-1347 (KT 7515) preserves metabolism and growth of trophic factor-deprived neurones. *Journal of Neuroscience* **22(1),** 103-113.

Hartley, C.L., Anderson, V.E.R., Anderson, B.H. and Robertson, J. (1997). Acrylamide and 2,5-hexanedione induce collapse of neurofilaments in SH-SY5Y human neuroblastoma cells to form perikaryal inclusion bodies. *Neuropathology* and *Applied Neurobiology* **23,** 364-372.

Hartley, C.L., Johnston, H.B., Nicol, S., Chan, K.M., Baines, A.J., Anderton, B.H. and Thomas, S.M. (1996). Phenotypic morphology and the expression of cytoskeletal markers during long-term differentiation of human SH-SY5Y neuroblastoma cells. *Toxicology in Vitro* **10,** 539-550.

Hartmann-Petersen, R., Seeger, M. and Gordon, C. (2003). Transferring substrates to the 26S proteasome. *Trends in Biochemical Sciences* **28(1),** 26-31.

Hasegawa, T., Matsuzaki, M., Takeda, A., Kikuchi, A., Akita, H., Perry, G., Smith, M.A. and Itoyama, Y. (2004). Accelerated α-synuclein aggregation after differentiation of SH-SY5Y neuroblastoma cells. *Brain Research* **1013,** 51-59.

Hashiguchi, M., Saito, T., Hisanaga, S. and Hashiguchi, T. (2002). Truncation of CDK5 activator p35 induces intensive phosphorylation of Ser^{202}/Thr^{205} of human tau. *Journal of Biological Chemistry* **277(46),** 44525-44530.

Heikkila, R.E., Hess, A. and Duvoisin, R.C. (1984). Dopaminergic neurotoxicity of 1-methyl-4-phenyl-1,2,3,6-tetrahydropyridine in mice. *Science* **224,** 1451-1453.

Heikkila, R.E., Hess, A. and Duvoisin, R.C. (1985). Dopaminergic neurotoxicity of 1-methyl-4-phenyl-1,2,5,6-tetrahydropyridine in the mouse: Relationships between monoamine oxidase, MPTP metabolism and neurotoxicity. *Life Sciences* **36,** 231-236.

Henchcliff, C. and Burke, R.E. (1997). Increased expression of cyclin-dependent kinase 5 in induced apoptotic neuron death in rat substantia nigra. *Neuroscience Letters* **230,** 41-44.

Hidding, U., Mielke, K., Waetzig V., Brecht, S., Hanisch, Behrens, A., Wagner, E. and Herdegen, T. (2002). The c-Jun N-terminal kinases in cerebral microglia: immunological functions in the brain. *Biochemical Pharmacology* **64,** 781-788.

Höglinger, G., Carrard, G., Michel, P., Medja, F., Lombès, A., Ruberg, M., Friguet, B. and Hirsch, E.C. (2003). Dysfunction of mitochondrial complex I and the proteasome: interactions between two biochemical deficits in a cellular model of Parkinson's disease. *Journal of Neurochemistry* **86,** 1297-1307.

Huang, Y., Cheung, L., Rowe, D. and Halliday, G. (2004). Genetic contributions to Parkinson's disease. *Brain Research Reviews* **46(1),** 44-70.

Humbert, S., Dhavan, R. and Tsai, L-H. (2000). p39 activates cdk5 in neurons, and is associated with the actin cytoskeleton. *Journal of Cell Science* **113,** 975-983.

Hunot, S., Brugg, B., Ricard, D., Michel, P.P., Muriel, M., Ruberg, M., Faucheux, B.A., Agid, Y. and Hirsch, E.C. (1997). Nuclear translocation of NF-κβ is increased in dopaminergic neurons of patients with Parkinson's disease. *Proceedings of the National Academy of Science USA* **94,** 7531-7536.

Imai, Y. and Takahashi, R. (2004). How do Parkin mutations result in neurodegeneration? *Current Opinion in Neurobiology* **14,** 384-389.

Ito, H., Kamei, K., Iwamoto, I., Inaguma, Y., García-Mata, R., Sztul, E. and Kato, K. (2002). Inhibition of proteasomes induces accumulation, phosphorylation, and recruitment of HSP27 and αB-crystallin to aggresomes. *Journal of Biochemistry* **131,** 593-603.

Jalava, A., Heikkila, J., Lintunen, M., Åkerman, K. and Pahlman, S. (1992). Staurosporine induces a neuronal phenotype in SH-SY5Y human neuroblastoma cells that resembles that induced by the phorbol ester 12-O-tetradecanoyl phorbol-13 acetate (TPA). *Federation of European Biochemical Societies* **300(2),** 114-118.

Javitch, J.A., D'Amato, R.J., Strittmatter, S.M. and Synder, S.H. (1985). Parkinsonism-inducing neurotoxin, N-methyl-4-phenyl-1,2,3,6-tetrahydropyridine: Uptake of the metabolite N-methyl-4-phenylpyridine by dopamine neurones explains selective toxicity. *Proceedings of the National Academy of Science* **82,** 2173-2177.

Jenner, P and Olanow, C.W. (1996) Oxidative stress and the pathogenesis of Parkinson's disease. *Neurology* **47(Suppl 3),** S161-S170.

Jenner, P. (2001). Parkinson's disease, pesticides and mitochondrial dysfunction. *Trends in Neurosciences* **24(5),** 245-246.

Jenner, P. (2003). The contribution of the MPTP-treated primate model to the development of new treatment strategies for Parkinson's disease. *Parkinsonism and Related Disorders* **9,** 131-137.

Jha, N., Kumar, J., Boonplueang, R. and Anderson, J.K. (2002). Glutathione decreases in dopaminergic PC12 cells interfere with the ubiquitin protein degradation pathway: relevance for parkinson's disease. *Journal of Neurochemistry* **80,** 555-561.

Johannessen, J.N., Chiueh, C.C., Burns, R.S. and Markey, S.P. (1985). Differences in the metabolism of MPTP in the rodent and primate: parallel differences in sensitivity to its neurotoxic effects. *Life Sciences* **36,** 219-224.

Johnson, G.V.W., Cox, T.M., Lockhart, J.P., Zinnerman, M.D., Miller, M.L. and Powers, R.E. (1997). Transglutaminase activity is increased in Alzheimer's disease brain. *Brain Research* **751,** 323-329.

Johnston, J.A., Ward, C.L. and Kopito, R.R. (1998). Aggresomes: A cellular response to misfolded proteins. *Journal of Cell Biology* **143,** 1883-1898.

Joyce, J, N., Presgraves, S., Renish, L., Borwege, S., Osredkar, T., Hagner, D., Replogle, M., PazSoldan, M. and Millan, M.J. (2003). Neuroprotective effects of the novel D_3/D_2 receptor agonist and antiparkinsonian agent S32504, in vitro against 1-methyl-4-phenylpyridinium (MPP^+) and in vivo against 1-methyl-4-phenyl-1,2,3,6-tetrahydropyridine (MPTP): a comparison to ropinirole. *Experimental Neurology* **184,** 393-407.

Julien, J-P. (1999). Neurofilaments in health and disease. *Current Opinion in Neurobiology* **9,** 554-560.

Junn, E. and Mouradian, M. (2001). Apoptotic signalling in dopamine-induced cell death: the role of oxidative stress, p38 mitogen-activated protin kinase, cytochrome c and caspases. *Journal of Neurochemistry* **78,** 374-383.

Junn, E., Ronchetti, R.D., Quezado, M.M., Kim, S-Y. and Mouradian, M.M. (2003). Tissue transglutaminase-induced aggregation of α-synuclein: implications for Lewy body formation in Parkinson's disease and dementia with Lewy bodies. *Proceedings of the National Academy of Science* **100(4),** 2047-2052.

Kalmes, A., Deou, J., Clowes, A.W. and Daum, G. (1999). Raf-1 is activated by the p38 mitogen-activated protein kinase inhibitor, SB203580. *FEBS Letters* **444(1),** 71-74.

Kamata, H. and Hirata, H. (1999). Redox regulation of cellular signalling. *Cell Signalling* **11(1),** 1-14.

Kaplan, D.R. and Miller, F.D. (2000). Neurotrophin signal transduction in the nervous system. *Current Opinion in Neurobiology* **10,** 381-391.

Kass, G.E., Wright, J.M., Nicotera, P. and Orreniuss, S. (1988). The mechanism of 1-methyl-4-phenyl-1,2,3,6-tetrahydropyridine toxicity: role of intracellular calcium. *Archives of Biochemistry and Biophysics* **260(2),** 789-797.

Kato, Y., Kravchenko, V.V., Tapping, R.I., Han, J., Ulevitch, R.J. and Lee, J.D. (1997). BMK1/ERK5 regulates serum-induced early gene expression through transcription factor MEF2C. *EMBO Journal* **16,** 7054-7066.

Katsuse, O., Iseki, E., Marui, W. and Kosaka, K. (2003). Developmental stages of cortical Lewy bodies and their relation to axonal transport blockage in brains of patients with dementia with Lewy bodies. *Journal of the Neurological Sciences* **211(1-2),** 29-35.

Keller, J.N., Dimayuga, E., Chen, Q., Thorpe, J., Gee, J. and Ding, Q. (2004). Autophagy, proteasomes, lipofuscin, and oxidative stress in the aging brain. *The International Journal of Biochemistry and Cell Biology* **36,** 2376-2391.

Kerokoski, P., Suuronen, T., Salminen, A., Soininen, H. and Pirttila, T. (2002). Influence of phosphorylation of p35, an activator of cyclin-dependent kinase 5 (cdk5), on the proteolysis of p35. *Molecular Brain Research* **106**, 50-56.

Keyse, S.M. (2000). Protein phosphatases and the regulation of mitogn-activated protein kinase signalling. *Current Opinion in Cell Biology* **12**, 186-192.

Kitada, T., Asakawa, S., Hattori, N., Matsumine, H., Yamamura, Y., Minoshima, S., Yokochi, M., Mizuno, Y and Shimizu, N. (1998). Mutations in the parkin gene cause autosomal recessive juvenile parkinsonism. *Nature* **292**, 605-608.

Kopito, R.R. (2000). Aggresomes, inclusion bodies and protein aggregation. *Trends in Cell Biology* **10**, 524-530.

Krüger, R., Fischer, C., Schulte, T., Strauss, K.M., Müller, T., Woitalla, D., Berg, D., Hungs, M., Gobbele, R., Berger, K., Epplen, J.T., Riess, O. and Schöls, L. (2003). Mutation analysis of the neurofilament M gene in Parkinson's disease. *Neuroscience Letters* **351**, 125-129.

Krüger, R., Kuhn, W., Müller, T., Woitalla, D., Graeber, M., Kösel., S., Pruntek, H., Epplen, J.T., Schöls, L. and Reiss, O. (1998). Ala30Pro mutation in the gene encoding α-synuclein in Parkinson's disease. *Nature Genetics* **18**, 106-108.

Kurosaki, R., Muramatsu, Y., Michimata, M., Matsubara, M., Kato, H., Imai, Y., Itoyama, Y. and Araki, T. (2002). Role of nitric oxide synthase against MPTP neurotoxicity in mice. *Neurological Research* **24(7)**, 655-662.

Lai, M., Griffiths, H., Pall, H., Williams, A. and Lunec, J. (1993). An investigation into the role of reactive oxygen species in the mechanism of 1-methyl-4-phenyl-1,2,3,6-tetrahydropyridine toxicity using neuronal cell lines. *Biochemical Pharmacology* **45(4)**, 927-933.

Langston, J.W., Ballard, P., Tetrud, J.W. and Irwin, I. (1983). Chronic parkinsonism in humans due to a product of meperidine-analogue synthesis. *Science* **219(4587)**, 979-980.

Langston, J.W., Irwin, I., Langston, E.B. and Forno, L.S. (1984). 1-methyl-4-phenylpyridiunium ion (MPP$^+$): identification of a metabolite of MPTP, a toxin selective to the substantia nigra. *Neuroscience Letters* **48**, 87-92.

Lasek, R.J., Garner, J.A.. and Brady, S.T. (1984). Axonal transport of the cytoplasmic matrix. *Journal of Cell Biology* **99(1)**, 212s-221s.

Laurent, M. and Fleury, A. (1993). A dynamic model for post-translational modifications of microtubules. FEBS Letters 336(1), 1-7.

Lavedan, C., Buchholtz, S., Nussbaum, R.L., Albin, R.L. and Polymeropoulos, M.H. (2002). A mutation in the human neurofilament M gene in Parkinson's disease that suggests a role for the cytoskeleton in neuronal degeneration. *Neuroscience Letters* **322**, 57-61.

Layfield, R., Cavey, J.R. and Lowe, J. (2003). Role of ubiquitin-mediated proteolysis in the pathogenesis of neurodegenerative disorders. *Aging Research Reviews* **2**, 343-356.

Lee, H., Park, C. and Kim, Y. (2000). MPP$^+$ increases the vulnerability to oxidative stress rather than directly mediating oxidative damage in human neuroblastoma cells. *Experimental Neurology* **165,** 164-171.

Lee, M., Kwon, T.T., Mingwei, L., Peng, J., Friedlander, R.M. and Tsai, L. (2000). Neurotoxicity induces cleavage of p35 to p25 by calpain. *Nature* **405,** 360-364.

Lee, V.M-Y., Otvos, L., Carden, M.J., Hollosi, M., Dietzschold, B. and Lazzarinin, R.A. (1988). Identification of the major multiphosphorylation site in mammalian neurofilaments. *Proceedings of the National Academy of Science* **85,** 1998-2002.

Lee, Z., Kwon, S., Kim, S., Yi, S., Kim, Y. and Ha, K. (2003), Activation of in situ tissue transglutaminase by intracellular reactive oxygen species. *Biochemical and Biophysical Research Communications* **305,** 633-640.

Leist, M. and Nicotera, P. (1998). Apoptosis, excitotoxicity, and neuropathology. *Experimental Cell Research* **239,** 183-201.

Leroy, E., Boyer, R., Auburger, G., Leube, B., Ulm, G., Mezey, E., Harta, G., Brownstein, M.J., Jonnalagada, S. and Chernova, T., Dehejia, A., Lavedan, C., Gasser, T., Stein-bach, P.J., Wilkinson, K.D. and Polymeropolous, M.H. (1998), The ubiquitin pathway in Parkinson's disease. *Nature* **395,** 451-452.

Lesort, M., Attanavanich, K., Zhang, J. and Johnson, G.V.W. (1998). Distinct nuclear localisation and activity of tissue transglutaminase. *Journal of Biological Chemistry* **273(20),** 11991-11994.

Lesort, M., Tucholski, J., Miller, M.L. and Johnson, G.V.W. (2000a). Tissue transglutaminase: a possible role in neurodegenerative disease. *Progress in Neurobiology* **61,** 439-463.

Lesort, M., Tucholski, J., Zhang, J. and Johnson, G.V.W. (2000b). Impaired mitochondrial function results in increased tissue transglutaminase activity in situ. *Journal of Neurochemistry* **75,** 1951-1961.

Leterrier, J.F., Käs, J., Hartwig, J., Vegners, R. and Janmey, P.A. (1996). Mechanical effects of neurofilament cross bridges. *Journal of Biological Chemistry* **271(26).** 15687-15694.

Li, B., Ma, W., Jaffe, H., Zheng, Y., Takahashi, S., Zhang, L., Kulkarni, A.B. and Pant, H.C. (2003). Cyclin-dependent kinase-5 is involved in neuregulin-dependent activation of phosphatidylinositol 3-kinase and Akt activity mediating neuronal survival. *Journal of Biological Chemistry* **278(37),** 35702-35709.

Li, B., Sun, M., Zhang, L., Takahashi, S., Ma, W., Vinade, L., Kulkarni, A.B., Brady, R.O. and Pant, H, C. (2001). Regulation of NMDA receptors by cyclin-dependent kinase-5. *Proceedings of the National Academy of Science* **98(22),** 12742-12747.

Li, B., Zhang, L., Gu, J., Amin, N.D. and Pant, H.C. (2000). Integrin $\alpha_1\beta_1$- mediated activation of cyclin-dependant kinase 5 activity is involved in neurite outgrowth and human neurofilament protein H Lys-Ser-Pro tail domain phosphorylation. *Journal of Neuroscience* **20(16),** 6055-6062.

Li, B., Zhang, L., Takahashi, S., Ma, W., Jaffe, H., Kulkarni, A.B. and Pant, H.C. (2002). Cyclin-dependent kinase 5 prevents neuronal apoptosis by negative regulation of c-jun N-terminal kinase 3. *EMBO Journal* **21(3),** 324-333.

270

Li, M., Linseman, D.A., Allen, M.P., Meintzer, M.K., Wang, X., Laessig, T., Wierman, M.E. and Heidenreich. (2001). Myocyte enhancer factor 2A and 2D undergo phosphorylation and caspase-mediated degeneration during apoptosis of rat cerebellar granule neurons. *The Journal of Neuroscience* **21(17)**, 6544-6552.

Liu, F., Su, Y., Li, B., Zhou, Y., Ryder, J., Gonzalez-DeWhitt, P., May, P.C. and Ni, B. (2003). Regulation of amyloid precursor protein (APP) phosphorylation and processing by p35/Cdk5 and p25/Cdk-5. *FEBS Letters* **547**, 193-196.

Lo Presti, P., Poluha, W., Poluha, D.K., Drinkwater, E. and Ross, A.H. (1992). Neuronal differentiation triggered by blocking cell proliferation. *Cell Growth and Differentiation* **3(9)**, 627-635.

Lombet, A., Zujovic, V., Kandouz, M., Billardon, C., Carvajal-Gonzalez, S., Gompel, A. and Rostene, W. (2001). Resistance to induced apoptosis in the human neuroblastoma cell line SK-N-SH in relation to neuronal differentiation – role of Bcl-2 protein family. *European Journal of Biochemistry* **268(5)**, 1352-1362.

Lopez-Carballo, G., Moreno, L., Masia, S., Perez, P. and Barettino, D. (2002). Activation of the phosphatidylinositol 3-kinase/Akt signalling pathway by retinoic acid is required for neural differentiation of SH-SY5Y human neuroblastoma cells. *Journal of Biological Chemistry* **277(28)**, 25297-25304.

Lorand, L. and Graham, R.M. (2003). Transglutaminases: crosslinking enzymes with pleiotrophic functions. *Nature Reviews Molecular Cell Biology* **4**, 141-156.

Lotharius, J., Dugan, L.L. and O'Malley, K.L. (1999). Distinct mechanisms underlie neurotoxin-mediated cell death in cultured dopaminergic neurones. *The Journal of Neuroscience* **19(4)**, 1284-1293.

Lowry, O.H., Rosebrough, N.J., Farr, A.L. and Radall, R.J. (1951). Protein measurement with the Folin phenol reagent. *Journal of Biological Chemistry* **193**, 265-275.

Luo, Y., Umegaki, H., Wang, X., Abe, R. and Roth, G.S. (1998). Dopamine induces apoptosis through an oxidation-involved SAPK/JNK activation pathway. *The Journal of Biological Chemistry* **273(6)**, 3756-3764.

Macleod, M., Allsopp, T., McLuckie, J. and Kelly, J.S. (2001). Serum withdrawal causes apoptosis in SHSY 5Y cells. *Brain Research* **889**, 308-315.

Majeski, A.E. and Dice, J.F. (2004). Mechanisms of chaperone-mediated autophagy. *The International Journal of Biochemistry and Cell Biology* **36**, 2435-2444.

Mandelkow, E-M., Mandelkow, E. and Milligan, R.A. (1991). Microtubule dynamics and microtubule caps: a time resolved cryo-electron microscopy study. *Journal of Cell Biology* **114(5)**, 977-911.

Markey, S.P., Johannessen, J.N., Chiueh, C.C., Burns, R.S. and Herkenham, M.A. (1984). Intraneuronal generation of a pyridinium metabolite may cause drug-induced parkinsonism. *Nature* **311**, 464-469.

Maroney, A.C., Glicksman, M.A., Basma, A.N., Walton, K.M., Knight Jr, E., Murphy, C.A., Bartlett, B.A., Finn, J.P., Angeles, T., Matsuda, Y., Neff, N.T., and Dionne, C.A. (1998). Motorneurone apoptosis is blocked by CEP-1347 (KT 7515) a novel inhibitor of the JNK signalling pathway. *Journal of Neuroscience* **18(1)**, 104-111.

Marzalek, J.R., Williamson, T.L., Lee, M.K., Xu, Z., Hoffman, P.N., Beecher, M.W., Crawford, T.O. and Cleveland, D.W. (1996). Neurofilament sub-unit NF-H modulates axonal diameter by selectively slowing neurofilament transport. *Journal of Cell Biology* **135**, 711-724.

Masaki, R., Saito, T., Yamada, K. and Ohtani-Kanebo, R. (2000). Accumulation of phosphorylated neurofilaments and increase in apoptosis-specific protein and phosphorylated c-jun induced by proteasome inhibitors. *Journal of Neuroscience Research* **62**, 75-83.

Mathews, C.K. and Van Holde, K.E. (1996). *Biochemistry* (2nd ed). California: The Benjamin/Cummings Publishing Company Inc.

Mathiasen, J.R., McKenna, B.A.W., Saporito, M.S., Ghadge, G.D., Roos, R.P., Holskin, B.P., Wu, Z., Trusko, S.P., Connors, T.C., Maroney., Thomas, B.A., Thomas, J.C. and Bozyczko-Coyne, D. (2004). Inhibition of mixed lineage kinase 3 attenuates MPP$^+$-induced neurotoxicity in SH-SY5Y cells. *Brain Research* **1003**, 86-97.

Matsuzaki, M., Hasegawa, T., Takeda, A., Kikuchi, A., Furukawa, K., Kato, Y. and Itoyama, Y. (2004). Histochemical features of stress-induced aggregates in α-synuclein overexpressing cells. *Brain Research* **1004**, 83-90.

McLean, P.J., Kawamata, H., Shariff, S., Hewett, J., Sharma, N., Ueda, K., Breakefield, X.O. and Hyman, B.T. (2002). Torsin A and heat shock proteins act as molecular chaperones: suppression of alpha-synuclein aggregation. *Journal of Neurochemistry* **83**, 846-854.

McNaught, K. and Jenner, P. (2001). Proteasomal function is impaired in substantia nigra in Parkinson's disease. *Neuroscience Letters* **297**, 191-194.

McNaught, K., Belizaire, R., Isacson, O., Jenner, P. and Olanow, W. (2003). Altered proteasomal function in sporadic Parkinson's disease. *Experimental Neurology* **179**, 38-46.

McNaught, K.S.P., Shashidharan, P., Perl, D.P., Jenner, P. and Olanow, C.W. (2002). Aggresome-related biogenesis of Lewy bodies. *European Journal of Neuroscience* **16(11)**, 2136-2148.

Meredith, G.E., Halliday, G.M. and Totterdell, S. (2004). A critical review of the development and importance of proteinaceous aggregates in animal models of Parkinson's disease: new insights into Lewy body formation. *Parkinsonism and Related Disorders* **10**, 191-202.

Meredith, G.E., Totterdell, S., Petroske, E., Santa Cruz, K., Callison Jr, R. and Lau, Y-S (2002). Lysosomal malfunction accompanies alpha-synuclein aggregation in a progressive mouse model of Parkinson's disease. *Brain Research* **956**, 156-165.

Mielke, K. and Herdegen, T. (2000). JNK and p38 stresskinases – degenerative effectors of signal-transduction-cascades in nervous system. *Progress in Neurobiology* **61**, 45-60.

Mielke, K., Damm, A., Yang, D.D. and Herdegen, T. (2000). Selective expression of JNK isoforms and stress-specific JNK activity in different neural cell lines. *Molecular Brain Research* **75**, 128-137.

Miller, C.C. and Anderton, B.H. (1986). Transglutaminase and the neuronal cytoskeleton in Alzheimer's disease. *Journal of Neurochemisty* **46**, 1912-1922.

Miller, K.E. and Joshi, H.C. (1996). Tubulin transport in neurones. *Journal of Cell Biology* **133(6),** 1355-1366.

Miloso, M., Villa, D., Crimi, M., Galbiati, S., Donzelli, E., Nicolini, G. and Tredici, G. (2004). Retinoic acid-induced neuritogenesis of human neuroblastoma SH-SY5Y cells is ERK independent and PKC dependant. *Journal of Neuroscience Research* **75(2),** 241-252.

Mitchison, T.J. and Kirschner, M.W. (1984). Dynamic instability of microtubule growth. *Nature* **312,** 237-242.

Miyasaka, H., Okabe, S., Ishigro, K., Uchida, T. and Hirokawa, N. (1993). Interaction of the tail domain of high molecular weight subunits of neurofilaments with the COOH-terminal region of tubulin and its regulation by tau kinase. *Journal of Biological Chemistry* **26,** 22695-22702.

Mochizuki, H., Hayakawa, H., Migita, M., Shibata, M., Tanaka, R., Suzuki, A., Shimo-Nakanishi, Y., Urabe, T., Yamada, M., Tamayose, K., Shimada, T., Miura, M. and Mizuno, Y. (2001). An AAV-derived Apaf-1 dominant negative inhibitor prevents MPTP toxicity as antiapoptotic gene therapy for Parkinson's disease. *Proceedings of the National Academy of Science* **98(19),** 10918-10923.

Muchowski, P.J., Ning, K., D'Souza-Schorey, C. and Fields, S. (2002). Requirement of an intact microtubule cytoskeleton for aggregation and inclusion body formation by a mutant Huntington fragment. *Proceedings of the National Academy of Science* **99(2),** 727-732.

Muqit, M.M.K., Davidson, S.M., Payne Smith, M.D., MacCormac, L.P., Kahns, S., Jenson, P.H., Wood, N.W. and Latchmam, D.S. (2004). Parkin is recruited into aggresomes in a stress-specific manner: over-expression of parkin reduces aggresome formation but can be dissociated from parkin's effect on neuronal survival. *Human Molecular Genetics* **13(1),** 117-135.

Murakata, C., Kaneko, M., Gessner, G., Angeles, T.S., Ator, M.A., O'Kane, T.M., McKenna, B.A.W., Thomas, B.A., Mathiasen, J.R., Saporito, M.S., Bozyczko-Coyne, D. and Hudkins, R.L. (2002). Mixed lineage kinase activity of indolocarbazole analogues. *Bioorganic and Medicinal Chemistry Letters* **12(2),** 147-150.

Nagy, L., Saydak, M., Shipley, N., Lu, S., Basilion, J.P., Yan, Y.H., Syka, P., Chandraratna, R.A.S., Stein, J.P., Heyman, R.A. and Davies, P.J.A. (1996). Identification and characterisation of a versatile retinoid response element (retinoic acid receptor response element – retinoid X receptor response element) in the mouse tissue transglutaminase gene promotor. *Journal of Biological Chemistry* **271(8),** 4355-4356.

Nakagawa, T., Chen, J., Zhang, Z., Kanai, Y. and Hirokawa. (1995). Two distinct functions of the carboxyl-terminal tail domain of NF-M upon neurofilament assembly: Cross bridge formation and longitudinal elongation of filaments. *Journal of Cell Biology* **129(2),** 411-429.

Nakamura, K., Bindokas, V.P., Marks, J.D., Wright, D.A., Frim, D.M., Miller R.J. and Kang, U.J. (2000). The selective toxicity of 1-methyl-4-phenylpyridinium to dopaminergic neurons: The role of mitochondrial complex I and reactive oxygen species revisited. *Molecular Pharmacology* **58,** 271-278.

Nakamura, S., Kawamoto, Y., Nakano, S., Akiguchi, I. and Kimura, J. (1997). p35^{nck5a} and cyclin-dependent kinase 5 colocalise in Lewy bodes of brains with Parkinson's disease. *Acta Neuropathol* **94,** 153-157.

Nakaoka, H., Perez D.M., Baek, K.J., Das, T., Husain, A., Misono, K., Im, M.J. and Graham, R.M. (1994). G(H) – A GTP binding protein with transglutaminase activity and receptor signalling function *Science* **264(5165),** 1593-1596.

Nanda, N., Iismaa, S.E., Owens, W.A., Husain, A., Macknay, F. and Graham, R.M. (2001). Targeted inactivation of G_h/tissue transglutaminase II. *Journal of Biological Chemistry* **276(23),** 20673-20678.

Nguyen, M.D., Larivière, R.C. and Julien, J-P. (2001). Deregulation of Cdk5 in a mouse model of ALS: toxicity alleviated by perikaryal neurofilament inclusions. *Neuron* **8,** 135-147.

Nicklas, W.J., Vyas, I. and Heikkila, R.E. (1985). Inhibition of NADH-linked oxidation in brain mitochondria by 1-methyl-4-phenylpyridine, a metabolite of the neurotoxin, 1-methyl-4-phenyl-1,2,5,6-tetrahydropyridine. *Life Sciences* **36,** 2503-2508.

Niethammer, M., Smith, D.S., Ayala, R., Peng, J., Ko, J., Lee, M.S., Morabito, M. and Tsai, L.H. (2000). NUDEL is a novel Cdk5 substrate that associates with LIS1 and cytoplasmic dynein. *Neuron* **28,** 697-711.

Nixon, R. and Sihag. (1991). Neurofilament phosphorylation: a new look at regulation and function. *Trends in Neurosciences* **14(11),** 501-506.

Nixon, R.A. (1998). The slow axonal transport of cytoskeletal proteins. *Current Opinion in Cell Biology* **10,** 87-92.

O'Ferrall, E.K., Robertson, J. and Mushynski, W.E. (2000). Inhibition of abberant and constitutive phosphorylation of the high-molecular-mass neurofilament sub-unit by CEP-1347 (KT7515), an inhibitor of the stress-activated protein kinase pathway. *Journal of Neurochemistry* **75,**2358-2367.

Offen, D., Beart, P.M., Cheung, N.S., Pascoe, C.J., Hochman, A., Gorodin, S., Melamed, E., Bernard, R. and Bernard, O. (1998). Transgenic mice expressing human Bcl-2 in their neurons are resistant to 6-hydroxydopamine and 1-methyl-4-phenyl-1,2,3,6-tetrahydropyridine neurotoxicity. *Proceedings of the National Academy of Science USA* **95,** 5789-5794.

Oh-hashi, K., Maruyama, W., Yi, H., Takahashi, T., Naoi, M. and Isobe, K. (1999). Mitogen-activated protein kinase pathway mediates peroxynitrite-induced apoptosis in human dopaminergic neuroblastoma SH-SY5Y cells. *Biochemical and Biophysical Research Communications* **263,** 504-509.

Ohshima, T., Ward, J.M., Huh, C., Longenecker, G., Veeranna., Pant, H.C., Brady, R.O., Martin, L.J. and Kulkarni, A.B. (1996). Targeted disruption of the cyclin-dependet kinase 5 gene results in abnormal corticogenesis, neuronal pathology and perinatal death. *Proceedings of the National Academy of Science USA* **93,** 11173-11178.

Okamoto, S., Krainc, D., Sherman, K. and Lipton, S.A. (2000). Antiapoptotic role of the p38 mitogen-activated protein kinase-myocyte enhancer factor 2 transcription factor pathway during neuronal differentiation. *Proceedings of the National Academy of Science USA* **97(13),** 7561-7566.

Oliverio, S., Amendola, A., Rodolfo, C., Spinedi, A. and Piacentini, M. (1999). Inhibition of "tissue" transglutaminase increases cell survival by preventing apoptosis. *Journal of Biological Chemistry* **274(48),** 34123-34128.

Orr, H.T. (2004). Neuron protection agency. *Nature* **431,** 747-748.

Orrenius, S., Zhivotovsky, B. and Nicotera, P. (2003). Regulation of cell death: the calcium-apoptosis link. *Nature Reviews* **4,** 252-265.

Orth, M. and Schapira, A.H.V. (2002). Mitochondrial involvement in Parkinson's disease. *Neurochemistry International* **40,** 533-541.

Påhlman, S., Ruusala, A., Abrahamsson, L., Mattsson, M.E. and Esscher, T. (1984). Retinoic acid-induced differentiation of cultured human neuroblastoma cells: a comparison with phorbolester-induced differentiation. *Cell differentiation* **14,** 135-144.

Palazzo, A., Ackerman, B. and Gundersen, G.C. (2003). Tubulin acetylation and cell motility. *Nature* **421,** 230.

Parameswaran, K.N., Cheng, X., Chen, E., Velasco, P.T., Wilson, J.H. and Lorand, L. (1997). Hydrolysis of $\gamma.\varepsilon$ isopeptides by cytosolic transglutaminases and by coagulation factor $XIII_a$. *Journal of Biological Chemistry* **272,** 10311-10317.

Patrick, G.N., Zhou, P., Kwon, Y.T., Howley, P.M. and Tsai, L. (1998). p35, the neuronal-specific activator of cyclin-dependent kinase 5 (Cdk-5) is degraded by the ubiquitin-proteasome pathway. *Journal of Biological Chemistry* **273(37),** 24057-24064.

Patrick, G.N., Zuckerberg, L., Nikolic, M., de la Monte, S., Dikkes, P. and Tsai, L. (1999). Conversion of p35 to p25 deregulates Cdk5 activity and promotes neurodegeneration. *Nature* **402,** 615-621.

Patzke, H. and Tsai, J. (2002). Calpain-mediated cleavage of the cyclin-dependant kinase-5 activator p39 to p29. *The Journal of Biological Chemistry* **277,** 8054-8060.

Perez-Olle, R., Lopez-Toledano, M.A., Liem, R.K.H. (2004). The G336S variant in the human neurofilament-M gene does not affect its assembly or distribution: Importance of the functional analysis of neurofilament variants. *Journal of Neuropathology and Experimental Neurology* **63(7),** 759-774.

Petroske, E., Meredith, G.E., Callen, S., Totterdell, S. and Lau, Y-S. (2001). Mouse model of Parkinsonism: A comparison between subacute MPTP and chronic MPTP/probenecid treatment. *Neuroscience* **106(3),** 589-601.

Piacentini, M., Farrace, M.G., Pieredda, L., Matarrese, P., Ciccosanti, F., Falasca, F., Rodolfo, C., Giammarioli, A.M., Verderio, E., Griffin, M. and Malorni W. (2002). Transglutaminase overexpression sensitises neuronal cell lines to apoptosis by increasing mitochondrial membrane potential and cellular oxidative stress. *Journal of Neurochemistry* **81,** 1061-1072.

Pifl, C., Giros, B. and Caron, M.G. (1993). Dopamine transporter expression confers cytotoxicity to low doses of the Parkinsonism-inducing neuroroxin 1-methyl-4-phenylpyridinium. *Journal of Neuroscience* **13(10),** 4246-4253.

Pigino, G., Paglini, G., Ulloa, L., Avila, J. and Cáceres, A. (1997). Analysis of the expression, distribution and function of cyclin dependent kinase 5 (cdk5) in developing cerebellar macroneurons. *Journal of Cell Science* **110,** 257-270.

Piredda, L., Farrace, M.G., Bello, M.L., Malorni, W., Melino, G., Petruzzelli, R. and Piacentini, M. (1999). Identification of 'tissue' transglutaminase binding proteins in neural cells committed to apoptosis. *FASEB Journal* **13,** 355-364.

Pollanen, M.S., Bergeron, C. and Luitgard, W. (1993). Deposition of detergent-resistant neurofilaments into Lewy body fibrils. *Brain Research* **603(1),** 121-124.

Poltorak, M. and Freed, W.J. (1989). Immunoreactive phosphorylated epitopes on neurofilaments in neuronal perikarya may be obscured by tissue processing. *Brain Research* **480,** 349-354.

Polymeropolous, M.H., Lavedan, C., Leroy, E., Ide, S.E., Dehejia, A., Dutra, A., Pike, B., Root, H., Rubenstein, J., Boyer, R., Stenroos, E.S., Chandrasekharappa, S., Athanassiadou, A., Papapetropoulos, T., Johnson, W.G., Lazzarini, A.M., Douvoisin, R.C., Di Iorio, G., Globe, L.I. and Nussbaum, R.L. (1997). Mutation in the α-synuclein gene identified in families with Parkinson's disease. *Science* **276,** 2045-2047.

Polymeropoulos, M.H., Higgins, J.J., Globe, L.I., Johnson, W.G., Ide, S.E., Di Iorio, G., Sanges, G., Stenroos, E.S., Pho, L.T., Schaffer, A.A., Lazzarini, A.M., Nussbaum, R.L. and Duvoisin, R.C. (1996). Mapping of a gene for Parkinson's disease to chromosome 4q21-23. *Science* **274,**1197-1199.

Pomérance, M., Multon, M-C., Parker, F., Venot, C., Blondeau, J-P., Tocqué, B. and Schweighoffer, F. (1998). Grb2 interaction with MEK-kinase 1 is involved in regulation of jun-kinase activities in response to epidermal growth factor. *Journal of Biological Chemistry* **273(38),** 24301-24304.

Prahlad, V., Helfand, B.T., Langford, G.M., Vale, R.D. and Goldman, R.D. (2000). Fast transport of neurofilament protein along microtubules in squid axoplasm. *Journal of Cell Science* **113,** 3939-3946.

Prasad, K.N., Cole, W.C and Kumar, B. (1999). Multiple antioxidants in the prevention and treatment of Parkinson's disease. *Journal of the American College of Nutrition* **18(5),** 413-423.

Przedborski, S., Jackson-Lewis, V., Yokoyama, R., Shibata, T., Dawson, V.L. and Dawson, T.M. (1996). Role of neuronal nitric oxide in 1-methyl-4-phenyl-1,2,3,6-tetrahydropyridine (MPTP)-induced dopaminergic cytotoxicity. *Proceedings of the National Academy of Science USA* **93(10),** 4565-4571.

Rampello, L., Cerasa, S., Alvano, A., Buttà, V., Raffaele, R., Vecchio, I., Carvallaro, T., Cimino, E.,Incognito, T and Nicoletti, F. (2004). Dementia with Lewy bodies: a review. *Archives of Gerontology and Geriatrics* **39,** 1-14.

Ramsay, R.R. and Singer, T.P. (1986). Energy dependent uptake of N-methyl-4-phenylpyridinium, the neurotoxic metabolite of 1-methyl-4-phenyl-1,2,3,6-tetrahydropyridine, by mitochondria. *The Journal of Biological Chemistry* **261(17),** 7585-7587.

Ramsay, R.R., Kowal, A.J., Johnson, M.K., Salach, J.I. and Singer, T.P. (1987). The inhibition site of MPP^+, the neurotoxic bioactivation product of 1-methyl-4-phenyl-1,2,3,6-tetrahydropyridine is near the Q-binding site of NADH dehydrogenase. *Archives of Biochemistry and Biophysics* **259(2),** 645-649.

276

Rang, H.P., Dale, M.M. and Ritter, J.M. (1995). *Pharmacology* (3rd ed). Edinburgh: Churchill Livingstone.

Rao, R.V. and Bredesen, D.E.(2004). Misfolded proteins, endoplasmic reticulum stress and neurodegeneration. *Current Opinion in Cell Biology* **16,** 653-662.

Ray, S.K. Wilford, G.G., Ali, S.F. and Banik, N.L. (2000). Calpain upregulation in spinal cords of mice with 1-methyl-4-phenyl-1,2,3,6-tetrahydropyridine (MPTP)-induced Parkinson's disease. *Annals of the New York Academy of Sciences* **914,** 275-283.

Ren, Y., Zhao, J. and Feng, J. (2003). Parkin binds to α/β tubulin and increases their ubiquitination and degradation. *Journal of Neuroscience* **23(8),** 3316-3314.

Ross, R.A., Spengler, B.A., and Biedler, J.L. (1983). Coordinate morphological and biochemical interconversion of human neuroblastoma cells. *JNCI* **71(4),** 741-749.

Roux, P.P., Dorva, G., Boudreau, M., Angers-Loustau, A., Morris, S.J., Makkerh, J. and Barker, P.A. (2002). K252a and CEP1347 are neuroprotective compounds that inhibit mixed lineage kinase-3 and induce activation of Akt and ERK. *The Journal of Biological Chemistry* **277(51),** 49473-49480.

Roy, S., Coffee, P., Smith, G., Liem, R., Brady, S. and Black, M. (2000). Neurofilaments are transported rapidly but intermittently in axons: implications for slow axonal transport. *Journal of Neuroscience* **20(18),** 6849-6861.

Ruffels, J., Griffin, M. and Dickenson, J.M. (2004). Activation of ERK 1/2, JNK and PKB by hydrogen peroxide in human SH-SY5Y neuroblastoma cells: role of ERK 1/2 in H_2O_2 – induced cell death. *European Journal of Pharmacology* **483,** 163-173.

Ruiz-Leon, Y. and Pascual, A. (2003). Induction of tyrosine kinase receptor B by retinoic acid allows brain-derived neurotrophic factor-induced amyloid precursor protein gene expression in human SH-SY5Y neuroblastoma cells. *Neuroscience* **120,** 1019-1026.

Saito, T., Ishiguro, K., Onuki, R., Nagai, Y., Kishimoto, T. and Hisanaga, S-I. (1998). Okadaic acid-stimulated degradation of p35, an activator of CDK5, by proteasome in cultured neurons. *Biochemical and Biophysical Research Communications* **252,** 775-778.

Saito, T., Onuki, R., Fujita, Y., Kusakawa, G., Ishiguro, K., Bibb, J.A., Kishimoto, T. and Hisanaga, S. (2003). Developmental regulation of the proteolysis of the p35 cyclin-dependent kinase 5 activator by phosphorylation. *Journal of Neuroscience* **23(4),** 1189-1197.

Samuels, B.A. and Tsai, L-H. (2003). Cdk5 is dynamo at the synapse. *Nature Cell Biology* **5(8),** 689-690.

Saporito, M.S., Brown, E.M., Miller, M.S. and Carswell, S. (1999). CEP-1347/KT-7515, an inhibitor of c-jun N-terminal kinase activation, attenuates the 1-methyl-4-phenyl tetrahydropyridine-mediated loss of nigrostriatal dopaminergic neurones in vivo. *Journal of Pharmacology and Experimental Therapeutics* **288,** 421-427.

Saporito, M.S., Thomas, B.A. and Scott, R.W. (2000). MPTP activates c-Jun NH_2-terminal kinase (JNK) and its upstream regulatory kinase MKK4 in nigrostriatal neurons in vivo. *Journal of Neurochemistry* **75,** 1200-1208.

Satoh, T., Nakatsuka, D., Watanabe, Y., Nagata, I., Kikuchi, H. and Namura, S. (2000). Neuroprotection by MAPK/ERK kinase inhibition with U0126 against oxidative stress in a mouse neuronal cell line and rat primary cultured cortical neurones. *Neuroscience Letters* **288,** 163-166.

Schaeffer, H.J. and Weber, M.J. (1999). Mitogen-activated protein kinases: specific messages from ubiquitous messengers. *Molecular and Cellular Biology* **19(4),** 2435-2444.

Schapira, A.H.V. (2004). Disease modification in Parkinson's disease. *Lancet Neurology* **3,** 362-368.

Schapira, A.H.V., Cooper, J.M., Dexter, D., Jenner, P., Clark, J.B. and Marsden C.D. (1989). Mitochondrial complex I deficiency in Parkinson's disease. *Lancet* **8649,** 1269.

Schluter, O.M., Fornai, F., Alessandrini, M.G., Takamori, S., Geppert, M., Jahn, R. and Sudhof, T.C. (2003). Role of alpha-synuclein in 1-methyl-4-phenyl-1,2,3,6-tetra-hydropyridine-induced parkinsonism in mice. *Neuroscience* **118(4),** 985-1002.

Schmidt, M.L., Murray, J., Lee, V.M-Y., Hill, W.D., Wertkin, A. and Trojanowski, J.Q. (1991). Epitope map of neurofilament protein domains in cortical and peripheral nervous system Lewy bodies. *American Journal of Pathology* **139(1),** 53-65.

Shamoto-Nagai, M., Maruyama, W., Kato, Y., Isobe, K., Tanaka, M., Naoi, M. and Osawa, T. (2003). An inhibitor of mitochondrial complex I, rotenone, inactivates proteasome by oxidative modification and induces aggregation of oxidised proteins in SH-SY5Y cells. *Journal of Neuroscience Research* **74,** 589-597.

Sharma, M., Sharma, P. and Pant, H.C. (1999c). CDK-5-mediated neurofilament phosphorylation in SH-SY5Y human neuroblastoma cells. *Journal of Neurochemistry* **73,** 79-86.

Sharma, P., Sharma, M, Amin, N.D., Albers, W. and Pant, H.C. (1999a). Regulation of cyclin-dependent kinase 5 catalytic activity by phosphorylation. *Proceedings of the National Academy of Science USA* **96,** 11156-11160.

Sharma, P., Steinbach, P., Sharma, M., Amin, N.D., Barchi Jr., J.J. and Pant, H. (1999b). Identification of the substrate binding site of cyclin-dependent kinase 5. *Journal of Biological Chemistry* **274(14),** 9600-9606.

Sharma, P., Veeranna., Sharma, M., Amin, N.D., Sihag, R.K., Grant, P., Ahn, N., Kulkarni, A.B. and Pant, H.C. (2002). Phosphorylation of MEK1 by cdk-5/p35 down-regulates the mitogen-activated protein kinase pathway. *Journal of Biological Chemistry* **277(1),** 528-534.

Shea T.B., Yabe, J.T., Ortiz, D., Pimenta, A., Loomis, P, Goldman, R.D. Amin, N. and Pant, H.C. (2004a). CDK-5 regulates axonal transport and phosphorylation of neurofilaments in cultured neurones. *Journal of Cell Science* **117,** 933-941.

Shea, T.B. and Beermann, M.L. (1994). Respective roles of neurofilaments, microtubules, MAP1B, and tau in neurite outgrowth and stabilisation. *Molecular Biology of the Cell* **5,** 863-875.

Shea, T.B. and Flanagan, L.A. (2001). Kinesin, dynein and neurofilament transport. *Trends in Neuroscience* **24(11),** 644-648.

Shea, T.B., Beermann, M.L. and Nixon, R.A. (1995). Aluminium treatment of intact neuroblastoma cells alters neurofilament subunit phosphorylation, solubility, and proteolysis. *Molecular and Chemical Neuropathology* **26(1),** 1-14.

Shea, T.B., Dahl, D.C., Nixon, R.A. and Fischer, I. (1997b). Triton-soluble phosphovariants of the heavy neurofilament sub-unit in developing an mature mouse central nervous system. *Journal of Neuroscience Research* **48,** 515-523.

Shea, T.B., Jung, C. and Pant, H.C. (2003). Does neurofilament phosphorylation regulate axonal transport? *TRENDS in Neurosciences* **26(8),** 397-400.

Shea, T.B., Jung, C., Yabe, J., Ma, D. and Fischer, I. (1998). Extensive phosphorylation and axonal transport of Triton-soluble neurofilament subunits. *Sub-cellular Biochemistry* **31,** 527-561.

Shea, T.B., Majocha, R.E., Marotta, C.A. and Nixon, R.A. (1988). Soluble, phosphorylated forms of the high molecular weight neurofilament protein in perikarya of cultured neuronal cells. *Neuroscience Letters* **97,** 291-297.

Shea, T.B., Sihag, R.K. and Nixon, R.A. (1990). Dynamics of phosphorylation and assembly of the high molecular weight neurofilament sub-unit in NB2a/d1 neuroblastoma. *Journal of Neurochemistry* **55,** 1784-1792.

Shea, T.B., Wheeler, E. and Jung, C. (1997a). Aluminium inhibits neurofilament assembly, cytoskeletal incorporation, and axonal transport. Dynamic nature of aluminium-induced perikaryal neurofilament accumulations as revealed by subunit turnover. *Molecular and Chemical Neuropathology* **32(1-3),** 17-39.

Shea, T.B., Zheng, Y.L., Ortiz, D. and Pant, H.C. (2004b). Cyclin-dependent kinase 5 increases perikaryal neurofilament phosphorylation and inhibits neurofilament axonal transport in response to oxidative stress. *Journal of Neuroscience Research* **76(6),** 795-800.

Shelton, B. and Johnson, G.V.W. (2004). Cyclin-dependent kinase-5 in neurodegeneration. *Journal of Neurochemistry* **88,** 1313-1326.

Shepherd, G.M. (1994). *Neurobiology* (3rd ed). New York: Oxford University Press.

Shoesmith Berke, S.J. and Paulson, H.L. (2003). Protein aggregation and the ubiquitin proteasome pathway: gaining the UPPer hand on neurodegeneration. *Current Opinion in Genetics and Development* **13,** 253-261.

Shringarpure, R., Grune, T., Mehlhase, J. and Davies, K.J.A. (2003). Ubiquitin conjugation is not required for the degradation of oxidised proteins by proteasome. *Journal of Biological Chemistry* **278(1),** 311-318.

Siegel, G.J. (1999). *Basic neurochemistry, molecular and cellular aspects* (6th ed). Philadelphia: Lipincott-Raven Publishers.

Singh, U.S., Kunar, M.T., Kao, Y-L. and Baker, K.M. (2001). Role of transglutaminase II in retinoic acid-induced activation of RhoA-associated knase-2. *EMBO Journal* **20(10),** 2413-2423.

Singh, U.S., Pan, J., Kao, Y., Joshi, S., Young, K.L. and Baker, K.M. (2003). Tissue transglutaminase mediates activation of Rho A and MAP kinase pathways during retinoic acid-induced neuronal differentiation of SH-SY5Y cells. *Journal of Biological Chemistry* **1(3),** 391-399.

Smith, D.S. and Tsai, L-H. (2002). Cdk5 behind the wheel: a role in trafficking and transport. *Trends in Cell Biology* **12(1),** 28-36.

Smith, P.D., Crocker, S.J., Jackson-Lewis, V., Jordan-Scutto, K.L., Hayley, S., Mount, M.P., O'Hare, M.J., Callaghan, S., Slack, R.S., Przedborski, S., Anisman, H. and Park, D.S. (2003). Cyclin-dependent kinase 5 is a mediator of dopaminergic neuron loss in a mouse model of Parkinson's disease. *Proceedings of the National Academy of Science* **100(23),** 13650-13655.

Song, X. and Ehrich, M. (1997a). Alterations of cytoskeletal tau protein of SH-SY5Y human neuroblastoma cells after exposure to MPTP. *Neurotoxicology* **19(1),** 73-82.

Song, X. and Ehrich, M. (1997b). MPTP affects cholinergic parameters in SH-SY5Y human neuroblastoma cells. *In Vitro Toxicology* **10(4),** 437-453.

Song, X. and Ehrich, M. (1998). Uptake and metabolism of MPTP and MPP+ in SH-SY5Y human neuroblastoma cells. In *vitro and Molecular Toxicology* **11(1),** 314.

Song, X., Perkins, S., Jortner, B.S. and Ehrich, M. (1997). Cytotoxic effects of MPTP on SH-SY5Y human neuroblastoma cells. *Neurotoxicology* **18(1),** 341-354.

Spillantini, M.G., Crowther, R.A., Jakes, R., Hasegawa, M. and Goedert, M. (1998). α-synuclein in filamentous inclusions of Lewy bodies from Parkinson's disease and dementia with Lewy bodies. *Proceedings of the National Academy of Science USA* **95,** 6469-6473.

Spillantini, M.G., Schmidt, M.L., Lee, V.Y., Trojanowski, J.Q., Jakes, R. and Goedert, M. (1997). α-synuclein in Lewy bodies. *Nature* **388,** 839-840.

Stanciu, M. and DeFranco, D.B. (2002). Prolonged nuclear retention of activated extracellular signal-related protein kinase promotes cell death generated by oxidative toxicity or proteasome inhibition in a neuronal cell line. *The Journal of Biological Chemistry* **277(6),** 4010-4017.

Stanciu, M., Wang, Y., Kentor, R., Burke, N., Watkins, S., Kress, G., Reynolds, I., Klann, E., Angiolieri, M.R., Johnson, J.W. and DeFranco, D.B. (2000). Persistent activation of ERK contributes to glutamate-induced oxidative toxicity in a neuronal cell line and primary cortical neuron cultures. *The Journal of Biological Chemistry* **275(16),** 12200-12206.

Stull, N.D., Polen, D.P. and Iacovitti, L. (2001). Antioxidant compounds protect dopamine neurones from death due to oxidative stress in vitro. *Brain Research* **931,** 181-185.

Sun, D., Leung, C.L. and Liem, R.H. (1996). Phosphorylation of the high molecular weight neurofilament protein (NF-H) by Cdk5 and p35. *Journal of Biological Chemistry* **271(24),** 14245-14251.

Sun, W., Kesavan, K., Scharfer, B.C., Garrington, T.P., Ware, M., Johnson, N.L., Gelfand, E.W. and Johnson, G.L. (2001). MEKK2 associates with the adapter protein Lad/RIBP and regulates the MEK5-BMK1/ERK5 pathway. *Journal of Biological Chemistry* **276(7),** 5093-5100.

Suzuki, Y.J., Forman, H.J. and Sevanian, A. (1997). Oxidants as stimulators of signal transduction. *Free Radical Biology and Medicine* **22(1/2)**, 269-285.

Tanaka, E.M. and Kirschner, M.W. (1991). Microtubule behaviour in the growth cones of living neurones during axon elongation. *Journal of cell biology* **115**, 345-363.

Terada, S. (2003). Where does slow axonal transport go? *Neuroscience Research* **47**, 367-372.

Terada, S., Kinjo, M. and Hirokawa, H. (1996). Oligomeric tubulin in large transporting complex is transported via kinesin in squid giant axons. *Cell* **103**, 141-155.

Tibbles, L.A. and Woodgett, J.R. (1999). The stress-activated protein kinase pathways. *Cellular and Molecular Life Sciences* **55**, 1230-1254.

Tieu, K., Zuo, D.M. and Yu, P.H. (1999). Differential effects of staurosporine and retinoic acid on the vulnerability of the SH-SY5Y neuroblastoma cells: Involvement of Bcl-2 and p35 proteins. *Journal of Neuroscience Research* **58**, 426-435.

Tipton, K.F. and Singer, T.P. (1993). Advances in our understanding of the mechanisms of the neurotoxicity of MPTP and related compounds. *Journal of Neurochemistry* **61(4)**, 1191-1206.

Tolentino, P.J., DeFord, S.M., Notterpek, L., Glenn, C.C., Pike, B.R., Wang, K.K.W. and Hayes, R.L. (2002). Up-regulation of tissue-type transglutaminase after traumatic brain injury. *Journal of Neurochemistry* **80**, 579-588.

Tran, P.T., Walker, R.A. and Salmon, E.D. (1997). A metastable intermediate state of microtubule dynamic instability that differs significantly between plus and minus ends. *Journal of Cell Biology.* **138(1)**, 105-117.

Tseng, H., Zhou, Y., Shen, Y. and Tsai, L. (2002). A survey of Cdk5 activator p35 and p25 levels in Alzheimer's disease brains. *Federation of European Biochemical Societies* **523**, 58-62.

Tuchloski, J. and Johnson, G.V.W. (2003). Tissue transglutaminase directly regulates adenylyl cyclase resulting in enhanced c-AMP-response element-binding protein (CREB) activation. *Journal of Biological Chemistry* **278(29)**, 26838-26843.

Tucholski, J. and Johnson, G.V.W. (2002). Tissue transglutaminase differentially modulates apoptosis in a stimuli dependent manner. *Journal of Neurochemistry* **81**, 780-791.

Tucholski, J., Kuret, J. and Johnson, G.VW. (1999). Tau is modified by tissue transglutaminase in situ: Possible functional and metabolic effects of polyamination *Journal of Neurochemistry* **73(5)**, 1871-1880.

Tucholski, J., Lesort, M. and Johnson, G.V.W. (2001). Tissue transglutaminase is essential for neurite outgrowth in human neuroblastoma SH-SY5Y cells. *Neuroscience* **102(2)**, 481-491.

Urani, C., Brambilla, E., Santagostino, A. and Camatini, M. (1994). 1-methyl-4-phenyl-1,2,3,6-tetrahydropyridine (MPTP) affects the actin cytoskeleton and calcium level of Swiss 3T3 mouse fibroblasts. *Toxicology* **91**, 117-126.

Veeranna., Amin, N.D., Ahn, N.G., Jaffe, H. Winters, C.A., Grant, P. and Pant, H.C. (1998). Mitogen-activated protein kinases (ERK1,2) phosphorylate Lys-Ser-Pro (KSP) repeats in neurofilament proteins NF-H and NF-M. *Journal of Neuroscience* **18(11),** 4008-4021.

Verderio, E., Gaudry, C., Gross, S., Smith, C., Downes, S. and Griffin, M. (1999). Regulation of cell surface tissue transglutaminase: effects on matrix storage of latent transforming growth factor-β binding protein-1. *Journal of Histology and Cytochemistry* **47(11),** 1417-1432.

Verderio, E., Nicholas, B., Gross, S. and Griffin, M. (1998). Regulated expression of tissue transglutaminase in Swiss 3T3 fibroblasts: effects of the processing of fibronectin, cell attachment, and cell death. *Experimental Cell Research* **239,** 119-138.

Vidaluc, J-L. (1996). MPTP as a molecular paradigm for neurodegeneration. A review of its connections with relevant molecules. *Current Medicinal Chemistry* **3,** 117-138.

Waetzig, V. and Herdegen, T. (2004). Neurodegenerative and physiological actions of c-jun N-terminal kinases in the mammalian brain. *Neuroscience Letters* **361,** 64-67.

Wang, W., Shi, L., Xie, Y., Ma, C., Li, W., Su, X., Huang, S., Chen, Z., Zhu, Z, Mao, Z., Han, Y. and Li, M. (2004). SP600125, a new JNK inhibitor, protects dopaminergic neurones in the MPTP model of Parkinson's disease. *Neuroscience Research* **48,** 195-202.

Wang, X., Martindale, J.L., Liu, Y. and Holbrook, N.J. (1998). The cellular response to oxidative stress: influences of mitogen-activated protein kinase signalling pathways on cell survival. *Biochemical Journal* **333,** 291-300.

Watanabe, H., Muramatsu, Y., Kurosaki, R., Michimata, M., Matsubara, M., Imai, Y. and Araki, T. (2004). Protective effects of neuronal nitric oxide synthase inhibitor in mouse brain against MPTP neurotoxicity: an immunohistological study. *European Neuropsychopharmacology* **14(2),** 93-104.

Wei, W., Wang, X. and Kusiak, J.W. (2002). Signalling events in amyloid β-peptide-induced neuronal death and insulin-like growth factor I protection. *Journal of Biological Chemistry* **277(20),** 17649-17656.

Wigley, W.C., Fabunmi, R.P., Lee, M.G., Marino, G.R., Mualem, S., DeMartino, G.N. and Thomas, P.J. (1999). Dynamic association of proteasomal machinery with the centrosome. *Journal of Cell biology* **145(3),** 481-490.

Wu, J and Zern, A. (2004). Tissue transglutaminase, a key enzyme involved in liver diseases. *Hepatology Research* **29,**1-8.

Wullner, U., Loschmann, P-A., Schulz, J.B., Schmid, A., Dringe, R., Eblen, F., Turski, L. and Klockgether, T. (1996). Glutathione depletion potentiates MPTP and MPP$^+$ toxicity in nigral dopaminergic neurones. *Neuro Report* **7,** 921-923.

Xia, X.G, Harding, T., Weller, M., Bieneman, A., Uney, J.B. and Schulz, J.B. (2001). Gene transfer of the JNK interacting protein-1 protects dopaminergic neurones in the MPTP model of Parkinson's disease. *Proceedings of the National Academy of Science* **98(18),** 10433-10438.

Xia, Z., Dickens, M., Raingeaud, J., Davis, R.J. and Greenberg, M.E. (1995). Opposing effects of ERK and JNK-p38 MAP kinases on apoptosis. *Science* **270,** 1326-1311.

Xu, Z., Marszalek, J.R., Lee, M.K., Wong, P.C., Folmer, J., Crawford, T.O., Hsieh, S., Griffin, J.W. and Cleveland, D.W. (1996). Subunit composition of neurofilaments specifies axonal diameter. *Journal of Cell Biology* **133(5),** 1061-1069.

Yabe, J.T. and Shea, T.B. (2000). Phospho-dependent association of neurofilament proteins with kinesin in situ. *Cell motility of the Cytoskeleton* **42,** 230-240.

Yabe, J.T., Chylinski, T., Wang, F., Pimenta, A., Kattar, S.D., Linsley, M., Chan, W. and Shea, T.B. (2001). Neurofilaments consist of distinct populations that can be distinguished by C-terminal phosphorylation, bundling, and axonal transport rate in growing axonal neurites. *Journal of Neuroscience* **21(7),** 2195-2205.

Yabe, J.T., Pimenta, A. and Shea, T.B. (1999), Kinesin-mediated transport of neurofilament protein oligomers in growing axons. *Journal of Cell Science* **112,** 3799-3814.

Yee, V.C., Pedersen, L.C., Le Trong, I., Bishop, P., Stenkamp, R.E. and Teller, D.C. (1994). Three-dimentional structure of a transglutaminase: human blood coagulation factor XIII. *Proceedings of the National Academy of Science USA* **91,**7296-7300.

Yuste, V.J., Sanchez-Lopez, I., Sole, C., Encinase, M., Bayascas, J.R., Boix, J. and Comella, J.X. (2002). The prevention of the staurosporine-induced apoptosis by Bcl-X$_L$, but not by Bcl-2 or caspase inhibitors, allows the extensive differentiation of human neuroblastoma cells. *Journal of Neurochemistry* **80,** 126-139.

Zang, L.Y. and Mistra, H.P. (1992). Superoxide radical production during the auto-oxidation of 1-methyl-4-phenyl-2,3-dihydropyridinium perchlorate. *Journal of Biological Chemistry* **267,** 17547-17552.

Zhang, J., Guttermann, R.P. and Johnson, G.V.W. (1998b). Tissue transglutaminase is an in situ substrate of calpain: regulation of activity. *Journal of Neurochemistry* **71,** 240-247.

Zhang, J., Lesort, M., Guttmann, R.P. and Johnson, G.V.W. (1998a) Modulation of the *in situ* activity of tissue transglutaminase by calcium and GTP. *Journal of Biological Chemistry* **273(4),** 2288-2295.

Zhang, J., Tucholski, J., Lesort, M., Jope, R.S. and Johnson, G.V.W. (1999). Noval bimodal effects of the G protein tissue transglutaminase on adrenoreceptor signalling. *Biochemical Journal* **343,** 541-549.

Zhang, J.W., Guttermann, R.P. and Johnson, G.V.W. (1998b). Tissue transglutaminase is an in situ substrate of calpain: Regulation of activity. *Journal of Neurochemistry* **71(1),** 240-247.

Zhao, J., Ren, Y., Jiang, Q. and Feng, J. (2003). Parkin is recruited to the centrosome in response to inhibition of proteasomes. *Journal of Cell Science* **116(19),** 4011-4019.

Zhao, M., New, L., Kravchenko, V.V., Kato, Y., Gram, H., Di Padova, F., Olsen, E.N., Ulevitch, R.J. and Han, J. (1999). Regulation of the MEF2 family of transcription factors by p38. *Molecular and Cellular Biology* **19(1),** 21-30.

Ziering, A., Berger, L., Heineman, S.D. and Lee, J. (1947). Piperidine derivatives. Part III. 4-arylpiperidines. *Journal of Organic Chemistry* **12,** 894-903.

The Nottingham Trent University
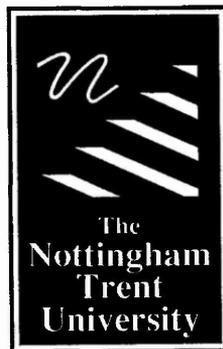
Libraries &
Learning
Resources